NUREG-1806, Vol. 1

Technical Basis for Revision of the Pressurized Thermal Shock (PTS) Screening Limit in the PTS Rule (10 CFR 50.61)

Summary Report

U.S. Nuclear Regulatory Commission
Office of Nuclear Regulatory Research
Washington, DC 20555-0001

AVAILABILITY OF REFERENCE MATERIALS IN NRC PUBLICATIONS

NRC Reference Material

As of November 1999, you may electronically access NUREG-series publications and other NRC records at NRC's Public Electronic Reading Room at http://www.nrc.gov/reading-rm.html.
Publicly released records include, to name a few, NUREG-series publications; *Federal Register* notices; applicant, licensee, and vendor documents and correspondence; NRC correspondence and internal memoranda; bulletins and information notices; inspection and investigative reports; licensee event reports; and Commission papers and their attachments.

NRC publications in the NUREG series, NRC regulations, and *Title 10, Energy*, in the Code of *Federal Regulations* may also be purchased from one of these two sources.

1. The Superintendent of Documents
   U.S. Government Printing Office
   Mail Stop SSOP
   Washington, DC 20402–0001
   Internet: bookstore.gpo.gov
   Telephone: 202-512-1800
   Fax: 202-512-2250
2. The National Technical Information Service
   Springfield, VA 22161–0002
   www.ntis.gov
   1–800–553–6847 or, locally, 703–605–6000

A single copy of each NRC draft report for comment is available free, to the extent of supply, upon written request as follows:

Address: U.S. Nuclear Regulatory Commission
Office of Administration
Mail, Distribution and Messenger Team
Washington, DC 20555-0001
E-mail: DISTRIBUTION@nrc.gov
Facsimile: 301–415–2289

Some publications in the NUREG series that are posted at NRC's Web site address http://www.nrc.gov/reading-rm/doc-collections/nuregs are updated periodically and may differ from the last printed version. Although references to material found on a Web site bear the date the material was accessed, the material available on the date cited may subsequently be removed from the site.

Non-NRC Reference Material

Documents available from public and special technical libraries include all open literature items, such as books, journal articles, and transactions, *Federal Register* notices, Federal and State legislation, and congressional reports. Such documents as theses, dissertations, foreign reports and translations, and non-NRC conference proceedings may be purchased from their sponsoring organization.

Copies of industry codes and standards used in a substantive manner in the NRC regulatory process are maintained at—

The NRC Technical Library
Two White Flint North
11545 Rockville Pike
Rockville, MD 20852–2738

These standards are available in the library for reference use by the public. Codes and standards are usually copyrighted and may be purchased from the originating organization or, if they are American National Standards, from—

American National Standards Institute
11 West 42nd Street
New York, NY 10036–8002
www.ansi.org
212–642–4900

Legally binding regulatory requirements are stated only in laws; NRC regulations; licenses, including technical specifications; or orders, not in NUREG-series publications. The views expressed in contractor-prepared publications in this series are not necessarily those of the NRC.

The NUREG series comprises (1) technical and administrative reports and books prepared by the staff (NUREG–XXXX) or agency contractors (NUREG/CR–XXXX), (2) proceedings of conferences (NUREG/CP–XXXX), (3) reports resulting from international agreements (NUREG/IA–XXXX), (4) brochures (NUREG/BR–XXXX), and (5) compilations of legal decisions and orders of the Commission and Atomic and Safety Licensing Boards and of Directors' decisions under Section 2.206 of NRC's regulations (NUREG–0750).

NUREG-1806, Vol. 1

Technical Basis for Revision of the Pressurized Thermal Shock (PTS) Screening Limit in the PTS Rule (10 CFR 50.61)

Summary Report

Manuscript Completed: May 2006
Date Published: August 2007

Prepared by
M. EricksonKirk, M. Junge, W. Arcieri,
B.R. Bass, R. Beaton, D. Bessette,
T.H.J. Chang, T. Dickson, C.D. Fletcher,
A. Kolaczkowski, S. Malik, T. Mintz,
C. Pugh, F. Simonen, N. Siu,
D. Whitehead, P. Williams, R. Woods,
S. Yin

Division of Fuel, Engineering and Radiological Research
Office of Nuclear Regulatory Research
U.S. Nuclear Regulatory Commission
Washington, DC 20555-0001

Abstract

During plant operation, the walls of reactor pressure vessels (RPVs) are exposed to neutron radiation, resulting in localized embrittlement of the vessel steel and weld materials in the core area. If an embrittled RPV had a flaw of critical size and certain severe system transients were to occur, the flaw could very rapidly propagate through the vessel, resulting in a through-wall crack and challenging the integrity of the RPV. The severe transients of concern, known as pressurized thermal shock (PTS), are characterized by a rapid cooling of the internal RPV surface in combination with repressurization of the RPV. Advancements in our understanding and knowledge of materials behavior, our ability to realistically model plant systems and operational characteristics, and our ability to better evaluate PTS transients to estimate loads on vessel walls led the NRC to realize that the earlier analysis, conducted in the course of developing the PTS Rule in the 1980s, contained significant conservatisms.

This report summarizes 21 supporting documents that describe the procedures used and results obtained in the probabilistic risk assessment, thermal hydraulic, and probabilistic fracture mechanics studies conducted in support of this investigation. Recommendations on toughness-based screening criteria for PTS are provided.

Foreword

The reactor pressure vessel is exposed to neutron radiation during normal operation. Over time, the vessel steel becomes progressively more brittle in the region adjacent to the core. If a vessel had a preexisting flaw of critical size and certain severe system transients occurred, this flaw could propagate rapidly through the vessel, resulting in a through-wall crack. The severe transients of concern, known as pressurized thermal shock (PTS), are characterized by rapid cooling (i.e., thermal shock) of the internal reactor pressure vessel surface that may be combined with repressurization. The simultaneous occurrence of critical-size flaws, embrittled vessel, and a severe PTS transient is a very low probability event. The current study shows that U.S. pressurized-water reactors do not approach the levels of embrittlement to make them susceptible to PTS failure, even during extended operation well beyond the original 40-year design life.

Advancements in our understanding and knowledge of materials behavior, our ability to realistically model plant systems and operational characteristics, and our ability to better evaluate PTS transients to estimate loads on vessel walls have shown that earlier analyses, performed some 20 years ago as part of the development of the PTS rule, were overly conservative, based on the tools available at the time. Consistent with the NRC's Strategic Plan to use best-estimate analyses combined with uncertainty assessments to resolve safety-related issues, the NRC's Office of Nuclear Regulatory Research undertook a project in 1999 to develop a technical basis to support a risk-informed revision of the existing PTS Rule, set forth in Title 10, Section 50.61, of the Code of Federal Regulations (10 CFR 50.61).

Two central features of the current research approach were a focus on the use of realistic input values and models and an explicit treatment of uncertainties (using currently available uncertainty analysis tools and techniques). This approach improved significantly upon that employed in the past to establish the existing 10 CFR 50.61 embrittlement limits. The previous approach included unquantified conservatisms in many aspects of the analysis, and uncertainties were treated implicitly by incorporating them into the models.

This report summarizes a series of 21 reports that provide the technical basis that the staff will consider in a potential revision of 10 CFR 50.61; it includes a description of analysis procedures and a detailed discussion of findings. The risk from PTS was determined from the integrated results of the Fifth Version of the Reactor Excursion Leak Analysis Program (RELAP5) thermal-hydraulic analyses, fracture mechanics analyses, and probabilistic risk assessment. These calculations demonstrate that, even through the period of license extension, the likelihood of vessel failure attributable to PTS is extremely low ($\approx 10^{-8}$/year) for all domestic pressurized water reactors. Limited analyses are continuing to further evaluate this finding. Should the $\approx 10^{-8}$/year value be confirmed, this would provide a basis for significant relaxation, or perhaps elimination, of the embrittlement limit established in 10 CFR 50.61. Such changes would reduce unnecessary conservatism without affecting safety because the operating reactor fleet has little probability of exceeding the limits on the frequency of reactor vessel failure established from NRC guidelines on core damage frequency and large early release frequency through the period of license extension.

Brian W. Sheron, Director
Office of Nuclear Regulatory Research
U.S. Nuclear Regulatory Commission

Contents

Appendices

Figures

Tables

Executive Summary

This report summarizes the results of a 5-year study conducted by the U.S. Nuclear Regulatory Commission (NRC), Office of Nuclear Regulatory Research (RES). The aim of this study was to develop the technical basis for revision of the Pressurized Thermal Shock (PTS) Rule, as set forth in Title 10, Section 50.61, of the *Code of Federal Regulations* (10 CFR 50.61), "Fracture Toughness Requirements for Protection Against Pressurized Thermal Shock Events," consistent with the NRC's current guidelines on risk-informed regulation. This report, together with other supporting reports documenting the study details and results, provides this basis.

This executive summary begins with a description of PTS, how it might occur, and its potential consequences for the reactor pressure vessel (RPV). This is followed by a summary of the current regulatory approach to PTS, which leads directly to a discussion of the motivations for conducting this project. Following this introductory information, we describe the approach used to conduct the study, and summarize our key findings and recommendations, which include a proposal for revision of the PTS screening limits. We then conclude the executive summary with a discussion of the potential impact of this proposal on regulations other than 10 CFR 50.61.

Description of PTS

During the operation of a nuclear power plant, the RPV walls are exposed to neutron radiation, resulting in localized embrittlement of the vessel steel and weld materials in the area of the reactor core. If an embrittled RPV had an existing flaw of critical size and certain severe system transients were to occur, the flaw could propagate very rapidly through the vessel, resulting in a through-wall crack and challenging the integrity of the RPV. The severe transients of concern, known as pressurized thermal shock (PTS), are characterized by a rapid cooling (i.e., thermal shock) of the internal RPV surface and downcomer, which may be followed by repressurization of the RPV. Thus, a PTS event poses a potentially significant challenge to the structural integrity of the RPV in a pressurized-water reactor (PWR).

A number of abnormal events and postulated accidents have the potential to thermally shock the vessel (either with or without significant internal pressure). These events include a pipe break or stuck-open valve in the primary pressure circuit, a break of the main steam line, etc. During such events, the water level in the core drops as a result of the contraction produced by rapid depressurization. In events involving a break in the primary pressure circuit, an additional drop in water level occurs as a result of leakage from the break. Automatic systems and operators must provide makeup water in the primary system to prevent overheating of the fuel in the core. However, the makeup water is much colder than that held in the primary system. As a result, the temperature drop produced by rapid depressurization coupled with the near-ambient temperature of the makeup water produces significant thermal stresses in the thick section steel wall of the RPV. For embrittled RPVs, these stresses could be sufficient to initiate a running crack, which could propagate all the way through the vessel wall. Such through-wall cracking of the RPV could precipitate core damage or, in rare cases, a large early release of radioactive material to the environment. Fortunately, the coincident occurrence of critical-size flaws, embrittled vessel steel and weld material, and a severe PTS transient is a very low-probability event. In fact, only a few currently operating PWRs are projected to closely approach the current statutory limit on the level of embrittlement during their planned operational life.

Current Regulatory Approach to PTS

As set forth in 10 CFR 50.61, the PTS Rule requires licensees to monitor the embrittlement of their RPVs using a reactor vessel material surveillance program qualified under Appendix H to 10 CFR Part 50, "Reactor Vessel Material Survellience Program Requirements." The surveillance results are then used together with the formulae and tables in 10 CFR 50.61 to estimate the fracture toughness transition temperature (RT_{NDT}) of the steels in the vessel's beltline and how those transition temperatures increase as a result of irradiation damage throughout the operational life of the vessel. For licensing purposes, 10 CFR 50.61 provides instructions on how to use these estimates of the effect of irradiation damage to estimate the value of RT_{NDT} that will occur at end of license (EOL), a value called RT_{PTS}. 10 CFR 50.61 also provides "screening limits" (maximum values of RT_{NDT} permitted during the plant's operational life) of +270°F (132°C) for axial welds, plates, and forgings, and +300°F (149°C) for circumferential welds. These screening limits correspond to a limit of $5\text{x}10^{-6}$ events/year on the annual probability of developing a through-wall crack [RG 1.154]. Should RT_{PTS} exceed these screening limits, 10 CFR 50.61 requires the licensee to either take actions to keep RT_{PTS} below the screening limit (by implementing "reasonably practicable" flux reductions to reduce the embrittlement rate, or by deembrittling the vessel by annealing [RG 1.162]), or perform plant-specific analyses to demonstrate that operating the plant beyond the 10 CFR 50.61 screening limit does not pose an undue risk to the public [RG 1.154].

While no currently operating PWR has an RT_{PTS} value that exceeds the 10 CFR 50.61screening limit before EOL, several plants are close to the limit (3 are within 2°F, while 10 are within 20°F). Those plants are likely to exceed the screening limit during the 20-year license renewal period that is currently being sought by many operators. Moreover, some plants maintain their RT_{PTS} values below the 10 CFR 50.61 screening limits by implementing flux reductions (low-leakage cores, ultra-low-leakage cores), which are fuel management strategies that can be economically deleterious in a deregulated marketplace. Thus, the 10 CFR 50.61 screening limits can restrict both the licensable and economic lifetime of PWRs.

Motivation for this Project

It is now widely recognized that the state of knowledge and data limitations in the early 1980s necessitated conservative treatment of several key parameters and models used in the probabilistic calculations that provided the technical basis for the current PTS Rule. The most prominent of these conservatisms include the following factors:

- highly simplified treatment of plant transients (very coarse grouping of many operational sequences (on the order of 10^5) into very few groups ($\approx$10), necessitated by limitations in the computational resources needed to perform multiple thermal-hydraulic calculations)
- lack of any significant credit for operator action
- characterization of fracture toughness using RT_{NDT}, which has an intentional conservative bias
- use of a flaw distribution that places *all* flaws on the interior surface of the RPV, and, in general, contains larger flaws than those usually detected in service
- a modeling approach that treated the RPV as if it were made entirely from the most brittle of its constituent materials (welds, plates, or forgings)
- a modeling approach that assessed RPV embrittlement using the peak fluence over the entire interior surface of the RPV

These factors indicate the high likelihood that the current 10 CFR 50.61 PTS screening limits are unnecessarily conservative. Consequently, the NRC staff believed that reexamining the technical basis for these screening limits, based on a modern understanding of all the factors that influence PTS, would most likely provide strong justification for substantially relaxing these limits. For these reasons, RES undertook this study with the objective of developing the technical basis to support a risk-informed revision of the PTS Rule and the associated PTS screening limit.

Approach

As illustrated in the following figure, three main models (shown as solid blue squares), taken together, allow us to estimate the annual frequency of through-wall cracking in an RPV:

- probabilistic risk assessment (PRA) event sequence analysis
- thermal-hydraulic (TH) analysis
- probabilistic fracture mechanics (PFM) analysis

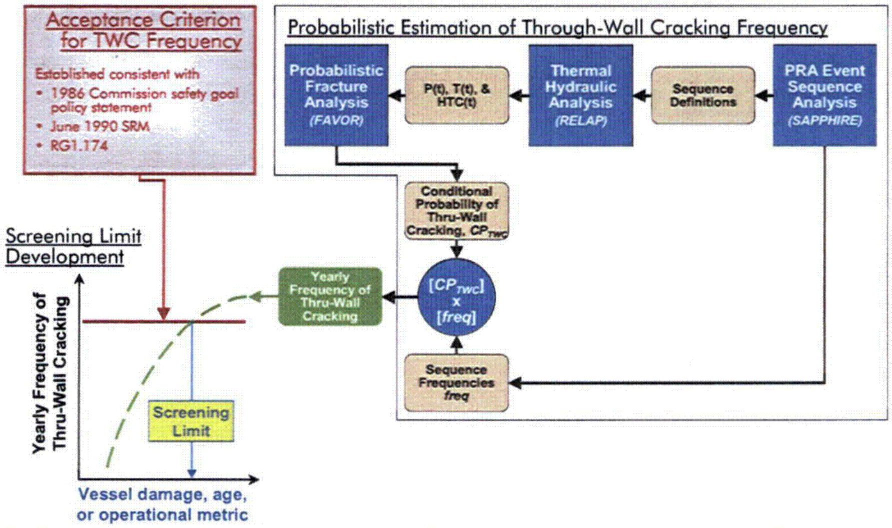

Schematic showing how a probabilistic estimate of through-wall cracking frequency (TWCF) is combined with a TWCF acceptance criterion to arrive at a proposed revision of the PTS screening limit

First, a PRA event sequence analysis is performed to define the sequences of events that are likely to cause a PTS challenge to RPV integrity, and estimate the frequency with which such sequences can be expected to occur. The event sequence definitions are then passed to a TH model that estimates the temporal variation of temperature, pressure, and heat-transfer coefficient in the RPV downcomer, which is characteristic of each sequence definition. These temperature, pressure, and heat-transfer coefficient histories are then passed to a PFM model that uses the TH output, along with other information concerning plant design and construction materials, to estimate the time-dependent "driving force to fracture" produced by a particular event sequence. The PFM model then compares this estimate of fracture driving force to the fracture toughness, or fracture resistance, of the RPV steel. This comparison allows us to estimate the probability that a crack could grow to sufficient size that it would penetrate all the way through the RPV wall if that particular sequence of events actually occured. The final step in the analysis involves a simple matrix multiplication of the probability of through-wall cracking (from the PFM analysis) with the frequency at which a particular event sequence is expected to occur (as defined by the event-tree analysis). This product establishes an estimate of the annual frequency of through-wall cracking that can be expected for a particular plant after a particular period of operation when subjected to a particular sequence of events. The annual frequency of through-wall cracking is then summed for all event sequences to estimate the total annual frequency of through-wall cracking for the vessel. Performance of such analyses for various operating lifetimes provides an estimate of how the annual frequency of through-wall cracking can be expected to vary over the lifetime of the plant.

The probabilistic calculations just described are performed to establish the technical basis for a revised PTS Rule within an integrated systems analysis framework. Our approach considers a broad range of factors that influence the likelihood of vessel failure during a PTS event, while accounting for uncertainties in these factors across a breadth of technical disciplines. Two central features of this approach are a focus on the use of realistic input values and models (wherever possible), and an *explicit* treatment of uncertainties (using currently available uncertainty analysis tools and techniques). Thus, our current approach improves upon that employed in developing SECY-82-465, which included intentional and unquantified conservatisms in many aspects of the analysis, and treated uncertainties *implicitly* by incorporating them into the models.

Key Findings

The findings from this study are divided into the following five topical areas: (1) the expected magnitude of the through-wall cracking frequency (TWCF) for currently anticipated operational lifetimes, (2) the material factors that dominate PTS risk, (3) the transient classes that dominate PTS risk, (4) the applicability of these findings (based on detailed analyses of three PWRs) to PWRs *in general*, and (5) the annual limit on TWCF established consistent with current guidelines on risk-informed regulation. In this summary, ***the conclusions are presented in boldface italic***, while the supporting information is shown in regular type.

TWCF Magnitude for Currently Anticipated Operational Lifetimes

- ***The degree of PTS challenge is low for currently anticipated lifetimes and operating conditions.***
  - Even at the end of license extension (60 operational years, or 48 effective full-power years (EFPY) at an 80% capacity factor), the mean estimated TWCF does not exceed $2x10^{-8}$/year for the plants analyzed. Considering that the RPVs at the Beaver Valley Power Station and Palisades Nuclear Power Plant are constructed from some of the most irradiation-sensitive materials in commercial reactor service today, these results suggest that, provided that operating practices do not change dramatically in the future, the operating reactor fleet is in little danger of exceeding either the TWCF limit of $5x10^{-6}$/yr expressed by Regulatory Guide 1.154 [RG 1.154] or the value of $1x10^{-6}$/yr recommended in Chapter 10 of this report — even after license extension.

Material Factors and their Contributions to PTS Risk

- ***Axial flaws, and the toughness properties that can be associated with such flaws, control nearly all of the TWCF.***
  - Axial flaws are much more likely than circumferential flaws to propagate through the RPV wall because the applied fracture driving force increases continuously with increasing crack depth for an axial flaw. Conversely, circumferentially oriented flaws experience a driving force peak mid-wall, providing a natural crack arrest mechanism. It should be noted that crack initiation from circumferentially oriented flaws is likely; it is only their through-wall propagation that is much less likely (relative to axially oriented flaws).
  - It is, therefore, the toughness properties that can be associated with axial flaws that control nearly all of the TWCF. These include the toughness properties of plates and axial welds at the flaw locations. Conversely, the toughness properties of both circumferential welds and forgings have little effect on the TWCF because these can be associated only with circumferentially oriented flaws.

Transients and their Contributions to PTS Risk

- ***Transients involving primary side faults are the dominant contributors to TWCF, while transients involving secondary side faults play a much smaller role.***
  - The severity of a transient is controlled by a combination of three factors:
    - initial cooling rate, which controls the thermal stress in the RPV wall
    - minimum temperature of the transient, which controls the resistance of the vessel to fracture
    - pressure retained in the primary system, which controls the pressure stress in the RPV wall
  - The significance of a transient (i.e., how much it contributes to PTS risk) depends on these three factors and the likelihood that the transient will occur.
  - Our analysis considered transients in the following classes (as shown in the following table):
    - primary side pipe breaks
    - stuck-open valves on the primary side
    - main steam line breaks
    - stuck-open valves on the secondary side
    - feed-and-bleed
    - steam generator tube rupture
    - mixed primary and secondary initiators

Factors contributing to the severity and risk-dominance of various transient classes

Transient Class		Transient Severity: Cooling Rate	Transient Severity: Minimum Temperature	Transient Severity: Pressure	Transient Likelihood	TWCF Contribution
Primary Side Pipe Breaks	Large-Diameter	Fast	Low	Low	Low	Large
	Medium-Diameter	Moderate	Low	Low	Moderate	Large
	Small-Diameter	Slow	High	Moderate	High	~0
Stuck-Open Valves, Primary Side	Valve Recloses	Slow	Moderate	High	High	Large
	Valve Remains Open	Slow	Moderate	Low	High	~0
Main Steam Line Break		Fast	Moderate	High	High	Small
Stuck-Open Valve(s), Secondary Side		Moderate	High	High	High	~0
Feed-and- Bleed		Slow	Low	Low	Low	~0
Steam Generator Tube Rupture		Slow	High	Moderate	Low	~0
Mixed Primary & Secondary Initiators		Slow	Mixed		Very Low	~0

Color Key			
Color Key	Enhances TWCF Contribution	Intermediate	Diminishes TWCF Contribution

  - The table above provides a qualitative summary our results for these transient classes in terms of both transient severity and the likelihood that the transient will occur. The color-coding of table entries indicates the contribution (or lack thereof) of these factors to the TWCF of the various classes of transients. This summary indicates that the risk-dominant transients (medium- and large-diameter primary side pipe breaks, and stuck-open primary side valves that later reclose) all have multiple factors that, in combination, result in their significant contributions to TWCF.
    - For medium- to large-diameter primary side pipe breaks, the fast to moderate cooling rates and low downcomer temperatures (generated by rapid depressurization and emergency injection of low-temperature makeup water directly to the primary) combine to produce a high-severity transient. Despite the moderate to low likelihood that these transients will occur, their severity (if they do occur) makes them significant contributors to the total TWCF.

- For stuck-open primary side valves that later reclose, the repressurization associated with valve reclosure coupled with low temperatures in the primary combine to produce a high-severity transient. This, coupled with a high likelihood of transient occurrence, makes stuck-open primary side valves that later reclose significant contributors to the total TWCF.
- The small or negligible contribution of all secondary side transients (main steam line break, stuck-open secondary valves) results directly from the lack of low temperatures in the primary system. For these transients, the minimum temperature of the primary for times of relevance is controlled by the boiling point of water in the secondary (212°F (100°C) or above). At these temperatures, the fracture toughness of the RPV steel is sufficiently high to resist vessel failure in most cases.

Applicability of These Findings to PWRs in General

- ***Credits for operator action, while included in our analysis, do not influence these findings in any significant way.*** Operator action credits can dramatically influence the risk-significance of ***individual*** transients. Therefore, appropriate credits for operator action need to be included as part of a "best estimate" analysis because there is no way to establish *a priori* if a particular transient will make a large contribution to the total risk. Nonetheless, the results of our analyses demonstrate that these operator action credits have a small ***overall effect*** on a plant's ***total TWCF***, for reasons detailed below.
  - <u>Medium- and Large-Diameter Primary Side Pipe Breaks</u>: No operator actions are modeled for any break diameter because, for these events, the safety injection systems do not fully refill the upper regions of the reactor coolant system (RCS). Consequently, operators would never take action to shut off the pumps.
  - <u>Stuck-Open Primary Side Valves that May Later Reclose</u>: Reasonable and appropriate credit for operator actions (throttling of the high-pressure injection (HPI) system) has been included in the PRA model. However, these credits have a small influence on the estimated values of vessel failure probability attributable to transients caused by a stuck-open valve in the primary pressure circuit (SO-1 transients) because the credited operator actions only prevent repressurization when SO-1 transients initiate from Hot Zero Power (HZP) conditions and when the operators act promptly (within 1 minute) to throttle the HPI. Complete removal of operator action credits from the model only slightly increases the total risk associated with SO-1 transients.
  - <u>Main Steam Line Breaks</u>: For the overwhelming majority of transients caused by a main steam line break (MSLB), vessel failure is predicted to occur between 10 and 15 minutes after transient initiation because the thermal stresses associated with the rapid cooldown reach their maximum within this timeframe. Thus, all of the long-term effects (isolation of feedwater flow, timing of HPSI control) that can be influenced by operator actions have no effect on vessel failure probability because such factors influence the progression of the transient *after failure has occurred* (if it occurs at all). Only factors affecting the initial cooling rate (i.e., plant power level at time of transient initiation, break location inside or outside of containment) can influence the conditional probability of through-wall cracking (CPTWC), and operator actions do not influence such factors in any way.
- ***Because the severity of the most significant transients in the dominant transient classes is controlled by factors that are common to PWRs in general, the TWCF results presented herein can be used with confidence to develop revised PTS screening criteria that apply to the entire fleet of operating PWRs.***
  - <u>Medium- and Large-Diameter Primary Side Pipe Breaks</u>: For these break diameters, the fluid in the primary cools faster than the wall of the RPV. In this situation, ***only*** the thermal conductivity of the steel and the thickness of the RPV wall control the thermal stresses and, thus, the severity of the fracture challenge. Perturbations in the fluid cooldown rate controlled by break diameter, break location, and season of the year do not play a role. Thermal conductivity is a physical property,

so it is very consistent for all RPV steels, and the thicknesses of the three RPVs analyzed are typical of PWRs. Consequently, the TWCF contribution of medium- to large-diameter primary side pipe breaks is expected to be consistent from plant-to-plant and can be well represented for all PWRs by the analyses reported herein.

- Stuck-Open Primary Side Valves that May Later Reclose: A major contributor to the risk-significance of SO-1 transients is the return to full system pressure once the valve recloses. The operating and safety relief valve pressures of all PWRs are similar. Additionally, as previously noted, operator action credits only slightly affect the total risk associated with this transient class.
- Main Steam Line Breaks: Since MSLBs fail early (within 10–15 minutes after transient initiation), only factors affecting the initial cooling rate can have any influence on the CPTWC values. These factors, which include the plant power level at event initiation and the location of the break (inside or outside of containment), are not influenced by operator actions in any way.

- ***Sensitivity studies performed on the TH and PFM models to investigate the effect of credible model variations on the predicted TWCF values revealed no effects significant enough to recommend changes to the baseline RELAP and FAVOR models, or to recommend cautions regarding the robustness of those models.***
- ***An investigation of design and operational characteristics for five additional PWRs revealed no differences in sequence progression, sequence frequency, or plant thermal-hydraulic response significant enough to call into question the applicability of the TWCF results from the three detailed plant analyses to PWRs in general.***
- ***An investigation of potential external initiating events (e.g., fires, earthquakes, floods) revealed that the contribution of those events to the total TWCF can be regarded as negligible.***

Annual Limit on TWCF

- ***The current guidance provided by Regulatory Guide 1.174 [RG 1.174] for large early release is appropriately applied to setting an acceptable annual TWCF limit of $1x10^{-6}$ events/year.***
    - While many post-PTS accident progressions led only to core damage (which suggests a TWCF limit of $1x10^{-5}$ events/year limit in accordance with Regulatory Guide 1.174), uncertainties in the accident progression analysis led to our recommendation to adopt the more conservative limit of $1x10^{-6}$ events/year based on LERF.

Recommended Revision of the PTS Screening Limits

We recommend using different reference temperature (*RT*) metrics to characterize an RPV's resistance to fractures initiating from different flaws at different locations in the vessel. Specifically, we recommend a reference temperature for flaws occurring along axial weld fusion lines (RT_{AW} or $RT_{AW\text{-}MAX}$), another for flaws occurring in plates or in forgings (RT_{PL} or $RT_{PL\text{-}MAX}$), and a third for flaws occurring along circumferential weld fusion lines (RT_{CW} or $RT_{CW\text{-}MAX}$). In each of these reference temperature pairs, the first metric is a weighted value that accounts for the differences between plants in weld fusion line area or plate volume, while the second metric is a maximum value that can be estimated based only on the information in the NRC's Reactor Vessel Integrity Database (RVID). We also recommend using different *RT* values together to characterize the fracture resistance of the vessel's beltline region, in recognition of the fact that the probability of vessel fracture initiating from different flaw populations varies considerably in response to factors that are both understood and predictable. Correlations between these *RT* metrics and the TWCF attributable to axial weld flaws, plate flaws, and circumferential weld flaws show little plant-to-plant variability because of the general similarity of PTS challenges among plants.

RT-based screening limits were established by setting the total TWCF (i.e., that attributable to axial weld flaws and plate flaws and circumferential weld flaws) equal to the reactor vessel failure frequency acceptance criterion of 1×10^{-6} events per year. The following figures graphically represent these screening limits (for the maximum *RT* metrics), along with an assessment of all operating PWRs relative to these limits. In these figures, the region of the graphs between the red locus and the origin has TWCF values below the 1×10^{-6} acceptance criterion, so these combinations of reference temperatures would be considered acceptable and require no further analysis. By contrast, the region of the graph outside of the red locus has TWCF values above the 1×10^{-6} acceptance criterion, indicating the need for additional analysis or other measures to justify continued plant operation. Clearly, operating PWRs do not closely approach the 1×10^{-6}/year limit. At EOL, at least 70°F, and up to 290°F, (39 to 161°C) separate plate-welded PWRs from the proposed screening limit; this separation between plant-specific values and the proposed screening limit reduces by 10–20°F (5.5 to 11°C) at end of license extension (EOLE, defined as 60 operating years or 48 EFPY). Additionally, no forged plant is anywhere close to the limit of 1×10^{-6} events per year at either EOL or EOLE. This separation of operating plants from the screening limit contrasts markedly with the current situation, where the most embrittled plants are within 1°F (0.5°C) of the screening limit set forth in 10 CFR 50.61. These differences in the "proximity" of operating plants to the current (10 CFR 50.61) and proposed screening limits are illustrated by the bar graph on the next page.

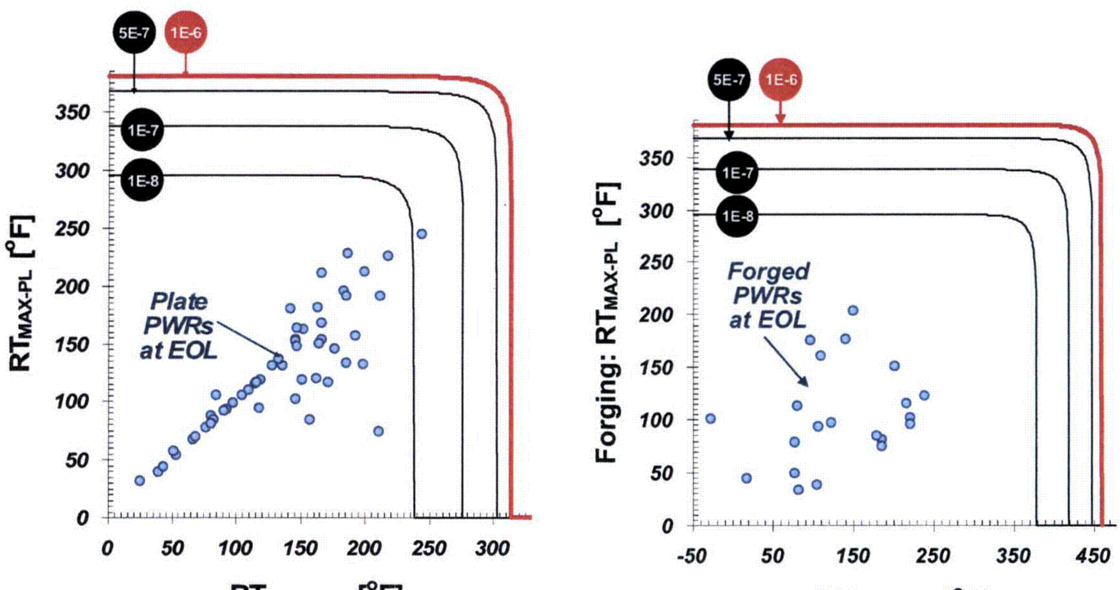

Comparison of RT-based screening limits (curves) with assessment points for operating PWRs at EOL (Left: plate vessels, Right: forged vessels)

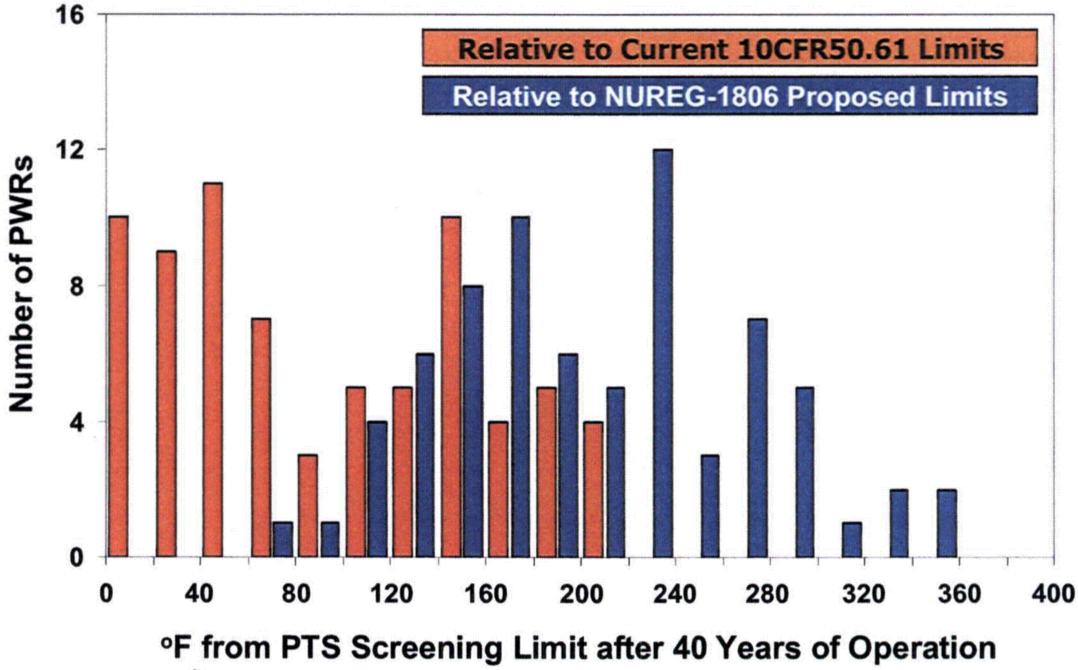

Difference between the proximity of operating PWRs to the current RT_{PTS} screening limits and to the screening limits proposed based on the work presented in this report.

These *RT*-based screening limits (and similar limits described in the text for application to weighted *RT* values) apply to PWRs in general, subject only to the following provisos:

- When assessing a forged vessel where the forging has a very high reference temperature (RT_{PL} above 225°F (107°C)) ***and*** the forging is believed to be susceptible to subclad cracking, a plant-specific analysis of the TWCF produced by the subclad cracks should be performed. However, no forging is projected to reach this level of embrittlement, even at EOLE.
- When assessing an RPV having a wall thickness of 7-in. (18-cm) or less (7 vessels), the proposed *RT* limits are conservative.
- When assessing an RPV having a wall thickness of 11-in. (28-cm) or greater, the proposed *RT* limits may be nonconservative. For the three plants meeting this criterion, either the *RT* limits would need to be reduced or known conservatisms in the current analysis would have to be removed to demonstrate compliance with the TWCF limit of 1×10^{-6} event/year. However, because these three plants are Units 1, 2, and 3 of the Palo Verde Nuclear Generating Station, which have vessels with very low embrittlement projected at EOL and EOLE, there is little practical need for such plant-specific analysis.

Aside from relying on different *RT* metrics than 10 CFR 50.61, this proposed revision of the PTS screening limit differs from the current screening limit in the absence of a "margin term." Use of a margin term is appropriate to account (at least approximately) for factors that occur in application but were not considered in the analysis upon which the screening limit is based. For example, the 10 CFR 50.61 margin term accounts for uncertainty in copper, nickel, and initial RT_{NDT}. However, our model explicitly considers uncertainty in all of these variables, and represents these uncertainties as being larger (a conservative representation) than would be appropriate in any plant-specific application of the proposed screening limit. Consequently, use of the 10 CFR 50.61 margin term with the new screening limits is inappropriate. In general, the following additional reasons suggest that use of *any* margin term with the proposed screening limits is inappropriate:

(1) The *TWCF* values used to establish the screening limit represent 90^{th} percentile values or greater.

(2) The results from our three plant-specific analyses apply to PWRs *in general*, as demonstrated in Chapters 8 and 9 of this report.

(3) Certain aspects of our modeling cannot reasonably be represented as "best estimates." On balance, there is a conservative bias to these non-best-estimate aspects of our analysis because residual conservatisms in the model far outweigh residual nonconservatisms.

Abbreviations

¼-T FLAW	Surface-breaking flaw defined by ASME Boiler and Pressure Vessel Code as having a depth equal to one-quarter of the vessel wall thickness and a length equal to six times the flaw depth
1D	One-Dimensional
ABAQUS	Commercial finite element code developed by Hibbett, Karlsson, and Sorenson in Pawtucket, Rhode Island
ACRS	Advisory Committee on Reactor Safety (NRC)
ADV	Atmospheric Dump Valve
AFW	Auxiliary Feedwater
APET	Accident Progression Event Tree
APEX	Advanced Plant Experiment
ASME	American Society of Mechanical Engineers
ASTM	American Society for Testing and Materials
ATWS	Anticipated Transient without Scram
B&W	Babcock and Wilcox
BWOG	Babcock and Wilcox Owners' Group
BCC	Body-Centered Cubic
BWR	Boiling-Water Reactor
CDF	Core Damage Frequency
CE	Combustion Engineering
CEOG	Combustion Engineering Owners' Group
CFD	Computational Fluid Dynamics
CL	Cold Leg
CFR	*Code of Federal Regulations*
CFT	Core Flood Tank
CPI	Conditional Probability of Crack Initiation
CPTWC	Conditional Probability of Through-Wall Cracking
CSAU	Code Scaling, Applicability, and Uncertainty Methodology
CSNI	Committee on the Safety of Nuclear Installations
CST	Condensate Storage Tank
CVN	Charpy V-Notch
ECC	Emergency Core Cooling
ECCS	Emergency Core Cooling System
EFPY	Effective Full-Power Years
EFW	Emergency Feedwater
EOL	End of License (40 operating years, 32 EFPY)
EOLE	End of License Extension (60 operating years, 48 EFPY)

EPRI	Electric Power Research Institute
ESFAS	Engineered Safety Features Actuation System
F&B	Feed-and-Bleed
FAVOR	Fracture Analysis of Vessels, Oak Ridge
FCI	Frequency of Crack Initiation
GMAW	Gas Metal Arc Weld
H2TS	Hierarchical, Two-Tiered Scaling
HCLPF	High Confidence of Low Probability of Failure
HEP	Human Error Probability
HFE	Human Failure Event
HPI	High-Pressure Injection
HPSI	High-Pressure Safety Injection
HRA	Human Reliability Analysis
HSSI	Heavy Section Steel Irradiation (Project)
HZP	Hot Zero Power
IAEA	International Atomic Energy Agency
ID	Inner Diameter
IPE	Individual Plant Examination
IPEEE	Individual Plant Examination of External Events
IPTS	Integrated Pressurized Thermal Shock
ISLOCA	Interfacing Systems Loss-of-Coolant Accident
ITV	Intermediate Test Vessel
IVO	Imatran Voima Oy
LAS	Low-Alloy Steel
LBLOCA	Large-Break Loss-of-Coolant Accident (pipe diameters above ~8-in. (~20-cm))
LEFM	Linear Elastic Fracture Mechanics
LER	Licensee Event Report
LERF	Large Early Release Frequency
LOCA	Loss-of-Coolant Accident
LOF	Lack of Inter-Run Fusion
LOFT	Loss-of-Fluid Test facility
LPI	Low-Pressure Injection
LPSI	Low-Pressure Safety Injection
MBLOCA	Medium-Break Loss-of-Coolant Accident (pipe diameters of ~4 to 8-in. (~10 to 20-cm))
MFIV	Main Feedwater Isolation Valve
MFW	Main Feedwater
MIST	Multi-loop Integral System Test
MRJ	Materials Reliability Project
MSIV	Main Steam Isolation Valve
MSLB	Main Steam Line Break

NDT	Nil-Ductility Temperature
NEA	Nuclear Energy Agency (OECD)
NRC	U.S. Nuclear Regulatory Commission
NRR	Office of Nuclear Reactor Regulation (NRC)
NUREG/CR	NRC Technical Report Designator (Contractor-prepared Report published by the U.S. Nuclear Regulatory Commission)
OD	Outer Diameter
OECD	Organization for Economic Cooperation and Development
ORNL	Oak Ridge National Laboratory
PFM	Probabilistic Fracture Mechanics
PIRT	Phenomena Identification and Ranking Table
PNNL	Pacific Northwest National Laboratories
PORV	Power-Operated Relief Valve
Ppb	Parts per Billion
PRA	Probabilistic Risk Assessment
PRODIGAL	Probability of Defect Initiation and Growth Analysis
PTS	Pressurized Thermal Shock
PTSE	Pressurized Thermal Shock Experiment
PVRUF	Pressure Vessel Research Users' Facility
PWR	Pressurized-Water Reactor
QHO	Quantitative Health Objective, as defined by the Commission's Safety Goal Policy Statement [NRC FR 86]
RCP	Reactor Coolant Pump
RCS	Reactor Coolant System
RELAP	Reactor Leak and Power excursion code
REMIX	a computer program used to determine the temperature of a plume in the downcomer when the flow in the loops is stagnant
RES	Office of Nuclear Regulatory Research (NRC)
RG	Regulatory Guide
RLE	Review-Level Earthquake
ROSA	Rig of Safety Assessment
RPS	Reactor Protection System
RPV	Reactor Pressure Vessel
RT	Reference Temperature
RVFF	Reactor Vessel Failure Frequency
RVID	Reactor Vessel Integrity Database
RWST	Refueling Water Storage Tank
SAPHIRE	Systems Analysis Programs for Hands-on Integrated Reliability Evaluations
SAW	Submerged Arc Weld
SBLOCA	Small-Break Loss-of-Coolant Accident (pipe diameters below ~4-in. (~10-cm))
SCC	Stress Corrosion Cracking
SECY	Secretary of the (U.S. Nuclear Regulatory) Commission

SEMISCALE	a 1:1705 scaled experimental facility that simulates the primary system of a 4-loop PWR plant
SG	Steam Generator
SGTR	Steam Generator Tube Rupture
SIAS	Safety Injection Actuation Signal
SIT	Safety Injection Tank
SMAW	Submerged Metal Arc Weld
SO-1	Stuck-open valve in the primary pressure circuit
SO-2	Stuck-open valve in the secondary pressure circuit
SQA	Software Quality Assurance
SRM	Staff Requirements Memorandum
SRV	Safety/Relief Valve
SSC	System, Structure, or Component
SSE	Safe-Shutdown Earthquake
SSRV	Secondary System Relief Valve
TBV	Turbine Bypass Valve
TH	Thermal-Hydraulics
TMI	Three Mile Island
TSE	Thermal Shock Experiment
TWCF	Through-Wall Cracking Frequency
UMD	University of Maryland
UPTF	Upper Plenum Test Facility
USE	Charpy V-Notch Upper-Shelf Energy
V&V	Verification and Validation
VCIF	Vessel Crack Initiation Frequency
(W)	Westinghouse
WOG	Westinghouse Owners' Group
WPS	Warm Pre-Stress

Nomenclature

Symbols Used in Thermal-Hydraulics

α	thermal diffusivity, m^2/s
β	bulk coefficient of expansion, 1/C
μ	viscosity, kg/m-s
ν	kinematic viscosity, m^2/s
ρ	density, kg/m^3
σ	stress, kg/s^2
τ	characteristic time
C_p	heat capacity, m^2/s^2-C
g	gravitational acceleration, m/s^2
Gr	Grashof Number
h	convective heat transfer coefficient, W/m^2-C
D	diameter, m
J	joules, $kg\text{-}m^2/s^2$
k	conductivity, W/m-C
l	length, m
Nu	Nusselt Number
Pr	Prandtl Number
P	pressure, $kg/m\text{-}s^2$
q	heat flux, W/m^2
Re	Reynolds Number
Ri	Richardson Number
s	seconds
t	thickness, m
t	time, s
u	velocity, m/s
T	temperature, C
W	watts, $kg\text{-}m^2/s^3$

Symbols Used in Fracture Mechanics

$2a$	Flaw depth measured through the vessel wall thickness
$2c$	Flaw length measured parallel to the axial or circumferential direction of the vessel
Cu	Copper content, weight%
J_{Ic}	A fracture toughness measure defined by ASTM E1820, which quantifies the resistance of metals to crack initiation by the initiation, growth, and coalescence of microvoids
J-R	A fracture toughness measure defined by ASTM E1820, which quantifies the resistance of metals to ductile tearing
K_{Jc}	A fracture toughness measure defined by ASTM E1921, which quantifies the resistance of metals to crack initiation by cleavage mechanisms
K_{Ia}	A fracture toughness measure defined by ASTM E1221, which quantifies the ability of metals to arrest (stop) a running cleavage crack
K_{Ic}	A fracture toughness measure defined by ASTM E399, which quantifies the resistance of metals to crack initiation under plane strain conditions
$K_{Ic(min)}$	The minimum K_{Ic} fracture toughness possible at a particular temperature
$K_{APPLIED}$	Linear elastic crack driving force
$\mathcal{L}$	For a buried defect, distance from the wetted clad surface on the vessel ID to the inner crack tip
ℓ	The length of the fusion line of an axial weld
Ni	Nickel content, weight%
P	Phosphorus content, weight%
RT_{AW}	A fracture toughness reference temperature, which characterizes the RPV's resistance to fractures initiating from flaws found along the axial weld fusion lines. It corresponds to the maximum RT_{NDT} of the plates/welds that lie to either side of the weld fusion lines, and is weighted to account for differences in weld fusion line length (and, therefore, number of simulated flaws) between vessel courses.
RT_{PL}	A fracture toughness reference temperature, which characterizes the RPV's resistance to fractures initiating from flaws found in plates that are not associated with welds. It corresponds to the maximum RT_{NDT} occurring anywhere in the plate.
RT_{CW}	A fracture toughness reference temperature, which characterizes the RPV's resistance to fractures initiating from flaws found along the circumferential weld fusion lines. It corresponds to the maximum RT_{NDT} of the plates/welds that lie to either side of the weld fusion lines.
RT_{NDT}	Transition fracture toughness reference temperature defined by ASME NB-2331
$RT_{NDT(u)}$	Unirradiated value of RT_{NDT}
RT_{PTS}	RT_{NDT} projected end of license to account for the effects of irradiation (defined in 10 CFR 50.61)
t_{WALL}	Vessel wall thickness
t_{CLAD}	Stainless steel cladding thickness

T_{30}	The temperature at which the mean CVN energy is 30 ft-lbs (41J)
$T_{35/50}$	Charpy V-notch energy transition temperature defined as the temperature at which the CVN energy is at least 50 ft-lbs (68J) and the lateral expansion of the specimen is at least 0.035-in. (0.89-mm) [See the definition on page 2-7]
T_{NDT}	Nil-ductility temperature defined by ASTM E-208
ΔT_{30}	The shift in the CVN 30 ft-lb (41J) transition temperature produced by radiation damage
σ_{flow}	Flow strength, average of tensile yield and tensile ultimate strength
ϕt	Fluence

Glossary

Terms Used in Probabilistic Risk Assessment

Abnormal operating procedure	A procedure (i.e., list of actions) used to address unique or special plant circumstances identified while using emergency operating procedures (EOPs). These abnormal operating procedures are usually called by EOPs, but may be indicated directly by some plant conditions.
Accident progression event tree	The event tree used to model the part of the accident sequence that follows the onset of core damage, including containment response to severe accident conditions, equipment availability, and operator performance.
Binning	The process of taking a large number of sequences and combining then into a smaller number of groups, that are expected to have similar characteristics (e.g., TH conditions), to allow effective utilization of limited resources.
Core damage	Uncovery and heatup of the reactor core to the point at which prolonged oxidation and severe fuel damage is anticipated and involving enough of the core to cause a significant release.
Dominant scenario	An accident sequence (scenario) that is usually represented by the top 10 or 20 events or groups of events modeled in a PRA, which accounts for a large fraction of the specified end state.
Emergency operating procedure	The primary procedure (i.e., list of actions) used to respond to a plant disturbance resulting from an initiating event.
Event tree	A logic diagram that begins with an initiating event or condition and progresses through a series of branches that represent expected system or operator performance that either succeeds or fails and arrives at either a successful or failed end state.
Fault tree	A deductive logic diagram that depicts how a particular undesired event can occur as a logical combination of other undesired events.
Large Early Release	The rapid, unmitigated release of airborne fission products from the containment to the environment occurring before the effective implementation of offsite emergency response and protective actions, such that there is a potential for early health effects.
Latin Hypercube sampling	A stratified sampling technique, in which the random variable distributions are divided into equal probability intervals, and probabilities are then randomly selected from within each interval.
Mitigating equipment	Systems or components, used to respond to an initiating event, of which successful operation prevents the occurrence of an undesired event or state.
Pre-initiator human failure event	Human failure events that represent the impact of human errors committed during actions performed prior to the initiation of an accident (e.g., during maintenance or the use of calibration procedures).
Post-initiator human failure event	Human failure events that represent the impact of human errors committed during actions performed in response to an accident initiator.

Prompt fatality	A fatality that results from substantial radiation exposures incurred during short time periods (usually within weeks, though up to 1 year for pulmonary effects).
PTS bin	A group of sequences that are expected to have similar TH characteristics and are represented by one unique set of TH characteristics during a FAVOR calculation.
Risk-informed	An approach to analyzing and evaluating activities, which bases decisions on the results of traditional engineering evaluations, supported by insights derived from the use of PRA methods.
Scenario	See Sequence.
Screening	The process of eliminating items from further consideration based on their negligible contribution to the probability of an undesired end state or its consequences.
Sequence	A representation in terms of an initiating event followed by a sequence of failures or successes of events (i.e., system, function, or operator performance) that can lead to undesired consequences, with a specified end state (e.g., potential for PTS).

Terms Used in Thermal-Hydraulics

Blowdown	Rapid depressurization of a system in response to a break.
Break flow	Flow of water (liquid and vapor) out a pipe break or a valve.
Break energy	Energy content of the fluid flow out a break.
Bottom-up	To break up a complex system into its subsystems, and then break up each subsystem into its components, examine individual local phenomena and processes that most affect each component, and build up the total complex system from these individual pieces (like manufacturing a car).
Coast down	Time required for a pump to stop rotating once power is shut off due to inertia.
Decay heat	Heat generated from radioactive decay of fission products.
Enthalpy	Sum of internal energy and volume multiplied by pressure.
Flash	Change of phase from saturated liquid to vapor resulting from decrease in pressure.
Flow quality	Mass fraction of flow stream that is steam. Higher quality flow would have a high mass fraction of steam.
Forced flow	Flow driven by a pump.
Inventory	Mass of water.
Loop flow	Mass flow rate of coolant in a circuit.
Makeup water	Water reservoir available for inventory control.
Natural circulation	Flow driven by buoyancy (gravity).
Pressure drop	Change in pressure due to conversion of mechanical energy to internal energy.
Protection system	Electrical controls to actuate engineering safety features.
Quality	Mass fraction of steam in a two-phase steam-water mixture.

Saturation temperature	A temperature corresponding to phase change from liquid to vapor.
Sensible heat	The product of specific heat and temperature change of subcooled liquid.
Subcooled	A system is *subcooled* if it exists entirely in a liquid state. The *degree of subcooling* is the number of degrees that the temperature of the system would have to be raised to cause boiling.
Throttled	Operation of a control valve to regulate flow.
Top-down	To characterize a complex system by establishing the governing behavior, or phenomenon, that is most important, and then proceed from that starting point to successive lower levels, by identifying the processes that have the greatest influence on the top-level phenomenon.
Trip	A "trip" occurs when a breaker opens in response to its trip mechanism (an arm that holds the breaker closed moves to allow the breaker to open). When a reactor trips, all of the breakers that provide power to the rod control system open, causing the rods to be inserted in the core and stopping the nuclear reaction. When a pump trips, the breaker opens, thereby disconnecting power and causing the pump to stop.
Water solid	A situation in which there is no steam in the system (i.e., it is all liquid). A "water solid" system is *subcooled.*

Terms Used in Fracture Mechanics

Brittle	Fracture occurring without noticeable macroscopic plastic deformation (stretching) of the material.
Cleavage fracture	Microscopically, cleavage is a fracture mode that occurs preferentially along certain atomic planes through the grains of the material. Cleavage can only occur in ferritic steels (i.e., steels having a body-centered cubic lattice structure). Macroscopically, cleavage fracture is often called "brittle" fracture because little noticeable plastic deformation (stretching) of the material occurs. (Note, however, that plastic flow at the micro-scale is a necessary precursor to cleavage.) Macroscopically, cleavage fracture is also characterized as being a sudden event, with cracks of very large dimensions developing over durations measured in fractional seconds. A useful, although inexact, analogue for cleavage fracture in common experience is the breaking of glass.
Ductile fracture	Microscopically, ductile fracture occurs through the initiation, growth, and eventual coalescence of micro-voids in the material into a macroscopic crack. These micro-voids tend to initiate at local heterogeneities in the material (e.g., inclusions, carbides, clusters of dislocations). Macroscopically, ductile fracture is associated with considerable plastic deformation (stretching) of the material. Relative to cleavage fracture, ductile fracture occurs very slowly, with crack growth rates measured in seconds rather than in micro-seconds (for cleavage).
Fracture toughness	A general term referring to a material's resistance to fracture. The term may be modified to refer to fractures by different mechanisms: <u>Arrest fracture toughness</u> measures a material's ability to stop a running cleavage crack. <u>Cleavage fracture toughness</u> measures a material's ability to resist crack initiation in cleavage. <u>Ductile fracture toughness</u> measures a material's ability to resist crack initiation attributable to ductile mechanisms on the upper shelf.

Lower shelf	At low temperatures, the toughness behavior of steels occurs by transgranular cleavage and is said to be on the lower shelf. On the lower shelf, a fracture is unstable, and is often referred to as a "brittle" fracture.
Reference temperature	A characteristic temperature used to locate the transition curve of a ferritic steel on the temperature axis.
Transition (or transition curve)	Between lower shelf and upper shelf temperatures, the fracture behavior of a ferritic material is said to be in "transition." At low temperatures in transition, fracture occurs by cleavage. As temperature increases through the transition regime, fracture occurs by ductile crack initiation and growth, a process which is terminated by cleavage. At still higher temperatures, cleavage cannot occur, and upper shelf conditions exist.
Upper shelf	At high temperatures, the toughness behavior of steels occurs by ductile mechanisms (micro-void initiation, growth, and coalescence) and is said to be on the upper shelf. On the upper shelf, afracture is stable and dissipates considerable amounts of energy.

Terms Used in Uncertainty Analysis

Aleatory	Aleatory uncertainties arise as a result of the randomness inherent in a physical or human process. Consequently, aleatory uncertainties are fundamentally irreducible. If the uncertainty in a variable is characterized as being aleatory, the entire distribution of the variable is carried through each simulation run.
Epistemic	Epistemic uncertainties are caused by limitations in our current state of knowledge (or understanding) of a given process. Epistemic uncertainties can, in principle, be reduced by an increased state of knowledge. If the uncertainty in a variable is characterized as being epistemic in a probabilistic simulation, individual values of the variable are randomly selected from a distribution and propagated through the calculation. This procedure models the understanding that the "correct" value of the variable is knowable, at least in principal. Thus, for epistemic uncertainties, individual simulation runs are deterministic, while the totality of all simulation runs captures the uncertainty characteristic of the epistemic variable.

1 Motivation for and Objective of this Study

1.1 Description of Pressurized Thermal Shock

During the operation of a nuclear power plant, the walls of the reactor pressure vessel (RPV) are exposed to neutron radiation, resulting in localized embrittlement of the vessel steel and weld materials in the area of the reactor core. If an embrittled RPV had an existing flaw of critical size and certain severe system transients were to occur, the flaw could very rapidly propagate through the vessel, resulting in a through-wall crack and challenging the integrity of the RPV. The severe transients of concern, known as pressurized thermal shock (PTS), are characterized by a rapid cooling (i.e., thermal shock) of the internal RPV surface and downcomer, which may be followed by repressurization of the RPV. Thus, a PTS event poses a potentially significant challenge to the structural integrity of the RPV in a pressurized-water reactor (PWR).

A number of abnormal events and postulated accidents have the potential to thermally shock the vessel (either with or without significant internal pressure). These events include a pipe break or stuck-open valve in the primary pressure circuit, or a break of the main steam line, among others. During such events, the water level in the core drops as a result of the contraction produced by rapid depressurization. In events involving a break in the primary pressure circuit, an additional drop in water level occurs as a result of leakage from the break. Automatic systems and operators must provide makeup water in the primary system to prevent overheating of the fuel in the core. However, the makeup water is much colder than that held in the primary system. As a result, the temperature drop produced by rapid depressurization coupled with the near-ambient temperature of the makeup water produces significant thermal stresses in the thick section steel wall of the RPV. For embrittled RPVs, these stresses could be sufficient to initiate a running crack, which could propagate all the way through the vessel wall. Such through-wall cracking of the RPV could precipitate core damage or, in rare cases, a large early release of radioactive material to the environment. Fortunately, the coincident occurrence of critical-size flaws, embrittled vessel steel and weld material, and a severe PTS transient is a very low-probability event.

1.2 PTS Limits on the Licensable Life of a Commercial Pressurized Water Reactor

In the early 1980s, attention was focused on the possibility that PTS events could challenge the integrity of the RPV wall for two reasons:

- Operational experience suggested that overcooling events, while not common, did in fact occur.
- The results of in-reactor materials surveillance programs suggested that the steels used in RPV construction were prone to loss-of-toughness over time as a result of neutron irradiation-induced embrittlement.

This possibility of accident loading combined with degraded material conditions motivated investigations aimed at assessing the risk of vessel failure posed by PTS for the purpose of establishing the operational limits needed to ensure that the likelihood of RPV failures caused by PTS transients is kept sufficiently low. These efforts led to the publication of a Commission paper [SECY-82-465], which provided the technical basis for subsequent development of what has come to be known as the "PTS Rule," as set forth in Title 10, Section 50.61, of the *Code of Federal Regulations* (10 CFR 50.61), "Fracture Toughness

Requirements for Protection Against Pressurized Thermal Shock Events" [10 CFR 50.61].

Currently, 10 CFR 50.61 requires licensees to monitor the embrittlement of their RPVs using a reactor vessel material surveillance program qualified under Appendix H to 10 CFR Part 50, "Domestic Licensing of Production and Utilization Facilities." The surveillance results are used together with the formulae and tables in 10 CFR 50.61 to estimate the fracture toughness transition temperature (RT_{NDT}†) of the steels in the vessel's beltline and how those transition temperatures increase as a result of irradiation damage throughout the operational life of the vessel. For licensing purposes, 10 CFR 50.61 provides instructions on how to use these estimates of the effect of irradiation damage to estimate the value of RT_{NDT} that will occur at end of license (EOL), a value called RT_{PTS}. 10 CFR 50.61 also provides "screening limits" (maximum values of RT_{NDT} permitted during the plant's operational life) of +270°F (132°C) for axial welds, plates, and forgings, and +300°F (149°C) for circumferential welds. These screening limits correspond to a limit of $5x10^{-6}$ events/year on the annual probability of developing a through-wall crack [RG 1.154]. Should RT_{PTS} exceed these screening limits, 10 CFR 50.61 requires that the licensee to either take actions to keep RT_{PTS} below the screening limit (by implementing "reasonably practicable" flux reductions to reduce the embrittlement rate, or by deembrittling the vessel by annealing [RG 1.162]), or perform plant-specific analyses to demonstrate that operating the plant beyond the 10 CFR 50.61 screening limit does not pose an undue risk to the public [RG 1.154]. While no currently operating PWR has an RT_{PTS} value that exceeds the 10 CFR 50.61 screening limit before EOL, several plants are close to the limit (3 are within 2°F while 10 are within 20°F, see Figure 1.1). Those plants that are close to are likely to exceed the screening limit during the 20-year license renewal period that is currently being sought by many operators. Moreover, some plants maintain their RT_{PTS} values below the 10 CFR 50.61 screening limits by implementing flux reductions (low-leakage cores, ultra-low-leakage cores), which are fuel management strategies that can be economically deleterious in a deregulated marketplace. Thus, the 10 CFR 50.61 screening limits can restrict the licensable and the economic lifetime of PWRs. As detailed in the next section, there is considerable reason to believe that these restrictions are not necessary to ensure public safety and, in fact, place unnecessary burden on licensees.

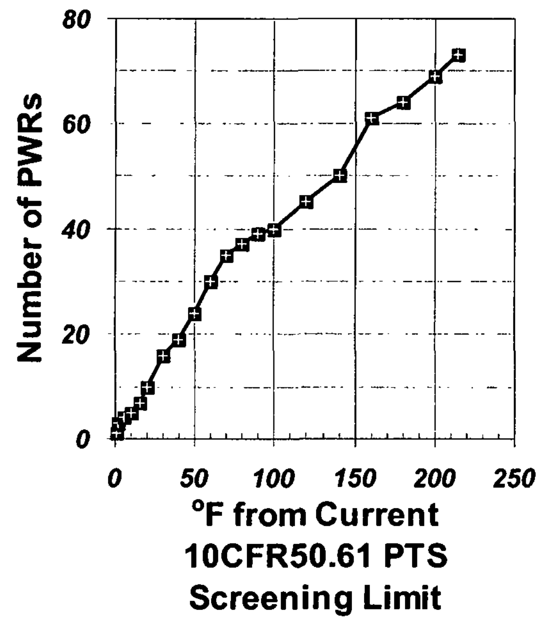

Figure 1.1. Proximity of currently operating PWRs to the 10 CFR 50.61 screening limit for PTS

† The RT_{NDT} index temperature was intended to correlate with the fracture toughness transition temperature of the material. Fracture toughness, and how it is reduced by neutron irradiation embrittlement, are key parameters controlling the RPV's resistance to any loading challenge. For a more detailed description of RT_{NDT} (in specific) and fracture toughness (in general), see [***EricksonKirk PFM***].

1.3 Technical Factors Suggesting Conservatism of the Current PTS Rule

It is now widely recognized that state of knowledge and data limitations in the early 1980s necessitated conservative treatment of several key parameters and models used in the probabilistic calculations that provided the technical basis [SECY-82-465] of the current PTS Rule [10 CFR 50.61]. The most prominent of these conservatisms include the following factors:

- highly simplified treatment of plant transients (very coarse grouping of many operational sequences (on the order of 10^5) into very few groups (≈ 10), necessitated by limitations in the computational resources needed to perform multiple thermal-hydraulic calculations)
- lack of any significant credit for operator action
- characterization of fracture toughness using RT_{NDT}, which has an intentional conservative bias [ASME NB2331]
- use of a flaw distribution that places *all* flaws on the interior surface of the RPV, and, in general, contains larger flaws than those usually detected in service
- a modeling approach that treated the RPV as if it were made entirely from the most brittle of its constituent materials (welds, plates, or forgings)
- a modeling approach that assessed RPV embrittlement using the peak fluence over the entire interior surface of the RPV

These factors indicate the high likelihood that the current 10 CFR 50.61 PTS screening limits are unnecessarily conservative. Consequently, the staff of the U.S. Nuclear Regulatory Commission (NRC) believed that reexamining the technical basis for these screening limits, based on a modern understanding of all the factors that influence PTS, would most likely provide strong justification for substantially relaxing these limits.

1.4 Statement of Objective

For the reasons stated in Section 1.3, the NRC's Office of Nuclear Regulatory Research (RES) undertook this study with the objective of developing the technical basis to support a risk-informed revision of the PTS Rule and the associated PTS screening limit, and thereby providing the basis for potential rulemaking.

1.5 Guide to this Report

As discussed in Chapter 4, this report summarizes a much larger documentary package, and updates a previous report [***Kirk 12-02***]. We begin in Chapter 2 by describing PTS, its potential precursors, and the historical occurrence of PTS in reactor operations. We also summarize the key findings on which the current rule is based, and we detail the provisions of the current rule. Chapter 3 describes this study in detail and discusses its guiding principles, our investigative approach, and our fundamental assumptions. Additionally, we detail the many organizations and individuals that have contributed to this project. Chapter 4 provides a "map" to the documents from which this summary report was drawn and describes the information available in each of those detailed reports. In Chapters 5, 6, and 7, we synopsize the key features of our probabilistic risk assessment (PRA) and human reliability analysis (HRA), our thermal-hydraulic (TH) analysis, and our probabilistic fracture mechanics (PFM) analysis, respectively. Chapters 6 and 7 also address experimental validation of our TH and PFM methodologies. Chapter 8 presents the results of our baseline plant-specific analysis of three PWRs, while Chapter 9 examines the general applicability of these results to the larger population of all commercial PWRs. In Chapter 10, we develop a limit on the risk posed by PTS that is consistent with current regulatory guidance. Chapter 11combines the information from Chapters 8 through 10 to develop a proposed revision to the 10 CFR 50.61 screening limit. Finally, Chapter 12 summarizes our findings and discusses some considerations for rulemaking.

2 Pressurized Thermal Shock Background

In this chapter, we provide background information on PTS. We begin with a general description of the progression of a PTS event, including its precursors and their effect on both the primary pressure circuit and the RPV itself (Section 2.1). We then discuss the historical incidence of PTS (Section 2.2). Finally, we summarize the findings of SECY-82-465, which provide the technical basis for the current PTS Rule (Section 2.3), and we review the rule's provisions (Section 2.4).

2.1 General Description of the Progression of a PTS Event

In the following sections, we describe the event sequence that can give rise to a PTS event (Section 2.1.1), the effect of those events on both the primary and secondary pressure circuits (Section 2.1.2), and the challenge that these transients can pose to the structural integrity of the RPV (Section 2.1.3).

2.1.1 Precursors

Normally, the RPV is very hot because of the high temperature of the water it contains (600°F 315°C)). Several types of malfunctions or accidents can cause the vessel to suddenly fill with cool water or cause the reactor coolant water temperature to decrease rapidly. Such rapid cooling causes the vessel to experience thermal shock. If the RPV is then subjected to high pressure, the phenomenon is referred to as PTS.

Most significant PTS scenarios fall into one of the following two categories:

- breaks in the primary side of the reactor coolant system (RCS) (see Sections 2.1.2.1 and 2.1.2.2)
- breaks in the secondary system (see Section 2.1.2.3).

Here, we use the term "break" to refer to pipe breaks (e.g., hot leg break, cold leg break, main steam line break, steam generator tube rupture), as well as stuck-open valves. Initially, a stuck-open valve transient behaves much like a transient initiated by a pipe break. However, later in stuck-open valve transients the valve can unstick (and, therefore, reclose), so repressurization is possible. Our analysis considers potential failures of the following valves:

- <u>Primary Side/RCS</u>: Power-operated relief valves (PORVs) and safety relief valves (SRVs)
- <u>Secondary Side</u>: Main steam isolation valves (MSIVs), steam generator atmospheric dump valves (ADVs), main steam safety valves (MSSVs), and so on.

Figure 2.1 illustrates the arrangement of the major components of both the primary and secondary systems in a PWR.

2.1.2 Thermal-Hydraulic Response of the Vessel

2.1.2.1 Pipe Breaks in the Primary System

When a break occurs in the primary system, mass is lost from the RCS. The level of water in the pressurizer (PZR) decreases, thereby causing a decrease in RCS pressure. If the RCS pressure or PZR level decreases too far, the reactor protection system (RPS) will generate a reactor trip signal, which in turn will insert the control rods and stop the fission process. Additionally, the engineered safety features actuation system (ESFAS) will generate a safety injection actuation signal (SIAS). The SIAS will start the high-pressure injection (HPI) and low-pressure injection (LPI) pumps, which will start the supply of emergency core cooling (ECC) water to the RCS, as pressure allows.

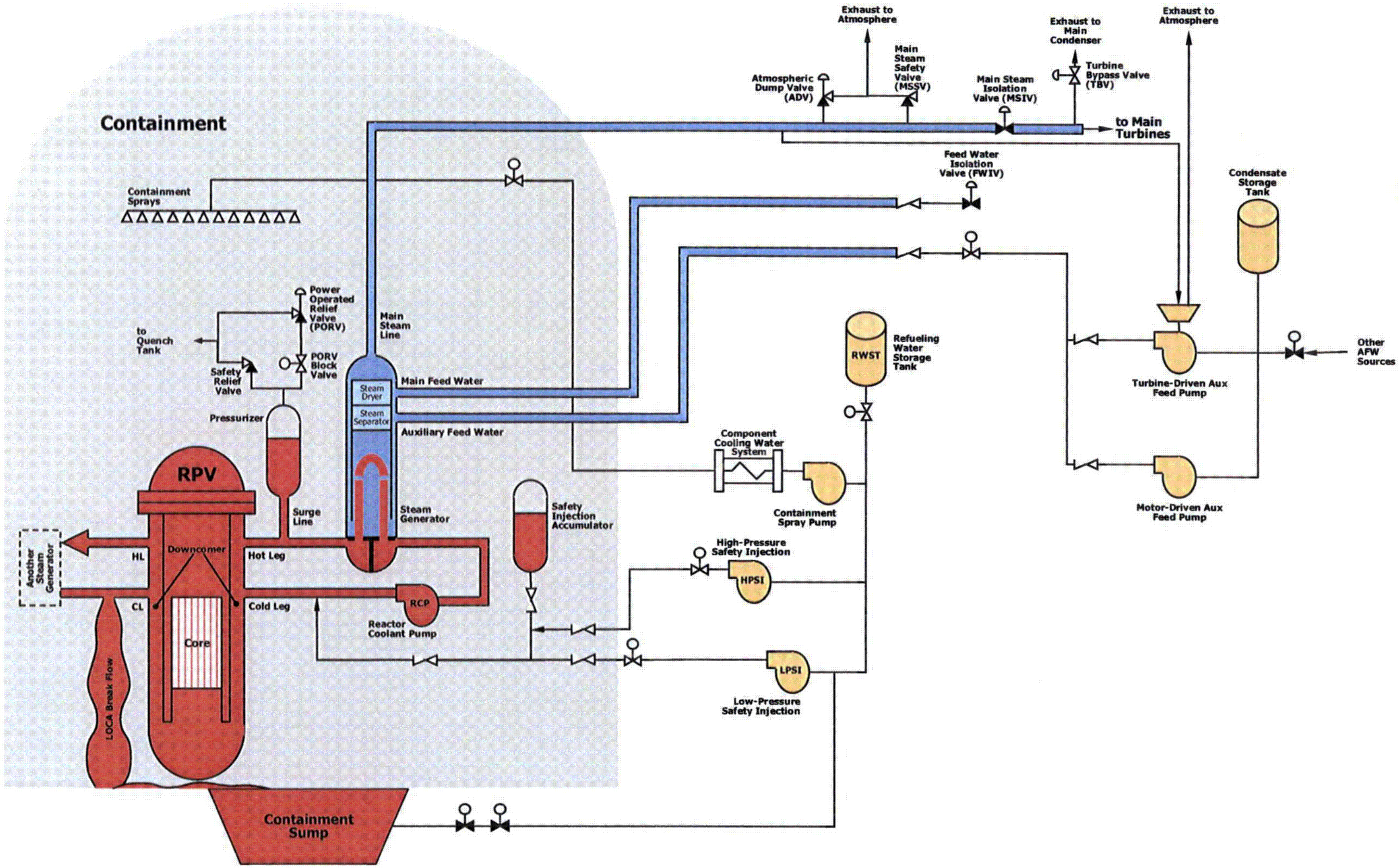

Figure 2.1. Schematic illustration of the main components of the primary (red) and secondary (blue) systems in a pressurized-water reactor

Further progress of the transient depends upon the ability of HPI to make up for the mass lost through the break.

For very small breaks (less than ~1.4-in. (3.5-cm) in diameter), HPI is sufficient to make up the lost mass and, thereby, maintain RCS mass and pressure control. For larger breaks, HPI is insufficient to replace the lost mass, so PZR level and RCS pressure continue to fall. As the pressure continues to fall, the safety injection tanks (SITs) discharge and, eventually, the LPI begins injecting colder water into the RCS. The ECC injection rates are substantially greater for large breaks (compared to small breaks), and result in much greater cooldown of the primary system and subsequently the RPV wall.

The controlling feature of such loss-of-coolant accidents (LOCAs) is the size of the break. The larger the break, the faster the transient proceeds, and the more severe the cooldown. Larger breaks cause a greater pressure decrease, which results in larger ECC flows. This causes the downcomer temperature to drop rapidly. The rate of temperature decrease (which is controlled by the break size) and the minimum temperature achieved (which is controlled by the temperature of the ECC water and whether ECC water is recirculated from the sump) are the dominant TH factors that influence the severity of the transient. Since RCS pressure is low, it not a significant factor.

2.1.2.2 Stuck-Open Primary Safety Relief Valves

During stuck-open valve transients, a primary SRV is assumed to stick open as a result of mechanical binding or other possible causes. This binding of the valve may release later in the transient, resulting in valve reclosure. Phenomenologically, stuck-open valve scenarios are similar to small hot leg break LOCAs, until the valve recloses. The "break" areas of stuck-open valve scenarios are typically in the small-break LOCA range of ≈1.5 to 2+-in. (≈3.8 to 5+-cm).

Following valve reclosure, HPI will gradually fill the RCS. As the RCS fills, the primary system pressure will increase above the saturation pressure of the coolant, thereby reestablishing subcooling in the loops. When operating procedures allow, the HPI can be controlled to avoid overfilling the RCS. If, however, the operator fails to attend to HPI control in a timely manner, the RCS can continue to fill until the primary system is water solid, meaning there is no longer any steam in the system. Since water is nearly incompressible, the RCS pressure rises very rapidly, and the pressure created by HPI will reopen the SRVs. RCS pressure will then remain at the SRV setpoint of 17.25 MPa (2500 psi) for as long as the HPI remains on.

The controlling features of stuck-open valve scenarios are the length of time the valve is open, and the repressurization associated with the primary system becoming water solid. The longer the SRV stays open, the cooler the downcomer temperature becomes. Timely operator control of HPI is an important factor influencing transient severity because it determines the maximum pressure achieved in the primary system. Thus, for these scenarios, both downcomer temperature and RCS pressure are important.

2.1.2.3 Breaks in the Secondary System

Secondary side breaks can include both actual breaks of the steam line and the sticking-open of one or more of the numerous control and safety valves in the steam system. A stuck-open valve is, therefore, also referred to as a "break," consistent with the terminology adopted to describe stuck-open valves in the primary system Break sizes can range from a single valve sticking open to a complete main steam line break (MSLB). Similar to LOCAs, *time* and *break size* are directly related. The larger the break, the faster the transient proceeds, and the more severe the cooldown.

Following break initiation, the response of engineered safety features systems may result in safety injection actuation, actuation of main feedwater isolation valves (MFIVs) and/or MSIVs, as well as automatic control of auxiliary feedwater (i.e., through isolation of a turbine-driven pump). If the break is downstream of the MSIVs, the steam line break will be terminated when the MSIV shuts. For larger MSLBs, MSIV closure is automatic and occurs rapidly after break initiation. For smaller steam line breaks, however, the operators will isolate the affected steam generator by securing flow to the generator and manually isolating the MSIVs. Therefore, downstream breaks are not PTS-significant. However, the main steam SRVs and ADVs are upstream of the MSIVs and, consequently, are not affected by an MSIV closure. For breaks occurring upstream of the MSIVs, steam will continue to blowdown until the affected steam generator is completely depressurized.

Steam generator depressurization causes cooling of the primary system. As steam continues leaking out of the break, the secondary side pressure continues to decrease, and the water in the generator remains saturated. Consequently, as the secondary side pressure decreases, the secondary side temperature also decreases. The primary side and secondary side remain "thermally coupled" during secondary side break scenarios, meaning that the primary system temperature will track the temperature of the affected steam generator. This primary system cooling increases the density of the primary water, so the volume of the water in the RCS shrinks. For sufficiently large secondary breaks, the shrinkage may be sufficient to actuate the emergency core cooling system (ECCS), causing direct injection of water at a temperature between that of external storage tanks (≈40°F (4.4°C)) and that of water recirculated from the sump (~120°F (49°C)). The flow of this colder water increases the cooling rate of the primary, thereby increasing transient severity. However, HPI does not reduce the minimum temperature of the primary below the boiling point of water in the secondary because the large heat transfer area in the affected steam generator (which is now at saturated conditions) is more than sufficient to bring the HPI water temperature up to the boiling point in the secondary system.

If the break is outside of containment, the lowest temperature expected would be 212°F (100°C) (saturation for atmospheric pressure); however, the final temperature could be higher (~250°F (120°C)) if the break is in containment. In this case, the minimum temperature of the primary system depends on the final containment pressure following blowdown of the steam generator.

The controlling features of steam line break scenarios are the size of the break, control of feedwater to the broken steam generator, proper steaming of the unaffected generator, and control of HPI if HPI is actuated. Large steam line breaks resemble large LOCAs in terms of the rate of downcomer cooling. The differences between large steam line breaks and primary system pipe breaks (LOCAs) are as follows:

- The downcomer does not get as cold during secondary side breaks. Temperatures typically range from 212°F to 250°F (100°C to 121°C) for secondary side breaks, depending on whether the break is outside or inside of containment and, if inside, what the containment pressure is. By contrast, temperatures for primary system pipe breaks (LOCAs) can be as low as ≈40°F (4.4°C) for LOCAs because the minimum temperature is controlled by the boiling point of water, rather than ambient outside temperatures.
- Natural circulation flow rates (characteristic of large steam line breaks) are higher than loop stagnation flow rates (characteristic of large LOCAs). This higher flow ensures thorough mixing in the downcomer of the reactor coolant and ECCS flow (provided that coolant flow is initiated). The need to consider thermal plumes or streaming effects can thus be eliminated *a priori* for breaks in the secondary system.

2.1.3 Response of the Vessel to PTS Loading

As detailed in Section 2.1.2, all PTS precursors cause rapid cooling of the primary system. Depending on the transient, this cooling may or may not be accompanied by significant pressure. Both of these factors (rapid cooling and pressure) produce stresses in the vessel wall. The thermal stresses are (approximately) equal both along the axis of the vessel and around its circumference because of its cylindrical geometry. At the beginning of the cooldown, the thermal stresses are tensile on the inner diameter (ID) of the vessel, and are equilibrated by compressive stresses on its outer diameter (OD). As the transient continues, these thermal stresses reduce to zero to the extent that isothermal conditions are achieved in the vessel wall. The pressure stresses are twice as large in the circumferential direction as they are in the axial direction (again as a direct consequence of the cylindrical vessel geometry). Also, pressure stresses are constant through the thickness of the RPV wall.

The degree to which these stresses challenge the integrity of the vessel is controlled by a number of factors, the most important of which are as follows:

- the existence of a crack in the RPV, as well as its location, orientation, and size
- the material's resistance to cracking at the location of the flaw, which is measured by its "fracture toughness." Fracture toughness depends on a number of other factors (each defined at the flaw location), the most important of which are as follows:
    - temperature
    - irradiation damage (fluence)
    - chemical composition
    - fracture toughness before irradiation

Qualitatively, when high stresses occur in the presence of a large crack at a low temperature, and when the material at the location of the crack has low fracture toughness, initiation of the crack becomes more likely. The likelihood that this initiated crack will propagate all the way through the vessel wall (thereby producing a breach in the primary system and leading to a condition we have defined as "failure") again depends on the interplay between the applied stresses (and how they vary through the wall) with the material's ability to stop a running crack (known as "arrest fracture toughness"). The factors that influence fracture toughness (listed above) also influence arrest fracture toughness. While arrest is by no means certain, it is true that as the crack propagates into the vessel wall, arrest becomes progressively more likely for transients where the stresses are primarily thermal. For these "mostly thermal" transients (medium- and large-diameter primary side pipe breaks, for example) arrest becomes more likely as the crack progresses into the vessel wall because temperature tends to increase while irradiation damage tends to decrease. (Both of these changes increase arrest fracture toughness.) Conversely, the progression of a crack initiated by a transient that produces both thermal and pressure stresses is fundamentally different. In this situation, the stresses remain higher through the wall because of the contribution of the pressure stress. Additionally, the fracture driving force tends to increase as the crack travels through the wall, as a result of the effect of primary system pressure on the crack faces. For these reasons, in transients that produce both thermal and pressure stresses, almost all cracks that initiate also propagate all the way through the vessel wall.

2.2 Historical Incidence of PTS

In the technical basis document written to support the current PTS Rule [SECY-82-465], the staff summarized the operational events that had, to that date, presented PTS challenges to operating plants. These events are depicted in Figure 2.2, which illustrates the three key operational parameters influencing event severity. Specifically, those parameters are the final RCS temperature, severity of the thermal shock (*dT/dt*) caused by the event, and existence (or lack thereof) of high pressure. A more recent search of licensee event reports (LERs) submitted between 1980 and 2000 reveals the occurrence of 128 "potentially PTS-significant" events. Approximately half of those LERs report the minimum temperature reached by the RCS, and the data suggest that the most recent transients are nearly all benign, with all but one having minimum RCS temperatures above 500°F (260°C). Thus, while overcooling events have occurred, they have only rarely been severe enough to challenge the structural integrity of the RPV.

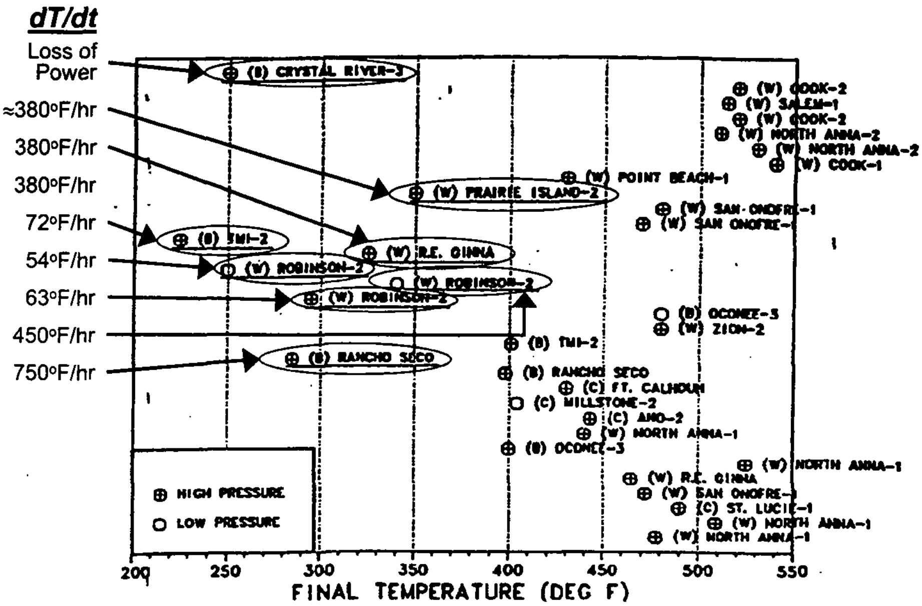

Figure 2.2. Figure 2.13 from SECY-82-465, depicting the final temperatures for 32 PTS precursor events experienced in commercial reactor service prior to 1982 (Cooling rates associated with the most significant transients have been superimposed on this graph.)

2.3 Summary of SECY-82-465 Findings

In the early 1980s, the nuclear industry and the NRC staff performed a number of investigations to assess the risk of vessel failure posed by PTS, and to establish the operational limits needed to ensure that the likelihood of RPV failures caused by PTS transients is maintained at an acceptably low level. These efforts led to the publication of a Commission paper [SECY-82-465] that provided the technical basis for subsequent development of what has come to be known as the "PTS Rule" [10 CFR 50.61]. The Commission paper included a number of probabilistic calculations performed to assess the influence of both contributory and mitigating factors (e.g., plant design, operator actions, operator training, material toughness, flaw population, and so on) on the outcome (vessel failure or non-failure) of a PTS event. The results of these calculations were used to develop a relationship between the probability of a through-wall crack developing in the RPV and the RT_{NDT} index temperature of the RPV. Regulatory Guide 1.154 [RG 1.154] later used this relationship, together with the judgment that an annual through-wall cracking frequency of 5×10^{-6} is acceptable, to establish "screening limits," or maximum values of RT_{NDT} permitted during the operating life of the plant. Specifically, the established limits were +270°F (132°C) for axial welds, plates, and forgings, and +300°F (149°C) for circumferential welds [10 CFR 50.61].

In the mid-1980s, the NRC conducted a number of follow-on studies concerning the risk associated with PTS events [ORNL 85a, 85b, 86]. These studies, featuring plant-specific analyses of H.B. Robinson Steam Electric Plant, Calvert Cliffs Nuclear Power Plant, and Oconee Nuclear Station, demonstrated that plants embrittled to the PTS screening limit of +270°F (132°C) had an annual probability of developing a through-wall crack below 5×10^{-6} events/reactor year. These plant-specific analyses demonstrate the conservatism of the generic analyses reported in SECY-82-465, which served as the basis for the provisions of 10 CFR 50.61.

2.4 Current Provisions of 10 CFR 50.61

As previously stated, 10 CFR 50.61 establishes "screening limits" (or maximum values of RT_{NDT} permitted during the operating life of the plant) of +270°F (132°C) for axial welds, plates, and forgings, and +300°F (149°C) for circumferential welds. Here, we discuss in greater detail the provisions of 10 CFR 50.61, as follows:

- Section 2.4.1: why an index-temperature approach is adopted to characterize transition fracture toughness in ferritic steels
- Section 2.4.2: the approach used to characterize irradiation effects on the index temperature
- Section 2.4.3: the specific provisions of 10 CFR 50.61
- Section 2.4.4: an evaluation of currently operating PWRs, relative to the PTS screening limits In 10 CFR 50.61

2.4.1 Index Temperature Approach to Characterize Transition Fracture Toughness in Ferritic Steels

"Fracture toughness" is a measure of a material's ability to deform without breaking in the presence of preexisting cracks. Physical evidence and numerous experimental observations demonstrate that the temperature dependence of the cleavage initiation fracture toughness of ferritic steels (K_{Ic} or K_{Jc}) does not depend on composition, heat treatment, material forming techniques (weld, plate, or forging), or irradiation conditions [Kirk 01a]. These factors influence only the position of the toughness transition curve on the temperature axis. This has led to widespread use of transition temperature approaches to characterize the cleavage fracture toughness of ferritic materials [WRC 175, Wallin 93a]. Such approaches employ empirical and/or physical evidence to establish the temperature dependence of fracture toughness that is common to all ferritic steels. Figure 2.3 shows the data used to establish the ASME K_{Ic} curve, one of the earliest transition temperature characterizations developed specifically using nuclear grade ferritic steels and weldments [WRC 175]. The formula for the curve in Figure 2.3 is as follows:

Eq. 2-1 $K_{Ic} = 33.2 + 2.806 \cdot \exp[0.02 \cdot (T - RT_{NDT} + 100)]$

where

RT_{NDT} is defined in accordance with ASME NB2331, as follows: $RT_{NDT} = MAX\{T_{NDT}, T_{35/50} - 60\}$.

T_{NDT} is the nil-ductility temperature (NDT) determined by testing specimens in accordance with ASTM E208.

$T_{35/50}$ is the transition temperature at which Charpy-V notch (CVN) specimens tested in accordance with ASTM E23 exhibit lateral expansion of at least 0.035-in. (0.89-mm) and absorbed energy of at least 50 ft-lbs (68J).

In Eq. 2-1, RT_{NDT} serves as an "index temperature" (i.e., a single value that characterizes the combined effects of alloying heat treatment, irradiation, etc. on fracture toughness)‡. Combining an index temperature with the (independently established) temperature dependence of fracture toughness (Eq. 2-1) defines the variation of toughness with temperature throughout the transition regime. The ease with which an index temperature can be experimentally established (relative to the much greater testing burden necessary to establish the complete toughness transition curve) makes transition temperature approaches attractive in applications where extensive material characterization is either economically infeasible or, for practical reasons, impossible.

‡ While RT_{NDT} is an index temperature that has customarily been used along with a fracture toughness transition curve (i.e., the ASME K_{Ic} curve), RT_{NDT} is ***not*** a *fracture toughness* index temperature. As specified by ASME NB-2331 (and as represented in Eq. 2-1), RT_{NDT} is defined based on non-fracture toughness tests that can, at best, be correlated with fracture toughness. [***EricksonKirk PFM***] provides a more detailed description of RT_{NDT}.

The monitoring of neutron irradiation embrittlement falls into both categories because of the expense associated with the testing of irradiated materials and the limited volumes of material that can be irradiated as part of a surveillance program.

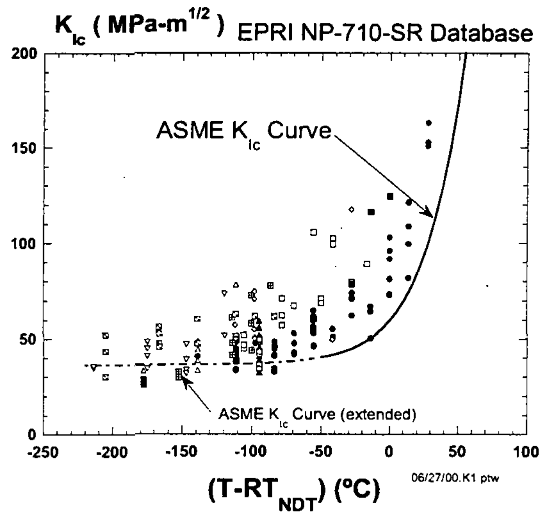

Figure 2.3. The empirical data used to establish the ASME K_{Ic} curve

2.4.2 Irradiation Effects on Index Temperature

As part of their required reactor vessel material surveillance programs qualified under Appendix H to 10 CFR Part 50, licensees attach surveillance capsules to the inner diameter and/or internal structures of the RPV. These capsules, which contain Charpy V-notch (CVN) specimens [ASTM E23], are removed over the lifetime of the RPV [ASTM E185], and the CVN specimens are tested to establish the index temperature T_{30} (the temperature at which the energy consumed in fracturing the CVN specimen is 30 ft-lbs). The difference between T_{30} after some amount of irradiation and T_{30} before irradiation begins is called ΔT_{30}, a metric which has long been used to assess the degree of irradiation damage imparted to the steel. (ΔT_{30} is closely related to the irradiation-induced shift in fracture toughness transition temperature. See [Kirk 01b] and [***EricksonKirk-PFM***].) These ΔT_{30} values from RPV surveillance programs provide the empirical basis to establish embrittlement trend curves that correlate the effect of irradiation exposure and chemical composition on ΔT_{30}. 10 CFR 50.61 adopts the following embrittlement trend curve [Randall 87]:

Eq. 2-2 $$\Delta T_{30} = (CF) f^{(0.28-0.1\log f)}$$

where

- *CF* — is a "chemistry factor" that characterizes the irradiation sensitivity of the steel. *CF* depends on copper content, nickel content, and product form. 10 CFR 50.61 includes tables of CF values.
- *f* — is the fast neutron fluence in neutrons per cm^2 (E>1Mev) divided by 10^{19}. For the purposes of 10 CFR 50.61, *f* is defined as the peak fluence at the clad-to-base metal interface at EOL.

2.4.3 Provisions of the Current Rule

10 CFR 50.61 uses the RT_{NDT} index temperature and the ΔT_{30} index temperature shift to estimate the effect of irradiation on RT_{NDT}, as follows:

Eq. 2-3 $$RT_{NDT(f)} = RT_{NDT(u)} + \Re \cdot \Delta T_{30} + M$$

where

- $RT_{NDT(f)}$ — is the estimated RT_{NDT} of the vessel material after irradiation to the fluence *f*. Toughness is determined from $RT_{NDT(f)}$ through its use as an index temperature for the ASME K_{Ic} and K_{IR} curves.
- $RT_{NDT(u)}$ — is the unirradiated RT_{NDT}. It can be determined based on either ASME NB2331 or other alternative techniques [NRC MEMO 82, NRC MTEB 5.2].
- $\Re$ — is 1 if ΔT_{30} is calculated from chemistry and fluence using Eq. 2-2. If ΔT_{30} is evaluated based on surveillance CVN data, $\Re$ is the ratio of the *CF* value estimated from the chemistry of the surveillance capsule to the *CF* value estimated from the heat average chemistry.

ΔT_{30} is defined by Eq. 2-2.

M is defined by **Eq. 2-4**.

Eq. 2-4 $$M = 2\sqrt{\sigma_I^2 + \sigma_\Delta^2}$$

where

σ_I is the standard deviation in the value of $RT_{NDT(u)}$.

σ_Δ is the standard deviation in the value of ΔT_{30}.

According to 10 CFR 50.61, a nuclear power plant licensee is required to estimate $RT_{NDT(f)}$ at EOL using **Eq. 2-2** for all materials in the vessel beltline. The highest of these values, defined as RT_{PTS}, is compared to the 10 CFR 50.61 PTS screening limit of +300°F (149°C) for circumferential welds and +270°F (132°C) for all other materials. If RT_{PTS} exceeds the screening limit, the licensee is required to either (1) implement flux reduction techniques to keep RT_{PTS} below the screening limit, (2) anneal the vessel according to Regulatory Guide 1.162 [RG 1.162], or (3) submit a safety analysis to the NRC demonstrating that the plant is safe to operate beyond the screening limit.

2.4.4 Evaluation of Operating Plants Relative to the Current PTS Screening Limits

Figure 1.1 compares RT_{NDT} values for all currently operating PWRs evaluated at the end of their originally licensed life (40 years) using Eq. 2-3 with the current 10 CFR 50.61 PTS screening limits. A number of points should be noted:

- No plants currently exceed the screening limit. However, since the operators of the Yankee Rowe Nuclear Power Plant failed to persuade the staff to permit operation in excess of the screening limit using the probabilistic procedures outlined in Regulatory Guide 1.154 [RG 1.154], all plants that have predicted that they would exceed the screening limit before EOL have elected to remain in statutory compliance by (1) implementing flux reduction, (2) pursuing new technological approaches coupled with exemption requests, or (3) using a combination of the two approaches.
- Currently, 10 plants project an RT_{NDT} at EOL ($\equiv RT_{PTS}$) within 20°F of the screening limit.
- While the most embrittled region in one-third of the operating PWRs is the circumferential weld, less than half of those plants (11 of 23) have their operation limited by the circumferential weld because of the higher PTS screening limit currently used to assess these plants (+300°F (149°C) *vs.* the +270°F (132°C) value used for axial welds, plates, and forgings).

3 PTS Reevaluation Project

This chapter describes the PTS Reevaluation Project, which the NRC's Office of Nuclear Regulatory Research (RES) initiated in 1999. The chapter is structured as follows:

- Model Structure: Section 3.1 provides an overview of the model used to evaluate the technical basis for a revised PTS screening limit.
- Uncertainty Treatment: Since the objective of this study is to develop the technical basis for a risk-informed revision of 10 CFR 50.61, a systematic treatment of uncertainties is a central feature of this project. Section 3.2 describes our framework for uncertainty treatment and propagation and provides an overview of how uncertainties were addressed in the PRA, TH, and PFM.
- Assumptions: Section 3.3 summarizes the fundamental assumptions made in developing our model.
- Contributors: Section 3.4 describes the organizations and individuals that have made key contributions over the course of this project.
- Peer Review: Given the complex interdisciplinary nature of this project, and at the request of the NRC's Advisory Committee on Reactor Safeguards (ACRS), the staff convened a panel of external experts to review the study's methodologies, findings, and recommendations. Section 3.5 describes the conduct of this review group and the staff's approach to addressing their comments.

3.1 Model Used to Evaluate a Revised PTS Screening Limit

3.1.1 Restrictions on the Model

The desired outcome of this study is to establish the technical basis for a new PTS screening limit. To enable all commercial PWR licensees to assess the state of their RPVs relative to such a new criterion without the need to make new material property measurements, the fracture toughness properties of the RPV steels need to be estimated using only information that is currently available (i.e., RT_{NDT} values, upper-shelf energy values, and chemical composition of beltline materials). All of this information is summarized in the NRC's Reactor Vessel Integrity Database [RVID2].

3.1.2 Overall Structure of the Model

Our overall model involves three major components, which are illustrated (along with their interactions) in Figure 3-1:

Component 1. *Probabilistic Evaluation of Through-Wall Cracking Frequency*: Estimate frequency of through-wall cracking as a result of a PTS event given the operating, design, and material conditions in a particular plant.

Component 2. *Acceptance Criterion for Through-Wall Cracking Frequency*: Establish a value of reactor vessel failure frequency (RVFF) consistent with current guidance on risk-informed decision-making.

Component 3. *Screening Limit Development*: Compare the results of the two preceding steps to determine if some simple, materials-based PTS screening limit can be established. Conceptually, plants falling below the screening limit would be deemed adequately resistant to a PTS challenge and would not require further analysis. Conversely, more detailed, plant-specific analysis would be needed to assess the safety of plant operation beyond the screening limit.

Each of these components is described in the following subsections.

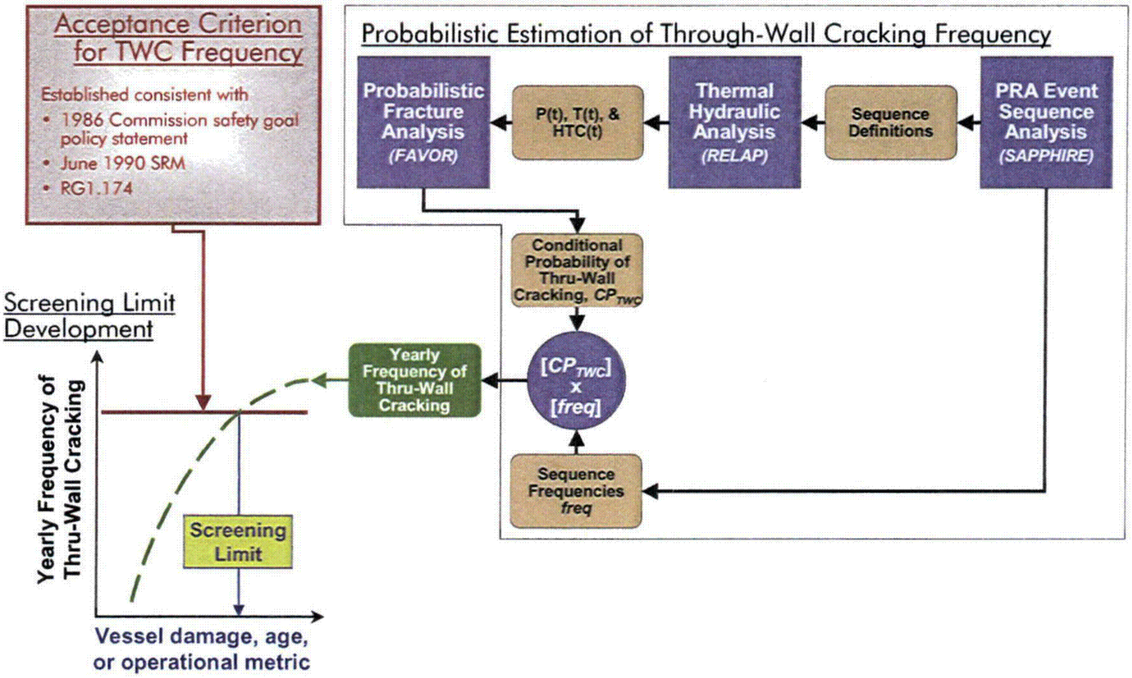

Figure 3-1. High-level schematic showing how a probabilistic estimate of through-wall cracking frequency (TWCF) is combined with a TWCF acceptance criterion to arrive at a proposed revision of the PTS screening limit.

3.1.2.1 Component 1: Probabilistic Estimation of Through-Wall Cracking Frequency

As illustrated in Figure 3-1, three main models (shown as solid blue squares), taken together, allow us to estimate the annual frequency of through-wall cracking in an RPV:

- PRA event sequence analysis
- TH analysis
- PFM analysis

In the following subsections, we first describe these three models and their sequential execution to give the reader an appreciation of their interrelationships and interfaces (Section 3.1.2.1.1). Secondly, we describe the iterative process we undertook, which involved repeated execution of all three models in sequence, to arrive at final models for each plant (Section 3.1.2.1.2). We then discuss the three specific plants we analyzed in detail (Section 3.1.2.1.3). Finally, we conclude with a discussion of the steps taken to ensure that our conclusions based on these three analyses apply to domestic PWRs *in general* (Section 3.1.2.1.4).

3.1.2.1.1 Sequential Description of How PRA, TH, and PFM Models are Used To Estimate TWCF

First, a PRA event sequence analysis is performed to define the sequences of events that are likely to cause a PTS challenge to RPV integrity, and estimate the frequency with which such sequences can be expected to occur. The event sequence definitions are then passed to a TH model, which estimates the temporal variation of temperature, pressure, and heat-transfer coefficient in the RPV downcomer characteristic of each sequence definition. These temperature, pressure, and heat transfer coefficient histories are then passed to a PFM model that uses the TH output, along with other information concerning plant design and construction materials, to estimate the time-dependent "driving force to fracture" produced by a particular event sequence. The PFM model then compares this estimate of fracture driving force to the fracture toughness, or fracture resistance, of the RPV steel. This comparison allows us to estimate the probability that a crack would be created and would penetrate all the way through the RPV wall if that particular sequence of events actually occurred. The final step in the analysis involves a simple matrix multiplication of the probability of through-wall cracking (from the PFM analysis) with the frequency at which a particular event sequence is expected to occur (as defined by the event-tree analysis). This product establishes an estimate of the annual frequency of through-wall cracking that can be expected for a particular plant after a particular period of operation when subjected to a particular sequence of events. The annual frequency of through-wall cracking is then summed for all event sequences to estimate the total annual frequency of through-wall cracking for the vessel. Performance of such analyses for various operating lifetimes provides an estimate of how the annual through-wall cracking frequency can be expected to vary over the lifetime of the plant.

3.1.2.1.2 Iterative Process Used To Establish Plant-Specific Models

The set of transients used to represent a particular plant are identified using a PRA event-tree approach, in which many thousands of different overcooling sequences are "binned" together into groups of transients believed to produce similar thermal-hydraulic outcomes. Judgments regarding which transients to put into which bin were guided by such characteristics as similarity of break size, operator action, etc., and resulted in "bins" such as medium-break primary system LOCAs, MSLBs, etc. From each of the tens or hundreds of individual event sequences in each bin, a single sequence was then selected and programmed into the Reactor Leak and Power (RELAP) TH excursion code to define the variation of pressure, temperature, and heat transfer coefficient *vs.* time. These TH transient definitions were then passed to the Fracture Analysis of Vessels, Oak Ridge (FAVOR) PFM code, which estimated the conditional probability of through-wall cracking (CPTWC) for each transient. When multiplied by the bin frequency estimates from the PRA, these CPTWCs become TWCF values, which (when rank-ordered) estimate the degree to which each bin contributes to the total TWCF of the vessel. At this stage, many bins were found to contribute very little or nothing at all to the total TWCF, and so received little further scrutiny. However, some bins invariably dominated the TWCF estimate. These bins were further subdivided by partitioning the bin frequency, and selecting a TH transient to represent each part of the original bin. This refined model was then reanalyzed using FAVOR, and the bins that provide significant contributions to TWCF are again examined. This process of bin partitioning, and selection of a TH transient to represent each newly partitioned bin, continued until the total estimated TWCF for the plant no longer changes significantly.

3.1.2.1.3 Plant-Specific Analyses Performed

In this study, we performed detailed calculations for three operating PWRs (Oconee 1, Beaver Valley 1, and Palisades), as shown in Figure 3-2. Together, these three plants sample a wide range of design and construction methods, and they contain some of the most embrittled RPVs in the operating fleet.

3.1.2.1.4 Generalization to All Domestic PWRs

Since the objective of this study is to develop the technical basis for revision of the 10 CFR 50.61 PTS screening limit that applies *in general* to all PWRs, we must understand the extent to which the three plant-specific analyses adequately address (in either a representative or a bounding sense) the range of conditions experienced by domestic PWRs *in general*.

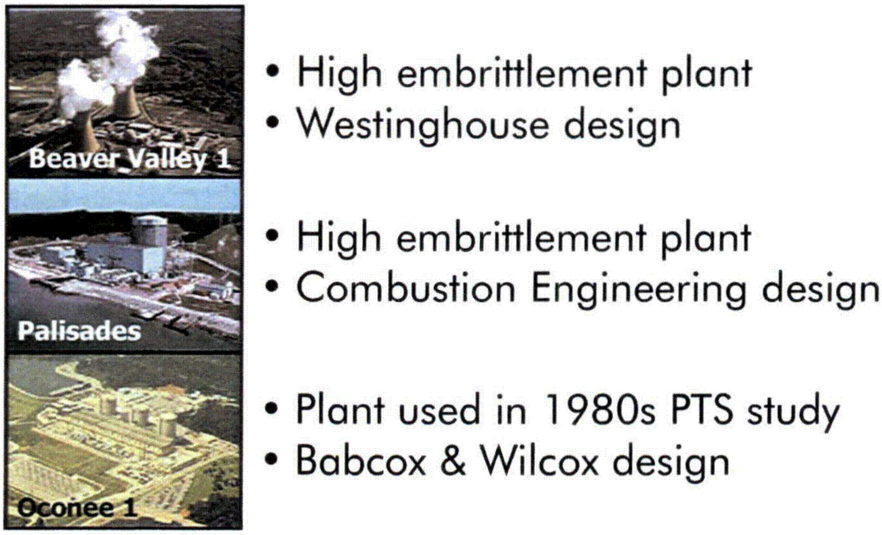

Figure 3-2. The three plants analyzed in detail in the PTS reevaluation effort.

To achieve this goal, we have took the following measures:

- We performed sensitivity studies on both the TH and PFM models to address the effect of credible changes to the models and/or their input parameters. The results of these studies provide insights regarding the robustness of our conclusions (based on three plants), when applied to the PWR population in general.
- We examined plant design and operational characteristics of five additional plants. In so doing, our aim was to determine whether the design and operational features identified as being important in our three plant-specific analyses vary significantly enough in the population of PWRs to question the generality of our results.
- In our three plant-specific analyses, we assumed that the only possible origins of PTS events are caused by events *internal* to the plant. However, the PRA categorized *external* events (such as fires, floods, and earthquakes), which can also be PTS precursors. We, therefore, examined the potential for external initiating events to create significant additional risk relative to the internal initiating events we already modeled in detail.

3.1.2.2 Component 2: Acceptance Criterion for Through-Wall Cracking Frequency

Since the issuance of SECY-82-465 and the original PTS Rule, the NRC has established a considerable amount of guidance on the use of risk metrics and risk information in regulation [e.g., NRC FR 86, and RG 1.174]. To ensure consistency with this guidance, the PTS Reevaluation Project staff identified and assessed options for a risk-informed criterion for RVFF (which Regulatory Guide 1.154 currently specifies in terms of TWCF).

As described in a May 2002 status report on risk metrics and criteria for PTS [SECY-02-0092], the options developed involved both qualitative concerns (the definition of RPV failure) and quantitative concerns (a numerical criterion for the reactor vessel failure frequency). These options reflected uncertainties in the margin between PTS-induced RPV failure, core damage, and large early release. The options also incorporated input received from the ACRS [NRC LTR 02], regarding concerns related to the potential for large-scale oxidation of reactor fuel in an air environment.

Our assessment of the options involved identifying technical issues unique to PTS accident scenario development, developing an accident progression event tree to structure consideration of the issues, performing a scoping study of containment performance during PTS accidents, and reviewing the options in light of this information. The scoping study involved collecting and evaluating available information, performing a few limited-scope thermal-hydraulic and structural calculations, and conducting a semi-quantitative analysis of the likelihood of various accident progression scenarios.

3.1.2.3 Component 3: Screening Limit Development

As illustrated schematically in the lower left corner of Figure 3-1, a screening limit for PTS can be established based on a simple comparison of *TWCF* estimates as a function of an appropriate measure of RPV embrittlement with the *TWCF* acceptance criterion (see Chapter 10). Beyond the work to establish both the *TWCF vs.* embrittlement curve and the limit value for *TWCF*, it is also necessary to establish a suitable vessel damage metric that, ideally, allows different conditions in different materials at different plants to be normalized. From a practical standpoint, "suitable" implies that the metric needs to be based on readily available information regarding plant operation and materials.

3.2 Uncertainty Treatment

At the outset of this project (1999), a staff member reviewed the NRC's existing approach for PRA modeling, focusing on how uncertainties should be treated, how they were propagated through the PRA, TH, and PFM models, and how that approach compared with the NRC's guidelines on work supporting risk-informed regulation [***Siu 99***]. This review established the general framework for model development and uncertainty treatment adopted in this study. In the following two sections, we first review this recommended framework (Section 3.2.1), and then discuss its actual implementation (Section 3.2.2). Section 3.2.2 provides an overview of the uncertainty treatment implemented in the PRA, TH, and PFM analyses and discusses how uncertainties are "passed" between these three main technical modules. Details of these implementations appear elsewhere in this report (Sections 5.2.6–5.2.7, 6.8.2, and 7.4, respectively) and in other documents [***Whitehead-PRA***, ***Chang***, and ***EricksonKirk-PFM***, respectively].

3.2.1 Recommended Framework

In this study, we performed probabilistic calculations to establish the technical basis for a revised PTS Rule within an integrated systems analysis framework [Woods 01]. Our approach considers a broad range of factors that influence the likelihood of vessel failure during a PTS event, while accounting for uncertainties in these factors across a breadth of technical disciplines [***Siu 99***]. Two central features of this approach are a focus on the use of realistic input values and models (wherever possible), and *explicit* treatment of uncertainties (using currently available uncertainty analysis tools and techniques). Thus, our current approach improves upon that employed in developing SECY-82-465, in which many aspects of the analysis included intentional and unquantified conservatisms, and uncertainties were treated *implicitly* by incorporating them into the models (RT_{NDT}, for example).

Our probabilistic models distinguish between aleatory and epistemic uncertainties. Aleatory uncertainties arise as a result of the randomness inherent in a physical or human process, whereas epistemic uncertainties are caused by limitations in our current state of knowledge (or understanding) of a given process. A practical way to distinguish between aleatory and epistemic uncertainties is that the latter can, in principle, be reduced by an increased state of knowledge. Conversely, because aleatory uncertainties arise as a result of randomness at a level below which a particular process is modeled, they are fundamentally irreducible. The distinction between aleatory and epistemic uncertainties is an important part of PTS analysis because different mathematical and/or modeling procedures are used to represent these different types of uncertainty.

3.2.2 Implementation

In this section, we describe our implementation of the uncertainty framework synopsized in Section 3.2.1, focusing specifically on the following aspects:

- How the framework was implemented in of the PRA, TH, and PFM analyses. Consistent with the framework, we systematically identify uncertainties and characterize their nature (as aleatory or epistemic). These uncertainties are then either quantified or addressed as part of the overall structure of the mathematical model.
- How uncertainties are "propagated" through the major components of the computational model used to estimate the TWCF illustrated in the upper right corner of Figure 3-1. This includes propagating uncertainties from PRA to TH, PRA to PFM, and TH to PFM.
- How the uncertainties considered in all three models (i.e., PRA, TH, and PFM) become manifest in the uncertainties in the estimated value of TWCF.

The first two points are described in Sections 3.2.2.1 through 3.2.2.3, for PRA, TH, and PFM, respectively. The final point is addressed in Section 3.2.2.4. Finally, Section 3.2.2.5 addresses the uncertainties associated with the potential "incompleteness" of our mathematical model relative to the physical reality we are trying to represent.

3.2.2.1 PRA

As illustrated in Figure 3-1, the PRA analysis has two major outputs:

- Bin Definition: the representation (or model) of the total PTS challenge using a finite number of event "bins," each of which represents an assortment of TH scenarios (that are believed to be similar)
- Bin Frequency: an estimate (central tendency and distribution) of the frequency with which the events represented by each bin are expected to occur

Each of these outputs has an associated uncertainty, as described in the following sections.

3.2.2.1.1 Bin Definition

Each bin represents an assortment of TH scenarios (i.e., PTS sequences) for the following reasons:

- Like most PRAs, ours includes the usual idealization that both equipment failures and operator actions are binary (i.e., a valve either sticks open or it does not, an operator either acts or fails to act)[§]. Clearly, reality is continuous; valves may stick open by various amounts and operators may act, but after some delay. This idealization leads to the situation where our mathematical representation (a single bin) represents a spectrum of potential outcomes, with each outcome having a distinct TH characteristic.
- Another common PRA feature that we adopt is to group "similar" transients together in a single bin. For example, all primary system pipe breaks having a break diameter of 8-in. (20-cm) and above are placed in a single bin called "large-break LOCAs." This approach is motivated by previous experience indicating that transients grouped in this manner have "similar" severity. Nonetheless, such "similarity" is an approximation. To continue with the large-break LOCA example, hot leg and cold leg breaks have different severities for the same break diameter, break diameter changes above 8-in. (20-cm) cause slightly different severities, and so on. All of these unmodeled effects occur for well-recognized physical reasons. Again, this idealization leads to the situation where our model (a single bin) represents a spectrum of potential outcomes, with each outcome having a distinct TH characteristic.

[§] As detailed in Section 5.2.6.1, this statement is not always true. When judged to be important, certain equipment failures and operator actions were further subdivided (e.g., 30% stuck-open valves, operator actions at 1 *vs.* 10 minutes, etc.). Nonetheless, the PRA model is still a discrete representation of a continuum, and each PRA bin still represents a spectrum of TH responses.

Thus, the structure of the PRA representation of the PTS challenge contains within it an uncertainty that is random and (hence) aleatory, having to do with all the ways that a PTS challenge could occur (i.e., PTS sequences). Discretizing the continuum of potential PTS sequences (which number in the tens or hundreds of thousands) into a tractable number of bins for detailed analysis (~hundreds) means that each bin contains many sequences, each of which can (in principle) produce a different TH response and, thereby, a different effect on the vessel.

As is often the case in PRA, only a portion of the entire aleatory uncertainty significantly affects the overall results of the analysis. The important part of the aleatory uncertainty is determined by the way the PRA model was developed and how the bins were defined. As described in Section 3.1.2.1.2, an initial PRA model is developed and individual TH sequences are selected to represent each bin. These TH definitions are then passed to the FAVOR PFM code, which estimates the CPTWC for each transient. When multiplied by the frequency estimates for each bin, these CPTWC values become TWCF values, which (when rank-ordered) estimate the degree to which each bin contributes to the total TWCF of the vessel. At this stage, many bins are found to contribute very little or nothing at all to the total TWCF. However, some bins invariably dominate the TWCF estimate. These bins are then further subdivided by partitioning the frequency of the bin, and selecting a TH transient to represent each part of the original bin. This refined model is then reanalyzed using FAVOR, and the bins that provide significant contributions to TWCF are again examined. This process of bin partitioning, and selection of a TH transient to represent each newly partitioned bin, continues until the total estimated TWCF for the plant no longer changes significantly. At this point, that portion of all possible PTS sequences (and, hence, the aleatory uncertainty) that significantly affects the overall results is determined and remains in the final model as representing the aleatory uncertainty associated with how a PTS challenge might occur.

3.2.2.1.2 Bin Frequency

For each bin, there is uncertainty regarding the true frequency of occurrence. The uncertainty in the frequency with which the events represented by each bin occurs depends upon the following three factors, each of which is also uncertain:

- uncertainty in the initiating event and its associated frequency
- uncertainty in the series of equipment successes and/or failures that may follow the initiating event, and the uncertainty in their associated probabilities
- uncertainty in the operator actions that may or may not be taken following the initiating event, and the uncertainty in their associated probabilities

Thus, the frequency of occurrence of each bin is a function of the frequencies and probabilities of these factors. (The bin frequency is estimated from the individual frequencies and probabilities using Latin Hypercube sampling techniques to develop the bin frequency histogram that is provided as input to the FAVOR post-processor (FAVPOST).) Each of these factors has an associated epistemic uncertainty, which is described by a distribution. These uncertainties are epistemic in nature because our belief as to the estimates of these frequencies and probabilities is influenced by our limited state of knowledge about these rare events; and better knowledge would clearly lead to reduced uncertainty.

3.2.2.2 TH

The approach used to address uncertainty in the TH analysis principally utilized sensitivity studies to quantify the effects of phenomenological and boundary condition uncertainties/variations on the severity of a TH sequence. The results of these studies were used in two ways:

(1) They were combined with probability estimates of the sensitivity parameters being evaluated to adjust the bin frequencies from the PRA analysis.

(2) They were used to justify further subdivision of the PRA bins. (See the discussion in Section 3.2.2.1.1.)

In this way, the TH uncertainty analysis accounts for certain parameters that can affect the thermal-hydraulic response of the plant, which were not explicitly considered in the PRA analysis (e.g., season of the year). Because the uncertainty analysis also produced insights regarding the effects of various system parameters and TH models on event severity, it also helped to identify the transient used to represent each PRA bin to the PFM analysis.

This method of accounting for TH uncertainty does not quantify the uncertainties associated with each TH sequence. Rather, it characterizes the uncertainties associated with each PRA bin. This is appropriate because, as illustrated in Figure 3.3, each TH sequence that is passed to the PFM analysis represents a much larger number of TH sequences that, together, constitute a PRA "bin." Provided the combined effects of the TH parameter and modeling uncertainties on the severity of this one representative sequence is small relative to both

- the uncertainty in the frequency of occurrence of all of sequences in the bin, and
- the variability in severity between the different sequences in the bin

then, the uncertainty associated with TH parameter and modeling uncertainties of the representative sequence can be considered negligible. The appropriateness of not accounting for these uncertainties because they are negligibly small is ensured by the iterative process used to define the PRA bins.

As described in Section 3.2.2.1.1, PRA bins that contribute significantly to the estimated TWCF were continually partitioned (including appropriate partitioning of the bin frequencies and selection of new TH sequences to represent each partitioned bin) until the total estimated TWCF for the plant did not change significantly with continued partitioning. Thus, any errors caused by not explicitly accounting for the TH parameter and modeling uncertainties associated with the TH sequence used to represent each PRA bin are not expected to influence the outcome of the analysis (i.e., the estimated values of TWCF).

3.2.2.3 PFM

Development of the PFM model featured a comprehensive review of all model components (both sub-models and parameters) with the aim of identifying, classifying, and quantifying the uncertainties in each [***EricksonKirk-PFM***]. In the great majority of cases, the best-estimate models (and associated uncertainties) were quantified, and these were propagated through the calculation. In some cases, inadequate empirical and/or physical evidence existed to support creation of a best-estimate with uncertainties. In these cases, conservative models and parameters were adopted [***EricksonKirk-SS***]). The judgment to include these conservatisms as part of the overall model is itself a treatment of uncertainty, not through quantification, but rather by influencing the structure of the overall PFM model.

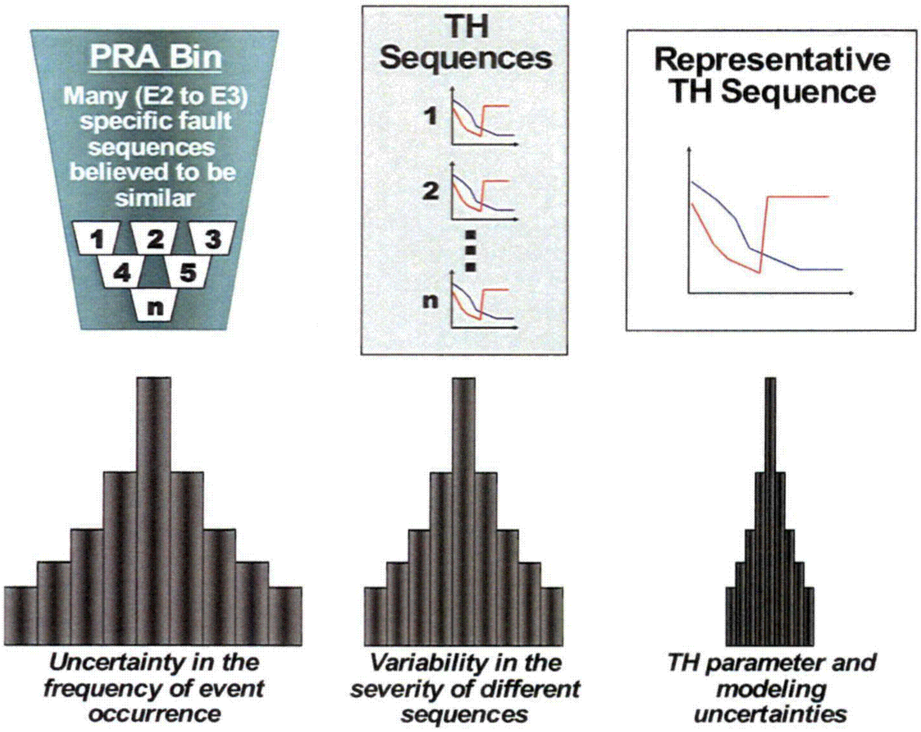

Figure 3.3. Characterization of TH uncertainties

The great majority of the parameters in the PFM model (e.g., RT_{NDT}, Cu, Ni, fluence, flaw parameters) were determined to have epistemic uncertainties. Statistical distributions were developed to characterize these uncertainties from representative data. In some cases, physical models guided these characterizations.

Conversely, the various fracture toughness parameters in the PFM model were all determined to have alleatory (irreducible) uncertainties. These alleatory uncertainties are a direct and natural consequence of the heterogeneity of the material at the same size scale as the crack-tip deformation fields. They also arise because the interaction of two factors (material resistance *vs*. applied loading) produces the measured parameter called fracture toughness (again, see [***EricksonKirk-PFM***] for full details).

The output of the PFM model is distributions quantifying the CPTWC for each transient analyzed. (This value is termed "conditional" because occurrence of the transient is assumed in the PFM calculation.) These distributions account for the uncertainties in the various toughness parameters, non-toughness parameters, and sub-models that together make up the PFM model.

3.2.2.4 What the Uncertainties in TWCF Represent

Sections 3.2.2.1, 3.2.2.2, and 3.2.2.3 described the uncertainties in the PRA, TH, and PFM models, respectively. Table 3.1 summarizes that discussion, and indicates that in each of these three areas, the important uncertainties have been either "accounted for" (in that they influenced the structure of the computational model) or "numerically quantified" (as part of the model). Thus, a description of what the uncertainties in the reported values of TWCF represent requires more than a strictly numerical answer. As described in a NUREG-series report on the theory and implementation of the FAVOR code [***Williams***], FAVPOST estimates the numerical value of TWCF by performing a matrix multiplication of the distribution of the frequency of each bin defined in the PRA analysis with the distribution of CPTWC estimated by the PFM analysis. However, these uncertainties and their quantifiable distributions arise as a direct consequence of the particular model we have used to calculate them and, as indicated in Table 3.1, the structure of the model itself accounts for a number of uncertainties that have not been numerically quantified. Thus, the uncertainties in our reported TWCF values represent all of the uncertainties discussed in this section and in the detailed companion reports [***Whitehead-PRA***, ***Chang***, and ***EricksonKirk-PFM***].

Table 3.1. Summary of uncertainty treatment in the three major technical areas

Technical Area	Uncertainty Type	Uncertainties that were accounted for in the structure of the model	Uncertainties that were numerically quantified
PRA	Aleatory	Discretization of all of the ways a PTS challenge could occur into a finite number of "bins"	---
	Epistemic	---	Bin frequency
TH	Aleatory	Boundary condition uncertainties	The effects of certain boundary condition uncertainties are reflected in the frequencies assigned to certain PRA bins.
	Epistemic	Model uncertainties	---
PFM	Aleatory	---	Uncertainties in fracture toughness values (e.g., K_{Ic}, K_{Ia}, J_{Ic})
	Epistemic	Adoption of conservative models (e.g., RT_{NDT}, flaw distribution, fluence attenuation)	Uncertainties in non-toughness values (e.g., Cu, Ni)

3.2.2.5 Incompleteness Uncertainty

As with any attempt to represent a complex physical system using a mathematical model, the question of "incompleteness uncertainty" arises. That is, "What has been left out of the model and, as a result, how confident should a decision-maker be in using the results of the analysis?". It is fundamentally impossible to quantitatively address uncertainties arising from unknown factors. However, our process for model building, verification and validation (V&V) of our computational models, conservatisms known to remain in the models, the various reviews to which our work has been subjected, and the potential implementation of our results in future rules all provide qualitative assurance that any incompleteness in the model should have a negligible effects on the results. We discuss each of these factors below:

- Process for Model Building: The PRA, TH, and PFM models were developed and continually improved throughout this study. Licensees from the three study plants provided input and review of both the PRA and TH models. The commercial nuclear power industry, working under the auspices of the Electric Power Research Institute (EPRI) Materials Reliability Project, was involved in reviewing all three models from the inception of the study. Additionally, subject-matter experts from the industry played a key role in both developing and reviewing the PFM model. To address uncertainties in a manner consistent with the framework proposed by Siu and synopsized in Section 3.2.1, various new models of both flaws and fracture toughness behavior were created for the PFM model. These new models have been presented for review and comment in various public and international venues, and have been published in both peer-reviewed journals and conference proceedings [Kirk 01a, Kirk 02a, Natishan 01, EricksonKirk 04].
- Computational V&V: Calculations made in PRA, TH, and PFM are performed using computer codes referred to as SAPHIRE, RELAP, and FAVOR, respectively. SAPHIRE and RELAP are commercially available programs and have been subjected to extensive review and V&V. The FAVOR PFM code was developed by RES for the express purpose of performing probabilistic

simulations of PTS. Accordingly, we have performed and reported V&V of FAVOR according to the software quality assurance (SQA) guidance in NUREG/BR-0167 [***Malik***].

- Known Conservatisms: While we devoted considerable effort throughout this study to perform "best estimate" analyses, it is nonetheless true that a number of conservatisms remain. Primary among these is the decision to treat through-wall cracking of the RPV as *equivalent to* occurrence of a large early release of radioactivity to the atmosphere. Chapter 10 discusses the reason for, and conservatism implicit in, this assumption. Furthermore, throughout the development of all the PRA, TH, and PFM models, there has been a tendency to address uncertainties by adopting conservative models or input values when the weight of physical and empirical evidence was inadequate to construct a "best-estimate" model. These types of conservatisms are discussed throughout Chapters 5–7 and in the supporting detailed reports [***Whitehead-PRA, Bessette, EricksonKirk-PFM***], and are summarized in Section 11.4.4.
- Reviews: As described under *Process for Model Building* above, our models were subjected to both internal and external review during their development. Additionally, we solicited and received reviews of the entire project from three sources. In December 2002, we published an interim report summarizing the results of computations performed up to that time [***Kirk 12-02***]. This report was reviewed by both the commercial nuclear power industry and staff from the NRC's Office of Nuclear Reactor Regulation (NRR), with both groups providing written comments [NEI Comments, NRR Comments]. These reviews indicated the need for numerous minor revisions, remodeling of some Oconee transients, and (most significantly) a fundamental restructuring and expansion of the documentation to improve both clarity and completeness. Addressing these comments resulted in this document (and the supporting documents, see Section 4.1), which have been subjected to review by an international group of experts. The comments provided by this panel (see Section 3.5 and Appendix B) have, again, resulted in improvements in both our documentation and our mathematical models. It is important to recognize that the combined effect of all of these changes (i.e., changes made in response to NEI, NRR, and external review panel comments) to the TWCF results [***Kirk 12-02***] has been to reduce the total TWCF by, on average, approximately one-third. Thus, while the comments received from the review panels have improved both the clarity of our documentation and the overall completeness and correctness of our models, the changes have not substantially altered either the overall structure of the models or the TWCF results that could be used to establish a new numerical value for the PTS screening criterion.
- Potential Implementation: Should NRR elect to use the information presented in this and supporting documents as the basis for rulemaking to revise the requirements of 10 CFR 50.61, it must be remembered that it is only a *screening limit* that is being revised. Exceeding a screening limit does not suggest that failure is imminent (or even likely). It merely signals the need for the licensee to take additional actions (either analytical or mitigative) to assure NRR that plant operation beyond the screening limit does not unduly increase the risk to the public. Additionally, the current structure of 10 CFR 50.61 requires that these actions be taken three years before the limits are actually exceeded. It also requires continued surveillance (according to the requirements of Appendix H to 10 CFR Part 50) to ensure the continued validity of assumptions made during development of the screening limit regarding irradiation embrittlement mechanisms. Maintenance of this rule structure mitigates the practical impact on the overall public risk posed by PTS, as a result of any incompleteness uncertainties associated with the recommended numerical value of the screening limit.

3.3 Fundamental Assumptions and Idealizations

Any mathematical model of a physical system inherently involves some level of assumption and/or idealization to make estimates of the parameters of interest tractable within the practical constraints associated with the particular problem of interest. As discussed in greater detail in Chapters 5, 6, and 7, the PRA, TH, and PFM models each involve a large number of sub-models and, thus, a large number of possible assumptions and/or idealizations. Assumptions and idealizations that occur within each of the PRA, TH, and PFM sub-models are, therefore, addressed in Chapters 5, 6, and 7, respectively, or within their supporting reports. In the following subsections, we discuss the fundamental assumptions and idealizations that pertain to the PRA, TH, and PFM sub-models *as a whole.*

3.3.1 Probabilistic Risk Assessment

As with any PRA or HRA, the analysis team found it necessary to make assumptions in this study. In addition to the typical assumptions made as part of a PRA (e.g., actual plant system configuration is represented by the as-built as-operated documented information), the analysis team made various additional assumptions during the detailed PTS analyses. These assumptions are grouped into seven categories, as follows:

1. Project execution
    a. Lessons learned from the Oconee analysis and preliminary PFM calculations for Beaver Valley and Palisades were used to simplify the model construction for Beaver Valley and Palisades.
2. Possible PTS Initiating Events
    a. Scenarios initiated by an anticipated transient without scram (ATWS) were screened from the PTS analyses for two reasons. First, ATWS events generally begin with severe undercooling (i.e., there is too much power for the heat removal capability) and likely involve other failures to achieve an overcooling situation. Second, with typical ATWS frequency estimates in the range of 10^{-5}/yr to 10^{-6}/yr combined with the need for other failures to occur to *possibly* cause a continuing and serious overcooling situation, ATWS-initiated sequences should not be significant contributors to PTS risk when compared to other modeled scenarios with initiator frequencies commonly in the range of 1/yr to 10^{-3}/yr.
    b. Interfacing systems loss-of-coolant accidents (ISLOCAs) could involve overcooling from the start of the event. However, significant ISLOCAs often fail, or are assumed to fail, mitigating equipment in PRAs, which ultimately causes an undercooling event, rather than an overcooling event; thus, ISLOCAs were not analyzed. Also, similar to ATWS, frequency estimates for ISLOCAs of sufficient size to cause a sever cooldown are in the range of 10^{-5}/yr to 10^{-6}/yr. Therefore, ISLOCAs should not be significant contributors to PTS risk when compared to other modeled scenarios with initiator frequencies commonly in the range of 1/yr to 10^{-3}/yr.
    c. It was asssumed that the frequency of inadvertent reactor/turbine trips under hot zero power (HZP) conditions is 20% of that occuring under full power conditions. The basis of this 20% factor is as follows:
        i. The plant operates at HZP approximately 2% of the time.
        ii. Except for inadvertent reactor/turbine trips attributable to transient conditions that arise while purposely changing feedwater and steam conditions along with changing power and other parameters in the plant, a review of transients occurring while at HZP provided no evidence that initiators

are significantly more prone to occur at HZP than at full power. While no statistical treatment of this observation was attempted, engineering judgment was used to suggest that reactor/turbine trips seem more likely under HZP than under full power conditions because operators are often adjusting feedwater and steam conditions during HZP, factors that increase the likleyhood of tripping the plant. On this baisis, a factor of 10 increase in the likelihood of trips under HZP (vs. full power condtions) was assumed.

iii. 2% x 10 = 20%

3. Scenario development

   a. Medium- and large-break LOCAs were modeled as leading directly to a significant thermal transient for the reactor vessel without the need to consider the response of mitigating systems.

   b. The status of pressurizer PORVs and SRVs (i.e., whether they were open or closed) was assumed to be unimportant in the development of small LOCA scenarios. The basis for this assumption was that the pressure drop resulting from the LOCA initiating event should preclude the demand to open a primary side PORV or SRV.

   c. The PTS models excluded certain systems, structures, and components (SSCs) (e.g., pressurizer sprays and heaters) because they typically were found to have little impact on PTS risk.

   d. The functions of some SSCs were simply assumed for certain scenarios (e.g., accumulators were assumed to inject their inventory if conditions in the primary were such that injection should occur—failure of accumulator check valves was not modeled).

   e. The analysts recognized the importance of *when* an operator action occurred or *when* a piece of equipment changed state to the degree of overcooling experienced during a PTS scenario. To account for this, the scenarios incorporated a ***limited*** set of important operator actions (e.g., operator fails to throttle high-pressure injection) and equipment state changes (e.g., stuck-open pressurizer SRV recloses).

4. Systems analysis

   a. The impact of heating and ventilation failures on equipment performance can be ignored because of the relatively slow effects on PTS-relevant equipment (e.g., failure of a pump as a result of room cooling failure typically takes a few hours by which time the PTS event is most likely over).

5. Data

   a. Engineering judgment was used to estimate the failure probabilities for some SSCs. The numerical values provided by these judgments were typically conservative (i.e., the values were chosen such that potential PTS scenarios would not be inadvertently eliminated).

6. Human reliability analysis

   a. Pre-initiator human failure events (HFEs) were not explicitly modeled in the Oconee and Beaver Valley PTS PRAs. Such human events were assumed to be included in the industry-wide data that was used to model system unavailabilities. For the Palisades analysis, pre-initiator HFEs were left "as-is" (i.e., the existing pre-initiator HFEs in the Palisades PRA model used in the PTS analysis were not modified).

   b. The time at which operators perform an action is taken to be either the earliest the action can be performed or the latest the action can be performed, whichever exacerbates PTS conditions (e.g., if the action involves the operator successfully throttling a pump by 20 minutes, then the action would be modeled as occurring at 20 minutes).

c. Given the uncertainty associated with the various plant conditions that could exist during hot shutdown, some human error probabilities (HEPs) were assumed to be greater than their corresponding full-power HEPs.

7. PTS bin development

   a. The assignment of the large number of potential PTS scenarios (tens of thousands) to a more limited number of PTS TH bins (tens to over one hundred) involved the analysts' judgments as to how various combinations of equipment and operator successes affected the TH response of the plant when compared to a limited set of initial TH calculations. If the analysts judged that a scenario's response would be similar to an existing TH calculation, the scenario was "binned" into the existing calculation's bin. If the analysts judged that a scenario's response could be sufficiently different from the existing calculations, a new TH calculation was requested, thereby creating a new bin.

   b. Typically, the analysts estimated the impact of the various equipment and operator combinations on two parameters (i.e., minimum downcomer temperature and primary pressure).

   c. Minimum downcomer temperature was the most important parameter that the analysts used to decide whether an existing TH bin could represent a scenario, or whether a new TH bin should be created.

   d. If the analysts determined that a PTS scenario could "fit" into more than one TH bin having similar characteristics (i.e., minimum downcomer temperatures approximately the same), they assigned the scenario to the bin believed to be more conservative (i.e., the scenario was assigned to the bin with the highest primary pressure).

3.3.2 Thermal-Hydraulics

The appropriateness of the RELAP TH analysis to assess PTS rests on the validity of the following fundamental assumptions:

- We assume that the TH methodology implemented in RELAP is appropriate to assess the conditions in the downcomer during a PTS event. RELAP estimates fluid temperatures and wall-to-fluid heat transfer coefficients that represent well-mixed conditions in the downcomer at the core elevation. This approach assumes that jets, thermal plumes, and thermal streaming are not significant factors for PTS-type loadings.
- We assume that it is appropriate to use the variation of pressure, temperature, and heat transfer coefficient with time characteristic of a *single* TH transient to represent an entire PRA bin (which may contain many tens or hundreds of transients).

In the following subsections, we discuss the appropriateness of each of these assumptions.

3.3.2.1 Appropriateness of the RELAP TH Model, in General

At the most basic level, a TH analysis requires calculation of conservation of mass and energy, from which pressure and temperature follow from the equation of state. From this information, the analysis then estimates the distribution of energy within the RCS. Within the downcomer, the interface between the thermal-hydraulic and fracture mechanics calculations is the heat flux between the downcomer fluid and the vessel wall. Heat flux quantifies the RCS energy distribution, which depends on both the temperature and heat transfer characteristics of the downcomer region. In this study, we used RELAP5/MOD3.2.2γ to estimate the heat flux and pressure boundary conditions. RELAP5 is a best-estimate systems code that models heat transfer and hydrodynamic processes without any intentional conservative or nonconservative modeling features. The code has been extensively documented [RELAP 01]. Our specific validation of RELAP5 addressed its ability to accurately estimate pressure, downcomer fluid temperature, and wall-to-fluid heat transfer coefficients for PTS loading conditions [***Fletcher***]. In these validation studies, which are summarized in Section 6.2, we compared RELAP5/MOD3.2.2γ predictions of pressure and temperature to measurements made in the most ideally scaled integral systems test facilities. These comparisons demonstrate that RELAP5/MOD3.2.2γ predictions of pressure and temperature appropriately characterize PTS loading events.

3.3.2.2 Appropriateness of the TH Model

RELAP5 calculates fluid temperatures and wall-to-fluid heat transfer coefficients that are characteristic of a well-mixed downcomer (at the core elevation). Dickson evaluated the suitability of this assumption using a predecessor of FAVOR [Dickson 87]. In that study, the base-case calculation represented a hot leg break with a diameter of 2-in. (5-cm) and a "nominal" plume strength of 140°F (60°C). (Plume strength equals the temperature difference between the colder water below the cold legs and the balance of the downcomer.) It should be noted that this "nominal" plume strength greatly exceeds any plumes that have been measured, as detailed in the following paragraph, and this "nominal" plume had no discernable effect of (relative to no plume at all) on the probability of through-wall cracking estimated by FAVOR. Furthermore, a doubling of the nominal plume strength produces only a 30% increase in the estimated probability of through-wall cracking. This study provided an indication that the well-mixed downcomer assumptions made by both RELAP and FAVOR are appropriate.

More recently, we have performed additional work to establish the adequacy of the assumption of a one-dimensional (1D) temperature boundary condition, as follows:

- A new integral experimental program was conducted at the APEX-CE test facility at Oregon State University to study cold leg and downcomer mixing [***Reyes-APEX***].
- We reviewed existing experimental databases, including integral system tests in the Loss-of-Fluid Test (LOFT) facility and the Rig of Safety Assessment (ROSA), as well as full-scale tests in the Upper Plenum Test Facility (UPTF), and reduced-scale mixing tests at Creare, Purdue University, and Imatron Voimy Oy (Finland).
- We performed mixing calculations using the REMIX code and computational fluid dynamics (CFD) codes.

In thermal-hydraulic evaluations of PTS [***Bessette***], we compare these experimental data and RELAP5/MOD3.2.2γ predictions of pressure and temperature to establish the adequacy of the uniform temperature approximation. As seen consistently in the experimental data, the downcomer is well-mixed. In integral system test data, the temperature variations seen in the in the axial or azimuthal directions is on the order of 9°F (5°C). Large temperature gradients (i.e., on the order of 180°F, or 100°C) are often seen in the cold leg following loop flow stagnation. However, temperature gradients in the cold leg do not translate to corresponding temperature variations in the downcomer because of the large eddy mixing occurring in the downcomer.

In summary, the maximum plume measured in any integral test facility representation of a PTS transient is on the order of 9°F (5°C). Probabilistic fracture mechanics calculations show that much larger plumes (strengths of ≈ 216°F, or 120°C) are needed to have even small effects on the estimated probability of through-wall cracking [***Bessette***, Section 5.5]. For these reasons, the modeling approaches of both the RELAP and FAVOR codes with regard to temperature uniformity throughout the downcomer are viewed as both appropriate and non-biasing for this application.

3.3.2.3 Appropriateness of a Using a Single TH Transient To Represent an Entire PRA Bin

In Section 3.1.2.1.2, we described the iterative process used to establish the single TH transient that represents an entire PRA bin (which may contain many tens or hundreds of transients). This process includes continual partitioning of the PRA bins that contribute significantly to the estimated TWCF until the total estimated TWCF for the plant does not change significantly with continued partitioning. Given that process, the appropriateness of using a single TH transient to represent an entire bin (which may contain tens or hundreds of sequences that can produce, in principal, a like number of different TH responses) is not justified based on the exact agreement of the representative TH transient to all of the other transients in the bin (which is not, and cannot, be guaranteed). Rather, the appropriateness is justified by the procedure detailed in Section 3.1.2.1.2, which ensures that further subdivision of the bins would not result in significant changes to the TWCF (the desired output of the analysis).

3.3.3 Probabilistic Fracture Mechanics

The appropriateness of the FAVOR PFM analysis to assess PTS rests on the validity of the following four fundamental assumptions:

- We assume (in general) that linear elastic fracture mechanics (*LEFM*) is an appropriate methodology to use in assessing the structural integrity of RPVs subjected to PTS loadings, and (in particular) that FAVOR predictions of the fracture response of RPVs in response to PTS loading are accurate.
- We assume that the effect of crack growth by subcritical mechanisms (i.e., environmentally assisted cracking and/or fatigue) is negligible and, consequently, the flaw population of interest is that associated with initial vessel fabrication.
- We assume that the fracture toughness of the stainless steel cladding is adequately high, and remains so even after irradiation, so there is no possibility of cladding failure as a result of the loading imposed by PTS transients.
- We assume that stresses are sufficiently low at locations in the vessel wall between $3/8 \cdot t_{wall}$ from the vessel ID and the OD, so the probability of failure associated with postulated defects in this region does not have to be calculated because it is zero.
- We assume that if a particular transient does not achieve a temperature in the downcomer below 400°F (204°C), it does not contribute to the vessel failure probability.

In the following subsections, we discuss the appropriateness of each of these assumptions.

3.3.3.1 Use of Linear Elastic Fracture Mechanics

One fundamental assumption in constructing our PFM model is that a linear elastic stress analysis of the vessel, and consequent fracture integrity assessment using the techniques of linear elastic fracture mechanics (*LEFM*), are accurate. Evidence supporting the appropriateness of this assumption is available in the following areas:

(1) In Section 7.10, we summarize the results of studies aimed at experimentally validating the appropriateness of *LEFM* techniques when applied to assessing the integrity of RPVs under thermal shock and PTS experiments. The results of three experimental series performed on scaled pressure vessels at ORNL in the 1970s and 1980s demonstrate the accuracy of *LEFM* techniques in these applications.

(2) One fundamental requirement for LEFM validity is that the dimensions of the plastic zone at the tip of a loaded crack must be very small compared with the dimensions of the crack being assessed and the structure in which the crack resides [Rolfe]. Under these conditions, the error introduced by plastic flow (which is not accounted for within LEFM theories) is acceptably small. To assess plastic zone sizes characteristic of the PTS problem, we had the FAVOR probabilistic fracture mechanics code report

all of the applied driving force to fracture ($K_{applied}$) values from an analysis of Beaver Valley Unit 1 at 60 EFPY, which contribute to the *TWCF*, (i.e., those that have a conditional probability of crack initiation greater than 0). The top graph in Figure 3-4 shows these $K_{applied}$ values overlaid on the K_{Ic} transition curve, while the bottom graph shows these same values expressed in the form of a cumulative distribution function. The lower graph indicates that 90% of the $K_{applied}$ values that contribute to the *TWCF* estimate lie between 20 and 35 ksi√in (22 – 38.5 MPa√m). Using these stress intensity factor values together with Irwin's equation for the plastic zone size under plane strain conditions [Rolfe] indicates that the plastic zone radii characteristic of PTS loading range from ~0.03 to ~0.13-in. (~0.76 to ~3.30-mm) depending upon the value of $K_{applied}$ (here taken to range from 20 to 35 ksi√in, or 22 – 38.5 MPa√m), and the value of the yield strengths (here taken to be 70 ksi (on average) for unirradiated materials and 90 ksi (on average) for irradiated materials (483 and 621, respectively). These values of plastic zone radii are small compared with the thickness of a PWR reactor vessel, indicating the appropriateness of LEFM techniques. Moreover, it can be noted that as the vessel ages, irradiation damage causes the yield strength to increase. Thus, as vessels approach EOL and extended EOL conditions, LEFM techniques become, if anything, more appropriate.

3.3.3.2 Assumption of No Subcritical Crack Growth

3.3.3.2.1 Due to Environmental Effects on the Low-Alloy Pressure Vessel Steel

Stress corrosion cracking (SCC) requires the presence of three factors: an aggressive environment, a susceptible material, and a significant tensile stress. If these three factors exist and SCC can occur, growth of intrinsic surface flaws in a material is possible. Since an accurate PTS calculation for the low-alloy steel (LAS) pressure vessel should address realistic flaw sizes, the potential for crack growth in the reactor vessel LAS as a result of SCC needs to be analyzed, in principle. However, for the reasons detailed in the following paragraphs, SCC for LAS in PWR environments is highly unlikely and, therefore, is appropriately assumed not to occur for the purposes of the FAVOR calculations reported herein.

The first line of defense against SCC of LAS is the cladding that covers much of the LAS surface area of the reactor vessel and main coolant lines. This prevents the environment from contacting the LAS and, therefore, obviates any possibility of SCC of the pressure boundary.

Additionally, several test programs have been conducted over the past three decades, all of which show that SCC in LAS cannot occur in normal PWR or boiling-water reactor (BWR) operating environments. SCC of LAS in the reactor coolant environment is controlled by the electrochemical potential (often called the free corrosion potential). The main variable that controls the LAS electrochemical potential is the oxygen concentration in the coolant. During normal operation of a PWR, the oxygen concentration is below 5ppb. The electrochemical potential of LAS in this environment cannot reach the value necessary to cause SCC [IAEA 90, Hurst 85, Rippstein 89, Congleton 85]. During refueling conditions, the oxygen concentration in the reactor coolant does increase. However, the temperature during an outage is low, rendering SCC kinetically unfavorable. During refueling outage conditions with higher oxygen concentrations but lower temperatures, the electrochemical potential of the LAS would still not reach the values necessary for SCC to occur [Congleton 85].

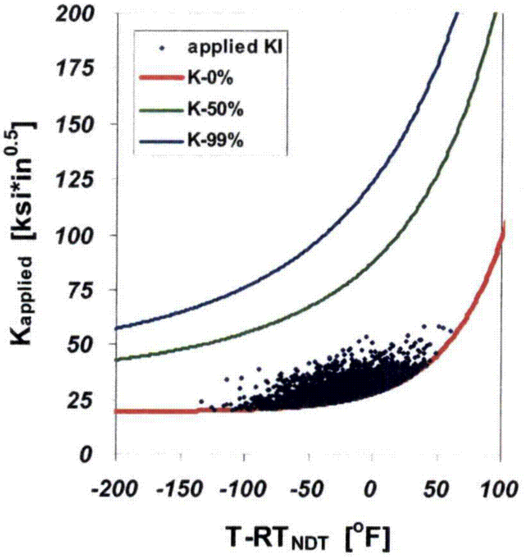

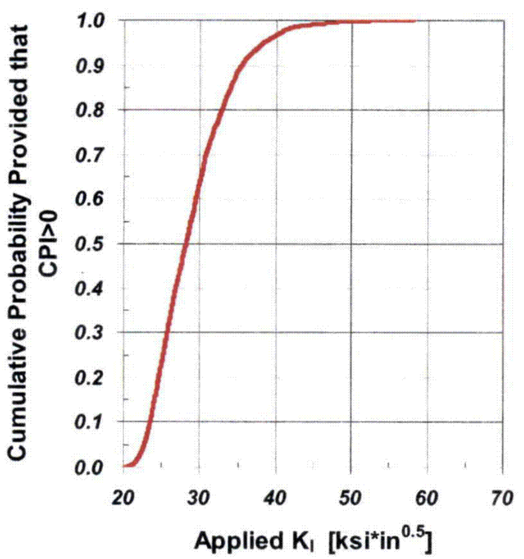

Figure 3-4. Illustration of the magnitude of $K_{applied}$ values that contribute to TWCF because they have a conditional probability of crack initiation > 0. The top graph shows all $K_{applied}$ values with $CPI > 0$ overlaid on the K_{Ic} transition curve from an analysis of Beaver Valley Unit 1 at 60 EFPY. The bottom graph shows these same results expressed in the form of a cumulative distribution function.

3.3.3.2.2 Due to Environmental Effects on the Austenitic Stainless Steel Cladding

As stated in Section 3.3.3.2.1, one assurance of the negligible effects of environmentally assisted crack growth on the low-alloy pressure vessel steel is the integrity of the austenitic stainless steel cladding that provides a corrosion-resistant barrier between the LAS and the primary system water. Under conditions of normal operation, the chemistry of the water in the primary pressure circuit is controlled with the express purpose of ensuring that SCC of the stainless steel cladding cannot occur. Even under chemical upset conditions (during which control of water chemistry is temporarily lost), the rate of crack growth in the cladding is exceedingly small. For example, Ruther et al. reported an upper bound crack growth rate of $\approx 10^{-5}$ mm/s ($\approx 4 \times 10^{-7}$ in/s) in poor-quality water (i.e., high oxygen) environments [Ruther 84]. The amount of crack extension that could occur during a chemical upset is therefore quite limited, and certainly not sufficient to compromise the integrity of the clad layer.

3.3.3.2.3 Due to Fatigue

Fatigue is a mechanism that initiates and propagates flaws under the influence of fluctuating or cyclic applied stress and can be separated into two broad stages: fatigue damage accumulation (potentially leading to crack initiation), and fatigue crack growth.

Fatigue is influenced by variables that include mean stress, stress range, environmental conditions, surface roughness, and temperature. Thermal fatigue can also occur as thermal stresses develop when a material is heated or cooled. Generally, fatigue failures occur at stresses having a maximum value less than the yield strength of the material. The process of fatigue damage accumulation, crack initiation, and crack growth closely relates to the phenomenon of slip attributable to static shear stress. Following a period of fatigue damage accumulation, crack initiation will occur by the progressive development and linking of intrusions along slip bands or grain boundaries. Growth of these initiated cracks includes fracture deformation sequences, plastic blunting followed by resharpening of the crack tip, and alternate slip processes.

The PWR vessel is specifically designed so that all of its components satisfy the fatigue design requirements in Section III of the Boiler and Pressure Vessel Code promulgated by the American Society of Mechanical Engineers (ASME), or equivalent. Several studies have shown that the 60-year anticipated fatigue "usage" of the vessel beltline region attributable to normal plant operations, including plant heatup/cooldown, design-basis transients, etc. is low, so fatigue-initiated cracks will not occur. Similarly, fatigue loading of the vessel is considered insufficient to result in propagation of any existing fabrication defects [EPRI 94, Kasza 96, Khaleel 00].

3.3.3.3 Assumption that the Stainless Steel Cladding will not Fail as a Result of the Loads Applied by PTS

Stainless steel, even in the clad form, typically exhibits initiation fracture resistance (J_{Ic} and J-R) values that far exceed those of the ferritic steels from which the RPV wall is made (see [Bass 04] for cladding data, compared to [EricksonKirk 04] for ferritic steel data). This is especially true for the levels of embrittlement at which vessel failure becomes a (small) probability because, at the fluences characteristic of the vessel ID location, the fracture toughness of ferritic steels can be considerably degraded by neutron damage, while the fracture toughness of austenitic stainless steels are essentially unaffected by these same levels of irradiation damage [Chopra 06]. This high toughness of the stainless steel cladding coupled with the small characteristic size of defects found in the cladding [***Simonen***] justifies the assumption that the stainless steel cladding will not fail as a result of the loads applied by PTS.

3.3.3.4 Non-Contribution of Flaws Deep in the Vessel Wall to Vessel Failure Probability

In FAVOR, flaws simulated to exist further than $\frac{3}{8} \cdot t_{wall}$ from the inner diameter surface are eliminated, *a priori*, from further analysis. This screening criterion is justified based on deterministic fracture mechanics analyses, which demonstrate that for the embrittlement and loading conditions characteristic of PTS, such flaws have zero probability of crack initiation. As illustrated in Figure 3.5, in practice, crack initiation almost always occurs from flaws that having their inner crack tip located within $0.125 \cdot t_{wall}$ of the inner diameter, further substantiating the appropriateness of eliminating cracks deeper than $\frac{3}{8} \cdot t_{wall}$ from further analysis.

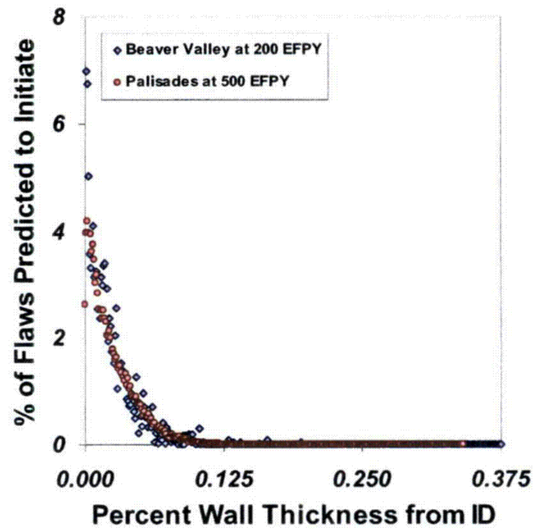

Figure 3.5. Distribution of crack initiating depths generated by FAVOR Version 03.1

3.3.3.5 Non-Contribution of Certain Transients to Vessel Failure Probability

When running a plant-specific analysis using FAVOR, we only calculated the CPTWC for TH transients that reach a minimum temperature at or below 400°F (204°C). This *a priori* elimination of transients is justified based on experience and deterministic calculations, both of which demonstrate that such transients lack adequate severity to have non-zero values of CPTWC, even for very large flaws and very large degrees of embrittlement. Additionally, the results of our plant-specific analyses (reported in Chapter 8) show that a minimum transient temperature of 352°F (178°C) must be reached before CPTWC will rise above zero, validating that our elimination of transients with minimum temperatures above 400°F (204°C) does not influence our results in any way.

3.4 Participating Organizations

This study could not have succeeded without the cooperation of a large number of individuals both within and outside the NRC. From its inception, the commercial nuclear power industry, working under the auspices of EPRI, has been a key participant in this project. Table 3.2 summarizes the key organizations and individuals, and their contributions to this study.

3.5 External Review Panel

In response to a letter [Bonaca 03] from the Chairman of the ACRS, the NRC's Executive Director for Operations (EDO) [Travers 03] identified a need to conduct formal peer review of the technical basis developed for potential revision of the screening criteria in the PTS Rule (10 CFR 50.61). In response to the EDO's direction, RES solicited a panel of experts to perform an independent review of this report, and all supporting documentation that comprises the basis for our recommended revisions to the PTS Rule. Two peer reviewers were selected from each of the three key technical areas (PRA, TH, and PFM). Each peer reviewer was asked to provide his or her individual comments on the entire PTS technical basis without developing a consensus on a unified set of comments, to satisfy the requirement that this peer review panel must not constitute a Federal advisory committee. The following individuals served on the peer review panel.

- **Dr. Ivan Catton:** Professor at the University of California, Los Angeles. Prof. Catton is an internationally recognized expert in thermal-hydraulics, and has served as a member of the NRC's ACRS.
- **Dr. David Johnson:** Vice President of ABS Consulting Inc., Irvine, California. Dr. Johnson is an internationally recognized expert in PRA. He is involved in major risk studies and in using those studies to support decision-making.
- **Dr. Thomas E. Murley:** The chair of this peer review panel, Dr. Murley is a former Director of the NRR. Dr. Murley played a key role in regulating the operation of nuclear power plants for many years in comprehensive, high-level, broad-scope management of programs on water-cooled nuclear reactor power plants' safety and risk assessments.
- **Dr. Upendra Rohatgi:** A researcher at the U.S. Department of Energy's Brookhaven National Laboratory, Upton, NY. Dr. Rohatgi has been extensively involved in the development of thermal-hydraulic computer codes for nuclear power plant applications. In the mid-1980s, he reviewed the thermal-hydraulic analyses performed for two of the plants analyzed in developing the current PTS Rule.
- **Mr. Helmut Schulz:** Head of the Department of Structural Integrity of Components at Gesellschaft fuer Anlagen-und Reaktorsicherheit (GRS), Cologne, Germany. As a senior manager, Mr. Schulz has been involved in directing the development of PFM methodologies and managing various international cooperative research projects concerning fracture mechanics under the auspices of the Committee on the Safety of Nuclear Installations (CSNI) and the Nuclear Energy Agency (NEA) of the Organization for Economic Cooperation and Development (OECD) in Europe.
- **Dr. Eric vanWalle:** Head of the Reactor Materials Research Department, Belgian Nuclear Research Center (SCK-CEN), Mol, Belgium. Dr. vanWalle is extensively involved in irradiation embrittlement characterization of RPV materials, and

various International Atomic Energy Agency (IAEA) and OECD/NEA cooperative research projects in fracture mechanics related to ensuring the structural integrity of nuclear power plants.

Appendix B provides more details of the peer review, including both the reviewers' comments regarding our technical basis and recommendations, and the staff's responses to those comments.

Table 3.2. Participating organizations

Sponsor/Organization		Individuals	Responsibilities
NRC	RES/DET/MEB	Mark EricksonKirk, Shah Malik, Tanny Santos, Debbie Jackson, Todd Mintz	Project management, materials, fracture mechanics
	RES/DRAA/PRAB	Roy Woods, Nathan Siu, Lance Kim, Mike Junge	PRA, human reliability analysis, event sequence analysis, risk goal
	RES/DSARE/SMSAB	Dave Bessette	Thermal-hydraulics analysis
	Oak Ridge National Laboratory	Terry Dickson, Richard Bass, Paul Williams	PFM Code FAVOR
	Pacific Northwest National Laboratory	Fred Simonen, Steve Doctor, George Schuster	Flaw distribution
	Brookhaven National Laboratory	John Carew	Fluence
	Sandia National Laboratories	Donnie Whitehead, John Forester, Vincent Dandini	PRA, human reliability analysis, event sequence analysis, external events analysis, generalization task
	SAIC	Alan Kolaczkowski, Susan Cooper, Dana Kelly	PRA, human reliability analysis, event sequence analysis, external events analysis, generalization task
	University of Maryland	Mohammad Modarres, Ali Mosleh, Fei Li, James Chang	Uncertainty analysis of PFM and TH
	The Wreathwood Group	John Wreathall	Human reliability analysis
	Buttonwood Consulting	Dennis Bley	Human reliability analysis
	INEEL	William Galyean	PRA, event sequence analysis
	ISL	Bill Arcieri, Robert Beaton, Don Fletcher	Thermal-hydraulic calculations using RELAP

Sponsor/Organization		Individuals	Responsibilities
EPRI	EPRI	Stan Rosinski	Program Management
	EPRI Materials Reliability Program (MRP) RPV Integrity Issue Task Group	Robert O. Hardies	ITG Chairman – Constellation Nuclear
	Westinghouse Electric Company	Ted Meyer, Bruce Bishop, Randy Lott, Steve Byrne, Robert Lutz, Barry Sloan, Eric Frantz	PRA, risk goal, PFM Code FAVOR, Fracture mechanics, materials, uncertainty analysis of PFM and TH
	Framatome ANP	Ken Yoon	Materials, fracture mechanics
	Sartrex Corporation	Ron Gamble	PRA, risk goal, PFM Code FAVOR
	Phoenix Engineering Associates	Marjorie EricksonKirk	Uncertainty analysis of PFM, fracture mechanics
	Constellation Nuclear – Calvert Cliffs	Robert O. Hardies	Plant-specific PTS
	First Energy – Beaver Valley	Dennis Weakland	Plant-specific PTS
	Duke Energy – Oconee	Jeff Gilreath, Steve Nadar	Plant-specific PTS
	Nuclear Management Company – Palisades	John Kneeland, Brian Brogan, Christer Dahlgren, Gary Pratt	Plant-specific PTS
	Applied Reliability Engineering	Dave Blanchard	Palisades PRA

4 Structure of this Report, and Changes Relative to Previous Reports

4.1 Report Structure

This report summarizes information found in a collection of other documents. As illustrated in Figure 4-1, various reports that concern either procedures or calculated results are available in each of three main technical areas (PRA, TH, and PFM). In this report, we do not attempt to provide a comprehensive summary of all aspects of the PFM, TH, and PRA procedures or results. Rather, in Chapters 5, 6, and 7, we focus on the key features of the PRA, TH, and PFM models, respectively, placing particular emphasis on changes between these models and those that were used to establish the technical basis for the current PTS Rule [10 CFR 50.61]. Chapter 8 goes on to detail the results of our "baseline" probabilistic calculations for Oconee Unit 1, Beaver Valley Unit 1, and Palisades. Chapter 9 summarizes various studies we have performed that collectively demonstrate the applicability of the results in Chapter 8 to PWRs in general, rather than just to the specific conditions analyzed herein. In Chapter 10, we discuss considerations associated with selecting an acceptable annual limit on TWCF, while in Chapter 11, we compare this limit to the results from Chapter 8 to establish a revision to the RT_{PTS} screening criteria currently expressed in 10 CFR 50.61.

4.2 Changes Relative to Previous Studies

To assist readers familiar with the details of calculations that form the basis for the current PTS rule [SECY-82-465] or the calculations previously reported from this effort [***Kirk 12-02***], we provide a guide to where our methodology and results differ from the previous studies, and provide pointers to locations in this and other documents where those changes are discussed in greater detail

4.2.1 Studies Providing the Technical Basis of the Current PTS Rule

As detailed in Section 3.2, one fundamental difference between our approach and that of SECY-82-465 is that here we consider all of the known factors that influence the likelihood of vessel failure during a PTS event, while accounting for uncertainties in these factors in a consistent manner across a breadth of technical disciplines (see [***Siu 99***] for details). Two central features of this approach are a focus on the use of realistic input values and models (wherever possible), and *explicit* treatment of uncertainties (using currently available uncertainty analysis tools and techniques). Thus, our current approach improves upon that employed in developing SECY-82-465, in which many aspects of the analysis included intentional and unquantified conservatisms, and uncertainties were treated *implicitly* by incorporating them into the models.

In addition to this overall change in modeling approach, the following specific changes were made in the three main technical areas:

<u>Modifications to PRA</u>

Table 5.1 (in Section 5.2.2) summarizes the differences between the current PRA and that used to support the current PTS Rule. These differences fall into the following three major categories:

(1) greater refinement and detail in the current PRA

(2) more realistic treatment of operator actions in the current PRA

Summary Report – NUREG-1806

	PFM	TH	PRA

Models, Validation, & Procedures	• Procedures, Uncertainty, & Experimental Validation: EricksonKirk, M.T., et al., "Probabilistic Fracture Mechanics: Models, Parameters, and Uncertainty Treatment Used in FAVOR Version 04.1," NUREG-1807.
	• FAVOR
	  • Theory Manual: Williams, P.T., et al., "Fracture Analysis of Vessels – Oak Ridge, FAVOR v04.1, Computer Code: Theory and Implementation of Algorithms, Methods, and Correlations," NUREG/CR-6854.
	  • User's Manual: Dickson, T.L., et al., "Fracture Analysis of Vessels – Oak Ridge, FAVOR v04.1, Computer Code: User's Guide," NUREG/CR-6855.
	  • V&V Report: Malik, S.N.M., "FAVOR Code Versions 2.4 and 3.1 Verification and Validation Summary Report," NUREG-1795.
	• Flaw Distribution: Simonen, F.A., et al., "A Generalized Procedure for Generating Flaw-Related Inputs for the FAVOR Code," NUREG/CR-6817, Rev. 1.
		• TH Model: Bessette, D., "Thermal Hydraulic Analysis of Pressurized Thermal Shock," NUREG/1809.
		• RELAP Procedures & Experimental Validation: Fletcher, C.D., et al., "RELAP5/MOD3.2.2 Gamma Assessment for Pressurized Thermal Shock Applications," NUREG/CR-6857.
		• Experimental Benchmarks: Reyes, J.N., et. al., Final Report for the OSU APEX-CE Integral Test Facility, NUREG/CR-6856.
		• Experimental Benchmarks: Reyes, J.N., Scaling Analysis for the OSU APEX-CE Integral Test Facility, NUREG/CR-6731
		• Uncertainty: Chang, Y.H., et al., "Thermal Hydraulic Uncertainty Analysis in Pressurized Thermal Shock Risk Assessment," University of Maryland.
			• Procedures & Uncertainty: Whitehead, D.W. and Kolaczkowski, A.M., "PRA Procedures and Uncertainty for PTS Analysis," NUREG/CR-6859.
			• Uncertainty Analysis Methodology: Siu, N., "Uncertainty Analysis and Pressurized Thermal Shock, An Opinion," USNRC, 1999.

Results	• Baseline: Dickson, T.L. and Yin, S., "Electronic Archival of the Results of Pressurized Thermal Shock Analyses for Beaver Valley, Oconee, and Palisades Reactor Pressure Vessels Generated with the 04.1 version of FAVOR," ORNL/NRC/LTR-04/18. • Sensitivity Studies: EricksonKirk, M.T., et al., "Sensitivity Studies of the Probabilistic Fracture Mechanics Model Used in FAVOR," NUREG-1808.	• Baseline: Arcieri, W.C., "RELAP5 Thermal Hydraulic Analysis to Support PTS Evaluations for the Oconee-1, Beaver Valley-1, and Palisades Nuclear Power Plants," NUREG/CR-6858. • Sensitivity Studies: Arcieri, W.C., et al., "RELAP5/MOD3.2.2Gamma Results for Palisades 1D Downcomer Sensitivity Study" • Consistency Check: Junge, M., "PTS Consistency Effort"	• Beaver: Whitehead, D.W., et al., "Beaver Valley PTS PRA" • Oconee: Kolaczkowski, A.M., et al., "Oconee PTS PRA" • Palisades: Whitehead, D.W., et al., "Palisades PTS PRA" • External Events: Kolaczkowski, A.M., et al., "Estimate of External Events Contribution to Pressurized Thermal Shock Risk" • Generalization: Whitehead, D.W., et al., "Generalization of Plant-Specific PTS Risk Results to Additional Plants"

Figure 4-1. Structure of documentation summarized by this report. When these reports are cited in the text, the citation appears in *italicized boldface* to distinguish them from literature citations.

(3) Use of the latest available data on initiating event frequencies and equipment failure probabilities in the current PRA

As noted in the table, since these improvements were made with the intent of increasing both the accuracy and comprehensiveness of the PRA representation of the plants, they neither systematically increase nor reduce the estimated risk from PTS.

Modifications to TH

The first PTS study was performed during the early 1980s. In that study, TH calculations were performed for Oconee Unit 1 with RELAP5/MOD1.5 (circa 1982) and for H.B. Robinson Unit 2 with RELAP5/MOD1.6 (circa 1984). The results of those calculations were documented in [ORNL 86, ORNL 85b].

By contrast, the TH calculations performed in the current study employed RELAP5/MOD3.2.2Gamma, which was released in 1999 [RELAP 99]. The changes in the RELAP5 code in the intervening 20 years have been extensive [RELAP 99]:

- RELAP5/MOD3.2.2Gamma uses a revised treatment of non-equilibrium modeling, including wall heat transfer models and coupling of the wall heat transfer and vapor generation models.
- Interphase friction models were revised, and now incorporate a new interphase drag model for the vertical bubbly and slug flow regimes.
- A general cross-flow modeling capability was installed, allowing cross-flow connections between most types of components and among the cell faces on those components.

Other changes were implemented as a result of the code assessments related to the RELAP5 analysis for the AP600 advanced passive reactor:

- The Henry-Fauske critical flow model was added to provide a standard-reference critical flow model upon which code calculations are based.
- Changes were made in code numerics to greatly reduce recirculating flows within model regions nodalized with a multidimensional approach.
- A mechanistic interphase heat transfer model was implemented to include the effects of noncondensible gases. This change greatly improved the simulation of condensation, preventing erratic behavior and code execution failures. This change is particularly important for situations where the plant accumulators empty and nitrogen is discharged into the reactor coolant system (a situation that typically led to code execution failure at the time of the first PTS study).

In the current study, no major changes were made from the RELAP5 plant input modeling approach used in the first PTS study [ORNL 86, ORNL 85a]. With only a few exceptions, the plant input models use the same nodalization schemes as before. Those nodalization schemes reflect plant modeling recommendations and guidance for the general modeling of plant transients, which evolved over years of RELAP4 and RELAP5 experimental assessments and plant applications preceding the first PTS study. However, the current study used capabilities in RELAP5/MOD3.2.2Gamma, including renodalization of the reactor vessel downcomer (using the general cross-flow modeling capability), conversion of the vessel/hot and cold leg connections and the hot leg-to-pressurizer surge line connection to the cross-flow format, and addition of junction hydraulic diameter input data as required by the conversion of the code to junction-based interphase drag. [***Bessette, Fletcher*** document how these RELAP5/MOD3.2.2Gamma capabilities influence the models used in the current study.]

Current computer calculation speeds and data storage capabilities exceed greatly those used during the first PTS study, allowing the number of transients that can be reasonably evaluated directly using RELAP5 to be expanded by more than an order of magnitude. In the first PTS study, budget and schedule considerations limited the number of transients evaluated per plant to about 10 to 15. By contrast, the current study used more than 500 RELAP5 transient calculations to characterize the risk of vessel failure.

Enormous advances in analysis tools (automated processes and plotting and data extraction routines) have also occurred. These tools lead to more comprehensive analyses, better communication and sharing of data, and more effective reporting of results.

<u>Modifications to PFM</u>

(1) A significant conservative bias in the unirradiated toughness index temperature (RT_{NDT}) model was removed. (See item 3 in Section 7.7.2.2 of this report and Section 3.2.2.3.1 of [***EricksonKirk-PFM***].)

(2) The spatial variation in fluence was recognized. (See item 1 in Section 7.7.2.2 of this report and Section 3.2.3.1 of [***EricksonKirk-PFM***].)

(3) Most flaws are now embedded, rather than on the surface, and are also smaller than before. (See Section 7.5 of this report and [***Simonen***].)

(4) Material region-dependent embrittlement properties were used. (See item 1 in Section 7.7.2.2 and Table 8.2 of this report.)

(5) Non-conservatisms in the crack arrest model were removed. (See item 2 in Section 7.8.2 of this report, Section 4.1 of [***EricksonKirk-PFM***], and [Kirk 02a].)

(6) Non-conservatisms in the embrittlement model were removed. (See Section 3.2.3 of [***EricksonKirk-PFM***]).

(7) The possibility of fracture on the upper shelf has been accounted for. (See item 1 in Section 7.8.2 of this report, Section 4.2 of [***EricksonKirk-PFM***], and [EricksonKirk 04].)

(8) The effect of warm pre-stress (WPS) has been accounted for. (See Section 7.7.1.1 of this report, Appendix B to [***EricksonKirk-PFM***])

(9) Uncertainties on chemical composition and $RT_{NDT(u)}$, which bound all known individual materials, have been included. (See Appendix D to [***EricksonKirk-PFM***].)

4.2.2 December 2002 Draft Report

In December 2002, we issued a draft report that detailed the results of plant-specific analyses performed on Oconee Unit 1, Beaver Valley Unit 1, and Palisades [***Kirk 12-02***]. Since that report was issued, we have made the following significant changes to our model:

Modifications to PRA

No significant changes were made to the PRA/HRA models since [***Kirk 12-02***].

Modifications to TH

The RELAP5 Oconee model was revised to incorporate comments received from Duke Power [***Arcieri-Base***]. In addition, momentum flux modeling in the downcomer was changed to avoid the erroneous prediction of recirculating flows in the downcomer that, for a small number of cases, were unphysically high. When erroneous predictions of recirculating flows occurred, the high liquid velocity resulted in correspondingly high calculations of the heat transfer coefficient. The entire set of Oconee cases was rerun.

Modifications to PFM

We revised the FAVOR PFM code. The information presented in [***Kirk 12-02***] was generated with FAVOR Version 02.4, whereas the information presented herein was generated with FAVOR Version 04.1. We made the following significant changes to FAVOR between these versions:

(1) As part of our V&V effort, we identified a bug in how FAVOR associated material properties with cracks that lie on the fusion line of welds. This bug was most significant when the toughness properties of the plates adjacent to the weld are lower and, thus, control the fracture response, as is the case with Beaver Valley Unit 1. Details of this bug fix can be found [***Malik***].

(2) FAVOR now considers the possibility of failure occurring by ductile tearing on the upper shelf. Section 7.8 of this report describes the upper-shelf model we used and our rationale for its introduction, while Section 4.2 of [***EricksonKirk-PFM***] and [***Williams***] provide full details of the FAVOR Version 04.1 upper-shelf model.

(3) FAVOR now models the effects of crack face pressure loading, as described in [***Williams***].

(4) FAVOR now accounts for the temperature dependence of thermal-elastic material properties, as described in [***Williams***].

5 Probabilistic Risk Assessment and Human Reliability Analysis

5.1 Introduction

This section describes the analysis activities associated with performing the PRA and HRA portions of the PTS reanalysis project.
As depicted in Figure 5.1, the PTS reanalysis project was a closely integrated effort among three primary technical disciplines:

(1) PRA (including HRA),
(2) TH modeling, and
(3) PFM.

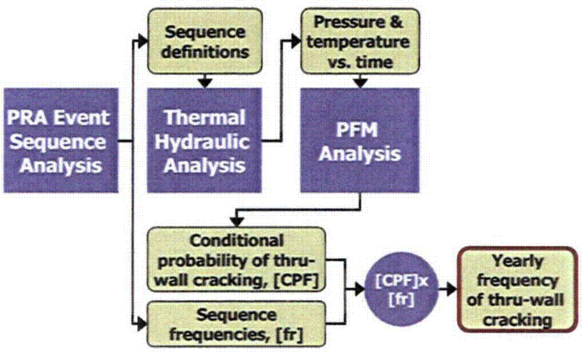

Figure 5.1. Integrated technical analyses comprising the PTS reanalysis project

As such, while this section focuses on the PRA and HRA (hereafter referred to as PRA unless specifically dealing with HRA) aspects of the reanalysis, important interfaces with the other technical disciplines are noted and cannot be completely separated from what was done in the PRA portion of the PTS reanalysis project.

A key final product of this reanalysis project is the estimation of TWCFs associated with severe overcooling scenarios. The PRA portion of the reanalysis project had three primary purposes:

(1) Define the overcooling scenarios (sequences) with the potential for being PTS challenges.

(2) Direct the TH analysis as to the specific sequences to be modeled to obtain plant TH response information to be forwarded to the PFM analysts.

(3) Estimate the frequencies, including uncertainties, for those overcooling sequences that are potentially important to the PTS results and provide that information to the PFM analysts.

In fulfilling the above purposes, the PRA analysts followed an iterative process.
The iterations were the result of (1) additional information becoming available from the other disciplines as the analyses evolved, and (2) feedback from the licensees participating in the three plant analyses (Oconee Unit 1, Beaver Valley Unit 1, and Palisades Unit 1).

For each purpose listed above, a specific product was produced. The first product, definition of the overcooling sequences, is in the form of event trees constructed by the PRA analysts for each of the three plant PTS analyses.
Event tree construction is a well-known and well-established PRA modeling tool that has been used in identifying and analyzing core damage scenarios, such as in the Individual Plant Examination (IPE) program. In this case, the same tool was used to identify and model overcooling sequences, rather than core damage sequences that could occur as a result of undercooling events. The sequences depicted by the PTS event trees represent those combinations of initiating events that disrupt normal plant operation (e.g., turbine trip), and

subsequent plant equipment and operator responses that are included in each plant model to represent overcooling sequences with the potential to be a PTS challenge.

The second product, direction by the PRA analysts to the TH analysts as to specific sequences to be modeled in their phase of the overall PTS analyses, was provided in the form of written and oral communications among the analysts. Each TH-modeled sequence was assigned a "case" number for identification purposes. For a given plant analysis, each TH "case" is a scenario that broadly represents many possible sequences on the event trees for that plant whose characteristics are similar enough that the sequences can be collectively represented by a single TH sequence (case). The TH analysts modeled each case to derive the time histories for reactor coolant pressure, reactor vessel downcomer temperature, vessel wall heat transfer characteristics, and other parameters important to defining the plant TH response during each case. This response information was subsequently provided to the PFM analysts to determine the vessel wall response (i.e., crack initiation and propagation) for the TH conditions. The modeling of multiple event tree sequences by a smaller number of "case" sequences involved a manual *binning* process that is summarized later in more detail.

The third product, sequence frequencies including uncertainties, was provided to the PFM analysts by the PRA analysts for those overcooling "case" bins that are potentially important to the PTS results. This information was provided in the form of electronic files containing a "case" bin identifier and statistical frequency information associated with that bin. These bin frequencies correspond to the "case" sequences modeled by the TH analysts and represent the combined frequencies of all event tree sequences combined into each bin. The PFM analysts then used the statistical frequency information, along with the TH information representing each bin, to estimate the TWCFs.

5.2 Methodology

A multi-step approach was followed to produce the PRA products for the PTS reanalysis project. Figure 5.2 depicts the steps followed to define the sequences of events that may lead to PTS (for input to the TH model), as well as the frequencies with which these sequences are expected to occur (for combination with the PFM results to estimate the annual frequency of through-wall cracking). Although the approach is illustrated in a serial fashion, its implementation involved multiple iterative passes through the various steps as the analyses and mathematical representations of each plant evolved. The following sections describe seven steps that together comprise the PRA analysis:

Step 1: Collect information (Section 5.2.1)

Step 2: Identify the scope and features of the PRA model (Section 5.2.2)

Step 3: Construct the PRA models (Section 5.2.3)

Step 4: Quantify and bin the PRA modeled sequences (Section 5.2.4)

Step 5: Revise PRA models and quantification (Section 5.2.5)

Step 6: Perform uncertainty analysis (Section 5.2.6)

Step 7: Incorporate uncertainty and finalize results (Section 5.2.7)

The reader should recognize that the PRA models described in this section consider *only* events internal to the operating plant (stuck-open valves, pipe breaks, etc.) as possible PTS precursors. A scoping study aimed at assessing the frequency and consequences of external initiating events (e.g., fires, floods, etc.) is detailed in a separate document [***Kolaczkowski-Ext***] and summarized in Section 9.4 of this report.

5.2.1 Step 1: Collect Information

During the initial phase of the PTS project, significant resources were expended to collect information regarding PTS in general and each plant in particular. General information-gathering activities included reviewing the basis for the current PTS Rule [10 CFR 50.61], and searching LERs for the years 1980–2000 to gain an understanding of the frequency and severity of real overcooling events [INEEL 00a]. Plant-specific information sources included the PRA analyses performed during the 1980s in support of the Integrated Pressurized Thermal Shock (IPTS) studies and the current PTS Rule [ORNL 85a, 85b, 86], as well as plant-specific design and operational information. Familiarity with all of this information provided the bases upon which the PRA analysis of each plant was conducted.

5.2.1.1 Generic Information

5.2.1.1.1 LER Review

The LER review identified a total of 128 events, demonstrating that overcooling events, or at least their precursors, do occur from time to time. These events are dominated by failure to properly control or throttle secondary side feed, a precursor that leads to relatively minor overcooling. Still, a few events have been associated with actual or potential loss of portions of secondary pressure control. These events predominantly involve equipment failures in the main feedwater, feed and steam control, and main steam systems. The results of the LER review also demonstrate that both active and passive (i.e., latent) human errors play a role, as many of the equipment failures were caused by improper maintenance or testing. Additionally, equipment in non-normal configurations can be an aggravating factor because contributing equipment faults have occurred that operators must identify, and for which they must compensate, to prevent overcooling.

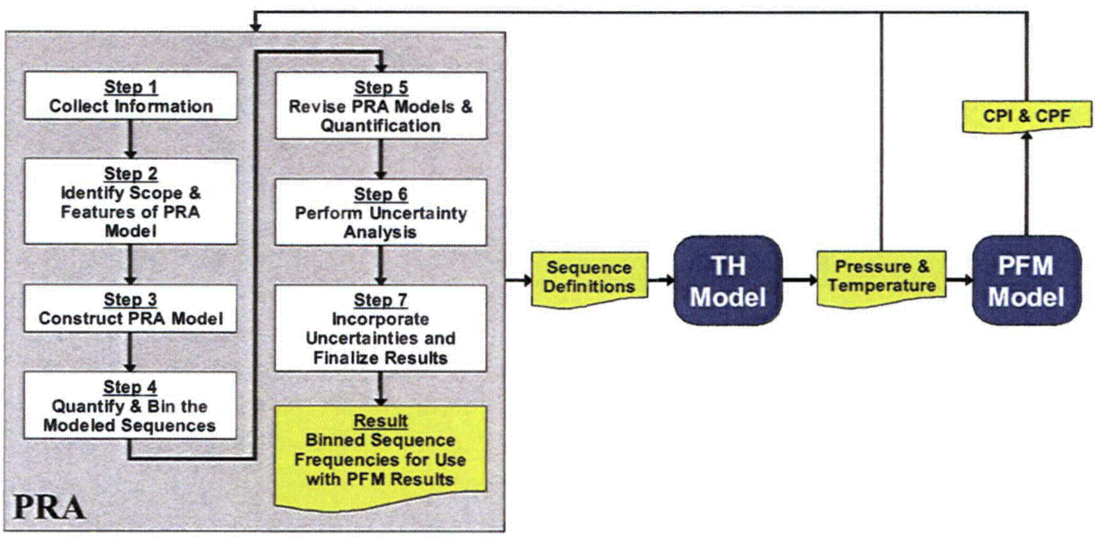

Figure 5.2. Diagrammatic representation of the PRA approach

5.2.1.1.2 Initiator Frequency and Probability Data

Initiator frequency and failure probability data are needed for initiating events, systems, and components as input to the PRA model. Since the goal of the PTS reevaluation project was to provide a PTS risk perspective for the operating fleet of PWRs, it was deemed appropriate to apply industry-wide PWR data for initiator frequencies and equipment failure probabilities in the plant-specific analyses. Hence, while the PRA model structure and the operational considerations it represented were based on plant-specific information, initiator frequencies and equipment failure probability data were generally based on industry-wide data.

Generic PWR data were obtained from two main sources. The first source, NUREG/CR-5750 [Poloski 99], summarizes industry-wide initiator experience for the years 1987–1995, along with failure probabilities for selected components. This information was updated twice. The first update was performed in an unpublished (at the time) addendum to NUREG/CR-5750 [Poloski 99], which extended the experience base through 1998. The second update dealt with loss-of-coolant initiators and was based on input intended to account for time-dependent material aging mechanisms that were not included in the experiential data [Tregoning 05]** The second source, NUREG/CR-5500 [Poloski 98], summarizes industry-wide experience for selected systems.

5.2.1.2 Specific Information

5.2.1.2.1 Previous PTS-PRA Analyses

Review of the PRA analyses performed in support of the IPTS studies and the current PTS Rule was another important input to the analyses.

Of particular relevance were NUREG/CR-3770 [ORNL 86] and WCAP-15156 [Westinghouse 99] (a more recent 1999 study) since these are past analyses of two of the plants covered in this work, Oconee 1 and Beaver Valley 1, respectively. Information in NUREG/CR-4183 [ORNL 85b] concerning H.B. Robinson, and NUREG/CR-4022 [ORNL 85a] concerning Calvert Cliffs, was also considered since these documents provided additional perspectives and analytical considerations useful to this work.

5.2.1.2.2 Plant-Specific Information

At the outset of each plant-specific analysis, information was requested from the licensees pertaining to plant design, procedures, training, and other aspects of plant operation relevant to building a PRA model for analyzing PTS. Information provided in response to these requests was supplemented by information gained during plant visits and ongoing interactions (oral, written, and email exchanges) with each licensee as the analyses evolved. In total, plant-specific information was derived from the following sources:

- summaries of any recent past actual overcooling events
- current PRA model and write-ups
- final safety analysis report sections
- piping and instrument diagrams and electrical drawings
- emergency and abnormal operating procedures
- miscellaneous system design-basis information and related material
- PTS-relevant training material
- operational aspects associated with hot-shutdown conditions
- observed multiple simulator exercises at each plant involving overcooling events that were setup and run as part of a collaborative effort between each licensee and the NRC contractor PRA analysts
- periodic interactions with the licensees regarding modeling details as each analysis evolved

** Generic initiator frequency and system failure probability information (as described in Section 5.2.1.1.2) was used for Oconee 1 and Beaver Valley 1, whereas the plant-specific PRA conducted by Consumers' Energy personnel (for Palisades) incorporated plant-specific information.

- feedback from each licensee as interim results from the analyses became available

5.2.2 Step 2: Identify the Scope and Features of the PRA Model

The format, structure, and details considered in the current analyses draw considerably from the earlier PRA analyses of PTS. Aside from recognition of the results and the reasons for the results from these past analyses, limitations and conservatism associated with the past studies were identified and, to the greatest possible extent, alleviated. Other improvements were adopted with the intent of increasing both the accuracy and comprehensiveness of the PRA representations of the plants. Table 5.1 summarizes the differences between the current PRA and that used to support the current PTS Rule. These differences fall into the following three major categories:

(1) greater refinement and detail in the current PRA
(2) more realistic treatment of operator actions in the current PRA
(3) use of the latest available data on initiating event frequencies and equipment failure probabilities in the current PRA

As noted in the table, since these improvements were made with the intent of increasing both the accuracy and comprehensiveness of the PRA representations of the plants, they neither systematically increase nor reduce the estimated risk from PTS.

In addition to identifying the areas for improvement of the PRA models that are addressed in Table 5.1, review of past PRA analyses of PTS provided information in four other areas:

(1) identifying the types of sequences that needed to be included in the PRA
(2) identifying what types of initiating events should be included
(3) identifying what functions and equipment status needed to be included
(4) identifying what human actions needed to be considered

The following four subsections describe the general features of the PRA models in each area. These features were established by a team approach involving analysts skilled in both system/sequence considerations and HRA considerations. Thus, the process for building PRA models involved integrated consideration of both system/sequence and human reliability factors.

5.2.2.1 Types of Sequences

The following list details the types of sequences included in the PRA models:

- overcooling scenarios
  - at full/nominal-power operation
  - under hot-shutdown conditions
- loss of RCS pressure scenarios
- virtually sustained RCS pressure scenarios (i.e., scenarios where RCS pressure initially decreases, necessitating start of HPI to restore pressure)
- late repressurization scenarios
- scenarios that provide immediate overcooling, as well as those that begin as loss-of-cooling scenarios (i.e., undercooling) and subsequently become overcooling scenarios

Two types of scenarios commonly modeled in PRAs are not included in the current PTS analyses (as previously discussed in Section 3.3.1):

(1) ATWS scenarios
(2) ISLOCA scenarios

Sequences resulting from such scenarios were not included, based on the following considerations. First, ATWS events generally initially begin as a severe undercooling event (i.e., there is too much power for the heat removal capability) and likely involve other failures to achieve an overcooling situation. While ISLOCAs, like the LOCAs modeled in the PTS study, could involve overcooling from the start of the event, significant ISLOCAs are often assumed to fail mitigating equipment in PRAs, which ultimately causes an undercooling event and core damage. Second, with typical ATWS and sizeable (not just small leaks), ISLOCA frequency estimates in the range of 10^{-5}/yr to 10^{-6}/yr (or even lower) and with the need

Table 5.1. Comparison of PRA analyses used in this study with the PRA analyses that supported 10 CFR 50.61

Difference Between Current PRA Analyses and the PRA Analyses that Supported 10 CFR 50.61			Effect on Calculated Risk	Comments
1	Refinement of Detail Considered by the Analysis	Slight expansion of the types of sequences and initiators considered	Increase	
2		Slight expansion of support systems both as initiators and as dependencies affecting equipment response	Increase	
3		Less gross binning of TH sequences because there are more "cases" into which to bin individual TH runs	Reduce	Current work features 50–100 cases per plant whereas previous studies only considered about a dozen cases (e.g., small steamline breaks and the opening of 1–2 secondary valves were previously binned with a large guillotine steamline break, thereby treating the cooling effects of the smaller scenarios much too conservatively).
4		External initiating events considered as potential PTS precursors	Increase	See Section 9.4.
5	Treatment of Operator Actions	Credit for operator actions is based on detailed consideration of numerous contextual factors associated with the modeled sequences, on multiple simulator observations at each plant, on the latest procedures and relevant training, and on numerous discussions with operating and training staffs. Detrimental acts of commission are also considered based on these same inputs, including procedural steps that call for operator actions that can exacerbate overcooling in certain situations.	Both Increase and Reduce	
6		A greater number of discrete operator action times are considered.	Reduce	Previous studies considered success or failure of operator action generally at 1 or 2 times after the start of the event. Currently, we consider up to 3 discrete times for some operator action.
7	Use of New Data	Includes the latest industry-wide (and some plant-specific) data for initiating event frequencies, equipment failure probabilities, and common-cause considerations.	Reduce	Largest factor is the significant drop in the initiator frequencies as a result of the decrease in scram rates resulting from institutional programs executed in the 1980s and 1990s.

for other failures to occur to possibly cause a continuing and serious overcooling situation, sequences involving ATWS or ISLOCAs should not be significant contributors to PTS risk. This is because other modeled scenarios that are likely to be significant contributors to PTS risk commonly have initiator frequencies in the range of 1/yr to 10^{-3}/yr, including other LOCAs that are already modeled in the PTS study.

5.2.2.2 Initiating Events

The following internal initiating events were included in the PRA models:

- small-, medium-, and large-break LOCAs
- transients commonly modeled in PRA analyses, including:
  - reactor-turbine trip
  - loss of main feedwater
  - loss of main condenser
  - loss of offsite power (including station blackout)
  - loss of support systems, such as AC or DC buses
  - loss of instrument air
  - loss of various cooling water systems
- steam generator tube rupture (SGTR)
- small and large steam line breaks with and without subsequent isolation

5.2.2.3 Functional/Equipment Considerations

The event trees in the PRA models that depict potential overcooling sequences are based on the status and interactions of four plant functions and associated plant equipment. Figure 5.3 presents a function-level event tree depicting the four functions and resultant general types of sequences treated in the PRA models. Each plant analysis features much more detailed event trees constructed at the initiator and equipment response level that incorporate the plant-specific design and operational features. These four functions (i.e., primary integrity, secondary pressure, secondary feed, and primary flow/pressure) are important to treat in the PTS analyses for the following reasons:

- <u>Primary integrity</u>: The status of this function influences the potential RCS pressure, which in turn influences the rate of cooldown (in some situations), the injection source capability, and the incoming and outgoing flow rates. All of these factors influence the vessel downcomer temperature.
- <u>Secondary pressure</u>: The status of this function influences the pressure and temperature in the RCS, since the RCS and the secondary side of the plant are thermal-hydraulically coupled in most scenarios. For example, a rapid drop in secondary pressure can cause rapid cooling of the RCS, affecting both the downcomer temperature and, potentially, the RCS pressure (depending on subsequent RCS injection flow and heat removal).
- <u>Secondary feed</u>: The status of this function influences the pressure and temperature in the RCS, since the RCS and the secondary side of the plant are thermal-hydraulically coupled in most scenarios. For example, overfeed can contribute to enhanced cooling of the RCS, affecting both the downcomer temperature and, potentially, the RCS pressure (depending on subsequent RCS injection flow and heat removal).
- <u>Primary pressure/flow</u>: The status of this combination of conditions influences the RCS pressure and flow conditions (forced flow or natural circulation) during the overcooling event as well as the nature of the injection that can add cooling to the vessel wall. The flow characteristics either exacerbate or mitigate flow stagnation, which can also affect the downcomer temperature.

In the plant event trees, the status of equipment relevant to each function is modeled in each PRA. This means that for each plant, the status of equipment relevant to each function is identified and included in the sequence modeling. For illustrative purposes, the following list summarizes the equipment associated with each function in the PRA models:

- <u>Primary integrity</u>: Status of pipe breaks, PORVs and associated block valves, pressurizer SRVs, and pressurizer heaters and spray considerations where appropriate.

- Secondary pressure: Status of steam line breaks, MSIVs and associated non-return valves, as well as related bypass and drain valve considerations where appropriate, turbine throttle and governor valves, steam dump/turbine bypass valves and associated isolation valves (if any), ADVs and associated isolation valves, and secondary steam relief valves (SSRVs).
- Secondary feed: Status of main feedwater (MFW), condensate, and auxiliary/emergency feedwater (AFW/EFW) systems.
- Primary pressure/flow: Status of high head safety injection, charging pumps and letdown considerations, accumulators/safety injection tanks, low head safety injection, and reactor coolant pumps (RCPs).

The status of other equipment that is relevant because of interactions with the equipment in this list is also modeled as appropriate. Such equipment includes the actuation and protection/isolation circuitry associated with the equipment in the preceding list, and support systems including cooling water, instrument air, and electric power and instrumentation. Heating and ventilation equipment was not considered in the analyses because of the slow effects of such a loss, and since the loss can often be easily identified and recovered.

5.2.2.4 Human Action Considerations

Plant records of overcooling events that have actually occurred demonstrate that operator actions and inactions can significantly influence the degree of overcooling and the RCS pressure for many types of overcooling events. Consequently, operator action directly influences, in both beneficial and detrimental ways, the potential for many types of event sequences to become serious PTS challenges. For example, early operator action to isolate the feed to a faulted (depressurizing or already depressurized) steam generator directly affects the amount of overcooling that occurs and/or how long such cooling is sustained. Consequently, any "realistic" PTS analysis needs to consider operator actions and inactions that influence overcooling sequences. Therefore, consistent with the guiding principles of this project to adopt best-estimate models and treat uncertainties explicitly whenever practicable, a rigorous treatment of human actions is included in the PRA models. The process to identify, model, and probabilistically quantify human factors derives largely from NUREG-1624, Revision 1 [NRC 00], which uses an expert elicitation approach. In this study, the experts included both NRC contractors and licensees. These individuals considered both errors of omission and acts of commission. This process identified several general classes of human failures (see Table 5.2), which have been incorporated into the PRA models. Table 5.2 also details which of the four primary functions (identified in Section 5.2.2.3) these failures most affect.

5.2.3 Step 3: Construct the PTS-PRA Models

The well-known and well-established event tree-fault tree PRA methodology was adopted as the basis for all plant-specific analyses. However, the modeling approach varied somewhat from plant-to-plant because of the order in which the plants were analyzed (lessons learned in the Oconee analysis impacted the Beaver Valley and Palisades modeling approach, for example). Additionally, the availability of information from TH and PFM at the time PRA modeling began influenced how the PRA model evolved. A summary is provided below of the modeling approaches for Oconee, Beaver Valley, and Palisades.

Table 5.2 General classes of human failures considered in the PTS analyses

Primary Integrity Control	Secondary Pressure Control	Secondary Feed Control	Primary Pressure/ Flow Control
I. Operator fails to isolate an isolable LOCA in a timely manner (e.g., close a block valve to a stuck-open PORV) II. Operator induces a LOCA (e.g., opens a PORV) that induces/enhances a cooldown	I. Operator fails to isolate a depressurization condition in a timely manner II. Operator isolates when not needed (may create a new depressurization challenge, lose heat sink...) III. Operator isolates wrong path/SG (depressurization continues) IV. Operator creates an excess steam demand such as opening turbine bypass/atmospheric dump valves	I. Operator fails to stop/throttle or properly align feed in a timely manner (overcooling enhanced or continues) II. Operator feeds wrong (affected) SG (overcooling continues) III. Operator stops/throttles feed when inappropriate (causes underfeed, may have to go to feed and bleed possibly causing overcooling)	I. Operator does not properly control cooling and throttle/terminate injection to control RCS pressure II. Operator trips RCPs when not appropriate and/or fails to restore them when desirable III. Operator does not provide sufficient injection or fails to trip RCPs appropriately (failure to provide sufficient injection is modeled as leading to core damage; thus, such sequences are not PTS-relevant)

5.2.3.1 PRA Modeling Differences Attributable to the Organization Constructing the Model

Both the Oconee and Beaver Valley PTS analyses use the same large event tree-small fault tree modeling format adopted by the PRAs that formed the technical basis for the current PTS Rule. This approach makes best use of the earlier work in constructing updated PRA models. Since the desired outputs do not require the explicit component faults for some systems included in the model, very simple system fault trees were used with corresponding system-level failure data to represent the failure or unavailability of these systems.

In contrast, a plant-specific PRA model developed by the licensee was used to provide the starting point for the PRA model of the Palisades plant used in this project. The licensee's PRA includes more detailed component-level fault trees for all the systems included in the PTS-PRA model. However, in all three analyses, the level of resolution in the results is sufficient for the purposes of assessing the PTS risk.

5.2.3.2 PRA Modeling Differences Attributable to the Order of Plant Analysis

The PRA model of Oconee was constructed first (at a time when feedback information from the TH analysis and from the PFM analysis was not yet available). Consequently, it was not possible to screen out of the model overcooling sequences having a benign TH response or very low estimated conditional probabilities of through-wall cracking (from the PFM analysis). Hence, the Oconee PRA model contains virtually all the possible overcooling sequences with virtually no *a priori* screening out of "low significance" sequences. Subsequent feedback from both TH and PFM verified that many of the sequences included in the Oconee model could justifiably been omitted from the PRA model.

Work on the Beaver Valley PRA model was initiated after the Oconee model had been constructed, at a time when the Oconee analysis results, while still evolving, were generally well-understood. Also, as the Beaver Valley PRA model was being constructed, some advanced TH and PFM results were already available for Beaver Valley sequences (identified from "lessons learned" from the Oconee analysis). Consideration of this TH/PFM information on Beaver Valley permitted *a priori* screening of the following general categories of sequences from the Beaver Valley PRA model:

- Sequences involving certain combinations of stuck-open pressurizer PORVs or SRVs were not modeled.
- Sequences involving certain combinations of secondary valve and simultaneous pressurizer PORV/SRV stuck-open events were not modeled.
- Sequences involving only secondary valve (single or multiple) stuck-open events were not modeled.
- Sequences involving overfeed of various steam generator (SG) combinations were not modeled.
- Sources of secondary depressurization downstream of the MSIVs were not explicitly modeled.
- SGTR sequences (including those involving lack of proper feed control and even with RCPs shutdown, possibly inducing RCS loop stagnation) were not modeled.
- Other sequences were screened from modeling on a case-by-case basis if the sequence frequency could be conservatively estimated as less than $\sim 10^{-8}$/yr. This screening limit was used because, when coupled with the maximum CPTWC (i.e., failure) calculated for any type of sequence (in the 10^{-3} range) a TWCF of $<10^{-11}$/yr would be generated. Such frequencies would clearly not be important to the overall PTS results, since some other sequences were known to involve TWCFs in the 10^{-8}/yr range.

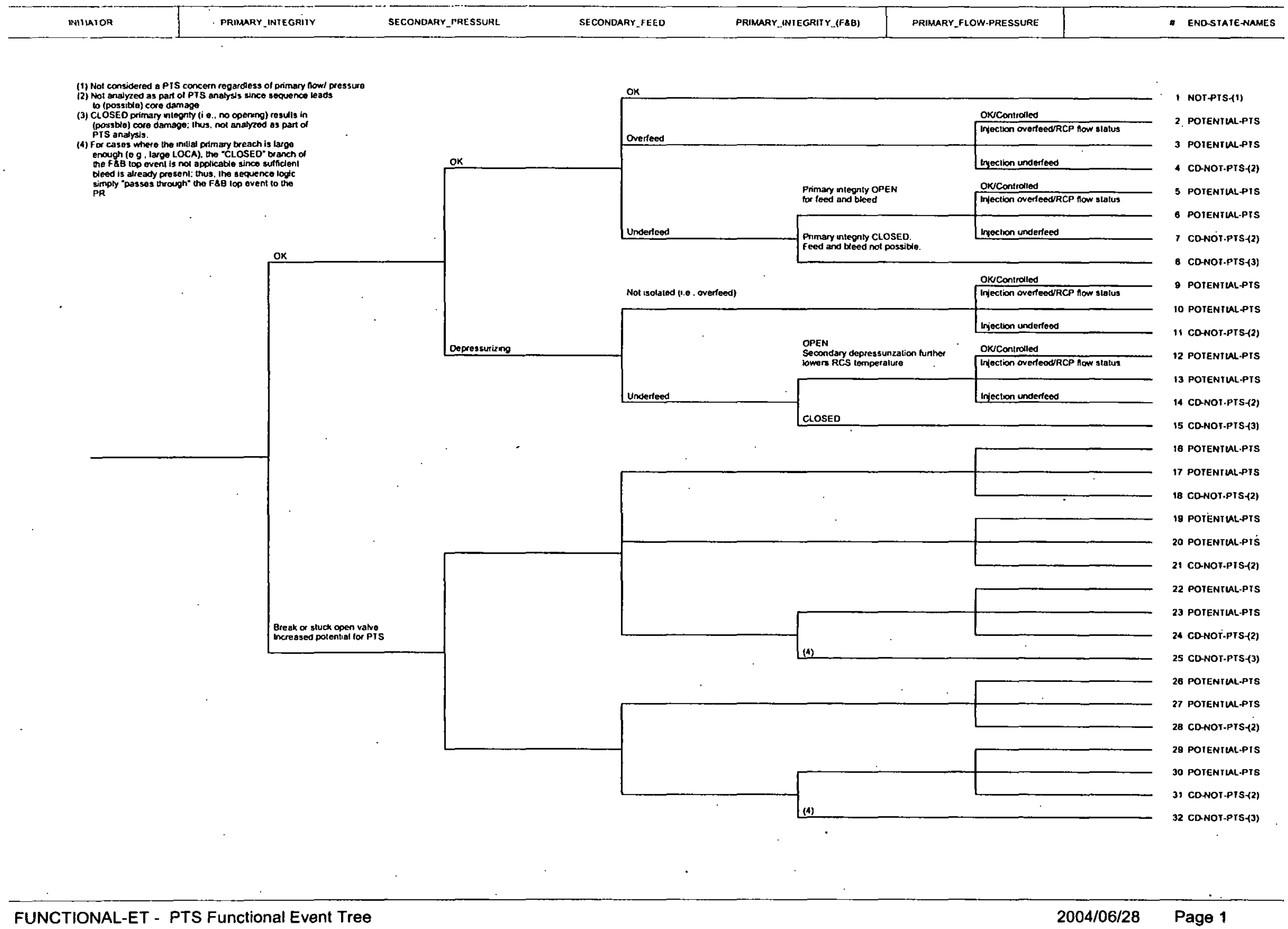

Figure 5.3. Functional event tree as the basis for PTS PRA analysis

Because the Palisades model was built starting with an already established licensee component-level PRA model with overcooling sequences, it is the most detailed model of the three. This preexisting Palisades model was augmented by the licensee, on the basis of NRC contractor review and input, to include possible scenarios and other factors not already in the preexisting model. Consequently, the "lessons learned" from the Oconee PRA also influenced the Palisades PRA model. In general, the Palisades PRA model addresses the same types of initiators and sequences, as do the Oconee and Beaver Valley models. However, the initiating event frequencies, equipment failure probability data, and human failure estimates are specific to Palisades.

5.2.4 Step 4: Quantify and Bin the PTS-PRA Modeled Sequences

For each plant, two conditions were modeled: full operating power and hot zero power (HZP). As identified in Section 5.2.3.2, little information was available to screen out potential PTS sequences for Oconee. Thus, because of a SAPHIRE code [SAPHIRE] limitation (i.e., the inability to store more than 100,000 sequences in a database); it became necessary to produce separate SAPHIRE models for full-power and HZP. Once the models (i.e., the event trees and fault trees) were constructed, the SAPHIRE code was used to generate the sequence logic for each event tree, and to solve the resulting sequences (90,629 sequences for each model) with no truncation attributable to frequency.

Given the number of potential PTS sequences for Oconee (181,258), it was necessary to group (i.e., bin) sequences with like characteristics into representative TH cases that could be analyzed with the RELAP TH code [RELAP].

Initial bins were constructed by developing event tree partitioning rules in SAPHIRE, and then applying those rules to produce the TH bins. Development of the partitioning rules required the analysts to examine the TH information available from preliminary analyses to identify the characteristics that would be important to the binning process.

Using this information, the analysts then made judgments as to whether existing TH characteristics could be used to represent new groups of sequences. If the analysts judged that existing characteristics were appropriate, either because they matched the examined sequences exactly or because the TH conditions from the new sequences were expected to be similar to, but not be worse than, the conditions from the existing analysis, the uniquely defining characteristics associated with the existing TH analyses were written in rule form for application in SAPHIRE. For those cases where the analysts were sufficiently unsure as to the appropriateness of using existing characteristics, new TH characteristics were identified. These new sets of characteristics were discussed with the TH analysts. If those discussions led to the conclusion that the expected TH conditions could be sufficiently different from prior TH analyses and the frequency of occurrence of the conditions was such that they could not be "added" to some existing TH bin without being unnecessarily conservative, a new TH calculation (and hence, TH "case") was identified. The TH characteristics associated with this new calculation were then written in rule form for subsequent application in SAPHIRE.

This iterative process continued until all accident sequence cut sets were associated with a specific TH bin. Thus, the final application of the developed rules involved the examination of each sequence cut set to determine which rule the cut set met, the subsequent "tagging" of the cut set, and the gathering of like-tagged cut sets into initial TH bins. Once all cut sets were gathered into the initial TH bins, the bins were re-quantified using a truncation limit of 10^{-10}/yr.

For Beaver Valley, essentially the same process was followed. The major difference between the Oconee and Beaver Valley analyses was in the number of sequences developed and solved (a total of 8,298 sequences for Beaver Valley for power and HZP). As discussed in the previous subsection, knowledge about what was and was not important in the Oconee analysis was used with preliminary sequence frequency estimates and CPTWC results from early Beaver Valley TH and PFM calculations to minimize the number of sequences actually modeled in the corresponding SAPHIRE databases. Given the significantly lower number of sequences, no truncation was performed on the initial TH bins.

For Palisades, the process was somewhat different, in that the SAPHIRE model included both power and HZP sequences in the same database (only 3,425 sequences total) and the sequences were solved using truncation value of a 10^{-9}/yr. Another difference between the Palisades and Oconee or Beaver Valley analyses was how the TH bins were created. In the Palisades analysis, each sequence end state was defined to a specific TH bin and all resulting cut sets were placed in the defined bin. (Note: use of this binning process rather than the one used in the Oconee or Beaver Valley analyses did not have any significant impact on the results, which are similar across the three plant analyses. It is simply that the binning process was somewhat less refined for bins that, based on experience with Oconee and Beaver Valley, were not expected to significantly influence the estimated TWCF values.)

5.2.5 Step 5: Revise PTS-PRA Models and Quantification

With preliminary results available, reviews were conducted by both licensee and internal project staff. This allowed for formal feedback from the licensee with regard to the PTS-PRA models, inputs, assumptions, and results, and gave the analysts an opportunity for self-review of the PRA performed to date. The purposes of the reviews were to determine the following:

- whether inaccuracies existed in the models, and whether additional potential PTS sequences needed to be modeled
- whether additional TH bins should be created to reduce unnecessary conservatism based on new or updated information obtained from preliminary CPTWC calculations or needs identified by the uncertainty analysis
- which human actions were associated with the important TH bins
- which of those human actions should be reexamined to produce even more realistic (i.e., less conservative) HEPs
- what combination of the above could be accomplished within the constraints of the project

For Oconee, the reviews identified the following needs:

- to add one more type of potential PTS sequence
- to add more TH bins to address uncertainty issues and reduce conservatism (note that conservatism is reduced by not having too many sequences represented by a bin that is described by plant conditions that are too conservative for the actual conditions of the sequences)
- to reexamine some human actions to produce updated HEPs to account for more specific conditions

The Beaver Valley reviews identified the following needs:

- to add more TH bins to address uncertainty issues and reduce conservatism
- to reexamine some human actions to produce updated HEPs to account for more specific conditions

Because the Palisades analysis was performed by the utility, the results of the review described here dealt only with issues identified by the NRC review of the licensees' PTS model. The review identified the following needs:

- to add more break sizes to the LOCA class of initiating events
- to modify probabilities for a few selected basic events
- to add more TH bins to address uncertainty issues

It should be mentioned that while formal reviews were performed, such as during the second plant visits at both Oconee and Beaver Valley, informal periodic reviews were conducted through frequent written and oral communications among the licensees and project staff. Appropriately, the models were revised and requantification was performed on the basis of these licensee inputs and as a result of self-evaluations by the project staff.

5.2.6 Step 6: Perform Uncertainty Analyses

The primary objective of the PRA portion of the PTS analyses was to produce frequencies of the set of representative plant responses to plant upsets (i.e., scenarios). These scenarios involve mitigating equipment successes and failures, as well as operator actions that result in various degrees of overcooling of the internal reactor vessel downcomer wall. The major areas of uncertainty associated with the PRA can be grouped into two broad categories:

- modeling of the representative plant scenarios
- estimation of the frequency of each modeled scenario

These areas of uncertainty and the techniques used to deal with the uncertainties are discussed in the following two subsections.

5.2.6.1 Modeling of Representative Scenarios to Characterize Aleatory Uncertainty

Each scenario in the PRA is represented by a collection of events described by the logic of the event tree and relevant fault trees for each initiating event identified in the analysis. The model initially assumed binary logic (e.g., the valve either fully recloses or sticks wide open with no intermediate states) for the events. The only explicit modeling of event timing involved the timing of operator actions (i.e., failure to take an action is modeled as failure to take that action in multiple discrete times — for example, by 10 minutes, by 20 minutes — each with a probability). Most uncertainties with regard to model structure (e.g., completeness, intermediate states) were not quantified. However, where deemed potentially important, a few aleatory uncertainties were addressed by purposely changing the model and assigning a probability to the applicability of the model change. Each of these changes became a different scenario (TH bin) with an associated frequency (e.g., area associated with a stuck-open SRV reduced 30%, timing of enclosure of a stuck-open SRV (3,000 s *vs.* 6,000 s), actual break size of small and medium LOCAs). Since it is unknown which scenario will occur following an initiating event, the complete set of scenarios, as represented by the event trees, characterize a large part of the aleatory uncertainty associated with the occurrence of a PTS challenge. The most important of these uncertainties that were explicitly handled in the analyses are addressed further in the next step, Step 7.

In addition, there is the overall uncertainty regarding the completeness of the PRA model(i.e., have all scenarios that potentially lead to PTS conditions been identified and modeled). This uncertainty issue was addressed non-quantitatively through both internal (i.e., NRC and its contractors) and external (i.e., licensee) reviews of the PRA model. As a result of this peer review process, the models are expected to produce a sufficiently complete set of potential PTS sequences and thus, any incompleteness in the models is expected to have a negligable effect on the results.

5.2.6.2 Quantification of Scenario Frequencies to Characterize Epistemic Uncertainty

Each scenario from the set of modeled scenarios is the interaction of what are treated as random events:

- initiating event (plant upset)
- series of mitigating equipment successes/failures (e.g., MFW trips, AFW starts, ADV challenges when one sticks open)
- operator actions (e.g., fails to close the ADV isolation valve by 20 minutes after the ADV sticks open)

Thus, the occurrence of each scenario is random, and the frequency of each scenario is obtained using the following equation:

Eq. 5-1

$$f_{scenario} = f_{initiating-event} \cdot Py_{equipment-response} \cdot Py_{Operator-Actions(s)}$$

where f denotes a frequency and Py denotes a probability.

Each of the variables used to obtain the scenario frequency has an epistemic uncertainty described by a distribution. The source of this information came primarily from the input data used in the analysis (i.e., the addendum to NUREG/CR-5750 [Poloski 99] for Oconee and Beaver Valley, and the plant-specific data used in the Palisades analysis). For a few specific model inputs, other data sources were also used to derive these uncertainty estimates. For the HEPs, both best-estimate values and uncertainty ranges and distributions were derived through the expert elicitation processes carried out in the human reliability analyses. Latin Hypercube sampling techniques were used to propagate these epistemic uncertainties to generate a probability distribution for each scenario frequency. Thus, the frequencies provided by the PRA analysts to the PFM analysts were described by histograms representing the resulting frequency distributions. In this way, these PRA uncertainty distributions were propagated through and combined with the PFM uncertainties to ultimately derive uncertainty distributions in the estimated TWCFs.

5.2.7 Step 7: Incorporate Uncertainty and Finalize Results

This section discusses important uncertainties (largely aleatory in nature) specifically addressed in the PRA and describes how each was handled. As described in the previous subsection, epistemic uncertainty in the frequency for each of the final TH bins was estimated using Latin Hypercube sampling techniques and is not described in this subsection.

The uncertainties discussed below were dealt with quantitatively; however, the degree of resolution associated with each specific uncertainty was limited. These uncertainties include:

- size of the LOCA within a LOCA category plus other factors (e.g., initial injection water temperature)
- size of the opening associated with single or multiple stuck-open SRV(s)
- time at which a stuck-open SRV recloses
- time at which operators take or fail to take action

These uncertainties were highlighted for specific treatment in the analysis based on (1) the scenarios found to be most important to the PTS results, and (2) a series of uncertainty analyses performed by the University of Maryland (UMD) project team members on many of the inputs and parameters potentially affecting the PTS results to see which uncertainties would most affect those results. The specific UMD analyses are discussed in [***Chang***]. The results of that work concluded that the above uncertainties are sufficiently important that they needed to be treated explicitly in the PRA model. These uncertainties and how they were addressed are discussed in the following paragraphs.

The actual break size of a LOCA for a specific LOCA class (i.e., small, medium, or large) can be any point on the spectrum of sizes defined by the two end points for that class. In addition, other factors (e.g., initial injection water temperature, break location, and injection flow rate) can contribute to the overall PTS model uncertainty, since these factors along with the specific break size affect the rate of cooling and subsequent plant response. Numerical probability results from the UMD uncertainty analysis were used to model and estimate the importance of the various modeling uncertainties examined in the UMD analysis, including different break sizes within a given class (which were assumed to be uniformly distributed). These numerical analyses provided a spectrum of different plant TH responses arising from uncertainties in these key parameters including break size. This spectrum of results was then represented by a number of discrete cases to cover the total spectrum of results (typically, five cases for small LOCAs, three for medium

LOCAs, and one for large LOCAs). Each case was assigned a probability by the UMD analysts based on how much of the total spectrum the discrete case represented. Each discrete case was assigned a new TH case number with corresponding TH curves, and the frequency of each new case was adjusted using the UMD assigned probability for that case. This was accomplished through the following steps:

- gather all cut sets from all sequences generated for a specific LOCA class into one bin
- reproduce the gathered cut sets a specified number of times corresponding to the number of discrete cases defined to represent the spectrum of results
- modify each set of reproduced cut sets to include the probability assigned to that discrete case

Thus, the new modified cut sets account for the uncertainty associated with various parameters examined in the UMD analysis, including possible variation of break sizes within a given LOCA class.

Just as with the LOCAs, the size of the opening associated with a stuck-open SRV can vary from sizes that are not PTS-significant to the valve fully stuck open. To deal with this and other relevant issues examined in the UMD analysis, the cut sets (and their associated frequencies) from stuck-open SRV sequences were modified to include a fraction that represented the uncertainty from the UMD work. In this case, it was assumed that the SRV opening size is uniformly distributed (any specific opening is equally likely) and the resulting fraction was included in the sequence frequency estimates to account for that fraction of possible SRV size openings that would be sufficient, from a cooling perspective, to be potentially important.

The time at which a stuck-open SRV recloses is unknown and can occur at any point after the valve sticks open. To approximate this, the frequencies associated with stuck-open SRV sequences with subsequent closure of the SRV were divided equally between two specific SRV reclosure times (i.e., 3,000 s and 6,000 s). These two time points were chosen after reviewing stuck-open SRV TH conditions. The 6,000 s point was chosen to coincide with the time when the change in downcomer wall temperature had "flattened out." The 3,000 s point was chosen to coincide with the time when sufficient cooling had occurred to the downcomer wall such that PTS could become an issue. Use of these two times provides a mechanism for determining some measure of the uncertainty associated with reclosure of stuck-open SRVs. Each case was assigned a 50% chance of occurring[††].

Just as the time at which a stuck-open SRV recloses is unknown, so too are the times at which operators perform actions. To address this issue, the times at which selected operator actions (i.e., those believed to be relatively important to PTS) were performed was varied. Typically, two or three different times were chosen to represent the uncertainty in when the action would be performed. Once the times were defined, typically (1) as early as could be expected, (2) as late as possible that would still affect the outcome, and (3) for some actions, some intermediate time, the probability of failing to perform the action by the specified time was developed. Use of these operator action times provides a means of estimating the uncertainty associated with when the operators actually perform their actions.

For the Oconee analysis, all issues identified above were incorporated into the analysis. For the Beaver Valley and Palisades analyses, results from the UMD analysis indicated that little uncertainty came from the sequences involving stuck-open SRVs that remained stuck open; thus, no modifications were made to those types of sequences in the Beaver Valley and Palisades analyses. However, all other

[††] Subsequent sensitivity analyses demonstrated that the 6,000 s time is nearly the worst time from a PTS challenge point of view. The worst conditional probabilities of vessel failure typically occur if the SRV is assumed to close at 7,000 s or a little beyond, but the vessel failure probabilities are within a factor of ~2 of those calculated for 6,000 s. See also the discussion in Section 8.5.3.3.2 and Comment #76 in Appendix B.

modifications were made for the analyses of Beaver Valley and Palisades.

6 Thermal-Hydraulic Analysis

6.1 Introduction and Chapter Structure

This section describes the thermal-hydraulic analysis performed on the Oconee-1, Beaver Valley-1, and Palisades nuclear power plants:

- The Oconee-1 coolant system is a lowered-loop, Babcock & Wilcox design with two steam generators, two hot legs, and four cold legs.
- The Beaver Valley-1 coolant system is a Westinghouse design with three steam generators, three hot legs, and three cold legs.
- The Palisades coolant system is a Combustion Engineering design with two steam generators, two hot legs, and four cold legs.

The discussion in this section begins in Section 6.2 with a general discussion of thermal-hydraulic issues for transients that contribute to the risk of vessel failure attributable to reactor coolant system overcooling. This section is followed by a description of the RELAP5 code and its implementation in the TH analysis in Section 6.3. The general structure of the RELAP5 code and an overview of the physical models contained in RELAP5 are included in this section.

The modeling of the plant primary and secondary systems including model initialization is discussed in Section 6.4. Section 6.5 presents an overview of the types of transients simulated, while Section 6.6 presents an overview of the results.

A summary discussion of the experimental validation of RELAP5 is presented in Section 6.7. Section 6.8 presents a discussion of sensitivity analysis and the analysis of uncertainty.

6.2 Thermal-Hydraulic Analysis of PTS Transients

The PTS analysis combines the thermal-hydraulic response of the reactor coolant system with the thermal response of the reactor vessel. These parameters, when combined with the PFM analysis, are used to estimate the probability of unstable crack propagation leading to possible vessel failure. The principal purpose of the TH analysis is to generate the time histories for key parameters for use in the FAVOR fracture mechanics analysis code, for various plant transients. The parameter responses passed to the FAVOR code are the reactor vessel downcomer fluid temperature, primary system pressure, and heat transfer coefficient on the inside of the vessel wall.

A wide variety of transients that could contribute to the risk of vessel failure were analyzed. These transients include reactor system overcooling attributable to a LOCA or a stuck-open primary side relief valve, a component failure that results in an uncontrolled release of steam from the secondary side (e.g., MSLB or stuck-open secondary side relief valve), or a control system failure that results in overfilling the steam generators. Combinations of failures are also of concern and were analyzed. The transients analyzed were defined from an event and fault tree analysis to determine possible transients (or accident sequences) and their frequencies of occurrence (see Chapter 5). Each transient and its associated frequency of occurrence are factored into the PFM analysis to estimate the risk of vessel failure.

As part of the analysis, key parameters and processes that affect the reactor vessel downcomer fluid temperature, primary system pressure and heat transfer coefficient on the inside of the vessel wall were defined. The Phenomena Identification and Ranking Table (PIRT) methodology was used to identify the most important processes that impact reactor system thermal-hydraulic response to a transient [Shaw 88, Zuber 89].

The PIRT methodology considered number of phenomenological processes and reactor system and plant boundary condition parameters. Examples of phenomenological processes include wall-to-fluid heat transfer in the downcomer, natural circulation flow, and steam generator heat transfer. Boundary condition examples include ECCS water injection temperature, break location (in the case of a LOCA), and timing of valve reclosure (for transients involving a stuck-open relief valve).

The PIRT methodology has been applied to the Yankee Rowe and H.B. Robinson plants for PTS events. In the case of Yankee-Rowe, the PIRT is based on a 1.3-in. [3.3-cm] cold leg break. This break is approximately equivalent to a 2.8-in. [7.1-cm] break when scaled up to the larger diameter of the three current plants. The H.B. Robinson PIRT was based on a 2-in. [5.08-cm] hot leg break. A PIRT was also performed as part of the assessment of RELAP5/MOD3.2.2Gamma against data from tests performed at experimental facilities that considered the wide variation in thermal-hydraulic conditions that can occur in PTS transients. This assessment is discussed in the RELAP5 PTS Assessment Report [***Fletcher***]. Table 6.1, excerpted from that report, provides a list of the parameters and processes considered and their ranking. This list considers a broader view of the types of transients that were analyzed, rather than focusing on a single transient.

The PIRT table presented in Table 6.1 was used to focus the RELAP5/MOD3.2.2Gamma assessment on the following parameters that can be observed in the experiments:

- break flow
- primary system pressurization
- natural circulation/flow stagnation
- boiler-condensation mode and reflux condensation
- mixing in the downcomer
- condensation, mixing, and stratification in the cold leg
- integral system response

These parameters were selected because of their primary or secondary importance on downcomer conditions. The following three phenomena were deemed to be most important to downcomer conditions during PTS events:

- natural circulation/flow stagnation
- integral system response
- primary system pressurization

Natural circulation/flow stagnation is important because if loop flow continues (or restarts during a transient), warm water at the average coolant system temperature will be flushed through the reactor vessel downcomer, increasing the downcomer fluid temperature. In contrast, if the loop flow is stagnant, the cold ECCS water will not be mixed with water from other parts of the reactor system and the downcomer temperature will be colder relative to the natural circulation case. Integral system response is important because the ECCS injection behavior (flow rates, timing, and to some extent temperatures) are functions of the overall system behavior. System pressurization is itself a primary figure of merit in the PTS analysis. The other phenomena listed above were considered because of their effect on these main phenomena or because they potentially impact downcomer conditions. Fluid mixing in the downcomer is among these phenomena. These phenomena as well as the overall RELAP5/MOD3.2.2Gamma assessment are further discussed in Section 6.7.

6.3 RELAP5 Code Description

6.3.1 RELAP5 Analysis Process

The RELAP5/MOD3.2.2Gamma computer code released in June 1999 was used for transient analysis to determine downcomer fluid conditions. The RELAP5 code was developed for best-estimate transient simulation of light-water reactor coolant systems during postulated accidents and transients. The code models the coupled behavior of the reactor coolant system, core, and secondary side system for loss-of-coolant accidents and operational transients such as anticipated transients without scram, loss of offsite power, loss of feedwater, and loss of flow. With RELAP5, a generic modeling approach is used that permits simulating a variety of thermal-hydraulic systems. Control system and secondary system components are included to permit modeling of plant controls, turbines, condensers, and secondary feedwater and steam systems.

Figure 6.1 and Figure 6.2 present top-level schematics of the RELAP5 modeling process and code structure.

The RELAP5 model input development process is portrayed on the left side of Figure 6.1. When modeling fluid systems with RELAP5, the physical systems are subdivided into networks of fluid cells that are interconnected by junctions. The RELAP5 model represents the fluid volumes, flow areas, path lengths and other characteristics of the physical system using a nodalization scheme of the fluid cells and junctions.

A RELAP5 input model is developed by assembling data that describes the thermal-hydraulic parameters of the physical system, such as pipe lengths, flow areas, volumes, and coefficients that simulate the pressure losses for flow through irregular geometry. The input model also requires the user to select various modeling options appropriate for the specific application, such as the critical flow model to be used and the locations in the model where it is to be activated.

The user must specify the initial conditions (pressures, temperatures, flow rates, etc.) for every model feature. In practice, RELAP5 plant transient event simulations begin from conditions that represent steady-state conditions. The initial condition input specifications cannot be made to an acceptable degree of accuracy using a manual approach. Instead, the user typically enters initial conditions that only approximate the desired ones and executes the plant model with RELAP5 in a steady-state mode until a smooth solution is attained with initial conditions that acceptably represent steady-state conditions. RELAP5 transient event simulations are then begun, starting from the accurate set of RELAP5-calculated steady-state initial conditions.

The user must specify the thermo-physical properties (such as thermal conductivity and heat capacity) for the materials of the model features that represent structures.

The user also defines the timing information for the calculation. This includes the problem start time, problem end time, a range of time step size and the interval between data points for the calculation printed and plotted output.

The RELAP5 code is executed using the input model described above and the code execution process is summarized in Figure 6.2. RELAP5 simultaneously solves the equations for the conservation of mass, momentum and energy for the fluid conditions and flows among the cells and junctions in the nodalization grid.

The code employs a set of steam tables to represent the steam, water and noncondensible gas physical properties (pressure, temperature, void fraction, quality, density, internal energy, etc.) in each cell as the transient calculation proceeds.

The transient calculation is advanced in time using discrete time steps, the selection of which is made to assure a stable solution. The code automatically makes this selection of time step size within the minimum and maximum time step range that is defined by the user via the input.

Table 6.1 Phenomena Identification and Ranking Table for Pressurized Thermal Shock in PWRs

Rank	Description	Comments
1	Break flow/diameter (or valve capacity)	Importance of LBLOCA has increased, pressure is less important
2	ECCS flow rate (Accumulator, HPI, LPI)	State on/off, shutdown head of pumps, accumulator initial pressure
3	Operator actions	Includes operating procedures, RCP trip, HPI throttling, feedwater isolation, etc.
4	Time of stuck valve reclosure	Pressurizer safety relief valves which reclose after sticking open
5	Plant initial state	Hot full power vs. hot zero power operation
6	Break location	Primary LOCA (hot leg, cold leg), MSLB (inside/outside containment; upstream/downstream MSIVs), SGTR
7	Unique plant features/design	Difference in steam generator design, number of loops, vent valves, etc.
8	Vessel to downcomer fluid heat transfer	Affects the rate at which heat is transferred from the vessel wall to the downcomer fluid. Affects risk of vessel failure in non-conduction limited situations.
9	ECCS injection temperatures	Seasonal/operational variations
10	Sump recirculation	ECCS temperature/flow changes after RWST drained
11	Feedwater control (or failure)	Post trip main feedwater behavior, steam generator overfeed events
12	Feedwater temperature	Oconee (using AFW instead of MFW during transient).
13	Reactor vessel wall heat conduction	In conjunction with vessel to downcomer fluid heat transfer, affects the rate at which heat is transferred from the vessel wall to the downcomer fluid. Important particularly on those situations where heat transfer from the wall is conduction limited.
14	Loop flow upstream of HPI	Scenario dependent, not as important for LBLOCAs
15	ECCS – RCS mixing in cold legs	Affects potential for formation of cold plumes in the downcomer
16	Flow distribution in downcomer	Affects mixing and potential for formation of cold plumes in the downcomer
17	Jet behavior, cold leg pipe to downcomer	
18	Loop injection upstream of safety injection	Scenario dependent, important for MSLB, not for LBLOCA
19	Steam generator energy exchange	
20	Timing of manual RCP trips	Risk of vessel failure lower if pumps remain on. Operator assumed to trip RCPs in accordance with plant procedures.
21	Interphase condensation and non-condensibles	RELAP5 overprediction of condensation
22	DC to core inlet bypass	Less important for LBLOCAs
23	Downcomer to upper plenum bypass	Less important for LBLOCAs
24	Upper head heat transfer coefficient under voided conditions	Less important for LBLOCAs

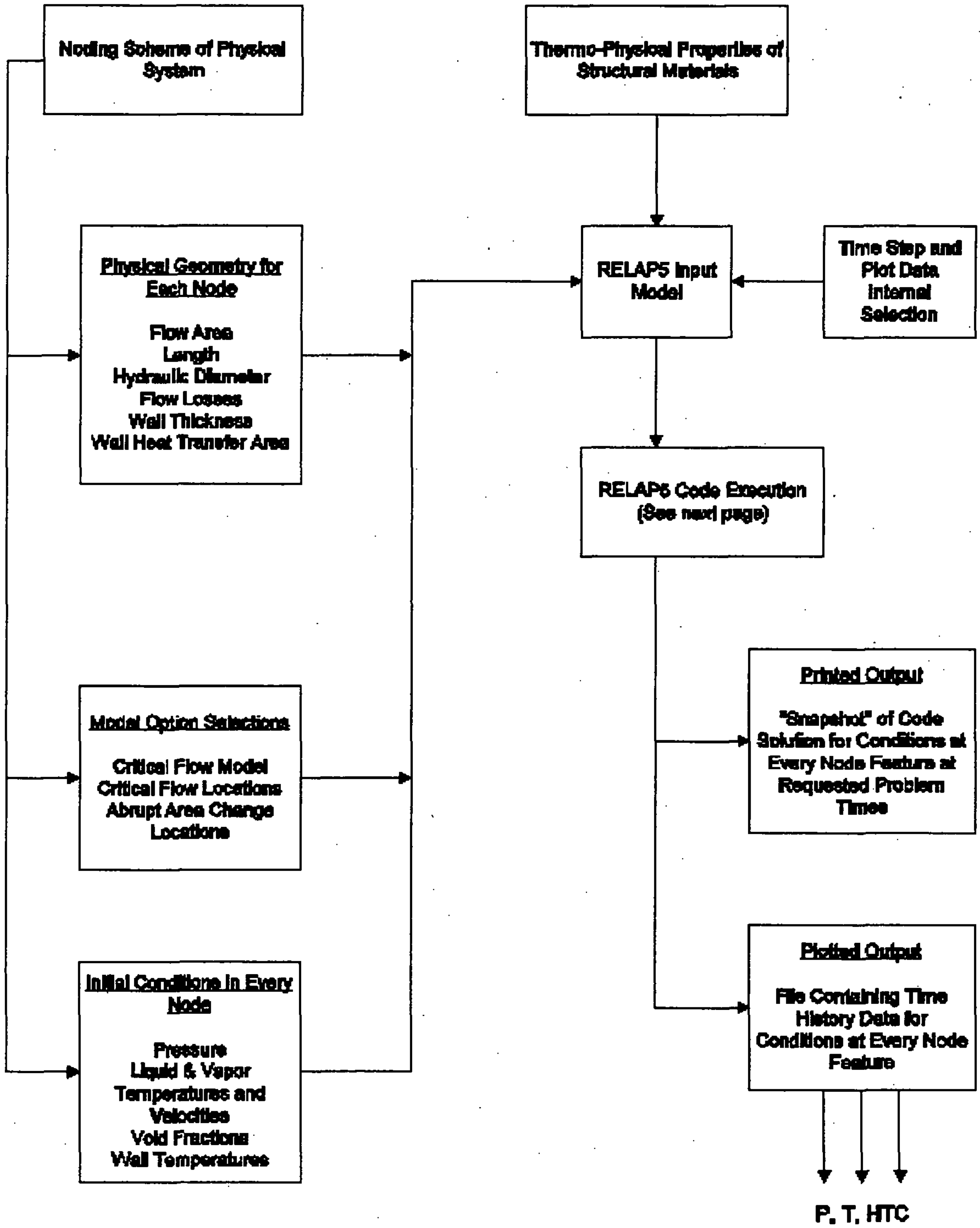

Figure 6.1. Schematic of RELAP5 Input and Output Processing

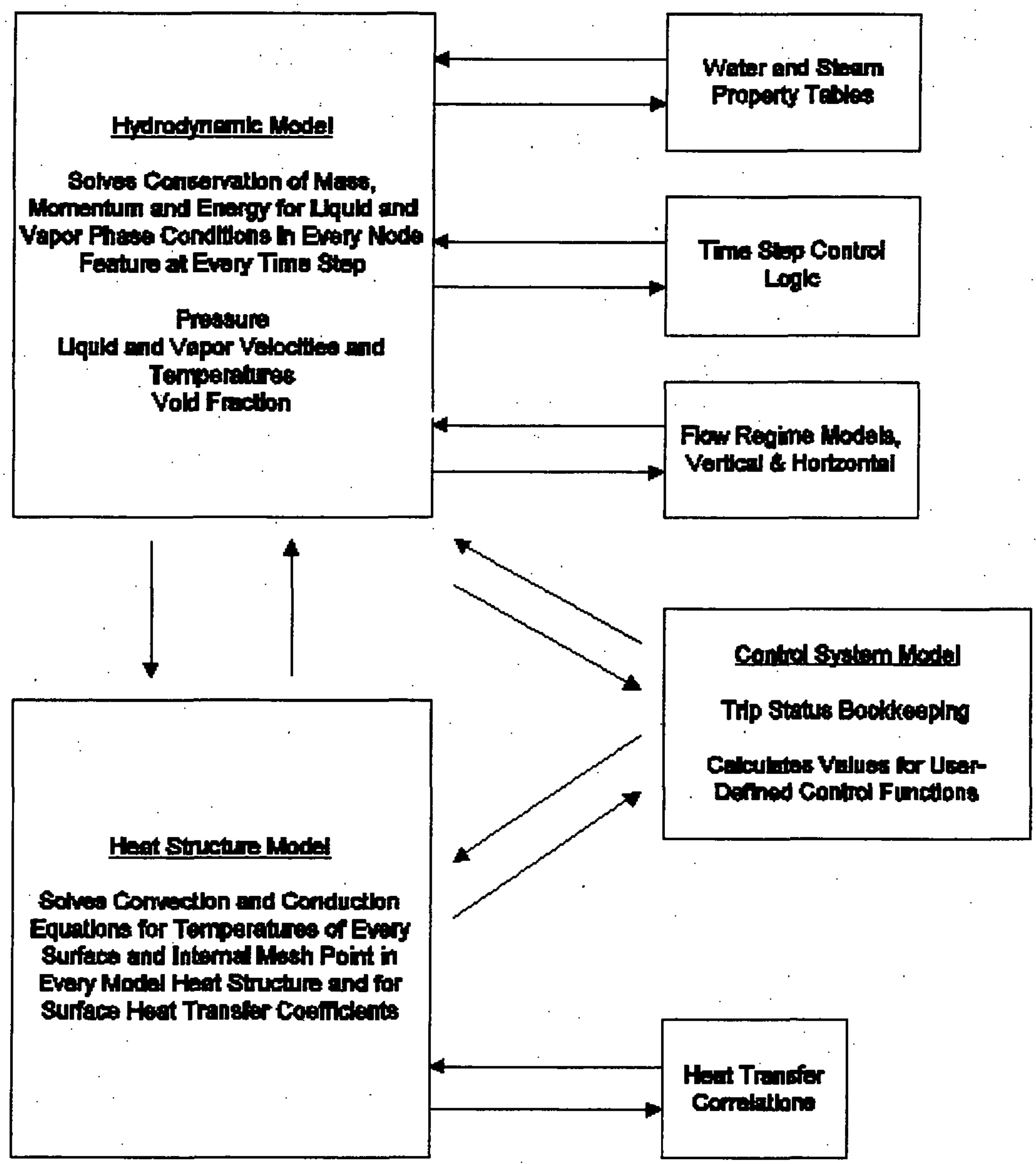

Figure 6.2. Schematic of RELAP5 Execution Processing

RELAP5 is based on a hydrodynamic model for single-phase and two-phase systems involving steam-water-noncondensible fluid mixtures in enclosed regions. The model is non-homogeneous (that is, the liquid and vapor phases at the same location may flow at different velocities) and non-equilibrium (that is, the liquid and vapor phases within the same region may exist at different temperatures).

The RELAP5 solution is based on a staggered-mesh arrangement in which the conditions representing the fluid state (pressures, temperatures, void fractions, etc.) are calculated at the center of each cell and the fluid flow behavior (liquid and vapor velocities and mass flow rates) is calculated at the junctions between the cells. The RELAP5-calculated behavior, therefore, represents flow of liquid and vapor from the center of one cell, through one-half of the length of that cell to the interconnecting junction, and through one-half of the length of the adjacent cell to the center of the adjacent cell.

The flow through the cell regions of the flow path is subjected to the influence of losses attributable to wall friction, and the flow through the junctions may be subjected to the influence of losses attributable to the presence of irregular configurations, such as pipe bends, valves, and orifices. In addition, the model considers the effects of friction between the liquid and vapor phases.

Flow regime maps that provide characteristics for fluid behavior in vertical and horizontal cell orientations are used to determine the distribution of steam and liquid within each cell. This distribution is considered consistently throughout the RELAP5 model (for example, influencing interphase friction, liquid and steam velocities, condensation, and vaporization and fluid-to-wall heat transfer).

The RELAP5 heat structure model is used to represent the structures of the physical system, such as fuel rods, steam generator tubes, and piping walls. Heat structures may include the effects of internal heating, such as with fuel rods or electrically powered pressurizer heaters. Heat structures are connected to the fluid cells and may be "single-sided" (connecting to a fluid cell on only one side, for example when modeling a cold leg piping wall) or "two-sided" (connecting to fluid on both sides, for example, when modeling the passage of heat from the primary to secondary coolant system through the steam generator tubes).

RELAP5 calculates wall-to-fluid heat transfer on a consistent basis, with the heat transfer based on the wall surface temperature and the fluid conditions (pressure, temperatures, velocities) in the fluid cell connected to the wall. The flow of heat within the heat structure is based on the wall surface temperature and a solution of the one-dimensional conduction heat transfer equation. A wall heat transfer mode map (analogous to the flow regime map described above) is used to determine the fluid-to-wall heat transfer process based on the wall temperature and fluid conditions (pressure, steam and liquid temperatures, void fraction, steam and liquid velocities).

RELAP5 capabilities include trip and control functions that allow the system model to represent the functions of automatic and operator actions in a plant. Examples of these actions include reactor trips, feedwater termination, relief valve operation, reactor coolant pump trips, and initiation of emergency core coolant flows. The RELAP5 trip and control features are also particularly important because they provide great flexibility for linking the hydrodynamic and heat structure models together and using them for simulating transient events that realistically represent the expected behavior the prototype plant systems.

RELAP5 output, as portrayed on the right side of Figure 6.1, includes both printed and plotted output. The printed output consists of a snapshot of the RELAP5 solution for the conditions of every model feature at user-selected times during the transient calculation. The plotted output consists of a file containing the time histories of the calculated solutions for every condition in every model feature. The user specifies the data interval of the plotted output. For the PTS application, it is the RELAP5-calculated time histories for reactor vessel downcomer fluid temperature, pressure, and wall heat transfer coefficient that are passed to the fracture mechanics analysts for use as boundary conditions in their analyses.

The RELAP5 plant and code assessment calculations for the PTS project were performed consistently using the same version of the code, which is RELAP5/MOD3.2.2Gamma. Complete documentation regarding the RELAP5 code and its application is found the RELAP5 Code Manuals [RELAP, various citations].

6.3.2 RELAP5 Numerics Issues

Two potential RELAP5 problems related to unphysical flow circulations exist that are significant for PTS analysis. These problems are discussed as follows.

The first potential problem relates to circulations for plants with two cold legs per coolant loop during event sequences that result in complete stagnation of the coolant loops (LOCAs with break diameters larger than 2 inches). Potential flow networks exist for these plants, consisting of the two common cold legs and the steam generator outlet plenum on each coolant loop and the reactor vessel downcomer. Circulating flows within these networks have been observed in RELAP5 calculations during periods when cold ECC injection water is injected into the cold legs. The calculated solution initially becomes unstable, resulting in the onset of a continuous flow through the network (with forward flow through one of the cold legs and reverse flow through the other cold leg).

Recirculating cold leg flows are believed to be numerically initiated as a result of round-off error, although once initiated, physically based buoyancy forces are created that could sustain such flows. The data from certain MIST and APEX tests used in the RELAP5 assessments (discussed later) provide potential, but inconclusive, evidence of circulating flows in cold leg networks in the test facilities. If present, cold leg network flow increases the downcomer fluid temperature as a result of mixing of the ECC injection water before it enters the downcomer. Because cold leg network flow is nonconservative for PTS, and because it is not clear whether such flows are physical, large artificial reverse flow loss coefficients were added in the cold legs near the reactor coolant pumps in the Oconee and Palisades models used for the LOCA cases. These artificial flow loss coefficients prevent negative flow in either of the two cold legs, thereby preventing circulating flows within the cold network and ensuring a solution for PTS that is conservative in this respect.

The second potential problem relates to large circulating flows calculated by RELAP5 to exist within the reactor vessel downcomer region that are not physically realistic. As with cold leg network circulation (described above), downcomer circulations were noted for LOCA sequences with break diameters greater than 2-in. (5-cm). The source of the circulation was traced to the application of the RELAP5 momentum flux model within downcomer regions that are represented using two-dimensional nodalization schemes (in the axial and azimuthal directions). The root cause of this problem in the RELAP5 code has not yet been determined; however, it was found that deactivating momentum flux for the junctions within the downcomer region prevented these physically unrealistic circulating flows. As a result, momentum flux was deactivated in the downcomer regions of the plant models used for the LOCA cases.

6.4 Plant Model Development

For all three plants examined, the thermal-hydraulic analysis methodology is similar. For each plant, the best available RELAP5 input model was used as the starting point. For Oconee, the base model was that used in the code scaling, applicability, and uncertainty [CSAU] study. For Beaver Valley, the base model was the H.B. Robinson-2 model used in the original PTS study in the mid-1980s. This model was reviewed by Westinghouse and revised and updated based on the review comments to reflect the Beaver Valley plant configuration. For Palisades, the base model was obtained from CMS Energy Corporation, the operators of the Palisades plant. This model was originally developed and documented by Siemens Power Corporation to support analysis of the loss of electrical load event for Palisades. The RELAP5 models are detailed representations of the power plants and include all major components for both the primary and secondary plant systems. RELAP5 heat structures are used throughout the models to represent structures such as the fuel, vessel wall, vessel internals, and steam generator tubes. The reactor vessel nodalization includes the downcomer, lower plenum, core inlet, core, core bypass, upper plenum and upper head regions. Plant-specific design features, such as the Oconee reactor vessel vent valves, are included. To illustrate the model features and level of detail, a nodeing diagram for the Palisades plant is included in Figure 6.3, Figure 6.4, and Figure 6.5. The modeling approaches used for Oconee and Beaver Valley are similar.

The downcomer model used in each plant was revised to use a two-dimensional nodalization. This approach was used to capture the possible temperature variation in the downcomer resulting from the injection of cold ECCS water into each cold leg. Capturing this temperature variation in the downcomer is not possible with a one-dimensional downcomer nodalization. In the revised models, the downcomer is divided into six azimuthal regions for each plant. The reason for choosing six azimuthal regions is to match the geometry of the hot and cold legs around the circumference of the reactor vessel and so that water from each of the cold legs would flow into a separate downcomer node.

The safety injection systems modeled for the Oconee, Palisades, and Beaver Valley plants include high-pressure injection (HPI), low-pressure injection (LPI), other ECCS components (e.g., accumulators, core flood tanks (CFTs), and/or safety injection tanks (SITs), depending on the plant designation), and makeup/letdown as appropriate. The secondary coolant system models include steam generators, main and auxiliary/emergency feedwater, steam lines, safety valves, main steam isolation valves (as appropriate) and turbine bypass and stop valves. Each of the models was updated to reflect the current plant configuration, including updating system setpoints (to best estimate values) and modifying control logic to reflect current operating procedures. Other model changes include adding control blocks to calculate parameters for convenience or information only (e.g., items such as minimum downcomer temperature).

Detailed information regarding the specific individual RELAP5 input models for the Oconee, Beaver Valley and Palisades plants can be found in [***Arcieri-Base***].

The RELAP5 model does not include an explicit containment model. A volume held at constant atmospheric pressure is used to represent the containment. This approach was used for the simulation of adverse containment conditions during a main steam line break in the containment. In this situation, the reactor coolant pumps are tripped because of high containment pressure.

The RELAP5 analysis considers the increase in injection water temperature resulting from switchover of the ECCS suction from the refueling water storage tank (RWST) to the containment sump. This switchover occurs when the water inventory in the RWST is depleted as a result of the combined pumping of the ECCS and containment spray pumps. After switchover, the ECCS and containment sprays operate in a recirculation mode, taking suction from the containment sump. At the point of suction switchover, ECCS injection water temperature will increase from a typical range of 283 to 305 K (50 to 90°F) to 325 to 335 K (120 to 140°F) or higher. Increase in ECCS injection temperature resulting from switchover to the containment sump is modeled to reflect the change in ECCS injection temperatures.

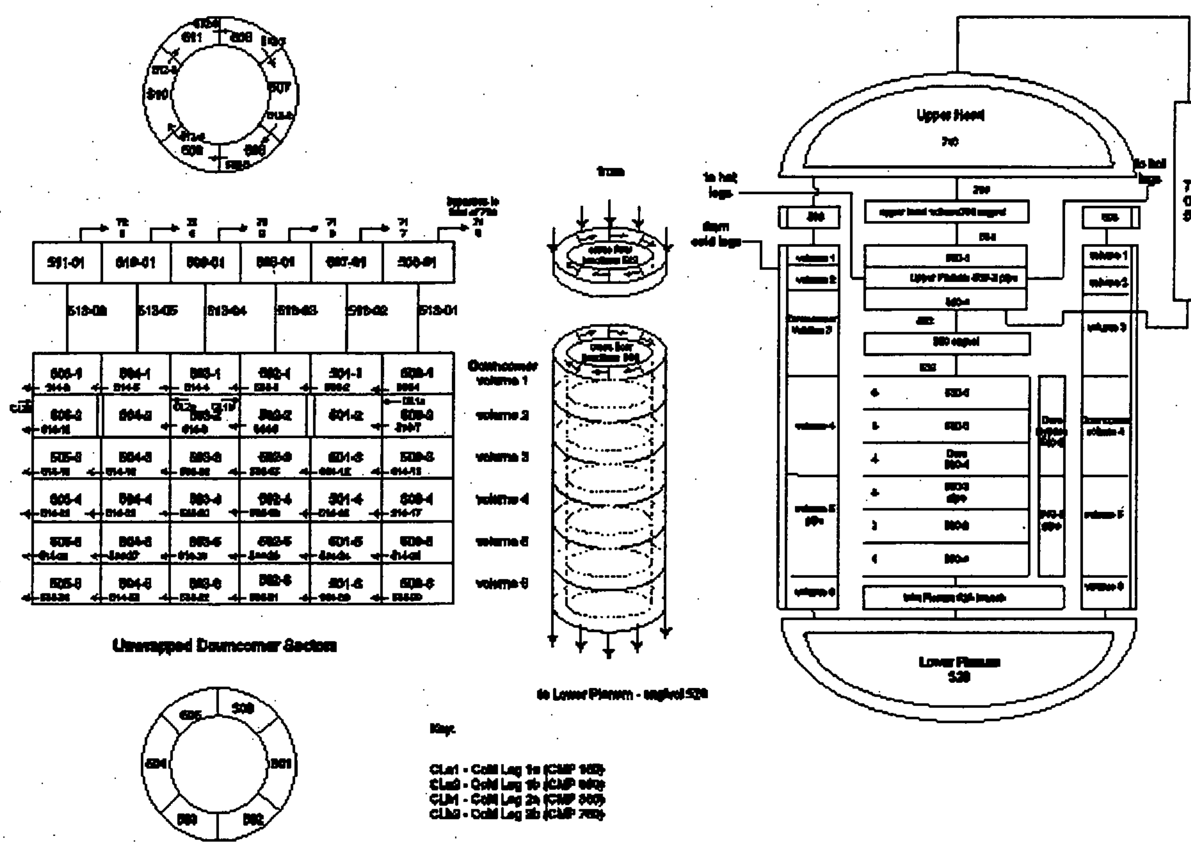

Figure 6.3. Palisades Reactor Vessel Nodalization

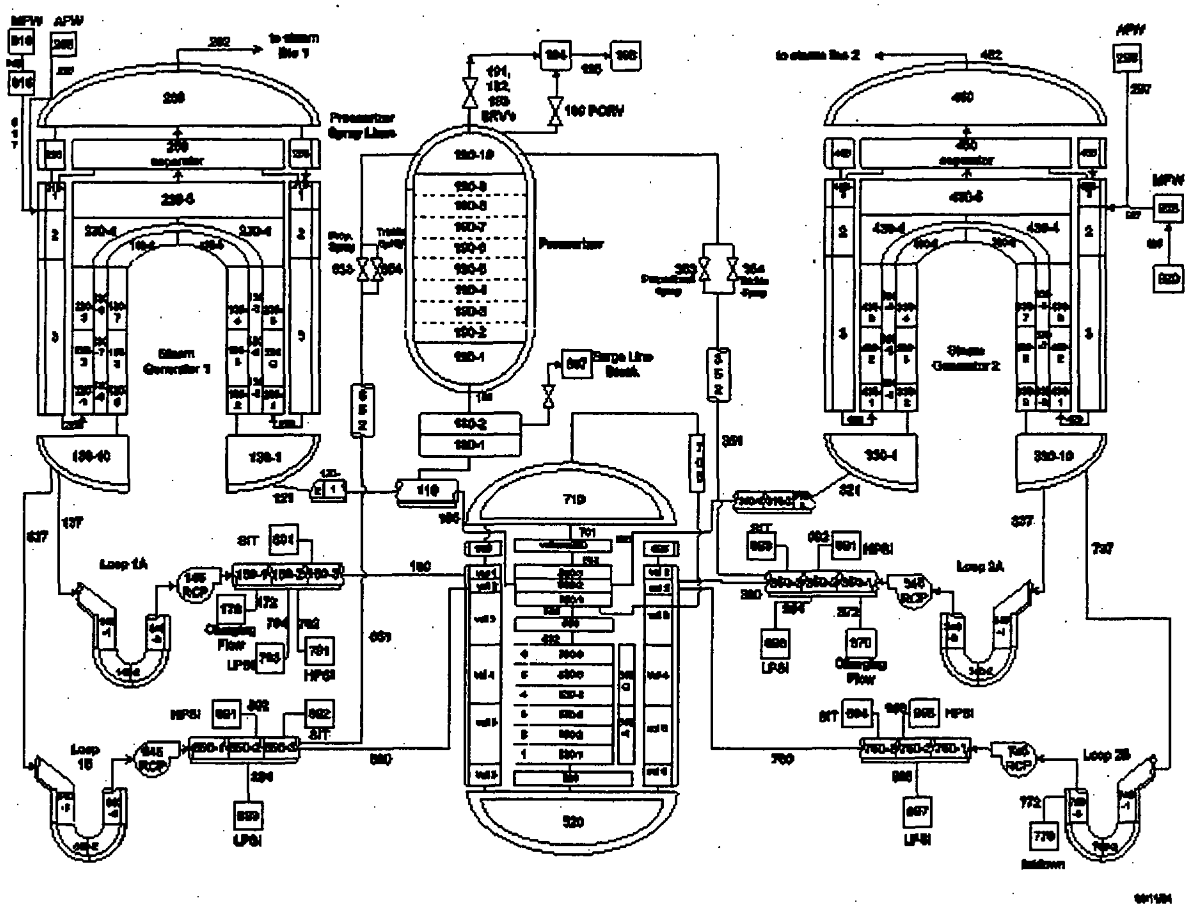

Figure 6.4. **Palisades Coolant Loop Nodalization**

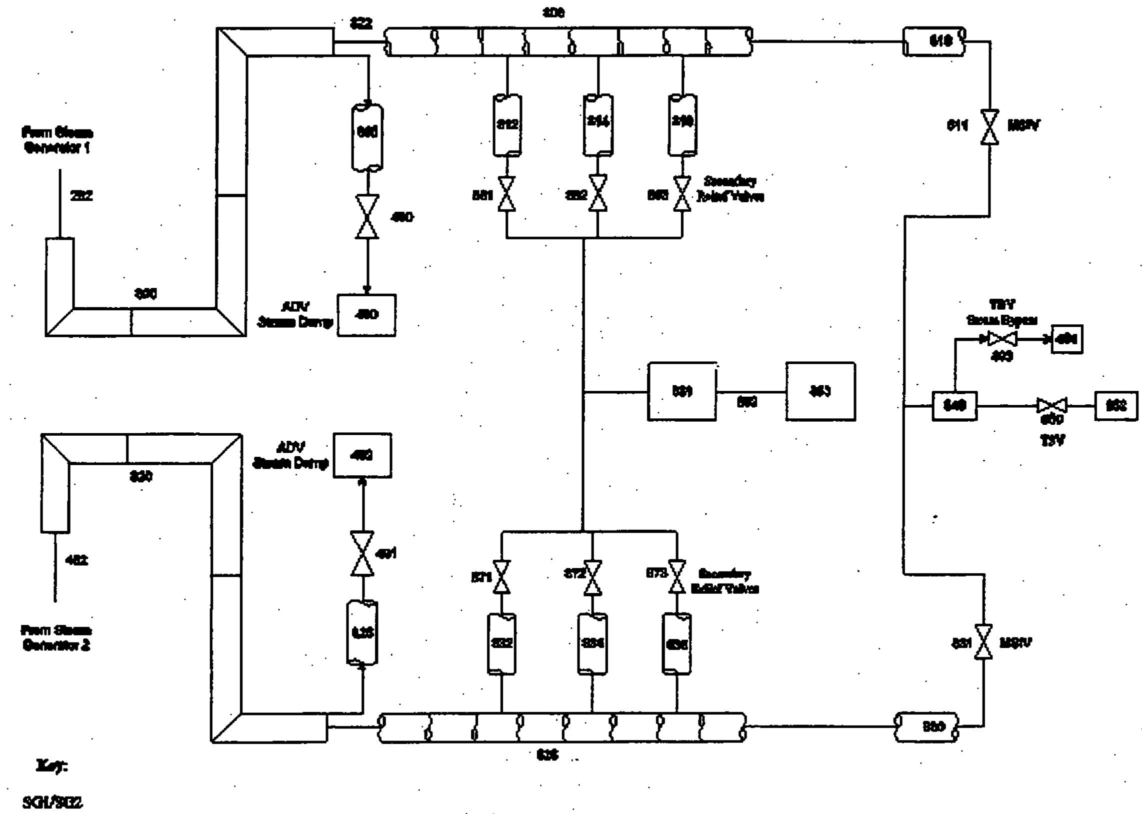

Figure 6.5. Palisades Main Steam System Nodalization

6.5 Transient Event Simulations

Transient events were selected for evaluation based on probabilistic risk assessment (PRA) analysis. Since each plant possesses unique thermal-hydraulic, hardware failure, and operational characteristics, there necessarily was variation in the transients events analyzed for the three plants. Examples of plant-to-plant differences important for PTS that affect transient selection include variations in shutoff heads for HPI pumps; initial pressure and temperature conditions in the accumulator (safety injection tank, core flood tanks); initial ECCS fluid temperature and allowed range; initial steam generator (SG) water masses; sizes and configurations of various valves and automatic controllers; and plant-specific operating procedures.

The development of the transient case list for each plant was an evolutionary process defined by the transient or sequence definition analysis. Generally, transients were selected based on the rate of primary system cooldown after transient initiation. Most transient event cases simulated generally fell into the categories of LOCAs and reactor/turbine trips with various complicating hardware and operator failures. Scenarios that consider stuck-open relief valves that either remain open or subsequently reclose later in the transient, system failures that cause steam generator overfeed, main steam line breaks, and others were analyzed. Evaluations were also performed for other types of events, such as steam generator tube rupture, recovery from a loss-of-all-feedwater event, and feed-and-bleed recovery from a LOCA with HPI failure.

The transient event simulations were run as RELAP5 restart calculations beginning from steady plant operating conditions. Total simulation time is 15,000 seconds for Palisades and Beaver Valley. For Oconee, the total simulation time is 10,000 seconds. .

6.5.1 Loss of Coolant Accidents

The smallest LOCA break size evaluated was 1.0-in. (2.54-cm) in diameter. Larger break diameters were also evaluated where the break flow area was progressively doubled, up to 22.63-in. (57.47-cm) in diameter. Break diameters considered in the analysis, therefore, range over the full break spectrum. The breaks for most LOCA cases are assumed to be on the hot side of the reactor coolant system (in the pressurizer surge line for smaller breaks and in the hot leg for larger breaks). The hot leg break location was selected for most evaluations because it results in the greatest reactor coolant system cooldown rate, an intentionally conservative treatment. The ECCS injection rates are also maximized in this situation. Evaluation of cold leg break LOCAs was also performed.

For all LOCA cases, the discharge and flow loss coefficients used for break junctions are assumed to be equivalent to those used in AP600 work. While these coefficients may not be appropriate for a specific break, the wide spectrum of break diameters accounts for any uncertainties in loss coefficients.

6.5.2 Reactor/Turbine Trips

The majority of cases analyzed are initiated by a reactor/turbine trip followed by various primary or secondary side failures. These failures include relief valve failures, steam generator level control failures, and others. In the RELAP5 model for all cases, a reactor trip is considered the same as a turbine trip. In reality, if a reactor trip signal is generated, there is a small delay before a turbine trip is generated. Since the long-term downcomer temperature and pressure are of interest, this delay is considered negligible. There are numerous cases where stuck-open valves (pressurizer or steam generator PORVs, safety relief valves, etc.) are modeled as failures following a reactor/turbine trip. In these cases, the valve is assumed to spuriously open at transient initiation. Primary side stuck valves (pressurizer SRVs or PORVs) are similar to LOCAs where the "break" is located at the top of the pressurizer, rather than in the surge line, hot leg, or cold leg. In most cases, the RELAP5 models use a single valve component to model several valves in parallel. For example, in Beaver Valley, three pressurizer PORVs are modeled with a single RELAP5 valve component. In order to have a single PORV fail by sticking open, the RELAP5 valve component is opened to one-third of the full flow area.

In a number of cases, the valve that stuck open was assumed to reclose at some later time. The time of reclosure was defined as either 3,000 seconds or 6,000 seconds depending on the transient definition from the PRA analysis. (Occasionally, a different time was chosen.) Various times were chosen since it would not be known when the valve would reclose (if it were to reclose). The 6,000-second reclosure time was selected as a point far enough out in time where the primary pressure and temperature reached a minimum.

Another set of failures is overfeeding of the steam generators. As with other cases, the initiating event is the reactor/turbine trip. These cases will result in an overcooling event. The failure could be anything from equipment/component failure to control failure or operator error. Cases have been run where a single steam generator is filled to the top, and the water level is maintained at that level. There are cases where multiple steam generators are filled to the top. Cases were run where the steam generator was filled to the top, then feedwater was stopped and the steam generator was allowed to boil dry.

6.5.3 Main Steam Line Break

Main steam line break cases were selected because they cause rapid depressurization of the steam generator. This rapid depressurization is one of the most limiting overcooling transients from a single failure on the secondary side. Large breaks considered were modeled as double-ended guillotine breaks. These breaks were assumed to occur at the connection of the steam line to the steam generator (upstream of the main steam isolation valves). Smaller steam line breaks were simulated with stuck secondary side valves (SRVs, ADVs, etc.) Turbine bypass valves were also assumed to stick open. In plants with main steam isolation valves, some of these stuck valves (breaks) were isolated by the MSIVs.

6.5.4 Operator Actions

Various operator actions are considered in the RELAP5 analyses based on the transient definition from the PRA analysis. For cases involving a primary system LOCA, the operator is assumed to take no action since automatic systems are presumed to operate and provide the core and primary system cooling. In these situations, the primary operator function is to monitor system conditions. For various transients involving reactor/turbine trips combined with component failures that lead to primary system overcooling, operator actions are a major factor and were modeled. Generally, the two categories of operator actions considered are (1) the operator correctly diagnoses the plant situation and performs the correct actions based on the emergency operating procedures, and (2) the operator fails to correctly diagnose the situation or takes an incorrect action.

A significant operator action for the plants analyzed is HPI control/throttling. Depending on the transient scenario, continued HPI injection can cause the system to refill and repressurize to the HPI pump shutoff pressure and/or the pressurizer PORV opening setpoint pressure. A good example of a transient where system repressurization can occur is a stuck-open primary safety valve that recloses after the system has depressurized. Continued HPI will cause the primary system to repressurize in this case unless the operator recognizes that the faulted valve has reclosed and takes action to control HPI injection.

Different plants have different HPI control methods. In Oconee, the operator can throttle HPI flow to obtain a desired flow rate and maintain a certain pressurizer water level. In Beaver Valley, however, the operator can either have a pump running or not. There is no "throttling"; rather, pumps are turned off if conditions are met. In Palisades, the operator

can throttle HPI if auxiliary feedwater is operating with the steam generator wide-range level greater than -84% and the reactor coolant system subcooling greater than 13.9 K (25°F). In this case, HPI is throttled to maintain pressurizer level between 40 and 60%.
HPI control is a crucial component in the overall PTS risk. An event where there is no HPI control can produce a much greater challenge to vessel integrity because of primary system repressurization than would the same event with HPI control because system repressurization does not occur. One significant variable in the HPI control is operator timing. Since the time that the operator will take control of the HPI is variable depending on the transient situation, several times are analyzed based on PRA input to determine the variation in overall system (downcomer) conditions. As an example, for Beaver Valley, cases were run where the operator does not control HPI, controls HPI 1 minute after the criteria for control are met, and controls HPI 10 minutes after the criteria are met.

Another example of an operator action is control of the reactor coolant pumps. The different plants use different criteria for tripping the RCP. At Oconee, the operator is assumed to trip the RCPs on low subcooling. At Beaver Valley, the RCP trip criterion is based on the difference between steam generator and pressurizer pressures. At Palisades, RCP trip criteria are based on primary system pressure and subcooling margin. In some events, the RCPs were not predicted to trip; however, various operating procedures could have caused the operators to trip the pumps. Therefore, in some cases, the RCPs were set to trip as an operator action. An additional note about RCPs is that they will be tripped if there are adverse containment conditions (i.e., main steam line break). Since the RELAP5 models used do not include the containment, the pumps were tripped manually if it was deemed necessary.

Failure of the operator to correctly diagnose the situation and take the correct action was also considered in the transient analysis. Failure to isolate the auxiliary/emergency feedwater to a faulted steam generator during a steam line break is an example of an operator failure considered in this analysis. This failure will result in an overcooling event where the faulted generator continues to remove heat, thus lowering the primary temperature. Timing of operator action was also analyzed. As an example, analyses were performed assuming that the operator stops AFW/EFW to the faulted generator (at 30 minutes for Beaver Valley). Time of operator action was determined by PRA analysis.

6.6 RELAP5 Analysis Results

The parameters that are used in the probabilistic fracture mechanics analysis are the reactor vessel downcomer fluid temperature, primary system pressure and reactor vessel wall heat transfer coefficient as a function of transient time. Post-processing of the RELAP5 results is performed to generate files that are transmitted to ORNL for analysis. Averaged values for the downcomer fluid temperature, system pressure, and downcomer fluid to vessel wall heat transfer coefficient were provided.

A large number of cases were analyzed for the Oconee, Beaver Valley, and Palisades plants to meet the requirements of the PRA analysis. A total of 177 cases were run for Oconee, 67 cases for Palisades, and 130 cases for Beaver Valley. These cases were needed to support the PRA model, particularly to support the development of transient bins needed to categorize the large number of transients that must be considered in developing a nuclear plant risk model. Because of the large number of cases, the results that are used in the probabilistic fracture mechanics analysis are separately presented in [***Arcieri-Base***].

6.7 RELAP5 Assessment Against Experimental Data

Assessments are performed to establish the suitability of the RELAP5/Mod 3.2.2Gamma code for analyzing plant transients that are significant risk contributors for PTS. The RELAP5 code version used for the assessment calculations is the same that is used for the PTS plant calculations. Assessment principally consists of performing an analysis for a particular experimental facility for a specific transient test. The results from a RELAP5 simulation of the test are compared against measurements from the experiment and conclusions are drawn regarding the code capabilities for predicting the physical behavior of the test.

Prior assessments of RELAP5 have been performed for a wide variety of transients over the 20-year development history of the code. Many of those assessments focused on tests representing LOCAs, for which the key system response is the integrity of the reactor core. It is noted that LOCAs as an event category are also an important vessel failure risk contributor for PTS, and so the extensive LOCA experimental database remains relevant and very useful for PTS applications. However, in contrast to the focus on core behavior during LOCAs, the focus for PTS-related transients is on the temperature and pressure conditions in the reactor vessel downcomer. Hence, the assessments discussed here focus on comparing RELAP5 results to experimental data for conditions in the downcomer.

The assessment of RELAP5/MOD3.2Gamma for representing PTS behavior, performed in the context of the PIRT discussion presented in Section 6.2, are summarized in the following sections. The assessments are documented in detail in the RELAP5 PTS Assessment Report [*Fletcher*].

6.7.1 Separate Effects Tests

RELAP5 was assessed against separate-effects experiments to evaluate RELAP5 capabilities for predicting specific localized behavior that is relevant for PTS. These separate-effects experiments included Marviken tests for assessing critical flow models, MIT pressurizer facility tests for assessing steam condensation and RCS pressurization behavior, UPTF full-scale tests for assessing condensation and steam-water flow phenomena and semiscale tests for assessing coolant loop natural circulation flow behavior. These assessments are discussed in this section.

6.7.1.1 Marviken Tests

Critical flow assessments were performed using data obtained from two experiments conducted at the Marviken facility. Marviken is a full-scale test facility fabricated from the 14,830-ft^3 (420-m^3) pressure vessel that was part of the Marviken nuclear power plant. RELAP5 is assessed against Marviken Tests 22 and 24.

During the experiments, the vessel is pressurized, the desired temperatures and liquid levels are established, and the break is opened, allowing a blowdown of the vessel to occur through a discharge pipe. The two tests differ mainly in the length of the discharge pipe that is employed.

The RELAP5 code utilizes the Henry-Fauske critical flow model to determine the break flow rate during periods when critical flow occurs.

A comparison of the measured and RELAP5-calculated vessel discharge flow rates for Marviken Test 22 is presented in Figure 6.6. The RELAP5 prediction of mass flow rate is in excellent agreement with the test data. The comparison of results for Test 24 is similar.

The Marviken assessments indicate that RELAP5 is capable of predicting critical break flow in an experimental system of the prototype scale. However, issues related to the exact configuration of breaks in PWR piping result in an additional general break flow prediction uncertainty. In order to account for this general uncertainty, the PTS plant calculations were performed using a spectrum of break diameters and locations. Break diameters from 1-in. (2.54-cm) to 22.63-in. (57.5-cm) in equal flow area increments were analyzed in the PTS plant evaluations.

6.7.1.2 MIT Pressurizer Test ST4

The MIT test facility is a small-scale, low-pressure representation of a PWR pressurizer. The insulated test vessel is 3.74-ft (1.14-m) tall with an inner diameter of 0.667-ft (0.203-m). Test ST4 was initialized with 1.41-ft (0.432-m) of saturated water in the bottom of the vessel at a pressure of 0.493 MPa [71.5 psia]. During the test, subcooled water is injected into the bottom of the vessel, increasing both the water level and pressure.

The capabilities of RELAP5 for simulating the steam condensation and the interfacial heat transfer between the stratified liquid and the vapor above the liquid were tested using comparisons to the measured data from this test. The mixing of the cold incoming water with hot water initially in the tank affects the prediction of the pressure increase, which for PTS is an important phenomenon. The simulation of this test is included in the set of standard problems that is executed routinely for RELAP5 developmental assessment.

A comparison of the measured and RELAP5-calculated pressure behavior is shown in Figure 6.7. The pressure increases as a result of the compression of the steam volume above the water surface. As the pressure increases, so too does the saturation temperature, leading to condensation of steam on the tank walls and liquid interface. RELAP5 predicted the trend of the pressure increase well, but somewhat

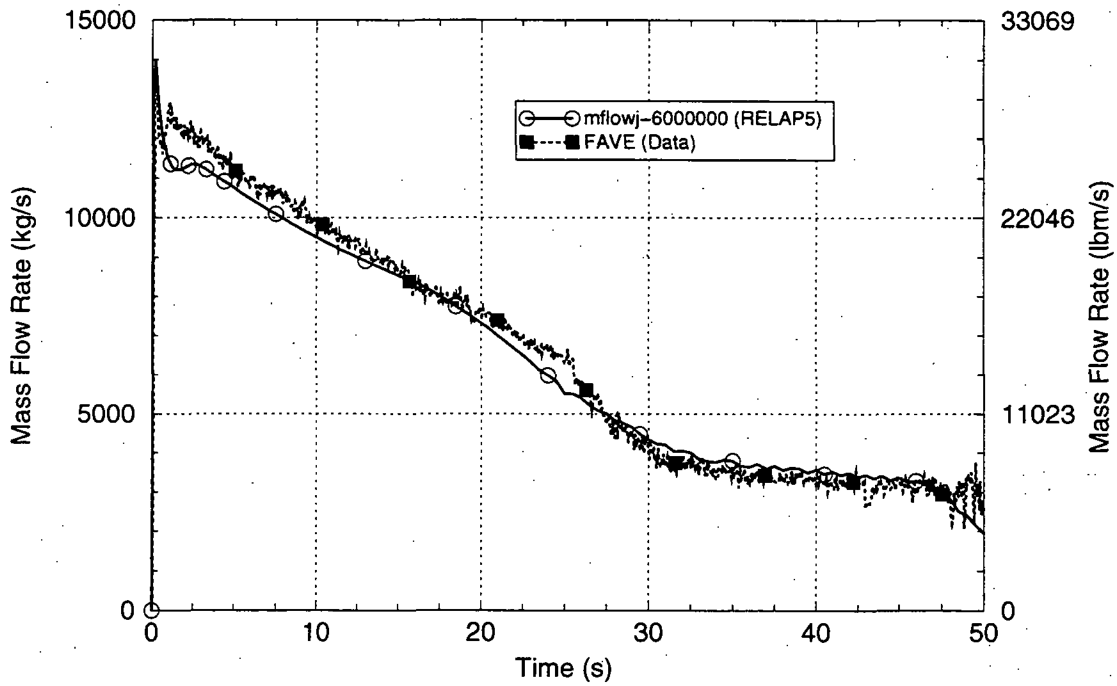

Figure 6.6. Mass Flow Rate at Nozzle Outlet (Marviken Test 22)

overpredicted the pressure. The pressure overprediction is attributed to an underprediction of the environmental heat losses with the model. Heat losses in a small facility like the MIT test facility can have a significant impact on system parameters such as pressure. Overall, the assessment indicates that RELAP5 is capable of well-predicting the pressure increases experienced when steam regions within the RCS of a PWR are compressed.

6.7.1.3 Upper Plenum Test Facility

The Upper Plenum Test Facility (UPTF) is a full-scale model of a four-loop 1,300 MWe PWR. Components included in this facility are the reactor vessel, downcomer, lower plenum, core simulator, upper plenum, and four coolant loops, each with reactor coolant pump and steam generator simulators. The test vessel, core barrel, and internals are a full-size representation of a PWR reactor vessel.

RELAP5 assessment was performed for Run 131 of UPTF Test 6. This test represents the interaction of steam and water in the reactor vessel downcomer and lower plenum regions of a PWR during the end-of-blowdown and refill portions of a large cold-leg break LOCA. The test investigates the behavior as the ECC water injected into the cold legs penetrates downward into the reactor vessel downcomer.

The test is run by injecting steam at a constant rate through the core and steam generator simulators at pressure and temperature conditions of 0.258 MPa [37.4 psia] and 458 K (364°F). The steam flows in the reverse direction, upward through the reactor vessel downcomer, toward the broken cold leg. When the steam flow behavior becomes steady, slightly subcooled emergency core cooling water at 392 K [246°F] is injected into the cold legs of the three intact loops.

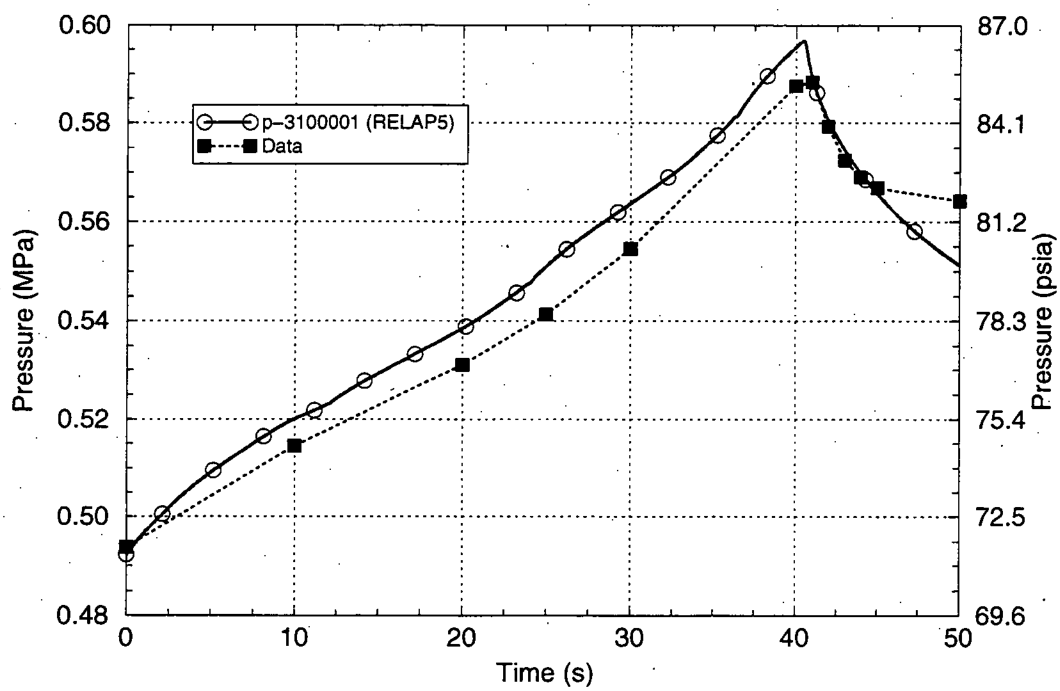

Figure 6.7. Pressure Rise (MIT Pressurizer Test ST4)

The RELAP5 simulation for UPTF Test 6, Run 131 indicates that the code well-predicts the measured downcomer pressure, lower plenum liquid level, and downcomer fluid temperature responses during the test. RELAP5 under predicted the downcomer fluid temperature by an average of 8 K (15°F) over the test period.

6.7.1.4 Semiscale Tests

Experiments were performed in the Semiscale Mod-2A test facility to evaluate single-phase, two-phase, and reflux steady-state coolant loop natural circulation behavior. This facility is a small-scale model of the primary coolant system of a four-loop PWR. The scaling factor between the test facility and full-scale plant is 1:1705. Two Semiscale Mod-2A tests, S-NC-2 and S-NC-3, are used for RELAP5 assessment.

The test facility represents the major components of a PWR, including, steam generators, reactor vessel, downcomer, reactor coolant pumps, pressurizer, and loop piping. The natural circulation experiments conducted at the facility utilized a single-loop configuration where the intact loop pump was replaced with a spool piece containing an orifice that simulated the hydraulic resistance of a locked pump rotor. The reactor vessel was also modified for these experiments to ensure a uniform heatup of the entire system and to avoid condensation in the vessel upper head region.

In Test S-NC-2, the steady-state loop natural circulation flow rate is measured as a function of the primary-side mass inventory. Single-phase, two-phase, and reflux steady-state modes were examined by varying the primary-side system mass while holding the SG secondary side conditions constant. During the test, a total of 17 separate steady-state conditions with different primary-side inventories ranging from 100 % to 61.2% of the full or maximum inventory were evaluated.

The RELAP5-calculated loop flow rates for Test S-NC-2 compare well with the test data for primary system inventories above 97% (single-phase liquid circulation and low-void two-phase circulation) and below 70% (reflux cooling circulation). For two-phase loop circulation, RELAP5 tended to overpredict the measured circulation rate for inventories between 70% and 90% and to underpredict it for inventories between 90% and 97%. The disagreement between the calculated and measured flow rates for inventories between 70% and 97% is attributed to overprediction of interphase drag by RELAP5.

In Test S-NC-3, the SG secondary side inventory is varied and the primary-side natural circulation flow rate is measured as a function of the reduced effective SG heat transfer area. As the SG inventory declines, the SG heat removal capability and the driving potential for primary-side loop circulation (the density difference between the core and the SG) is diminished, causing the primary flow rate to decline.

RELAP5 well-predicted the measured primary-side flow at effective SG heat transfer areas above 55% but overpredicted the primary-side flow at lower inventories.

In summary, RELAP5 well-predicted the two semiscale natural circulation tests for the conditions associated with high primary- and secondary-side coolant system inventories. The code also well-predicted the transitions to lower primary-side flow rates resulting from reduced primary- and secondary-side inventories. However, at reduced primary- and secondary-side inventories, the code generally tended to overpredict the primary-side flow rate and these overpredictions are believed to result from an overprediction of interphase drag.

Overpredicting the primary-side flow rate generally is nonconservative from the viewpoint of PTS analysis. Since the temperature of the coolant loop flow typically is much higher than the ECCS injection temperature, faster loop flows result in warmer temperatures for coolant entering the reactor vessel. The assessments indicate that under degraded inventory conditions, the primary-side flow rate may be overpredicted by a factor of about two. The maximum downcomer fluid temperature uncertainty that results from overpredicting the loop flow is estimated to be 19 K (34°F). However, it is noted that this uncertainty applies only during simulation of event sequences involving natural circulation, and then only during specific time periods within them when the primary or secondary system inventories are degraded. This uncertainty is evaluated as part of the integral system assessments that follow.

6.7.2 Integral System Response

RELAP5 was assessed against integral-effects experiments to evaluate code capabilities for predicting the system response in facilities scaled to pressurized water reactors. The assessments focus on the code capabilities for predicting the behavior of the reactor vessel downcomer conditions, which are of greatest significance for PTS analysis. The integral-effects experiments address phenomena in coolant system configurations specifically representing the geometries of Westinghouse, Combustion Engineering, and Babcock & Wilcox PWR plant designs. The integral-effects tests simulated PWR behavior under conditions expected during small, medium, and large break LOCAs; stuck-open pressurizer SRV events; and feed-and-bleed cooling operation scenarios.

These sequence categories make up the majority of the risk-dominant sequences in the PTS evaluation study for the Oconee-1, Beaver Valley-1 and Palisades PWRs.

The integral tests used in the assessments were performed in the ROSA-IV, ROSA/AP600, OSU-APEX, LOFT, and MIST experimental facilities. Comparisons of pressures and temperatures measured in these experiments to those predicted by RELAP are made in Sections 6.7.2.1 through 6.7.2.5. Section 6.7.2.6 makes comparisons between heat transfer coefficient estimates from these and other experimental data and those predicted by RELAP.

6.7.2.1 ROSA-IV Experiments

The ROSA-IV facility is a 1/48 volume-scaled, full-pressure representation of a Westinghouse 3,423 MWt four-loop PWR. The facility utilizes a full-height electrically heated core. The four PWR coolant loops are represented with two equal-volume loops. Components included in the loops are the hot leg, steam generator, reactor coolant pump, cold leg, pressurizer (on the intact loop) and ECCS systems (HPI, LPI, and accumulators).

RELAP5 was assessed against two ROSA IV experiments, SB-CL-18 and SB-HL-06.

ROSA-IV Test SB-CL-18 represents a 5% 6-in. (15.24-cm) equivalent diameter scaled break on the side of a cold leg with the reactor in full-power operation. The HPI and AFW systems are assumed to fail and a LOOP is assumed to occur at the time of the reactor trip.

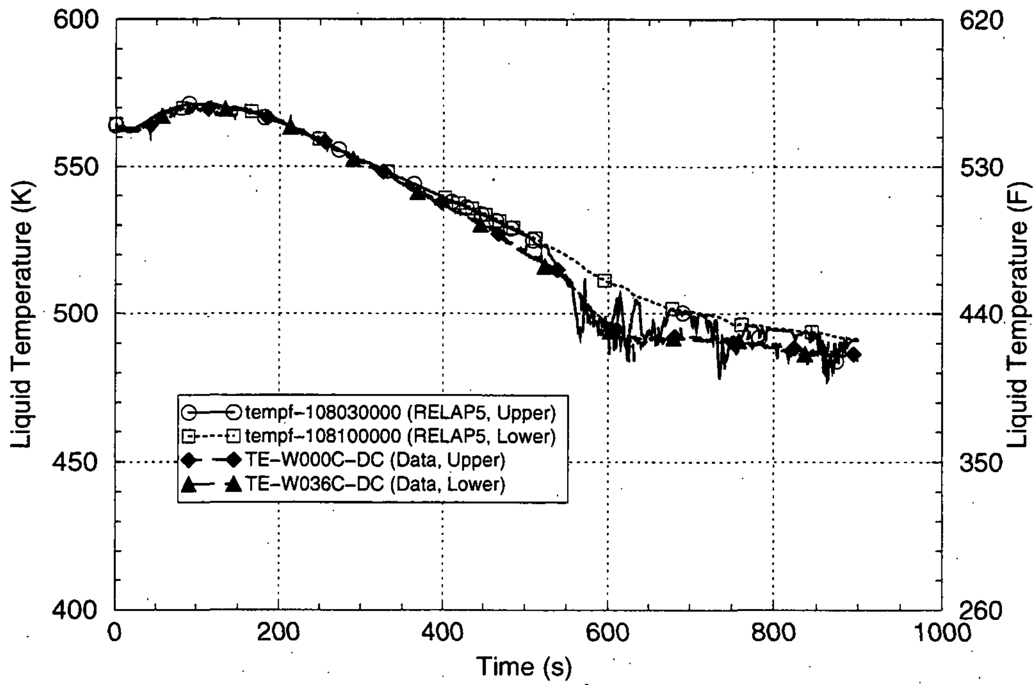

Figure 6.8. Reactor Vessel Downcomer Fluid Temperatures (ROSA-IV Test SB-CL-18)

The assessment of RELAP5 against the test data from ROSA-IV Test SB-CL-18 indicates that the code is capable of acceptably simulating the experiment behavior including the parameters of key importance for PTS (RCS pressure, coolant loop flow, and reactor vessel downcomer temperatures). Figure 6.8 compares the measured and RELAP5-calculated reactor vessel downcomer fluid temperatures. The data shown are for elevations within the downcomer corresponding to the top and bottom of the reactor core. RELAP5 overpredicted the downcomer fluid temperature by a maximum of 13 K (23°F) and underpredicted it by a maximum of 23 K (41°F). Over the test period, RELAP5 overpredicted the downcomer fluid temperature by an average of 0.16 K (0.29°F).

ROSA-IV Test SB-HL-06 represents a 0.5% 2-in. (5.08-cm) equivalent diameter scaled break on the top of the hot leg with the reactor in full-power operation. The HPI and AFW systems are assumed to fail and a LOOP is assumed to occur at the time of the reactor trip. When the core uncovered and the heatup began, the pressurizer PORV was opened to depressurize the primary system and initiate accumulator injection.

The assessment of RELAP5 against the test data from ROSA-IV Test SB-HL-06 indicates that the code is capable of acceptably simulating the experimental behavior including the parameters of key importance for PTS (RCS pressure, coolant loop flow, and reactor vessel downcomer temperatures). Figure 6.9 compares the measured and RELAP5-calculated reactor vessel downcomer fluid temperatures. The data shown are for elevations within the downcomer corresponding to the top and bottom of the reactor core. The large drop in the measured downcomer temperature at about 8,000 s resulted from a condensation-driven rapid movement of water into the pressurizer; this water movement was not seen in the RELAP5 calculation. Condensation is an expected uncertainty in code calculations and the current state of the art in thermal-hydraulic modeling does not allow accurate predictions of extreme transient condensation events. RELAP5 underpredicted the downcomer fluid temperature by a maximum of 70 K (126°F) and by an average of 10 K (18°F) over the test period.

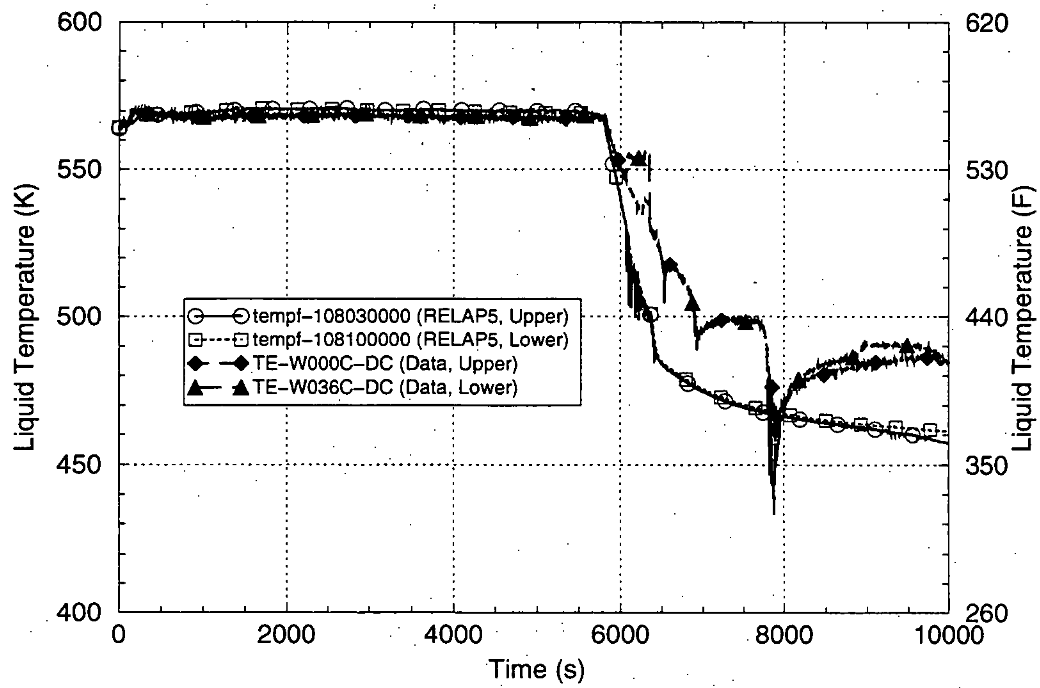

Figure 6.9. Reactor Vessel Downcomer Temperatures (ROSA-IV Test SB-HL-06)

6.7.2.2 ROSA AP-600 Experiments

The ROSA-AP600 facility is a 1/30 volume-scaled, full-pressure representation of a Westinghouse AP600 PWR. The facility utilizes a full-height electrically heated core. The two AP600 coolant loops are represented with two equal-volume loops in the test facility. Components represented in the loops are the hot leg, steam generator, one reactor coolant pump (compared with two pumps in the plant design), one cold leg (compared with two in the plant design), pressurizer (on one loop), and core makeup tanks (CMTs) on the other loop. The passive residual heat removal (PRHR) system, ADS, and IRWST are also represented in the test facility.

While there are configuration differences between the designs of AP600 and currently operating PWRs, assessments against ROSA/AP600 data are useful for PTS because the cold leg and reactor vessel downcomer regions of the facility are particularly well-instrumented and activation of the ADS effectively causes a transition from a small-break LOCA event sequence to a large-break LOCA event sequence, both of which are of interest for the PTS application. RELAP5 was assessed against two ROSA-AP600 experiments, AP-CL-03 and AP-CL-09.

Test AP-CL-03 represents a 0.1% 1-in. (2.54-cm) diameter scaled break on the bottom of a cold leg in the CMT loop. The reactor is operating at full power when the break opens. An additional failure, where one of the two ADS-4 valves on the CMT loop fails to open, is also assumed.

The comparisons of RELAP5-calculated and measured data for this experiment show that the complex system behavior and timing of the test are well-predicted with RELAP5. The RELAP5 prediction of coolant loop flow stagnation and draining are in good agreement with the test data.

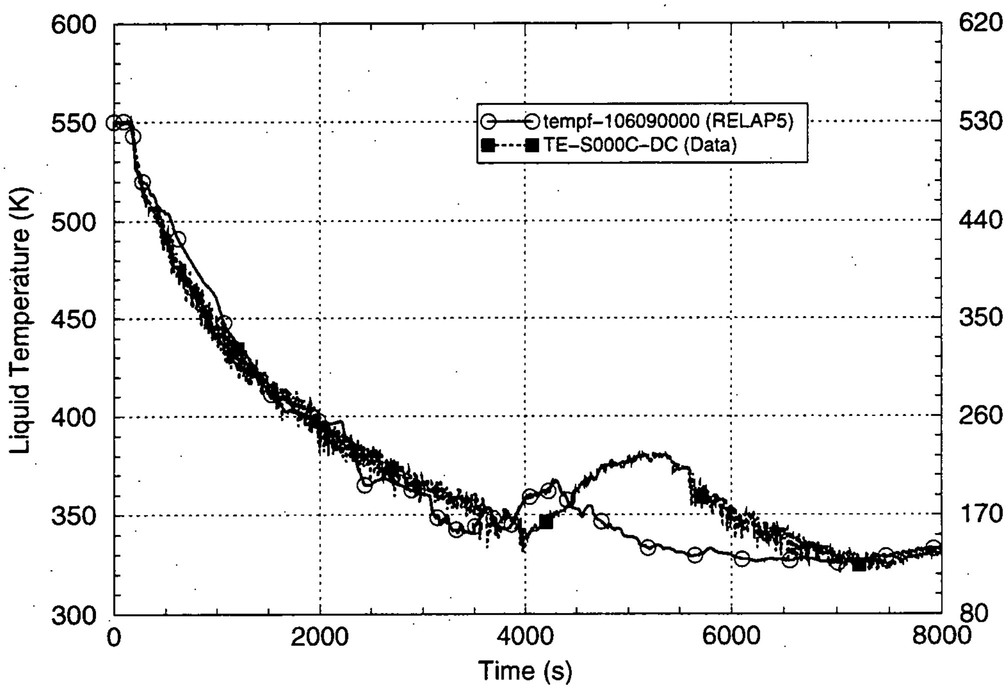

Figure 6.10. Reactor Vessel Downcomer Fluid Temperatures (ROSA/AP600 Test AP-CL-03)

The test exhibits thermal stratification within the cold legs; a layer of cold ECCS water resides under a layer of warmer water within the horizontal cold leg pipes. This thermal-stratification behavior cannot be represented with a one-dimensional computer code such as RELAP5. However, the assessment indicates only minimal effects of this code limitation on the calculated reactor vessel downcomer prediction. Figure 6.10 compares the RELAP5-calculated and measured reactor vessel downcomer fluid temperatures on the pressurizer-loop side of the downcomer at an elevation corresponding to the bottom of the reactor core. The fluid temperature code-data comparisons at other locations in the downcomer are similar. RELAP5 overpredicted the downcomer fluid temperature by a maximum of 59 K (106°F) and underpredicted it by a maximum of 72 K (130°F). RELAP5 underpredicted the downcomer fluid temperature by an average of 4 K (7°F) over the test period.

Test AP-CL-09 also represents a 0.1% 1-in. (2.54-cm) diameter scaled break on the bottom of a cold leg in the CMT loop. The reactor is operating at full power when the break opens. Although similar to Test AP-CL-03, Test AP-CL-09 represents additional passive safety system failures:

- Both CMT discharge valves fail closed.
- Half of the valves in each ADS stage fail closed.
- ADS (normally activated by low CMT level) activated 30 minutes after a low-low pressurizer pressure signal is generated.
- Check valve in accumulator discharge line on the CMT loop fails closed.
- Check valve in the IRWST discharge line on the CMT loop fails closed.
- Only one-half of the PRHR heat exchanger capability is available.

The comparisons of RELAP5-calculated and measured data for this experiment show that the complex system behavior and timing of the test are well-predicted with RELAP5.

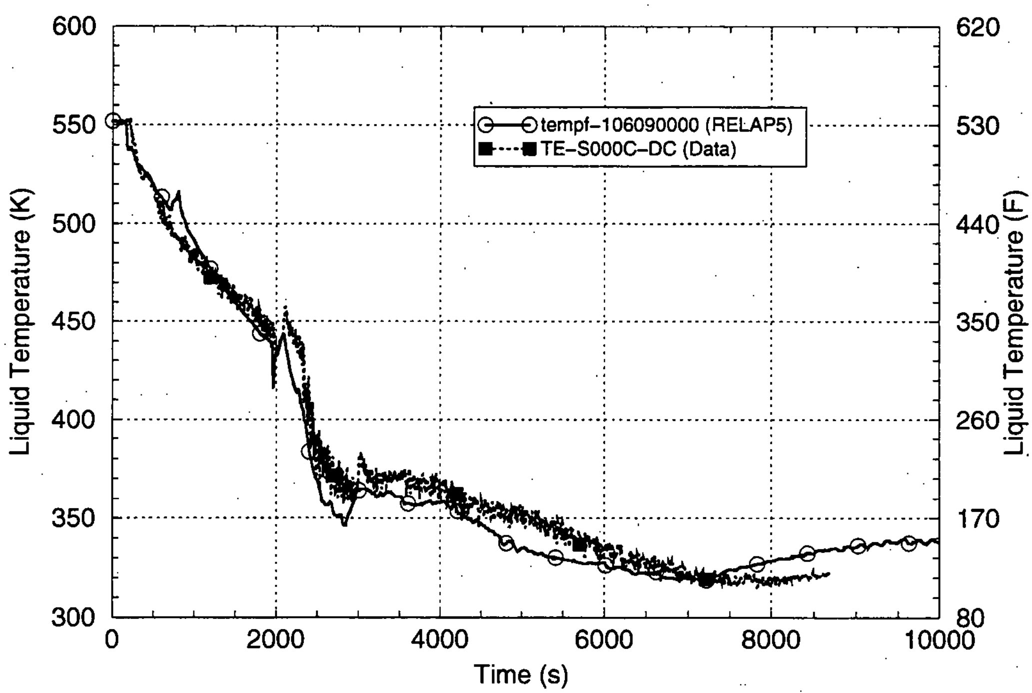

Figure 6.11. Reactor Vessel Downcomer Fluid Temperatures (ROSA/AP600 Test AP-CL-09)

As in Test AP-CL-03, thermal stratification behavior within the horizontal cold legs (which cannot be represented with RELAP5) is observed in Test AP-CL-09. Because of cold leg thermal stratification effects, the sequence order in which two loops stagnated in the RELAP5 calculation was the reverse of that seen in the test. However, good agreement is seen between the calculated and measured first-loop and second-loop stagnation times. The assessment indicates only minimal effects of this code limitation on the prediction of vessel downcomer fluid temperatures. Figure 6.11 compares the RELAP5-calculated and measured reactor vessel downcomer fluid temperatures on the pressurizer-loop side of the downcomer at an elevation corresponding to the bottom of the reactor core. The fluid temperature code-data comparisons at other locations in the downcomer are similar. RELAP5 overpredicted the downcomer fluid temperature by a maximum of 39 K (71°F) and underpredicted it by a maximum of 49 K (88°F). RELAP5 overpredicted the downcomer fluid temperature by an average of 1 K (2°F) over the test period.

6.7.2.3 APEX Tests

A series of tests specific for plants of Combustion Engineering (CE) design was conducted at the APEX facility operated by Oregon State University. The APEX facility is a ¼-height scale low-pressure integral systems facility that has been configured to model the thermal-hydraulic phenomena of CE plants. The purpose of these tests was to investigate mixing of high-pressure injection fluid in the cold leg and the downcomer and to evaluate the onset of coolant loop flow stagnation, which can lead to low temperatures in the reactor vessel downcomer. Two APEX tests were used for RELAP5 assessment, APEX-CE-13 and APEX-CE-05.

Test APEX-CE-13 represents a stuck-open pressurizer safety relief valve event with the reactor operating at full power. The stuck-open valve is subsequently assumed to reclose. This type of transient event is a significant contributor to PTS risk event because the RCS is first significantly cooled and then repressurized after the relief valve closes. To start the test, the ADS-2 valve atop the pressurizer was opened to simulate a stuck-open pressurizer safety relief valve. Simultaneously, two reactor coolant pumps were tripped, the HPI system was actuated and reactor core power was tripped. The ADS-2 valve was closed at 1 hour into the test and the test was terminated about 20 minutes later after the RCS had refilled.

The comparisons of RELAP5-calculated and measured data from Test APEX-CE-13 indicate that the code is capable of acceptably simulating the behavior of the key PTS parameters for this test. RELAP5 overpredicted the RCS cooldown rate during the period when the relief valve is open as shown in Figure 6.12. RELAP5 predicted a delayed onset of the repressurization and underpredicted the pressurization rate after the relief valve closed as seen in Figure 6.13. These differences between the calculated and measured responses are considered to be moderate and to result from difficulties in adequately modeling the system heat losses of small-scale facilities such as APEX. RELAP5 underpredicted the downcomer fluid temperature by an average of 2 K (4°F) over the test period.

Test APEX-CE-05 was performed to provide baseline mixing data for the injection of cold ECC water into the cold legs of the RCS. During the test, RCS temperatures and pressures consistent with full-power plant operation are first established and then the steam generators, RCPs and reactor core heaters are secured to create stagnant conditions in the RCS. High-pressure injection is initiated into the four cold legs and a pressurizer drain valve is opened to accommodate the injected fluid and control the pressurizer level and RCS pressure. For this test, the behavior of interest is the manner in which the cold water entering the vessel through the cold legs spreads downward and around the reactor vessel downcomer annulus. The thermocouple instrumentation of the facility was upgraded in order to observe this behavior.

The test data exhibit only very small variations in the downcomer temperatures around the periphery of the downcomer. The maximum azimuthal downcomer temperature variations are 9 K (16°F) at the elevation corresponding to the top of the core and are 5 K (9°F) at the elevation corresponding to the bottom of the core. No significant plumes were observed in the downcomer based on the temperature results of this test. Larger variations are seen in the axial direction in the downcomer, but these variations, which are related to the time required for fluid to transit though the downcomer, are short-lived. The downcomer temperature variations observed in the RELAP5 simulation of the test similarly are small.

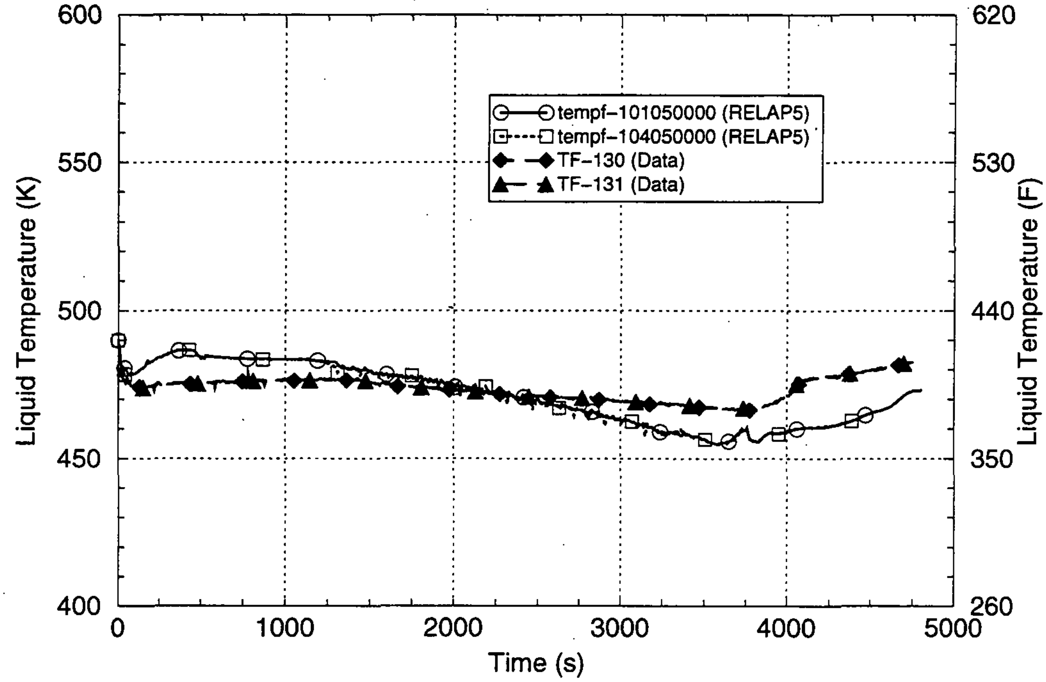

Figure 6.12. Reactor Vessel Downcomer Fluid Temperatures (Test APEX-CE-13)

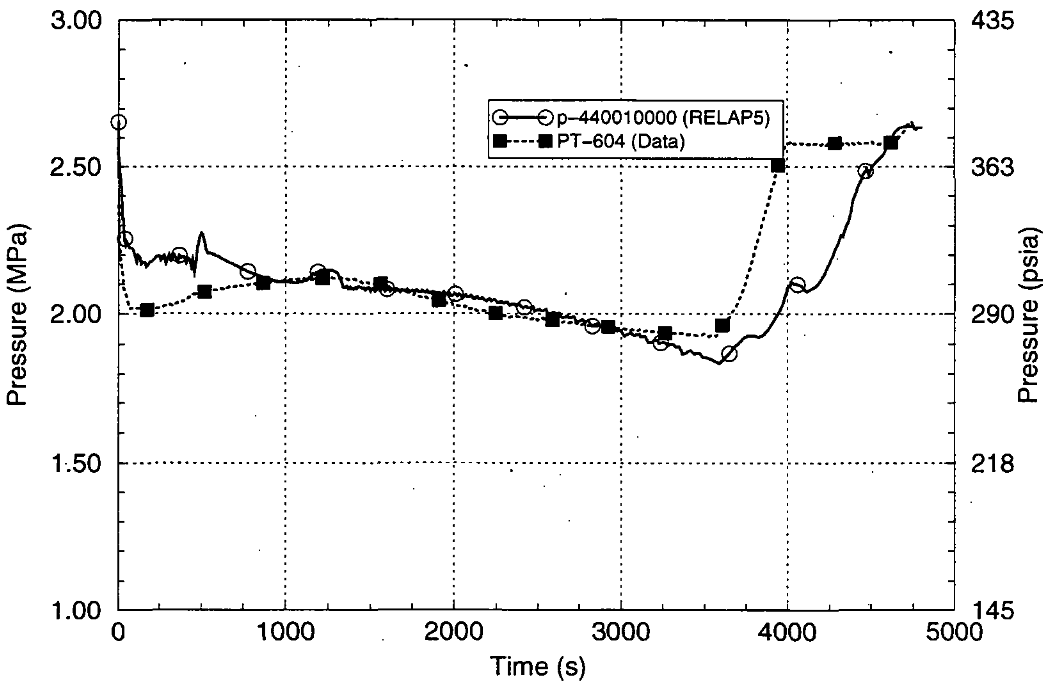

Figure 6.13. Pressurizer Pressure (Test APEX-CE-13)

Figure 6.14 compares the RELAP5-calculated and measured reactor vessel downcomer fluid temperature responses for Test APEX-CE-05 at a representative location (directly under one of the cold legs at an elevation corresponding to the top of the core). The figures show that RELAP5 predicts the downcomer fluid temperature excellently up to about 2,000 s, but then underpredicts it afterward. Over the test period, RELAP5 underpredicted the downcomer fluid temperature by an average of 5 K (9°F). The underprediction is attributed to more involvement of warm fluid residing within the cold legs in the mixing process in the experiment than in the calculation.

A second sensitivity RELAP5 calculation for Test APEX-CE-05 was performed in which large artificial flow loss coefficients for reverse flow were added in the reactor coolant pump suction regions of each cold leg. This modeling approach is used in PTS plant calculations to suppress circulations through the cold legs on the same coolant loop (in the forward direction through one cold leg and in the reverse direction in the other) for certain types of PTS events. This model change resulted in RELAP5-calculated reactor vessel downcomer fluid temperatures that were additionally lower (compared with the above calculation) by an average of 8 K (14°F) over the test period. This difference represents the expected downcomer temperature conservatism resulting from using the high artificial reverse flow loss coefficient modeling approach.

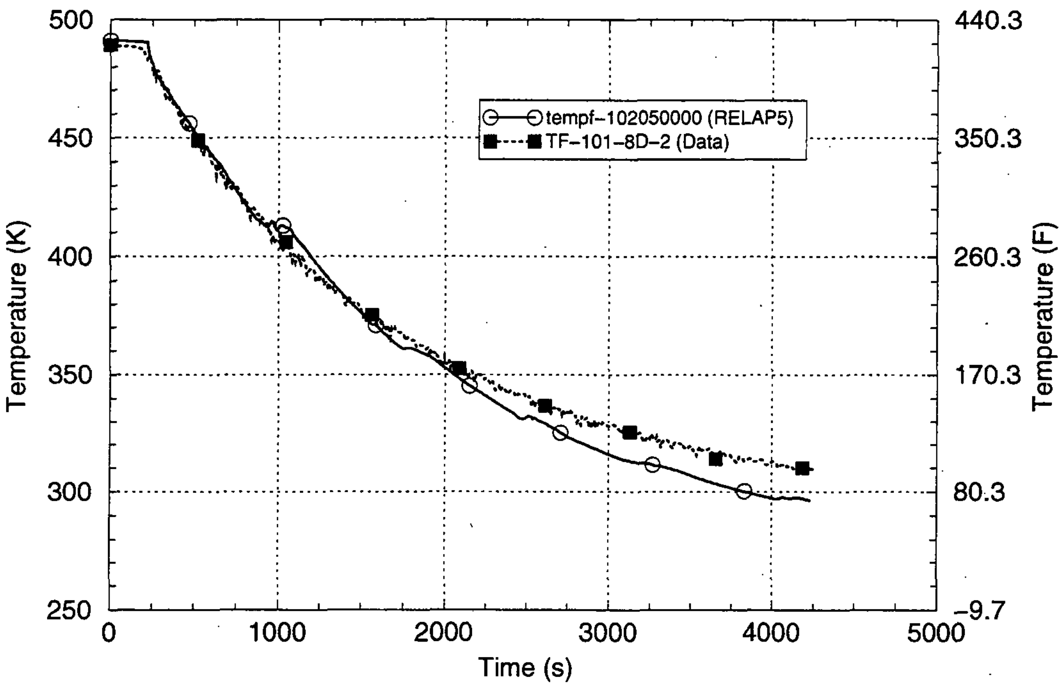

Figure 6.14. Reactor Vessel Downcomer Fluid Temperatures (Test APEX-CE-05)

6.7.2.4 LOFT Tests

The Loss-of-Fluid Test Facility (LOFT) is a 50-MWt volumetrically scaled PWR system. The LOFT facility was designed to obtain data on the performance of the engineered safety features of a commercial PWR system for postulated accidents, including LOCAs.

The LOFT nuclear core is approximately 5.51-ft (1.68-m) tall and 2-ft (0.61-m) in diameter, and is composed of nine fuel assemblies containing 1,300 nuclear fuel rods of representative PWR design. Three intact loops are simulated using a volume/power ratio scaling by the single circulating (intact) loop in the LOFT primary system. The broken loop is simulated by the scaled LOFT blowdown loop.

An ECCS is provided to simulate the engineered safety features in PWRs. An HPI system centrifugal pump and a nitrogen-pressurized accumulator supply emergency core cooling. The LPIsystem and accumulator discharge lines are orificed as required to simulate the delivery characteristics of various PWR emergency core cooling systems.

RELAP5 assessment was performed using three LOFT experiments, Test L3-7, Test L2-5 and Test L3-1.

Loft Test L3-7 represents plant recovery actions following a 1-in. (2.54-cm) equivalent diameter break in the cold leg of a PWR operating at full power. The primary purpose of this test is to establish a break flow approximately equal to the HPI flow at an RCS pressure of approximately 6.9 MPa [1,000 psia], to isolate the break and to demonstrate the stabilization of the plant at cold shutdown conditions.

During Test L3-7, the break was opened, the reactor and reactor coolant pumps were tripped, leading to coolant loop natural circulation flow. At 1,800 s, the AFW and HPI flows were terminated to hasten the loss of RCS fluid inventory and to establish the conditions leading into the system recovery to cold shutdown conditions. At 3,603 s, the AFW flow was reinstated and a SG steam bleed operation begun to effect a controlled depressurization of the intact loop SG secondary system. The HPI flow was reinstated at 5,974 s, and the test was terminated at 7,302 seconds.

The assessment indicates that RELAP5 is capable of acceptably simulating the behavior of the key PTS parameters for LOFT Test L3-7. The RELAP5 prediction of the RCS pressure is in good-to-excellent agreement with the measured data. The RELAP5 prediction of the reactor vessel downcomer fluid temperature is in good agreement with the measured data. Figure 6.15 shows a comparison of the measured and calculated reactor vessel downcomer fluid temperatures for this test at representative locations in the downcomer (on the broken loop and intact loop sides of the downcomer and at elevations in the downcomer corresponding to the elevations of the top and middle of the core). Over the test period, RELAP5 underpredicted the downcomer fluid temperature by an average of 8 K (14°F).

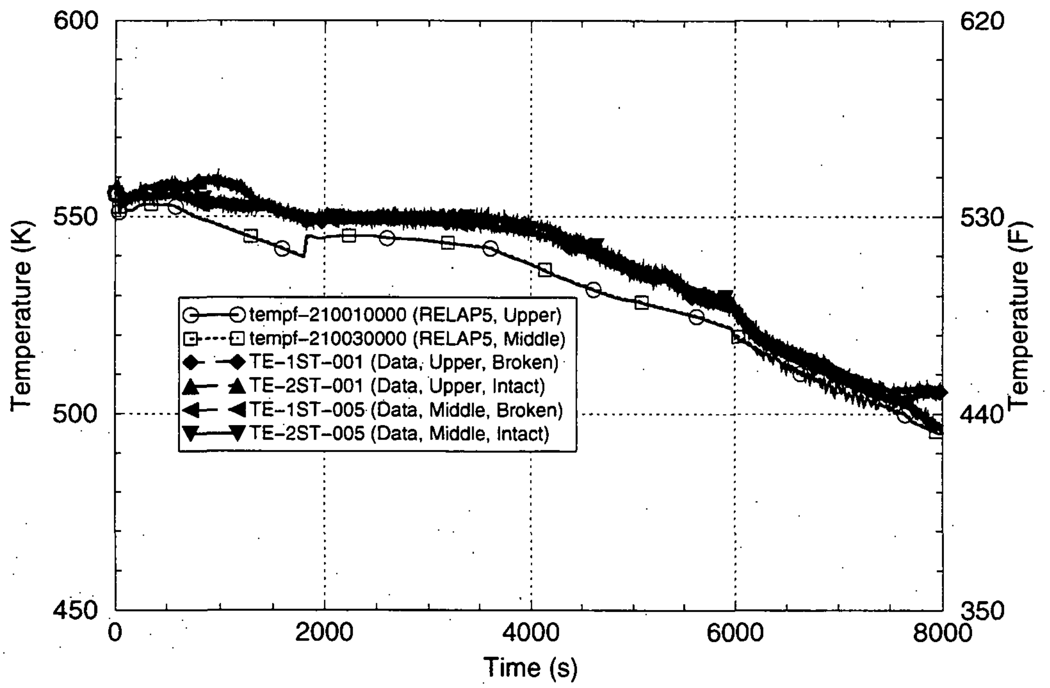

Figure 6.15. Reactor Vessel Downcomer Fluid Temperatures (LOFT Test L3-7)

Test LOFT L2-5 represents a double-ended offset guillotine break LOCA in the cold leg of a PWR operating at full power. The primary purpose of this test was to evaluate the performance of the ECCS for cooling the core. For the purposes of the PTS assessment, this test provides data for the very rapid blowdown and refilling of the RCS with cold ECCS which accompanies a very large break in the RCS. During the test, the break was opened and the reactor and reactor coolant pumps were tripped. Accumulator injection began when the RCS pressure had declined below the initial accumulator pressure and delayed injection of HPI and LPI ECC coolant began at 24 s and 37 s, respectively after the break opened.

The assessment indicated no major differences between the RELAP5-calculated and measured responses for LOFT Test L2-5. The RELAP5 predictions of the reactor vessel downcomer fluid temperature and RCS pressure are in good agreement with the measured data. Figure 6.16 shows a comparison of the measured and calculated reactor vessel downcomer fluid temperatures for this test at representative locations in the downcomer (on the broken loop side of the downcomer at elevations in the downcomer corresponding to the elevations of the top, middle and bottom of the core). Over the test period, RELAP5 underpredicted the downcomer fluid temperature by an average of 4 K (7°F).

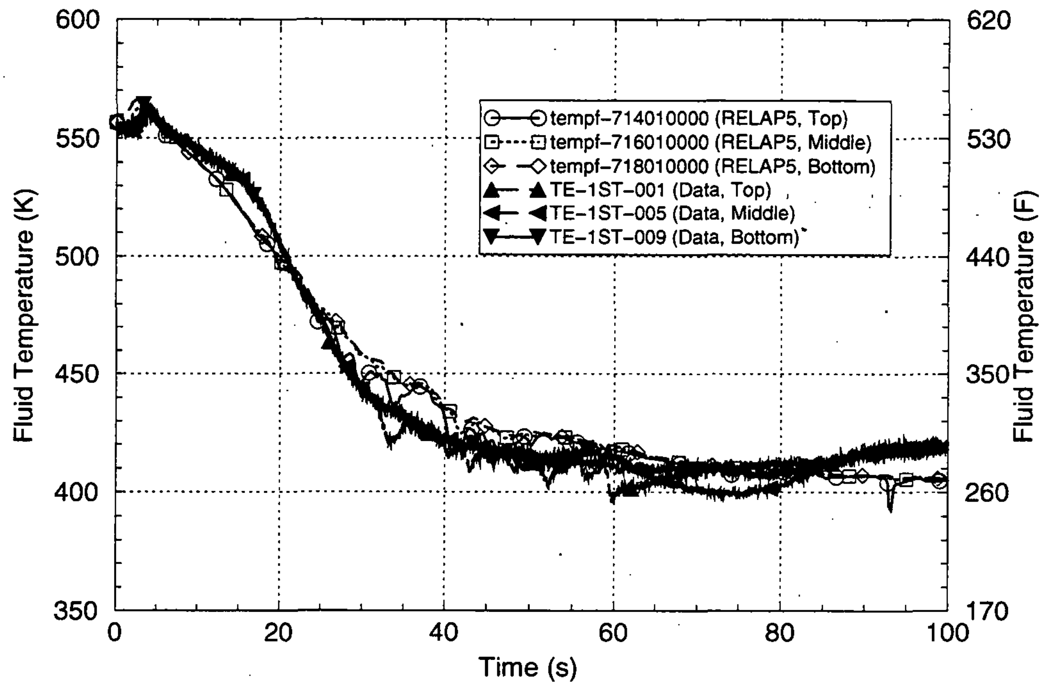

Figure 6.16. Reactor Vessel Downcomer Fluid Temperatures (LOFT Test L2-5)

LOFT Test L3-1 represents an equivalent 4-in. (10.16-cm) diameter break LOCA in the cold leg of a PWR operating at full power. The primary purpose of this experiment was to evaluate the performance of the ECCS for cooling the core.

During the experiment, the reactor and the reactor coolant pumps were tripped and ECC flows from the HPI and accumulator systems were initiated as the RCS pressure declined. The accumulator water inventory was fully discharged and the experiment was continued until 3,623 s using the HPI ECC flow alone. At that time a feed-and-bleed SG cooling process was implemented; the experiment was concluded at 4,368 s.

For the purposes of the PTS assessment, this test provides data for the rapid blowdown and stabilization of the RCS with ECCS injection for a break diameter that is toward the larger end of the small-break LOCA spectrum.

Test L3-1 also provides data useful for comparing RELAP5 simulation capabilities when using one-dimensional and two-dimensional reactor vessel downcomer modeling approaches. RELAP5 PTS plant simulations have shown considerable variation in calculated downcomer temperatures for cold leg LOCAs with break diameters near 4-in. (10.2-cm), depending upon whether the 1-dimensional or 2-dimensional RELAP5 downcomer modeling approach is used. RELAP5 calculations for LOFT Test L3-1 are performed using both downcomer modeling approaches in order to judge which approach is better for simulating cold leg breaks of this approximate size.

The assessment indicated that the behavior in the reactor vessel downcomer region is particularly difficult to predict for a break of this size and location. Accumulator injection has a potential for directly influencing the downcomer temperature, but mixing within the cold leg and upper downcomer regions significantly affects that influence. The prediction of mixing within the thermally stratified cold leg regions is beyond the capability of RELAP5. The break is large enough that the RCS depressurizes sufficiently to result in accumulator injection, but not so large as to allow for an accumulator discharge that is insensitive to the RCS pressure. Finally, the break location in the cold leg adds to the prediction difficulty because the most direct path for steam to reach the break is upward through the downcomer, against the downward flow of cold accumulator water. Therefore, interphase condensation modeling, known to be a weakness of RELAP5, appears to be particularly important for predicting the behavior for this particular break size and location

The assessment indicates that RELAP5 is capable of acceptably predicting the reactor coolant system parameters for this test. The downcomer fluid temperatures in the test were underpredicted using both the 1- and 2-dimensional downcomer modeling approaches. Over the test period, the underprediction is by an average of 7 K (13°F) when using the one-dimensional downcomer modeling scheme and by an average of 13 K (23°F) when using the 2-dimensional downcomer modeling scheme. Figure 6.17 compares the measured and calculated fluid temperatures for Test LOFT L3-1 at a representative location in the reactor vessel downcomer. The data shown are for a location on the broken loop side of the downcomer at an elevation corresponding to the middle of the reactor core. The code-data comparisons at other locations in the downcomer are similar.

The 2-dimensional reactor vessel downcomer modeling approach is judged to be the more appropriate approach for RELAP5 PTS applications because of (1) the better accumulator injection behavior it produced, (2) the ability it provides for predicting different fluid behavior in the intact and broken-loop sides of the reactor vessel downcomer, which has the potential to affect break flow and downcomer mixing, and (3) the more conservative downcomer fluid temperature predictions it produced.

More detailed information regarding the assessment of RELAP5 for LOFT Test L3-1 is found in Section 3.9 of [***Fletcher***].

6.7.2.5 MIST Tests

The Multi-loop Integral System Test (MIST) facility is a scaled full-pressure experimental facility that represents the B&W lowered-loop plant design with two hot legs and four cold legs. The plant-to-facility power scaling factor is 817, and the plant-to-facility volume scaling factor is 620 for the total primary system volume, excluding the core flood tanks. Major components include two once-through steam generators with full length tubes, two hot leg pipe segments, four cold leg pipe segments, four coolant pumps, a reactor vessel with an external downcomer, a pressurizer with spray and PORV connections, and one core flood tank. Boundary systems provide simulation of the HPI, auxiliary feedwater, and various types of failures such as steam generator tube ruptures and LOCAs.

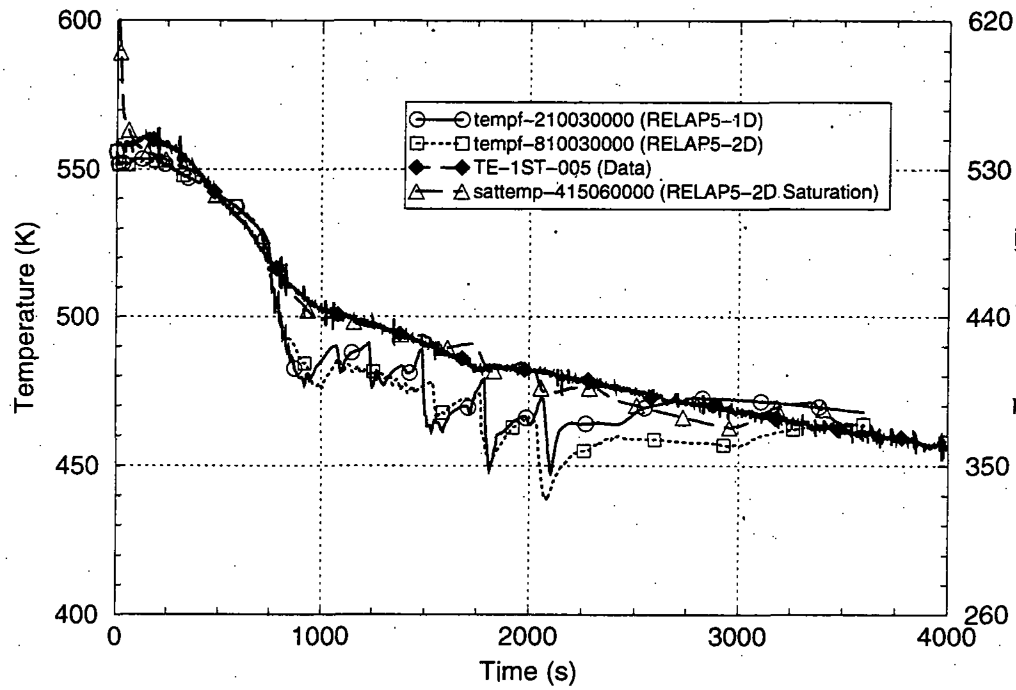

Figure 6.17. Reactor Vessel Downcomer Fluid Temperatures (LOFT Test L3-1)

RELAP5 assessment was performed for three MIST experiments, Test 360499, Test 3109AA, and Test 4100B2.

MIST Test 360499 is a HPI-power operated relief valve (HPI-PORV) feed-and-bleed simulation, starting from 110% flow, 10% scaled-power conditions. The system behavior for this test resembles a stuck-open pressurizer PORV event sequence with continued HPI injection and operator throttling based upon the RCS subcooling margin. Events such as this are significant contributors to the risk of PTS vessel failure.

The assessment for this test indicated that the RELAP5 prediction of the RCS pressure was excellent. However, the assessment indicated major differences between the calculated and measured responses within the cold legs on the two coolant loops. RELAP5 overpredicted the cold leg temperature in Loop A, and did not predict the coolant loop flow stagnation seen in the test. RELAP5 underpredicted the cold leg temperature in Loop B and did predict the coolant loop flow stagnation seen in the test.

Despite these difficulties, the RELAP5 prediction of the reactor vessel downcomer fluid temperature, which represents a mixture of the cold leg temperatures, was judged to be good. Figure 6.18 compares the calculated and measured reactor vessel downcomer fluid temperatures for MIST Test 360499 at a representative location in the downcomer (at an elevation corresponding to the bottom of the core). The code-data comparisons at other downcomer locations are similar. Over the test period, RELAP5 overpredicted the downcomer fluid temperature by an average of 3 K (5°F).

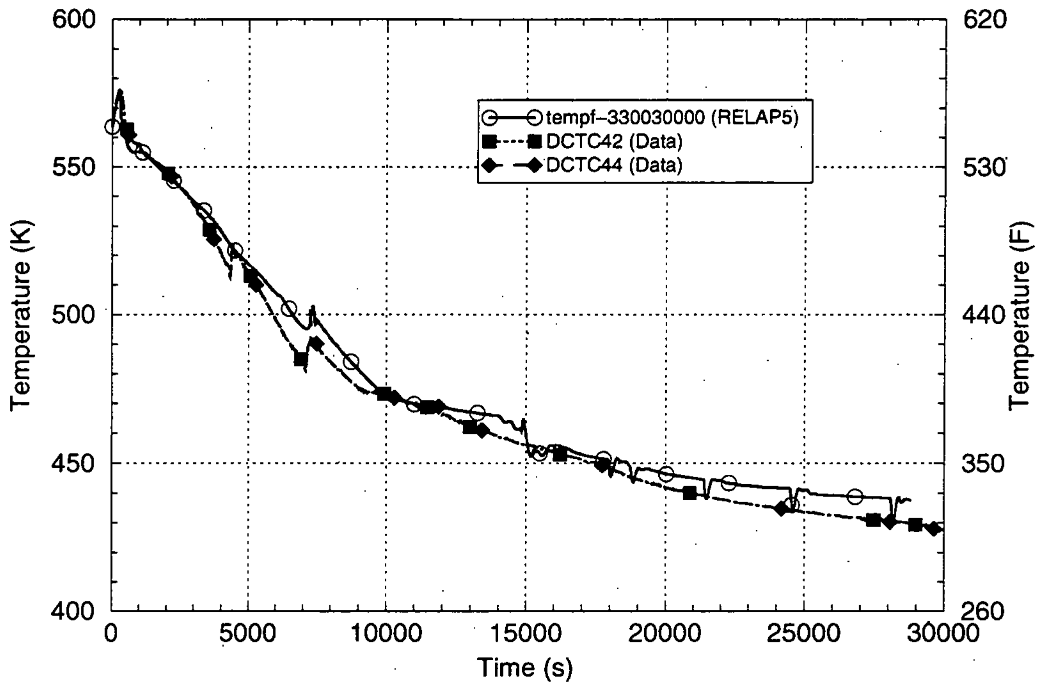

Figure 6.18. Reactor Vessel Downcomer Fluid Temperatures (MIST Test 360499)

MIST Test 3109AA represents a 1.6-in.^{2} (10-cm^2) break in the RCP discharge section of a PWR cold leg. This break size corresponds to a 1.4-in. (3.59-cm) diameter break in the PWR and is sufficiently small that HPI flow can compensate for break flow. At the start of the test, the facility is operating under natural-circulation loop flow conditions, with the RCP rotors locked.

The assessment indicated no major differences between the calculated and measured data for MIST Test 3109AA. The RELAP5 prediction of the RCS pressure is in good agreement with the measured data. The code well-predicted the interruption of loop natural circulation flow in both of the coolant loops. RELAP5 overpredicted the reactor vessel downcomer fluid temperature after about 1,000 s. Figure 6.19 compares the calculated and measured reactor vessel downcomer fluid temperatures for MIST Test 3109AA at a representative location in the downcomer (at an elevation corresponding to the top of the core). The code-data comparisons at other downcomer locations are similar. Over the test period, RELAP5 overpredicted the downcomer fluid temperature by an average of 10 K (18°F).

MIST Test 4100B2 represents a 15.5-in.^{2} (100-cm^2) [4.4-in. (11.2-cm) diameter] equivalent break in the RCP discharge section of a PWR cold leg. The break size is sufficiently large that HPI cannot compensate for the break flow. The test is initiated at conditions representing 3.5% scaled power and coolant loop natural circulation conditions with the RCPs tripped and their rotors locked. During the test, the core power is tripped and HPI and EFW flows are initiated.

The assessment for MIST Test 4100B2 shows moderate differences between the calculated and measured data for the most important parameters for PTS (RCS pressure and downcomer fluid temperature). Following the RCS blowdown, basic limitations of RELAP5 resulted in an underprediction of the stable RCS pressure by about 0.68 MPa [98 psi]. RELAP5 slightly underpredicted the downcomer fluid temperatures during the blowdown period, up to about 2,100 s. However, during the refill period RELAP5 overpredicted the reactor vessel

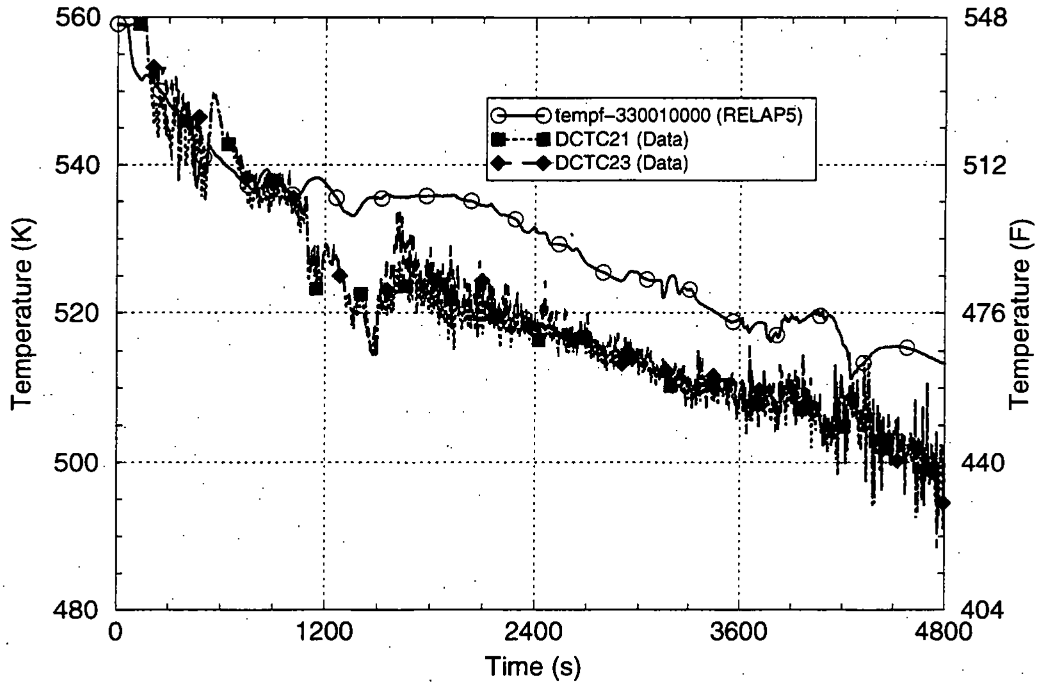

Figure 6.19. Reactor Vessel Downcomer Fluid Temperatures (MIST Test 3109AA)

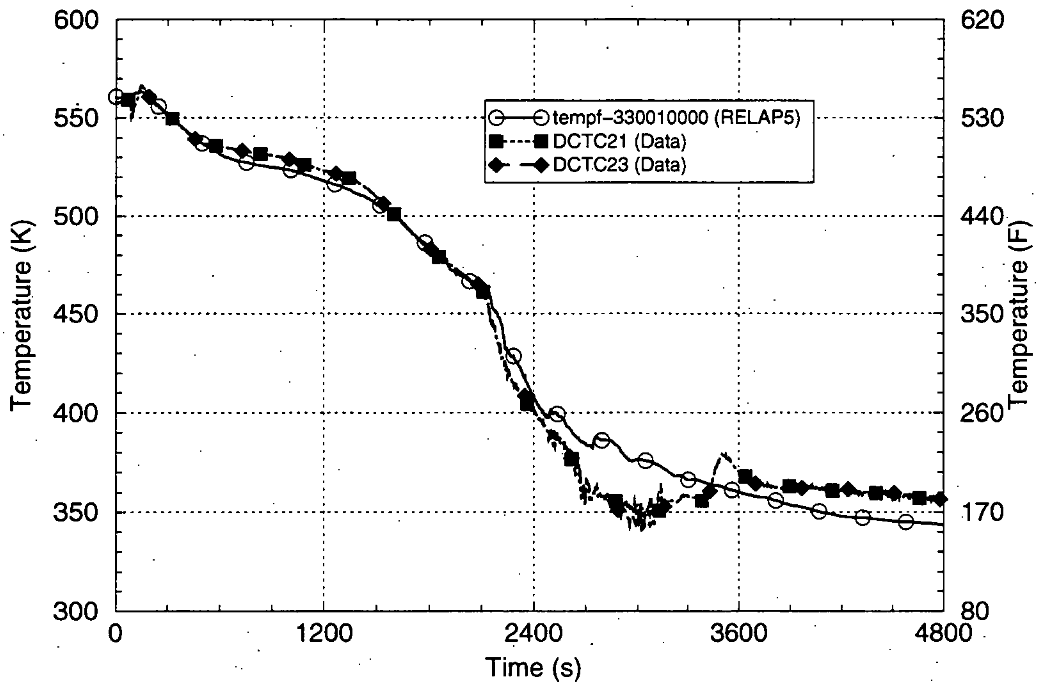

Figure 6.20. Reactor Vessel Downcomer Fluid Temperatures (MIST Test 4100B2)

downcomer fluid temperature by up to 32 K (58 °F). Figure 6.20 compares the calculated and measured reactor vessel downcomer fluid temperatures for MIST Test 4100B2 at a representative location in the downcomer (at an elevation corresponding to the top of the core). The code-data comparisons at other downcomer locations are similar. Over the test period, RELAP5 overpredicted the downcomer fluid temperature by an average of 0.37 K (0.67°F).

6.7.2.6 Reactor Vessel Wall Inside-Surface Heat Transfer Coefficient

For the reactor vessel wall heat transfer coefficient, quantitative assessment comparisons are more difficult than for RCS pressures and downcomer fluid temperatures because heat transfer coefficients are not directly measured in the experiments. Further, since most of the test facilities were designed to study core-coolability safety issues and not vessel downcomer overcooling issues, experimental instrumentation related to downcomer wall heat transfer (wall and fluid thermocouples, wall heat fluxes and downcomer fluid velocities) is generally limited. Quantitative assessments of RELAP5 capabilities for predicting the vessel wall heat transfer coefficient and other heat transfer-related parameters are provided in this section to the extent feasible considering the limited available data. Other investigations into reactor vessel wall heat transfer in general and RELAP5 capabilities in particular are also presented here to support the assessment conclusions regarding the wall heat transfer coefficient. The information in this section summarizes that presented in greater detail elsewhere [***Bessette***].

As described below, for the PTS application, the wall heat transfer regime of greatest interest is for wall-to-fluid convection for Reynolds numbers toward the low end of the turbulent range. This regime corresponds to the reactor vessel downcomer situation during periods with low coolant-loop natural circulation flow or periods after the coolant-loop flows have stagnated as a result of voiding in the upper regions of the RCS (as is caused by draining during LOCA events). Other heat transfer regimes are also experienced during portions of the PTS transient accident scenarios. Highly turbulent forced convection is experienced when reactor coolant pumps are operating or when there is robust coolant-loop natural circulation flow. Saturated and subcooled nucleate boiling are generally experienced for events where the RCS rapidly depressurized, the fluid saturation temperature quickly drops and the hot vessel wall passes heat to a flashing and boiling fluid. The attention is given here to the regime for convection because it (1) is frequently encountered in the PTS scenarios, and (2) results in a relatively low heat transfer coefficient. The other regimes (highly turbulent convection and boiling) result in large heat transfer coefficients. A detailed assessment of the accuracy of RELAP's heat transfer models is not warranted in these other regimes because the process of wall-to-fluid heat transfer is dominated by the surface boiling transport mechanism and not by the convective movement of fluid. Therefore, the heat transfer is less influenced by details of bulk fluid motion

6.7.2.6.1 Effect of Heat Transfer Coefficient on Wall Heat Flux

During normal steady plant operation, the reactor vessel wall temperature is the same as the downcomer fluid temperature (which is core inlet temperature). During PTS scenarios, the fluid temperature falls. The wall-to-fluid heat transfer processes from the hotter vessel wall to the colder fluid in the downcomer are of significance. The RCS cooldowns experienced in the PTS accident scenarios generally fall into three categories of (1) secondary-side events, such as main steam line breaks, (2) small primary-side LOCAs, such as hot or cold leg breaks or stuck-open pressurizer relief valve events, and (3) large primary-side LOCAs, such as double-ended hot or cold leg breaks. Each of these event categories is separately discussed in the following subsections.

6.7.2.6.1.1 Secondary Side Events

For secondary-side events, the RCS is rapidly cooled by overcooling to the steam generators but the RCS remains at high pressure and, often, forced flow of coolant through the RCS loops continues. The RCS fluid cools, but the extent of the cooldown is limited because the ultimate heat sink temperature is the saturation temperature at atmospheric pressure, which represents the final state in the secondary coolant system. The reactor vessel wall heat transfer coefficient remains high as a result of pump-forced flow or a robust coolant-loop natural circulation flow for cases where the reactor coolant pumps are tripped. As a result, the wall-to-fluid heat transfer process is controlled by heat conduction through the reactor vessel wall.

6.7.2.6.1.2 Small Primary Side LOCAs

For small primary-side LOCA events, the RCS depressurizes at a rate that is proportional to the break size. Fluid flashing caused by the RCS depressurization cools the RCS fluid as the saturation temperature falls. The ECC systems add cold water to the RCS at rates that increase with decreasing RCS pressure. This pressure dependency results because the ECC systems are made up of (1) tanks (accumulators, core flood tanks, and safety injection tanks) with cold water inventory stored at intermediate pressures, and (2) centrifugal pump systems (HPI, LPI, etc.) for which no flow is delivered above the pump shutoff heads and for which lower RCS pressures lead to greater cold water injection flow rates.

For the small LOCAs, the system pressure is defined by the RCS mass and energy balances associated with core heat addition, cold water injection, steam generator heat removal, and break flow. There is much interdependence among the PTS parameters of interest (pressure, fluid temperature, and heat transfer coefficient).

Larger break sizes lead to lower pressures (which tend to mitigate the PTS risk) while at the same time leading to higher ECC injection rates and lower fluid temperatures (which tend to increase the PTS risk). Further, the variations in the injection flow rate can directly affect the break flow (which, in turn, affects RCS pressure) and the RCS inventory, which affects tripping of reactor coolant pumps, coolant loop natural circulation and stagnation, vessel downcomer velocities and wall heat transfer coefficients. For small primary-side LOCA events, the potential for vessel failure as a consequence of PTS arises as a result of incomplete RCS depressurization and RCS draining, which causes the stagnation of the coolant-loop natural circulation flows and leads to pooling of cold water in the cold leg and downcomer regions.

Because for small breaks, the injection of cold ECC water is at a low rate, the RCS cooldown experienced for this category of LOCA events is relatively slow and there is a feedback between the heat transfer from the wall to the fluid and the fluid temperature itself. For this category of events, the downcomer wall heat transfer regimes generally fall into the range of turbulent forced convection from wall to subcooled liquid (even following coolant loop flow stagnation, the downcomer flow rates remain sufficiently high to resemble forced convection).

6.7.2.6.1.3 Large Primary Side LOCAs

For large primary-side LOCA events, the RCS completely depressurizes and the injections of cold ECC water from the HPI, LPI, and accumulator systems are at very high rates. The rapid decline in the fluid saturation temperature leads to limited periods of fluid flashing and boiling on the hot vessel wall. Heat transfer coefficients are very high for conditions of nucleate boiling. As a result of the large break size, the RCS cannot repressurize from the ECC injection. The high injection rate floods the cold legs and vessel downcomer regions with cold water and this quickly terminates the boiling process.

6.7.2.6.2 Comparison of Measured and RELAP5-Calculated Reactor Vessel Wall Heat Transfer Data

Only limited pertinent data are available from integral system tests for assessing RELAP5 reactor vessel wall-to-fluid heat transfer for geometries consistent with the plants and the conditions present in the PTS accident scenarios. Instruments are often not available for directly measuring heat transfer coefficient or heat flux. However, downcomer fluid and vessel wall thermocouple data along with fluid velocity data are occasionally available that permit a quantified comparison between the measured and RELAP5-calculated wall heat transfer process. This section summarizes vessel wall-to-fluid heat transfer comparisons pertinent for the PTS for tests performed in the UPTF, APEX-CE, and Creare test facilities.

6.7.2.6.2.1 UPTF Test 1 Run 21

The UPTF featured a full-scale representation of the reactor vessel, downcomer, and cold legs of a PWR. Test 1 Run 21 consisted of injecting cold HPI water into one of the four cold legs (Cold Leg 2) into a system that was initially filled with hot pressurized water. The experimental conditions are comparable to those experienced in a PWR following stagnation of the coolant loop natural circulation flow. This experimental facility and test were modeled with RELAP5 and the calculated results were compared with the measured test data. The RELAP5 model included a 2-dimensional nodalization scheme, comparable to those employed in the PTS plant analyses.

The measured velocity data at the core-bottom elevation in the downcomer exhibited a downward flow below Cold Leg 2 and upward flows through other azimuthal sectors of the downcomer as shown in Figure 6.21. (The direction of positive velocity is downward.) The RELAP5 simulation also showed a downward water flow below Cold Leg 2 (Figure 6.22), but with the cold water spreading into sectors adjacent to Cold Leg 2 by the time the flow reached the core bottom elevation. As a result, the RELAP5-calculated velocities are seen in these figures to be lower than the measured velocities. The fluid velocities in the downcomer (in both the test and calculation) were much greater than the superficial fluid velocity based on only the HPI flow in the downcomer. The test data indicated that the downcomer velocity is ~16 times the downcomer HPI superficial velocity.

An assessment of the RELAP5-calculated vessel wall heat transfer coefficient was made using fluid and wall thermocouple data. In downcomer regions away from Cold Leg 2, RELAP5 was found to underpredict the rates of decline in both the fluid and vessel wall temperatures by a similar extent and therefore to predict the heat transfer coefficient well (within ~15%). Below Cold Leg 2, RELAP5 was found to underpredict the wall-to-fluid differential temperature of the test as shown in Figure 6.23 and to also underpredict the wall-to-fluid heat flux (as indicated by the slower cooldown rate at the location of a thermocouple embedded 1-in. (25-mm) into the vessel wall at the core top elevation; see Figure 6.24). Since the RELAP5 underprediction of the differential temperature was much greater than the RELAP5 underprediction of the heat flux, RELAP5 was found to overpredict the wall-to-fluid heat transfer coefficient under Cold Leg 2 for UPTF Test 1-21 by a factor of ~2.

6.7.2.6.2.2 APEX-CE Test 5

The Advanced Plant Experiment facility (APEX-CE) is a reduced-height, pressure, and temperature facility scaled to Palisades, a CE-designed plant. The test consisted of injecting cold HPI water into all four cold legs of a system that was initially filled with hot pressurized water. The experimental conditions are comparable to those experienced in a pressurized water reactor following stagnation of the coolant loop natural circulation flow. This experimental facility and test were modeled with RELAP5 and the calculated results were compared with the measured test data. The RELAP5 model included a two-dimensional nodalization scheme, comparable to those employed in the PTS plant analyses.

The RELAP5 assessment concentrated on the first 1,700 s of the test period. There was excellent agreement between measured and calculated fluid and wall temperatures as shown in Figure 6.25 and Figure 6.26. The excellent match between the measured and calculated wall temperatures indicated that RELAP5 also predicts the wall heat flux well. However, a comparison between the measured and calculated wall-to-fluid differential temperatures indicated that RELAP5 underpredicted the test differential temperature by a factor of ~2 and, therefore, overpredicted the wall-to-fluid heat transfer coefficient for APEX-CE-5 by the same factor.

There are no direct measurements for downcomer flow velocity in the APEX-CE facility, but flow velocity indications were derived from thermocouple data. The calculations indicated that the RELAP5 and measured flow velocities are in good agreement and that (after scaling up for a full-height downcomer) the data indicate that the downcomer circulating flow velocity is a factor of ~20 greater than the superficial velocity of the HPI flowing alone in the downcomer region.

6.7.2.6.2.3 Creare Fluid Mixing Tests

Creare performed experiments in a one-half linear scale facility to investigate fluid mixing in a downcomer region for a stagnant coolant-loop situation. The facility represents the region of a single cold leg and one-fourth of the reactor vessel downcomer. The downcomer configuration included a thermal shield installed in the center of the downcomer span. Two NRC tests, MAY105 and MAY106 were performed to simulate cold water injection into an initially hot downcomer (RELAP5 simulations for these tests were not performed). Velocity measurements for two tests indicated velocity ratios (downcomer velocity to superficial downcomer velocity based on HPI flow) of 21 and 26. The downcomer flow was found to contain regions of up-flow and down-flow, with the down-flow velocities greater than the up-flow velocities. The downcomer flow pattern was found to be buoyancy induced.

Figure 6.27 shows that the heat transfer data for the Creare tests are proportional to the Dittus-Boelter correlation. An enhancement of the heat transfer by a factor of ~1.55 above the Dittus-Boelter correlation is seen in the figure for down flow regions but not elsewhere. The enhancement is attributed to entrance effects to which the thermal shield configuration may contribute. In modeling convective heat transfer, RELAP5 applies the maximum of Churchill-Chu for free convection and Dittus-Boelter for forced convection. At low flow velocities (e.g., < ~1 m/s), Churchill-Chu provides higher heat transfer coefficients than Dittus-Boelter.

6.7.2.6.2.4 Summary and Discussion

Three sets of experiments related to injection of cold water into stagnant initially hot water in the reactor vessel downcomer region of a pressurized water reactor have been described in this section. The situation represented by these tests is consistent with that following coolant-loop stagnation in many of the PTS accident scenario categories. The experiments all indicate that the buoyancy effects of cold water entering the downcomer through the cold legs set up a circulation within the downcomer region. The downcomer circulation velocities are seen to be larger than the superficial velocity (that which would result in the downcomer from the ECC injection flow alone) by factors of ~16 to 26.

In the UPTF and APEX-CE assessments, RELAP5 with a two-dimensional downcomer nodalization is seen to be able to capture on a first-order basis the flow pattern and velocities in the downcomer region. Based on comparison between measured and RELAP5-calculated wall and fluid temperature data, RELAP5 is seen to provide reasonable representations of the vessel wall inside surface heat transfer coefficient. For the UPTF test, RELAP5 is seen to provide a good representation (within ~15%) of the heat transfer coefficient for downcomer regions away from Cold Leg 2 (the only cold leg through which the cold water enters the vessel) and to overpredict the heat transfer coefficient by a factor of ~2 for the region under Cold Leg 2. For the APEX-CE test (for which cold water enters the vessel through all cold legs), RELAP5 is seen to overpredict the heat transfer coefficient for all downcomer regions, again by a factor of ~2. Creare data corroborate UPTF and APEX-CE data in showing enhanced large eddy circulating flows in the downcomer. The relatively high velocities result in good heat transfer as seen in the data and predicted by RELAP5. The integrated assessment of RELAP5 for downcomer heat transfer shows the predictions of the RELAP code to be either realistic or conservative.

6.7.2.6.3 Comparison of RELAP5-Calculated and CFD-Calculated Downcomer Flows

A comparison was made between RELAP5 and COMMIX CFD code solutions for the flow patterns experienced in the reactor vessel downcomer. The comparison was made during the coolant-loop flow stagnation period following a 2-inch (5.1-cm) hot-side break accident scenario in a three-loop Westinghouse plant.

The comparison indicated that RELAP5 adequately captured the overall flow patterns but not finer-scale eddy-flow behavior seen in the COMMIX run. The flow velocities from the COMMIX and RELAP5 calculations were similar and on the order of 19.7 to 39.4 in/s (0.5 to 1.0 m/s).

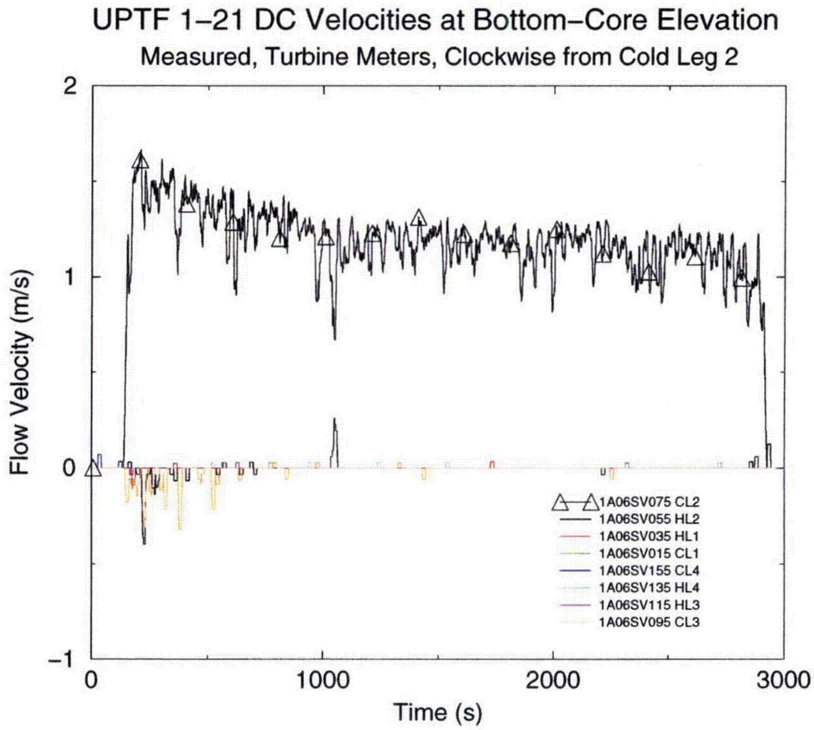

Figure 6.21. UPTF 1-21 DC Velocities at Bottom-Core Elevation Measured, Turbine Meters, Clockwise from Cold Leg 2, Filtered

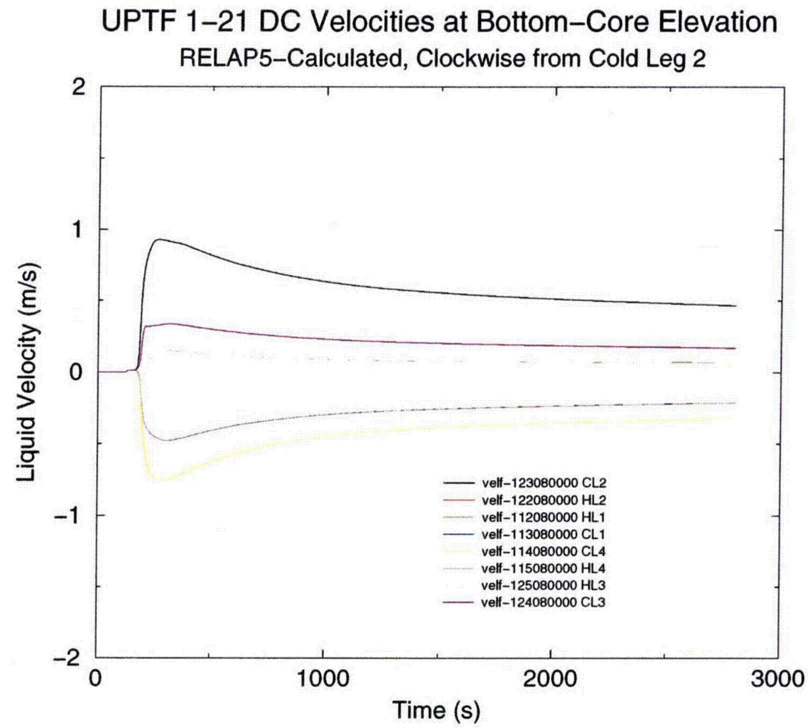

Figure 6.22. UPTF 1-21 DC Velocities at Bottom-Core Elevation RELAP5 (Calculated, Clockwise from Cold Leg 2)

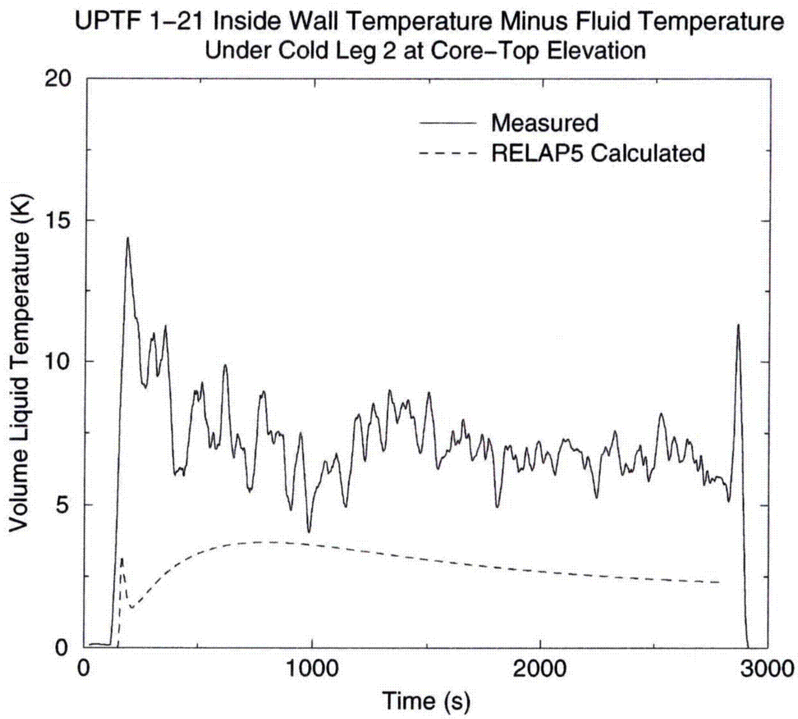

Figure 6.23. UPTF 1-21 Wall Temperature Minus Fluid Temperature Under Cold Leg 2 at Core-Top Elevation

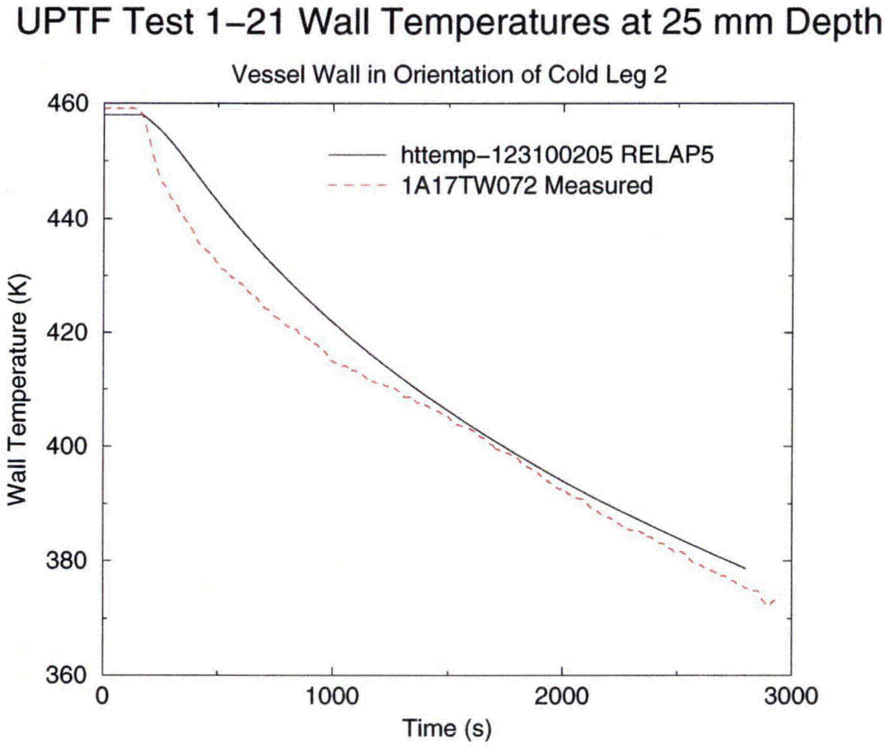

Figure 6.24. UPTF Test 1-21 Wall Temperatures at 25 mm Depth Vessel Wall in Orientation of Cold Leg 2

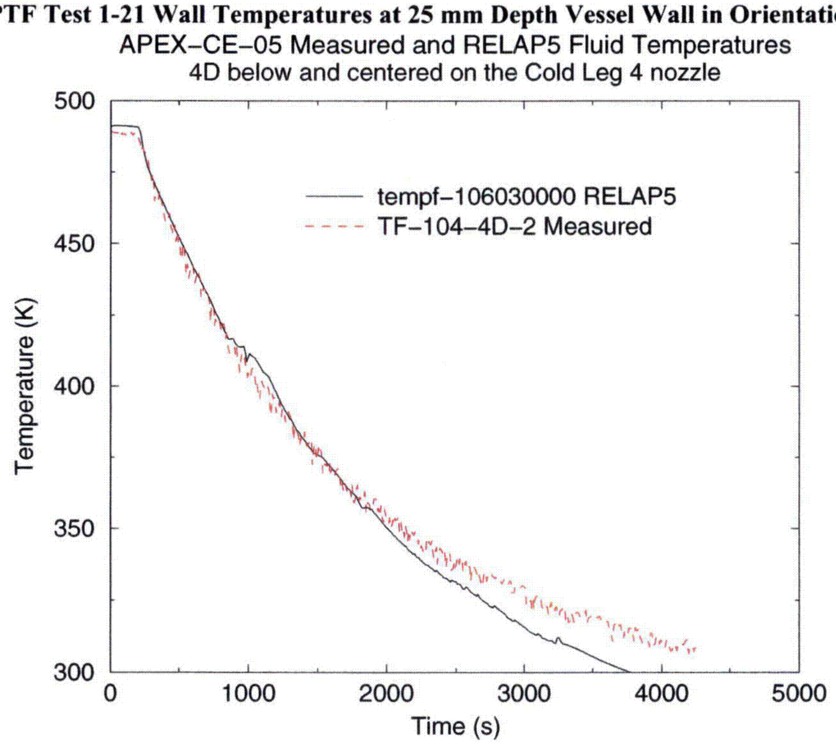

Figure 6.25. APEX–CE–05 Measured and RELAP5 Fluid Temperatures 4D below and centered on the Cold Leg 4 nozzle

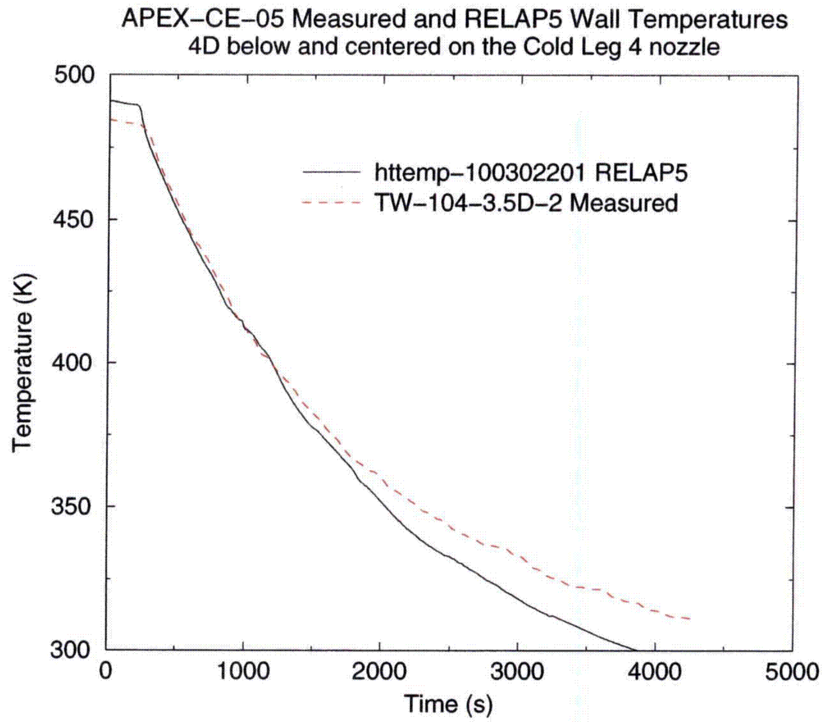

Figure 6.26. APEX-CE-05 Measured and RELAP5 Wall Temperatures 4D below and centered on the Cold Leg 4 nozzle

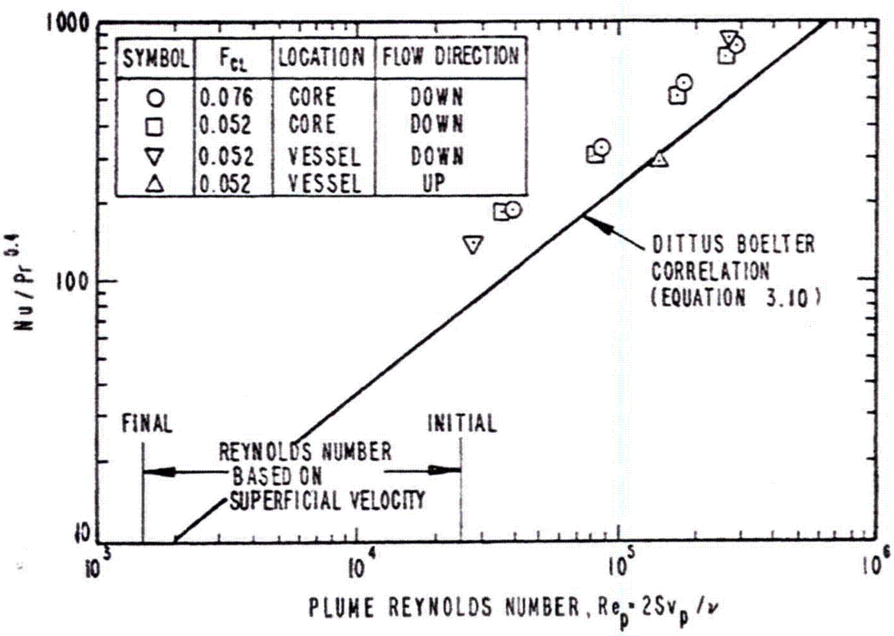

Figure 6.27. Creare Data Compared to Dittus-Boelter

6.7.3 RELAP5 Assessment Conclusions

An assessment has been performed of the RELAP5/MOD3.2.2Gamma computer code capabilities for predicting the parameters of importance for evaluating PTS risk during PWR plant accident scenarios, focusing on the RCS pressure and the temperature of the fluid in the reactor vessel downcomer region. The assessment is performed by comparing the results from RELAP5 simulations of pertinent separate-effects and integral-effects tests with measured test data for experiments in facilities scaled to PWRs. Qualitative judgments are made regarding the overall fidelity of the RELAP5 test predictions. Quantitative estimates also are made of the average uncertainties in the RELAP5 predictions for the important PTS parameters.

The RELAP5 PTS assessment uses data from six experiments in four different separate-effects experimental facilities and from eleven experiments in five different integral-effects experimental facilities.

The separate-effects experiments specifically address (1) pressurizer draining and filling; (2) critical break flow; (3) steam and water behavior in the reactor vessel lower plenum and downcomer regions during the end-of-blowdown and refill periods of LBLOCAs; and (4) single-phase, two-phase, and reflux cooling mode loop natural circulation phenomena under primary-side and secondary-side degraded inventory conditions. These represent phenomena that are significant for the prediction of the important PTS parameters.

The results of the 18 assessment cases generally indicated good and excellent agreement between the RELAP5 calculations and the measured test data. The conclusion from the RELAP5/MOD3.2.2Gamma PTS assessment is that the code is capable of well-predicting the phenomena of importance for evaluating PTS risk in PWRs. The average uncertainty in the RCS pressure prediction is characterized as ±0.2 MPa (±29 psi). The average uncertainty in the reactor vessel downcomer fluid temperature prediction is characterized as ±10 K (±18°F).

6.8 Sensitivity and Uncertainty Analysis

Sensitivity studies were performed to evaluate the effect of key parameters on the RELAP5 prediction of downcomer conditions. These sensitivity studies formed the basis for the assessment of uncertainty in the thermal-hydraulic analysis. The purpose of the uncertainty analysis was to provide adjustments to PRA bin probabilities based on key thermal-hydraulic parameters that significantly affect downcomer conditions, principally temperature.

6.8.1 Sensitivity Analysis

Table 6.2 presents a summary of the results of the sensitivity studies performed as part of the thermal-hydraulic analysis. Many of these sensitivity studies were used to guide the definition of the transients analyzed in this study and to guide the uncertainty assessment discussed later in this section. In addition to the sensitivity studies listed in Table 6.2, evaluations were performed on convective heat transfer from the reactor vessel to the downcomer fluid and on the effect of the in-vessel circulation flows on downcomer conditions.

The heat transfer coefficient model for mixed convection used in RELAP5/MOD3.2.2Gamma is computed as the maximum of the forced convection, laminar convection, and natural convection values. The correlations used are by Dittus-Boelter, Kays, and Churchill-Chu. However, the flow and heat transfer in the downcomer during flow stagnation conditions are more accurately described as buoyancy opposed mixed convection. In this situation, heat transfer is from the hot walls to subcooled fluid flowing downward under low flow conditions. Under these conditions, heat transfer may be enhanced compared to free convection as modeled in RELAP5, which would promote more rapid cooling of the vessel walls.

Sensitivity studies utilizing the Petukhov correlation for parallel plates (known as the ORNL ANS Interphase Model in

RELAP5/MOD3.2.2Gamma) in lieu of the Dittus-Boelter correlation were performed. Additionally, RELAP5/MOD3.2.2Gamma was modified to apply a multiplier to compensate for buoyancy effects in forced turbulent convection published by Swanson and Catton [Swanson 87]. This model was later refined to utilize the Petukhov-Gnielinski heat transfer correlation along with the multiplier proposed by Swanson and Catton.

Other studies were performed where the heat transfer coefficient calculated by RELAP5 was varied by ±30%. The results of these RELAP5 calculations were analyzed using FAVOR to determine the direct impact of heat transfer uncertainty on vessel failure probability. The results of the heat transfer coefficient sensitivity studies are discussed in Chapter 9.

In-vessel circulation flows that deliver water from the upper plenum region to the upper downcomer can occur during a transient (particularly a LOCA). Such flows would tend to warm the water in the upper downcomer and the cold legs. Experiments and CFD studies have shown that there can be significant counter-flow of warm water from the upper downcomer, and energy exchange in the cold leg between the warm stream and the cold ECC injection. These in-vessel flows tend to increase the downcomer temperature.

The B&W vent valve design allows for significant in-vessel circulation once the reactor coolant pumps are tripped. While the pumps are on, the vent valves are held shut by differential pressure. After the pumps are tripped, flow stagnation conditions can occur, and the resulting pressure difference between the upper plenum and the downcomer will cause the vent valves to open, resulting in significant flow of warm water from the upper plenum to the downcomer. The impact of vent valve function on the downcomer fluid temperature is transient-dependent, but can be on the order of 50 K (90°F) based on a 2.83-in. (7.18-cm) surge line break, as seen in the next section.

While Westinghouse and CE plants do not have vent valves, they do have a bypass flow path between the upper downcomer and the upper plenum. The area of this path is generally not precisely characterized in power plants, but amounts to approximately 3% of the total core flow during normal plant operation. Assuming typical values of entrance and exit loss coefficients, the approximate flow area becomes 0.580-ft^2 (0.054-m^2) (10-in. [25.4-cm] diameter equivalent). This value is about 7% of the flow area of the Oconee vent valves, which is 8.45-ft^2 (0.785-m^2). The RELAP5 results were reviewed to evaluate bypass flows, for a large number of Palisades and Beaver Valley transients. The calculations indicate that the flow through the bypass region is small compared to the B&W vent valve flow, implying that the effect of bypass flow on downcomer temperature is small for Westinghouse and CE plants.

6.8.2 Treatment of Uncertainties

6.8.2.1 Overview

The approach used to address uncertainty in the thermal-hydraulic analysis principally utilized sensitivity studies to quantify the effect of phenomenological and boundary condition uncertainties/variations on the severity of a TH sequence. The results of these studies were used in either of the following two ways:

(1) They were combined with probability estimates on the sensitivity parameters being evaluated to adjust the bin probabilities from the PRA analysis.

(2) They were used to justify further subdivision of the PRA bins.

In this way, the TH uncertainty analysis accounted for certain parameters that can affect the thermal-hydraulic response of the plant that were not explicitly considered in the PRA analysis (e.g., season of the year). Because the uncertainty analysis also produced insights regarding the effects of various system parameters and TH models on event severity, it also helped to identify the transient used to represent each PRA bin to the PFM analysis.

Table 6.2 Summary of PTS Sensitivity Studies

Parameter	Significance	Sensitivity Evaluation	Results
Break flow (or valve capacity)	Most important factor in determining the RCS cooldown and depressurization rate. Directly impacts ECCS injection flow.	Break spectrum analysis performed for the three plants analyzed. Range of break diameters considered is 1-in. (2.54-cm) to 22-in. (56-cm), sequentially increasing the flow area by a factor of 2. Analyses where the flow area was varied by ±30% were also performed.	Significant effect on downcomer conditions. Can be significant contributor to vessel failure risk. Uncertainty in break flow for a given break area is small, given the range of break areas evaluated.
Break location	Downcomer temperature generally warmer for cold leg breaks vs. hot leg breaks. Hot leg breaks generally result in lower downcomer temperatures because the break flow enthalpy is higher for a hot leg break than for the same size cold leg break. In addition, for cold leg breaks, the ECC flow into the broken cold leg tends to flow out the break. Therefore, less cold ECC water is delivered to the downcomer.	Effect of break location evaluated by analyzing both cold leg and hot leg breaks.	Significant effect on downcomer conditions. Either hot leg or cold leg breaks can be significant contributors to vessel failure risk.
HPI Flow (BC)	ECCS flow rates are specified from pump flow curves which are pressure dependent.	HPI flow rate varied by ±10%. Evaluations also done considering HPI pump failure.	Effect of flow rate sensitivity found to have an insignificant impact on downcomer conditions and is not a significant contributor to vessel failure risk. Transients involving pump failure resulted in warmer downcomer temperatures, but are generally small contributors to vessel failure risk.

Parameter	Significance	Sensitivity Evaluation	Results
Accumulator Injection Temperature	Injection of large volume of cold water as the system pressure reaches the injection pressure of the accumulators. Injection temperature is dependent upon the season (winter or summer) assumed.	Temperature varied from 294 K (70°F) to 314 K (105°F) depending on the plant analyzed and season assumed.	Significant effect on downcomer conditions, principally temperature in conjunction with HPI and LPI injection temperature sensitivity evaluation. Can be significant contributor to vessel failure risk.
Accumulator Injection Rate	Injection of large volume of cold water as the system pressure reaches the injection pressure of the accumulators.	The effect of pressure on flow was examined by varying the initial pressure from 3.8 MPa [550 psi], 4.1 MPa [600 psi] (nominal) and 4.5 MPa [650 psi].	Insignificant effect on downcomer conditions.
HPI and LPI Injection Temperature	Seasonal effect on the injection water temperature, which affects the downcomer water temperature. Done in conjunction with the accumulator injection temperature sensitivity.	Oconee – Temperature range considered is 278 K (40°F) to 303 K (85°F). Palisades – Temperature range considered is 278 K (40°F) to 311 K (90°F). Beaver Valley – summer temperature of 286 K (55°F) considered. Note that Beaver Valley maintains ECC water temperature at a constant 300 K (50°F) in accordance with Technical Specifications.	Significant effect on downcomer conditions. Affected transients can be significant contributors to vessel failure risk.
Decay Heat Load	Decay heat load directly affects downcomer conditions.	Hot full power conditions and hot zero power conditions considered. Hot zero power defined as 0.2% of full core power (~5.2 MWth).	Uncertainties in decay heat load small compared to the range of conditions considered.
HPI Flow Control	Direct impact of HPI flow rate on downcomer conditions. HPI throttling generally reduces downcomer temperature and system pressure.	For transients involving either closure of a stuck-open pressurizer SRV or main steam line break, the RCS may reach conditions for which operating procedures require HPI throttling or termination. For these transients, the scenarios analyzed varied the timing and conditions under which the operator controlled HPI flow.	Significant effect on downcomer conditions, principally temperature. Affected transients can be significant contributors to vessel failure risk.

Parameter	Significance	Sensitivity Evaluation	Results
Feedwater Control	Direct impact on downcomer conditions particularly if the steam generator is overfilled.	Various feedwater control scenarios ranging from normal control of steam generator level to failure of level control or operator error, resulting in filling of the steam generators until water entered the steam lines.	Range of sequences analyzed covers uncertainty in feedwater control. Generally, effects are insignificant unless combined with a valve failure or MSLB.
Secondary Pressure Control	Direct impact on downcomer conditions for MSLB or stuck-open secondary relief valve sequences.	A spectrum of PRA sequences were analyzed for failures of secondary side valves, including steam dump, steam generator safety/relief, and atmospheric release valves. The failures were combined in some instances with failure of feedwater control such that the faulted steam generator continued to be fed with auxiliary feedwater.	Significant effect on downcomer conditions. Affected transients can be significant contributors to vessel failure risk.

This method of accounting for TH uncertainty does not quantify the uncertainties associated with each TH sequence; rather, it characterizes the uncertainties associated with each PRA bin. This is appropriate because, as illustrated in Figure 3.3, each TH sequence that is passed on to the PFM analysis represents a much larger number of TH sequences that, together, constitute a PRA "bin." Provided the combined effects of the TH parameter and modeling uncertainties on the severity of this one representative sequence is small relative to both

- the uncertainty in the frequency of occurrence of all of the sequences in the bin, and
- the variability in severity between the different sequences in the bin, then

the uncertainty associated with TH parameter and modeling uncertainties of the representative sequence can be considered negligible. The appropriateness of not accounting for these uncertainties because they are negligibly small is ensured by the iterative process used to define the PRA bins. PRA bins that contribute significantly to the estimated TWCF were continually partitioned (including appropriate partitioning of their frequencies and selection of new TH sequences to represent each partitioned bin) until the total estimated TWCF for the plant did not change significantly with continued partitioning. Thus, any errors caused by not explicitly accounting for the TH parameter and modeling uncertainties associated with the TH sequence used to represent each PRA bin are not expected to influence the outcome of the analysis (i.e., the estimated values of TWCF).

The following section summarizes the TH uncertainty analysis. Full details can be found in a companion report [***Chang***].

6.8.2.2 Approach

The TH uncertainty characterization begins with identification of the event categories (e.g., LOCAs) that are expected to significantly challenge vessel integrity. If necessary, each of these event categories was then subdivided. For example, the LOCA event category called was subdivided as follows:

- Small LOCA: between 1.5-in. (3.8-cm) and approximately 4-in. (10-cm)
- Medium LOCA: approximately 4-in. (10-cm) and approximately 8-in. (20-cm)
- Large LOCA: greater than approximately 8-in. (20-cm)
- Stuck-open pressurizer safety relief valves
  - Without subsequent reclosure
  - With subsequent reclosure, resulting in system repressurization

The aim of event category subdivision was to better bound the uncertainty by not having one category attempt to represent too broad a range of thermal-hydraulic conditions. However, even within these subdivided event categories the response of the plant can vary due to sequence to sequence differences within each subdivision. To quantify this, the following uncertainties were identified:

- Aleatory Uncertainties
  - (1) Break diameter (1- to 22-in. (2.5- to 56-cm)): variation of ±30% considered.
  - (2) Break location (surge line or hot leg, cold leg)
  - (3) Decay heat level (full power, low (hot zero) power)
  - (4) Reactor coolant pump status (tripped vs. operating)
  - (5) Heat structure sensible heat (variation of ±30% considered)
  - (6) HPI state (normal operation, failed)
  - (7) HPI flow rate (±10%)
  - (8) Accumulator pressure ± 345 kPa (±50 psi), accumulator temperature: 21°C, 43°C (70°F, 110°F)
  - (9) Effect of seasonal variation on downcomer temperature (summer, winter)
- Epistemic Uncertainties
  - (1) In-vessel circulation attributable to vent valve function in Oconee (cases where valves failed were considered)
  - (2) Vessel wall-to-downcomer fluid heat transfer
  - (3) Flow resistance (loop flow)
  - (4) Break flow

6.8.2.2.1 Break Diameter and Location (Aleatory 1 and 2)

Downcomer conditions are strongly influenced by the break diameter (break flow) and break location. Various diameters (1.5-in. (3.8-cm) to 22-in. (56-cm)) and break locations (surge line, hot leg, and cold leg) are considered.

The thermal-hydraulic response of the reactor system is considerably different as the break diameter increases from 2-in. (5.08-cm) to 16-in. (40.64-cm). For the larger break cases of 8-in. (20.32-cm) or more, maximum ECCS delivery will occur (the HPI and LPI systems will be operating at pump runout conditions), resulting in the maximum rate of reactor coolant system (downcomer) cooldown and depressurization.

For smaller breaks in the range of 5.6-in (14.37-cm) or less, ECCS delivery flow will be limited by the break flow so that the rate at which reactor coolant system cooldown and depressurization will occur is more strongly tied to break diameter and location. In this range, the rate of reactor system cooldown and depressurization decreases with break diameter. Transients involving stuck-open primary side safety valves fall into this category.

ECCS performance is also affected by the break location. For hot leg or surge line breaks, the ECCS will flow from the cold legs through the downcomer to the break. For cold leg breaks, some of the ECCS flow will be discharged through the break.

Inherently, the rate of reactor system cooldown and depressurization is more uncertain in this range relative to break diameters greater than 8-in. (20.32-cm). Hence, the uncertainty analysis focused on break diameters less than 5.6-in (14.37-cm). A ±30% variation on break area to account for break flow uncertainty was considered for LOCA and stuck-open primary safety valve transients.

6.8.2.2.2 Heat Sources (Aleatory 3, 4, and 5)

Heat sources affecting downcomer conditions include the decay heat load, reactor coolant pump status, and the sensible heat in the reactor plant heat structures.

In the case of decay heat load, three sets of decay heat data corresponding to full-power operation, 0.7% of full-power operation, and 0.2% of full-power operation were analyzed. Later in the analysis, the low-power operations were combined into the hot zero power initiating state. Probabilities assigned to these states are 0.98 for hot full-power conditions and 0.02 for hot zero power conditions. Uncertainties in heat load due to RCP operation were considered by evaluating transients where the pumps are tripped vs. when they remain operating.

The principal effect of sensible heat in the heat structures is the rate at which heat is transferred from the system structure to the system fluid. A range of ±30% is considered in the uncertainty analysis.

6.8.2.2.3 High-Pressure Injection (Aleatory 6 through 9)

ECCS performance considered four factors, including (1) failure on demand, (2) injection flow rate, (3) injection temperature, and (4) injection timing. System failures include a partial or full system failure, where the injection flow at the required rate is not delivered. Failures of this type result in warmer downcomer temperatures. Transients involving HPI failure have been considered in the uncertainty analysis. Flow rate uncertainty was assessed using a ±10% variation in HPI flow. Flow rate uncertainties in the LPI or accumulators (or core flood tank) were also considered.

Uncertainty in injection temperature considers the effect of seasonal variations on the injection water source, which is the refueling water storage tank located outdoors. Table 6.2 lists the values used. Probabilities assigned to the seasonal variation are 0.25 for summer and winter and 0.50 for fall/spring. Uncertainty in injection timing of the accumulators was considered by varying the injection pressure over a range of ±50 psi. The pressures at which high- and low-pressure injection is initiated are judged to have a small uncertainty. Uncertainty in the RCS coolant loop total flow resistance focuses on the loop flow resistance. A 100% increase in flow resistance was considered.

6.8.2.2.4 Vent Valves (Epistemic 1)

Uncertainty in the in-vessel circulation, which affects the energy distribution in the reactor coolant system, focuses principally on Oconee because of the presence of the vent valves. For the uncertainty evaluation, failure of the valves to open was considered.

6.8.2.3 Definition of Sensitivity Indicator

Sensitivity analyses were performed with RELAP5 for each of the parameters discussed in Section 6.8.2.2. Downcomer temperature is the most important of the three thermal-hydraulic boundary conditions in the fracture analysis and therefore is the focus of the sensitivity analysis. The sensitivity indicator is the effect on the average downcomer temperature due to the change in a single sensitivity parameter over the transient time of interest, which is 10,000 seconds for this analysis. Each sensitivity indicator has an associated probability of occurrence determined from the parameter being varied. The following equation is used to compute the sensitivity indicator:

$$\Delta T = \overline{T}_{sen} - \overline{T}_{nom}$$

where $\overline{T}_{sen}$ is the sensitivity case downcomer temperature averaged over the 10,000 seconds interval and $\overline{T}_{nom}$ is the base case downcomer temperature averaged over the 10,000 second interval. To compute the sensitivity indicator, each sensitivity parameter is varied (one at a time) to an upper and lower bound and the average temperature difference is determined. This approach is called the nominal range sensitivity analysis and is described in more detail in [***Chang***].

The impact on the sensitivity indicator of a given sensitivity parameter depends strongly on the transient and therefore a large number of transients that include the types of transients considered in the PTS analysis (LOCAs, stuck-open primary safety valves, MSLBs, etc.) need to be considered.

6.8.2.4 Example of Results for a Surge Line Break

The case of a 2.83-in. (7.18-cm) surge line break LOCA for Oconee is used to illustrate the development of the sensitivity indicator. Figure 6.28 presents the sensitivity parameter ranking for the 2.83-in. (7.18-cm) surge line break LOCA for Oconee. For this case, the sensitivity indicator ranges from an increase of 100K (180°F) when HPI is assumed to fail to a decrease of 35 K (63°F) for hot zero power initialization. The sensitivity indicator depends on the transient being considered and sensitivity indicators were developed for the range of transients considered in the PTS analysis.

The uncertainty evaluation requires consideration of the effect of multiple parameters on the downcomer conditions. As an example, a transient may be initiated from hot zero power during the summertime. The sensitivity studies only evaluated the effect of increasing or decreasing a single parameter. To combine the effect of multiple parameters on the downcomer fluid temperature, the sensitivity indicators are added together. This approach is based on the assumption that the effect of any sensitivity parameter is independent of the effect of any other parameter so that the sensitivity indicators become linearly additive. Application of the linearly additive assumption avoids performing RELAP5 sensitivity studies on the large number of sensitivity parameter combinations. The linear additive assumption was applied to the various types of transients considered in the uncertainty analysis.

Validation of the linear additive assumption (LAA) was done by varying multiple sensitivity parameters in a single RELAP5 run based on a 2.83-in. (7.18-cm) surge line break LOCA model for Oconee. Five different combinations of sensitivity parameters were selected to cover a downcomer temperature range of 111 K (200°F).

Table 6.3 lists the five combinations of sensitivity parameters considered and the results of T_{sens} computed applying the linear additive assumption compared to direct computation using RELAP5. A plot of the results is shown in Figure 6.29. The 45-degree line in Figure 6.29 represents the perfect scenarios in which the expected values are same as the RELAP5 calculated values. The solid dots represent the realities. The difference between the solid dots and the squares on the 45-degree line is the deviation of the LAA from the RELAP5 results. Figure 6.29 shows that downcomer temperature computed using the linear additive assumption is in good agreement with the RELAP5 calculated results.

Given the important sensitivity indicators and associated probabilities, a statistical analysis is carried out to finalize selection of representative transients for each bin and to refine the frequencies for the bins defined during the front-end risk modeling. This statistical analysis is performed in two parts. First, the downcomer temperature is determined by adjusting the nominal downcomer temperature for each subcategory identified in Step 5 by the sensitivity indicator (downcomer temperature adjustment) for all combinations of sensitivity parameters being considered for that subcategory using the linear additive approach. Then, the probability of occurrence for each combination of sensitivity parameters is determined. Note that thousands of temperature points are generated for all of the combinations of sensitivity parameters considered.

Table 6.3 List of Combined Sensitivity Indicators Varied for LAA Verification

No.	Sensitivity Parameters Varied	T_{sens} using LAA	T_{sens} (°K) using RELAP5	$T_{sens,RELAP5} - T_{sens,LAA}$ (°K)
1	Winter conditions; p(CFT) +50 psi; 70% A_{brk}; RVVVs Close; 70% HTC	331.7	345.3	13.6
2	Summer; vent valves failed closed; 200% loop flow resistance	360.0	362.3	2.7
3	p(CFT) +50 psi; 110% nominal HPI mass flow; 70% nominal break area; 130% nominal heat transfer coefficient	387.6	391.4	3.8
4	Summer conditions; p(CFT) ÷50 psi ; 90% nominal HPI mass flow; 130% nominal break area; normal vent valve function; 200% loop flow resistance	415.5	406.9	-8.6
5	Summer conditions; 90% nominal HPI mass flow; 70% nominal break area; normal vent valve function; 130% nominal heat transfer coefficient.	438.2	448.8	10.7

Given the downcomer temperature and corresponding probability, a probability density function is constructed. The development of this function is illustrated in Figure 6.30 for Oconee for LOCAs between 1.5-in. (3.81-cm) and 4-in. (10.16-cm) in diameter. This figure shows the resulting cumulative distribution function found from integrating the probability density function that is used to obtain the probabilities used to adjust the bin frequencies.

The representative scenarios are determined from the probability density function by subdividing the probability into five bands between the 0.05 and 0.95 probability levels and determining the temperature at the median point in each band. The probabilities in the two regions near the tails are increased by 0.05. This adjustment is made because of potentially large errors in the sensitivity indicator in the tails of the probability density function (below 0.05 and above 0.95 probability level). In Figure 6.30, there are five bands shown on the cumulative density function plots along with the median values identified and the downcomer temperature corresponding to each median.

Selection of the representative scenario corresponding to the median temperature in each probability band in the cumulative density distribution plot is done by picking the sensitivity indicator result that corresponds to the median temperature and using the corresponding set of RELAP5 results for probabilistic fracture mechanics analysis. An example of the selection of representative scenarios along with the corresponding probabilities is presented in Table 6.4.

The uncertainty analysis was performed for the transients considered for the Oconee, Beaver Valley, and Palisades plants. There were some variations in the thermal-hydraulic categories considered, the sensitivity indicators evaluated and in the set of representative transients selected. These variations are attributable to differences principally in plant design and plant operating conditions. Otherwise, the approach used is the same for the three plants. Adjustments were made to the bin probabilities and representative sequences were selected based on the uncertainty analysis conducted for the three plants. Details can be found in [***Chang***].

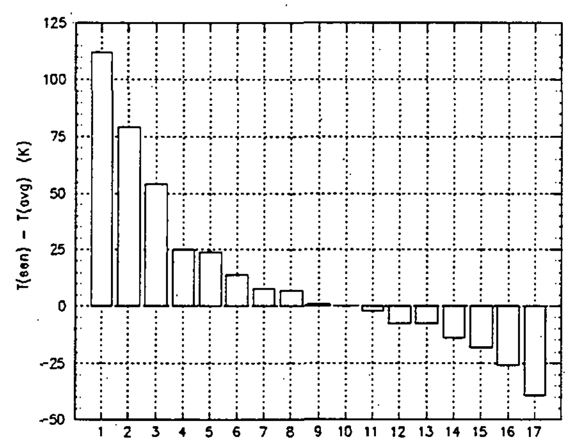

1	100% HPI fail
2	50% HPI fail
2	50% HPI fail
3	25% HPI fail
4	RVVVs Open
5	CL LOCA
6	90% m(HPI)
7	130% CHTC
8	Summer
9	P(CFT) -= 50 psi
10	Nominal
11	P(CFT) += 50 psi
12	110% m(HPI)
13	70% CHTC
14	Winter
15	High CL rev. K
16	RVVV Close
17	HZP

Figure 6.28. Sensitivity parameter ranking of a 2.8-in. (7.18-cm) surge line break LOCA

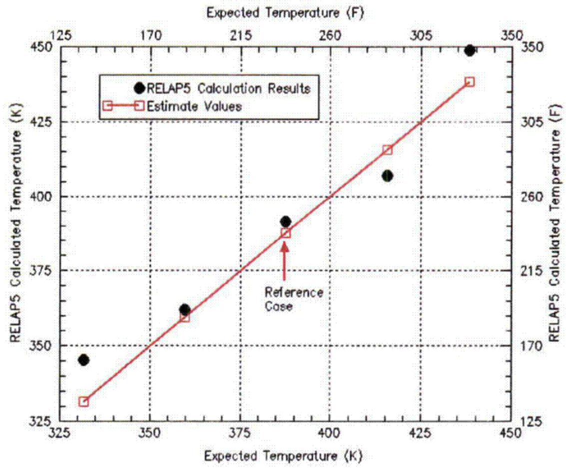

Figure 6.29. Confirmation of the Linearly Additive Assumption for a 2.8-in. (7.18-cm) surge line break LOCA

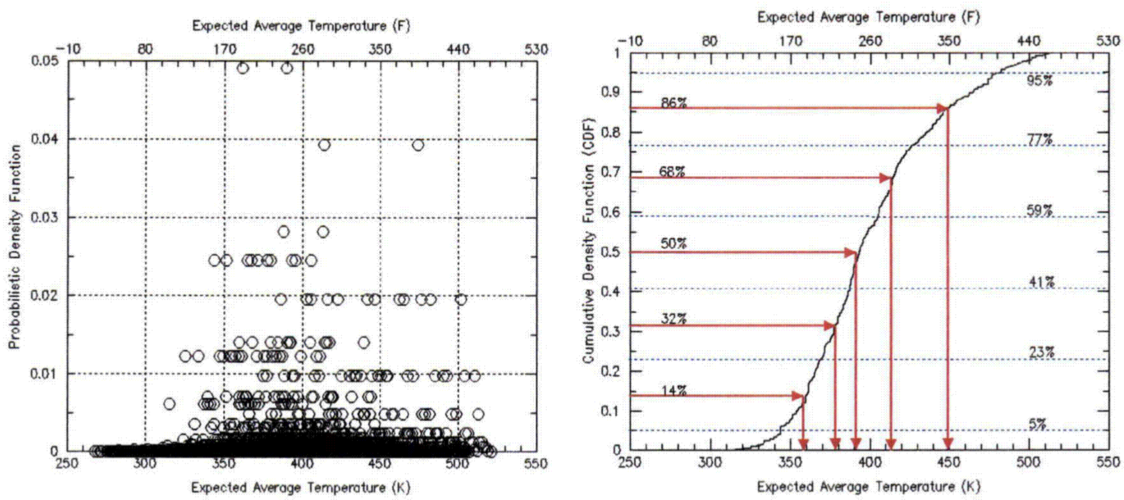

Figure 6.30. Illustration of the Statistical Results for Downcomer Temperature Distribution

Table 6.4 Example of Representative Scenario Selection

#	TH Bin #	Probability	Scenario Specification Descriptions
1	145	0.23	1E-3 m^2 cold leg LOCA with increased 30% break area (Winter)*
2	142	0.18	4E-3m^2 surge line with 30% reduced break area
3	141	0.18	4E-3m^2 surge line with 30% increased break area
4	172	0.18	8E-3m^2 cold leg LOCA
5	154	0.23	8E-3m^2 surge line LOCA with 30% reduced break area RPV vent valves closed

7 Probabilistic Fracture Mechanics Analysis

7.1 Interaction of PFM Model with PRA and TH models

Figure 7.1 illustrates how the PFM model connects to both the PRA and TH models discussed in Chapters 5 and 6, respectively. Specifically, the PFM model takes as input from TH the pressure, temperature, and heat transfer coefficient time histories that have been defined by TH for the sequences defined by PRA. The PFM model uses this TH information along with other information concerning plant design and materials of construction to estimate the time-dependent driving force to fracture produced by a particular event sequence. The PFM model compares this estimate of fracture driving force to the fracture toughness, or fracture resistance, of the RPV steel. This comparison allows us to estimate the probability that a particular sequence of events will produce a crack all the way through the RPV wall were that sequence of events actually to occur. The final step in the analysis involves a matrix multiplication of these through-wall cracking frequency estimates with the frequency at which a particular event sequence is expected to occur (as defined by PRA). This product establishes an estimate of the annual frequency of through-wall cracking that can be expected for a particular plant after a particular period of operation when subjected to a particular sequence of events. The annual frequency of through-wall cracking is then summed for all event sequences specified by PRA to estimate the total annual frequency of through-wall cracking for the vessel. Performance of such analyses for various operating lifetimes provides an estimate of how the annual through-wall cracking frequency can be expected to vary over the lifetime of the plant.

7.2 Components of the PFM Model

Figure 7.1 also shows that the PFM model is itself composed of four major sub-models (which themselves are composed of yet more sub-models and parameter inputs). The four major sub-models that make up the PFM model are as follows:

- A flaw distribution model: see Section 7.5 for an overview and [***Simonen***] for details.
- A neutronics model: see Section 7.6 for an overview and [***EricksonKirk-PFM***] for details.
- A crack initiation model: see Section 7.7 for an overview and [***EricksonKirk-PFM***] for details.
- A through-wall cracking model: see Section 7.8 for an overview and [***EricksonKirk-PFM***] for details.

Together, these four sub-models provide the information necessary to estimate both the fracture driving force ($K_{applied}$) generated by the PTS loading and the resistance of the material to fracture ($K_{Resistance}$). $K_{applied}$ depends upon the thermal-hydraulic inputs of pressure, temperature, and heat transfer coefficient (all *vs.* time), on the vessel dimensions, and on the location and size of the flaws that are quantified by the flaw distribution model. $K_{Resistance}$, more commonly called "fracture toughness," depends upon the chemical composition of the steel, the downcomer temperature from the thermal-hydraulics calculations combined with the heat conduction properties of the steel, and on the degree of neutron irradiation exposure experienced by the steel. Our calculations consider the potential for cracks to initiate in either a brittle manner by cleavage or in a ductile manner by microvoid initiation and coalescence. (The type of crack initiation that occurs depends upon the temperature.) We also consider the potential for cleavage cracks to stop, which is a phenomenon referred to as "crack arrest." These different failure modes all have different characteristics fracture toughness ($R_{esistance}$) values, as follows:

- K_{Ic} quantifies the resistance of the material to crack initiation in cleavage.
- J_{Ic} and *J-R* quantifies the resistance of the material to crack initiation by micro-void coalescence. Furthermore, the *J-R* curve describes the resistance of the material to further ductile crack growth.
- K_{Ia} quantifies the ability of the material to stop (arrest) a running cleavage crack.

These various values of $K_{Resistance}$ (K_{Ic}, J_{Ic}, *J-R*, and K_{Ia}) and their dependencies on chemical composition, temperature, and neutron irradiation exposure are estimated by a combination of the neutronics model, the crack initiation model, and the through-wall cracking model. Also, the crack initiation model and the through-wall cracking models estimate, respectively, the probability of crack initiation and the probability of through-wall cracking by comparing the value of $K_{applied}$ to the appropriate value of $K_{Resistance}$.

7.3 Objectives of this Chapter

The objectives of this chapter are as follows:

(1) Section 7.4: Describes our approach to model development and uncertainty characterization.

(2) Sections 7.5 through 7.8: Provide a summary discussion of the four major sub-models that make up the PFM model.

(3) Section 7.9: Provides a summary discussion of how all of these sub-models are implemented in the FAVOR probabilistic fracture mechanics code. (See [***Dickson-UG***] and [***Williams***] for details.)

(4) Section 7.10: Provides a summary discussion of an experimental validation of the linear elastic fracture mechanics (LEFM) techniques that underlie our approach. (See Appendix A of [***EricksonKirk-PFM***] for details.)

7.4 Approach to Model Development and Uncertainty Characterization

As discussed in Section 3.2, our approach to developing a risk-informed revision of 10 CFR 50.61 requires explicit identification of the type of uncertainty (aleatory or epistemic) to enable the development of an appropriate mathematical model. To do so, it is first necessary to establish independent, physically motivated, models that account for the effects of irradiation damage and temperature. We achieved this goal by the following three-step process:

(1) Uncertainty Identification: We began by constructing a graphical description of the current toughness model. This description, called a "root cause diagram," is illustrated schematically in Figure 7.2. Diagrams of this type show *all* of the parameters (shaded boxes) and *all* of the relationships (nodes) used to estimate the fracture toughness for a particular set of conditions. Decomposing the toughness / embrittlement model in this way permitted identification of individual sources of uncertainty, both in the parameters and in the relationships assumed between the parameters.

(2) Uncertainty Classification: Uncertainties were classified through an understanding of the basic physical mechanisms responsible for crack initiation, for crack arrest, and for irradiation damage. Without this physical understanding, it was impossible to distinguish the irreducible (i.e., aleatory) uncertainties associated with variability of the material from reducible (i.e., epistemic) uncertainties caused by limited data, imperfect models, and so on.

(3) Uncertainty Quantification: The physical understanding developed to classify uncertainty types also played a pivotal role in uncertainty quantification because a model of fracture toughness that can be regarded as representing the true behavior

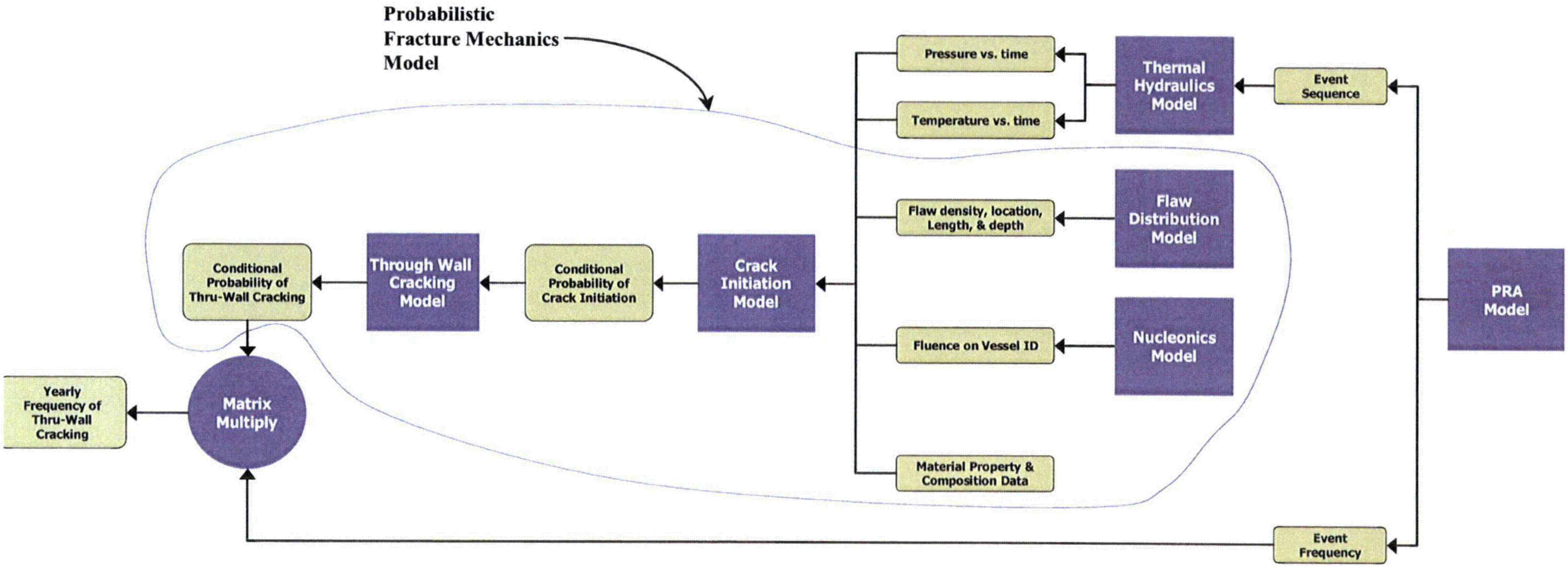

Figure 7.1. Illustration of the interrelationships between PFM model and the TH and PRA models, and the four principal sub-models that comprise the PFM model

of the material is needed to quantify the uncertainties present in any other model. Therefore, uncertainty quantification was achieved by comparing the RT_{NDT}-based toughness model developed for use in the PTS reevaluation project to this best-estimate model.

To be consistent with LEFM principles, LEFM-valid K_{Ic} and K_{Ia} values were used to calibrate the parameters of this best estimate model. However, the best-estimate model cannot be constructed as a purely empirical fit to these K_{Ic} and K_{Ia} values. Without the insights available from a physically based understanding it was impossible to discern if the trends demonstrated by the laboratory data can be expected to apply to the material and loading conditions of interest in commercial PWRs. Consequently, the "best estimate models" each had a form motivated by the physical processes responsible for the underlying phenomena.

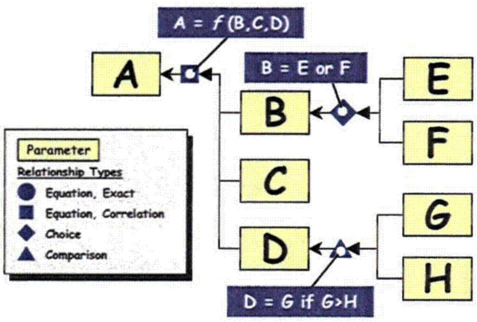

Figure 7.2. Illustration of a root cause diagram showing how uncertainties in input variables (E, F, G, and H) propagate through models (nodes), themselves potentially having uncertainty, to produce uncertainty in a resultant value (A)

7.5 Flaw Model

The flaw model provides estimates of the density (flaws per unit area or volume), size, and location in the vessel wall of initial fabrication defects‡‡. This flaw distribution, reported in detail by [***Simonen***], represents a major improvement in realism relative to that adopted in previous studies of PTS risk. Indeed, one of the major unknowns/uncertainties identified in the last comprehensive evaluation of PTS [SECY-82-465] was the distribution of flaws assumed to exist in the RPV wall. SECY-82-465 used flaw models based on the Marshall study, which included data from a limited population of nuclear vessels and from many non-nuclear vessels [Marshall 82]. These flaw measurements were part of routine pre-service NDE examinations performed 25 or more years ago at vessel fabrication shops. Given the limitations of the NDE technology available at the time, the Marshall flaw distribution provides a reasonable representation only for flaws having depth dimensions larger than ≈1-in. (2.54-cm). The Marshall distribution was nonetheless applied in SECY-82-465 and in the IPTS studies [ORNL 85a, 85b, 86] by extrapolating fits to the data to the much smaller flaws of concern in PTS calculations (less than ≈0.25-in. (0.64-cm)). Additionally, all flaws in the Marshall distribution were assumed to break the inner-diameter surface of the RPV despite the fact that the observations rarely, if ever, revealed surface breaking flaws in nuclear grade construction.

Table 7.1 summarizes the various sources of experimental data used by Simonen et al. to develop the flaw distributions used in FAVOR. While the volume of material represented in Table 7.1 improve greatly on the Marshall flaw distributions [Marshall 82], an inescapable conclusion is also that the quantity of available data is also quite small compared with the volume of RPV material in service. Consequently, it is not possible to ensure on an empirical basis alone that the flaw distributions developed based on these data apply to all PWRs in general. However, the flaw distributions proposed in [***Simonen***] rely on the experimental evidence gained from inspections of the materials summarized in Table 7.1 do not rest solely on this empirical evidence. Along with these data Simonen et al. used both physical models and expert opinions when developing their recommended flaw distributions. Additionally, where detailed

‡‡ Growth of initial fabrication defects attributable to sub-critical cracking mechanisms does not need to be considered; see Section 3.3.3.2.

information was lacking Simonen et al. made conservative judgments (for example, all NDE indications were modeled as cracks and, therefore, potentially deleterious to RPV integrity). This combined use of empirical evidence, physical models, expert opinions, and conservative judgments allowed Simonen et al. to propose flaw distributions for use in FAVOR that are believed to be appropriate/conservative representations of the flaw population existing in PWRs in general. (See Appendix C and [*Simonen*] for details.)

Table 7.1. Summary of sources of experimental data sources for the flaw distribution

Vessel	Weld	Plate	Clad
PVRUF	9150	855	1650
Shoreham	10375	975	--
Hope Creek	245	550	--
River Bend	2440	1465	--
Table entries represent volume of material examined in in^3.			

In the following sections, we summarize the findings of this study for buried flaws in welds (Section 7.5.1), buried flaws in plates (Section 7.5.2), and surface flaws in both plates and welds (Section 7.5.3). Section 7.5.4 contrasts our flaw distribution the results with the Marshall distribution used in SECY-82-465.

7.5.1 Buried Flaws in Welds

The Simonen study made the following observations regarding flaws that form as part of the axial or circumferential weld fabrication process:

(1) Flaws in welds are distributed uniformly through the thickness of the RPV weld. There is no tendency for a greater density of flaws to occur either near the root or cap passes.

(2) No surface breaking flaws were identified in all of the weld material examined, nor was a credible physical mechanism for surface flaw generation identified. Consequently, the flaw distributions used herein contain *only* buried flaws. This is a significant change from the Marshall flaw distribution, which contained *only* surface breaking flaws.

(3) Virtually all non-volumetric flaws found in welds were lack of side-wall fusion defects that exist on the fusion line between the deposited weld metal and the plate or forging being joined. Consequently, the number of flaws in a particular weld scales in proportion to the fusion line area. Additionally, this observation implies that axial welds contain *only* axially oriented flaws whereas circumferential welds contain *only* circumferentially oriented flaws.

(4) Data on flaw density exhibited statistically significant differences depending upon the welding process used (SAW, SMAW, GMAW, or repair weld). However, it is difficult in practice to ascertain from records precisely where different weld processes were used, or where repair welds were made. For this reason, we decided that the flaw distributions used in this study would represent blended combinations of the SAW, SMAW, and REPAIR flaw distributions. Percentages of SAW and SMAW were established on a vessel specific basis. The percentage of repair weld was assumed to be 2% for all vessels analyzed. A repair weld volume of 2% exceeds slightly the repair percentage of 1.5% that was observed by PNNL for both the Shoreham and PVRUF vessels.

(5) Flaw densities exhibited statistically significant differences depending upon the vessel examined (PVRUF or Shoreham). Since Simonen did not establish a model capable of explaining why the density and size of flaws can be expected to vary from vessel to vessel, it was decided to adopt for FAVOR calculations flaw densities based only on observations of the Shoreham vessel because the Shoreham welds had a higher flaw density than the PVRUF welds.

(6) Flaw depth dimensions did not exhibit statistically significant differences for the different welding process and vessels examined, so in this case the data from the different processes and vessels were pooled.

There was, however, clear differences in the distributions of flaws length depending on the welding processes and vessels examined, so the flaw length distributions were established on a case-by-case basis.

It should also be noted that the empirical data used as the primary evidence to establish the distribution of embedded weld flaws do not, and cannot, provide any information about the maximum size a flaw can be. For this reason, it was decided to truncate the non-repair flaw distribution at 1-in. (2.54-cm) and the repair flaw distribution at 2-in. (5.08-cm). In both cases, the selected truncation limit exceeds the maximum observed flaw size by a factor of 2. We performed a sensitivity study with FAVOR and ascertained that, within reasonable bounds on truncation limit dimension, the estimated through-wall cracking frequency is not influenced in any significant way by the truncation limit [Dickson 03].

7.5.2 Buried Flaws in Plates

As reflected by the information in Table 7.1, the empirical evidence available to support a plate flaw distribution is much more limited than the available information for welds. Data on flaw rates and sizes from these sources agree well with two flaw distributions for plates derived by applying flaw density adjustment factors to weld flaw distributions. These adjustment factors, which were proposed by a group of experts [***Simonen***], are as follows:

- The density of plate flaws of depth less than 0.24-in. (6-mm) is 10% of that for weld flaws.
- The density of plate flaws of depth above 0.24-in. (6-mm) is 2.5% of that for weld flaws.

Since reasonable agreement exists between the limited experimental data on plate flaws and the adjusted weld distributions it was decided to use the adjusted weld distributions as input to FAVOR. A truncation limit of 0.43-in. (1.09-cm) was selected because it exceeds the largest observed plate flaw by a factor of 2. Again, a FAVOR sensitivity study demonstrates that this truncation limit does not influence significantly the estimated TWCF [Dickson 03].

Finally, the data reported by [***Simonen***] failed to reveal any preferred orientation for plate flaws. To model this finding in the most accurate way possible without performing mixed-mode fracture calculations, half of the simulated plate flaws are orientated axially, while the remaining half are oriented circumferentially in the vessel.

7.5.3 Surface Flaws in Welds and Plates

The entire inner-diameter of a nuclear RPV is clad with a thin layer of stainless steel to prevent corrosion of the underlying ferritic steel. Lack of inter-run fusion (LOF) can occur between adjacent weld beads, resulting in circumferentially oriented cracks. (All cladding in RPVs was deposited circumferentially.) While the data in [***Simonen***] shows a high probability (1 to 10 flaws per meter of deposited cladding weld bead) of obtaining very shallow LOF defects (1% of the clad layer thickness), only two deep LOF defects, having depths of ~50% and ~63% of the clad layer thickness, were found in all of the cladding inspected. Simonen found no evidence of LOF defects that completely compromised the clad layer.

The only flaws we expect to challenge the integrity of the RPV during PTS loading are those that completely penetrate the clad layer because it is only in this situation that the crack has its tip residing in the ferritic RPV steel, which is subject to neutron irradiation embrittlement. Despite the lack of empirical evidence for such deep flaws, it was not believed appropriate to completely exclude such flaws from the flaw model used in our PFM analysis owing to the limited amount of clad material examined. For this reason, we developed a distribution for small *buried* cladding flaws based on a combination of the data available, expert judgment, and the predictions of the PRODIGAL weld flaw simulation code [PRODIGAL]. This distribution was adjusted as follows to estimate the number of the clad flaws that fully penetrate the cladding thickness:

- We estimated that only $1/1000^{th}$ of the observed density of *buried* cladding flaws would fully penetrate the cladding thickness.

- We assumed that these surface breaking defects exist only in single layer cladding. Multi-layer cladding was assumed to have no surface breaking flaws because the likelihood of two LOF defects aligning in two different weld layers is quite remote.
- Based on the physical mechanism of their formation, all LOF defects are aligned with the clad welding direction (circumferential).

In FAVOR, these surface-breaking circumferential flaws in the cladding can be simulated to occur anywhere in the vessel (i.e., in any weld, plate, and forging).

7.5.4 Comparison of the Current Flaw Distribution with that Proposed by the Marshall Committee

Figure 7.3 compares of the Marshall flaw distribution with the three components of the flaw distribution developed by Simonen. The following observations can be made:

- In general, the individual contributions to the new flaw distribution contain more flaws than the Marshall distribution, but the flaws in the new distribution are considerably smaller.
- While all of the flaws in the Marshall distribution are surface-breaking, only flaws associated with the cladding are surface-breaking in our new distribution, and these comprise only a small percentage of the total. Also, these cladding flaws are all circumferentially oriented because they follow the direction of weld deposition.
- The Marshall distribution focused on flaws in welds and did not distinguish between flaws in different product forms. The new distribution does, and it demonstrates that flaws in base metal are considerably smaller and occur less frequently than flaws in welds.

As illustrated in Figure 7.4, Dickson and Simonen report that the estimated TWCF drops by a factor of between 20 and 70 when the new flaw distribution is adopted instead of the Marshall distribution [Dickson 03].

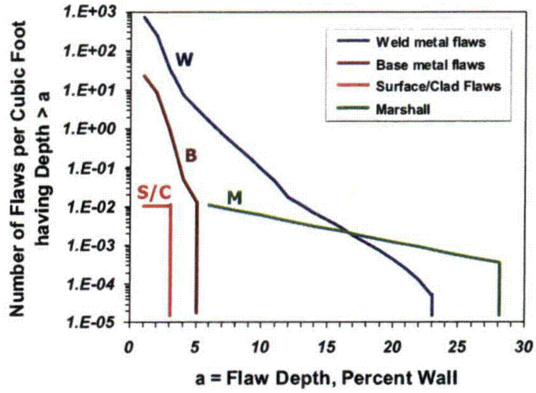

Figure 7.3. Comparison of the new flaw distribution to the Marshall flaw distribution

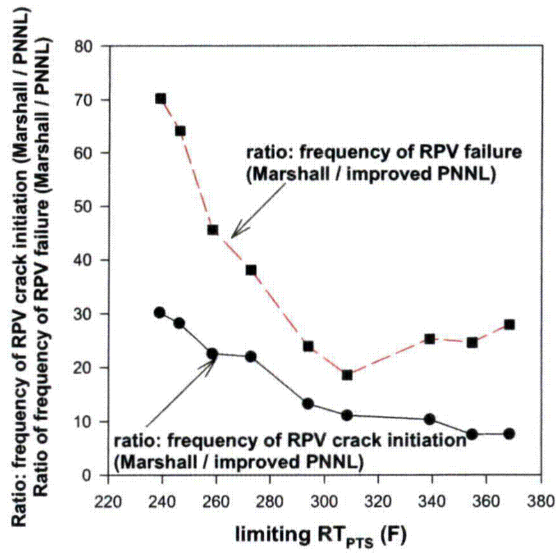

Figure 7.4. Illustration of the impact of the flaw distribution adopted in this study (improved PNNL) with that used in previous PTS calculations (Marshall flaw characterization) [Dickson 02] (analysis performed on Oconee at 60 EFPY)

7.6 Neutronics Model

The neutronics model is itself composed of two major components:

- a calculation of the fluence on the ID of the vessel performed according to NRC Regulatory Guide 1.190 [RG 1.190]
- attenuation of this fluence through the wall of the vessel to the location of the crack of

interest using the attenuation formula in Regulatory Guide 1.99 [RG 1.99].

7.6.1 ID Fluence

The variation of fluence over the inner diameter of the vessel is estimated using modeling procedures based on the guidance provided in the NRC Regulatory Guide 1.190 [RG 1.190], "Calculational and Dosimetry Methods for Determining Pressure Vessel Neutron Fluence." Fluences so calculated are considered best estimates because they are based on the most up-to-date calculational procedures.

While procedures used to calculate fluence have been updated from those that provided the basis of the current PTS Rule, the more significant change in our fluence treatment has been the refinement of our discretization of the circumferential and azimuthal variation of fluence. In previous studies, each major region in the beltline of the vessel (i.e., each weld, plate, or forging) was assigned a value of fluence equal to the peak value estimated to occur anywhere in the region. In contrast, our models capture the detailed azimuthal and axial variation of fluence, resulting in a much more realistic model of the fluence variation in the beltline region.

7.6.2 Through-Wall Fluence Attenuation

Similar to previous PTS calculations [SECY-82-465, ORNL 85a, ORNL 85b, ORNL 86] FAVOR adopts the Regulatory Guide 1.99, Revision 2, model of fluence attenuation through the thickness of the vessel [RG 1.99]. This model assumes that the fluence (and thus the damage caused by irradiation) drops exponentially as the through-wall distance from the inner radius of the RPV increases. The exponential coefficient adopted (-0.24) assumes that fluence attenuates at the same rate as displacements per atom (DPA) (a conservative assumption). A recent review of attenuation models [English 02] concluded that while the RG1.99R2 attenuation model is widely regarded as conservative, no better alternative model exists at the current time.

7.7 Crack Initiation Model

The crack initiation model is itself composed of the following major components:

- Fracture driving force model
  - LEFM driving force
  - Warm pre-stress
- Crack initiation resistance model
  - Unirradiated cleavage crack initiation toughness index temperature
  - Irradiation-induced shift in the cleavage crack initiation toughness index temperature
  - Cleavage crack initiation fracture toughness transition behavior

The probability of a crack initiating is determined by comparing the fracture driving force ($K_{applied}$) and the crack initiation resistance (K_{Ic}). If $K_{applied}$ for a given set of conditions (i.e., a particular TH transient and a particular flaw) exceeds the minimum value of the K_{Ic} distribution, the conditional probability of crack initiation (*CPI*) takes on a value greater than zero, which is calculated by FAVOR. Conversely, if $K_{applied}$ for a given set of conditions falls below the minimum value of the K_{Ic} distribution then *CPI*=0 (exactly zero, not a very small number).

In the following two subsections, we discuss the key features of the crack initiation model (Section 7.7.1) and the major differences between the current crack initiation model and that used in previous investigations of PTS risk (Section 7.7.2) [SECY-82-465, ORNL 85a, ORNL 85b, ORNL 86]. [***EricksonKirk-PFM***] provides a detailed discussion of the crack initiation model.

7.7.1 Key Features

7.7.1.1 Fracture Driving Force Model

Warm pre-stress (WPS) effects were first noted in the literature in 1963 [Brothers 63]. These investigators reported (as have many since them) that the apparent fracture toughness of a ferritic steel can be elevated in the fracture mode transition regime if the specimen is first "pre-stressed" at an elevated temperature. Once a specimen is subjected to a certain $K_{applied}$ and has not failed, the temperature can be reduced and the specimen will remain intact despite the fact that the process of reducing the temperature has also reduced the initiation fracture toughness (K_{Ic} or K_{Jc}) to values smaller than $K_{applied}$. In the past four decades, the physical mechanisms responsible for the WPS effect have been identified, studied extensively, and validated.

The types of loading that produce PTS challenges are characterized (generally) by a rapid cooldown on the inside the RPV. This type of loading produces values of $K_{applied}$ that initially increase, but later decrease as the transient progresses. Thus, depending upon the specifics of the transient (temperature gradients, flaw location, and so on) WPS may be effective, thereby preventing initiation of a cleavage crack even though $K_{applied}$ exceeds K_{Ic}. Nonetheless, to date, investigations of PTS have not included WPS as part of the PFM model [SECY-82-465, ORNL 85a, ORNL 85b, ORNL 86] for the following two reasons:

(1) TH transients were previously represented as smooth variations of both pressure and temperature with time. However, data taken from operating nuclear plants demonstrate that actual TH transients are not always so well behaved. This created the possibility that the short duration fluctuations of pressure and/or temperature with time characteristic of real transients might nullify the beneficial effect of WPS while the companion idealized transient might show WPS to be effective.

(2) In the past, the probabilistic risk assessment (PRA) models of human reliability (HR) were not sufficiently sophisticated to capture the potential for plant operators to repressurize the primary system as part of their response to an overcooling event. Since such a repressurization would usually nullify the benefit of WPS, it was viewed as nonconservative to account for the benefit produced by WPS within a model that may also ignore the potentially deleterious effects of operator actions.

This reevaluation of the PTS Rule features both more realistic representations of the TH transients and a much more sophisticated PRA/HR models that consider explicitly both acts of omission and commission on the part of plant operators. Consequently, we have incorporated WPS effects into the PFM model. Thus, in this model the following two requirements must ***both*** be met for a crack to initiate:

Eq. 7-1 $K_{applied} \geq K_{Ic(min)}$

$dK_{applied}/dt > 0$

7.7.1.2 Crack Initiation Resistance Model

Our model of the resistance of ferritic steels to cleavage crack initiation includes the following characteristics:

- a temperature dependency of fracture toughness that is universal to all ferritic steels and is uninfluenced by irradiation
- a scatter in fracture toughness that is universal to all ferritic steels and is not influenced by irradiation
- a finite lower bound to the distribution of (scatter in) crack initiation toughness values (i.e., a value of fracture driving force below which cleavage fracture *cannot* occur)
- an irradiation damage model that recognizes that the effects of irradiation are purely athermal (i.e., affecting *only* the position of the fracture toughness transition curve on the temperature axis)

These characteristics are all motivated by an understanding of the physical processes responsible for cleavage fracture. While the numerical coefficients of our model are obtained empirically (i.e., obtained by fitting toughness data) the functional forms of the fits are physically motivated. This physical basis provides an additional benefit in that it helps provide assurance that the models apply to all conditions of interest (i.e., to a variety of RPV steels and welds subject to range of irradiation conditions.

Our physical understanding of cleavage fracture also provides important guidance regarding how the uncertainty in fracture toughness should be modeled. Specifically, it is recognized that the distribution of non-coherent particles throughout the BCC iron lattice establishes the scatter in K_{Ic} and K_{Jc} data [Natishan 01, EricksonKirk 04]. It is possible, at least in principle, to know if a non-coherent particle exists at a particular point in the matrix, or not. This might suggest an epistemic nature to K_{Ic} and K_{Jc} scatter, were it not for the fact that K_{Ic} and K_{Jc} do not exist as point properties. K_{Ic} and K_{Jc} values always have an associated size scale, that being the plastically deformed volume. Upon loading, the presence of the crack elevates the stress state along the entire length of the crack front to the point that dislocations begin to move in the surrounding volume of material, which contains a distribution of dislocation barriers (e.g., non-coherent particles, grain boundaries, twin boundaries, etc.). Sufficient accumulation of dislocations at a barrier can elevate the local stress-state sufficiently to initiate a crack in the barrier, and, if the criteria for fracture are satisfied, propagate the crack through the entire surrounding test specimen or structure. Thus, the existence of a particular dislocation barrier at a particular location does not control K_{Ic} and K_{Jc}. Rather K_{Ic} and K_{Jc} are controlled by the *distribution* of these barriers throughout the lattice, and how this *distribution* interacts with the elevated stresses along the crack front. Since the distribution of these barriers throughout the lattice is random and occurs at a size-scale below that considered by the crack initiation toughness model, the uncertainty in K_{Ic} and K_{Jc} is irreducible. For this reason, the uncertainty in K_{Ic} is modeled as aleatory in FAVOR [***Williams***].

Beyond the aleatory uncertainty in K_{Ic}, our model of crack initiation toughness accounts for uncertainties in both the model and in the input parameters that are epistemic in nature. The major epistemic model uncertainty is the RT_{NDT} bias correction, which is discussed in the next section, because this represents a major change in the crack initiation model relative to that adopted in previous investigations of PTS. Epistemic uncertainties in input data (i.e., Cu, Ni, and P content, initial RT_{NDT}, and un-irradiated CVN upper-shelf energy) are accounted for and propagated through the FAVOR calculation. While the mean values of these distributions are the values the licensees have docketed [RVID2], the statistical distributions assumed to exist around these mean values were derived from *all data available* for the entire population of RPV-grade ferritic steels and their weldments. Consequently, these distributions overestimate (sometimes significantly so) the degree of uncertainty in these input variables relative to that which would characterize a *particular* weld, plate, or forging that would exist in the beltline of a *particular* PWR. While plant-specific studies might appropriately adopt less-scattered distributions, we have used generic distributions of the input variables to support our goal of developing a revision to 10 CFR 50.61 that applies to all PWRs.

7.7.2 Major Changes

In this section, we summarize the major changes between the calculational models adopted here and those used to support the current version of 10 CFR 50.61.

7.7.2.1 Fracture Driving Force Model

As discussed in Section 7.7.1.1, our models incorporate the effects of WPS, whereas previous studies of PTS have not. Adopting a WPS model can reduce the TWCF estimated for certain classes of transients. For example, the TWCF estimated for a primary side pipe break will be significantly smaller when the effects of WPS are considered, while the TWCF estimated for a stuck-open valve that recloses later during the transient (thereby repressurizing the primary system) may not be affected by WPS at all. In plant analyses of Oconee Unit 1 based on a complete set of transients (i.e., considering the potential for vessel failure from all potential PTS precursors), inclusion of WPS in the model reduces the estimated TWCF by between a factor of 2½ and 3 [Dickson 03]. Dickson's results show that while the degree of "benefit" associated with adopting a WPS model depends on the transients considered to produce PTS risk it is reasonably insensitive to the degree of embrittlement.

7.7.2.2 Crack Initiation Resistance Model

Relative to the models used in the studies that established the technical basis to the current PTS Rule [SECY-82-465, ORNL 85a, ORNL 85b, ORNL 86], our model has the following *major* differences (see [***EricksonKirk-PFM***] for a comprehensive discussion of *all* differences):

(1) Consideration of Systematic Material Property and Fluence Variations throughout the Beltline Region: In previous studies, the known systematic variations of material properties and fluence throughout the beltline region were treated in a highly simplified fashion. Specifically, the effect of radiation damage on each major region (i.e., each plate, weld, or forging) of the vessel was assessed assuming that the entire region was subjected to the maximum fluence occurring anywhere in the region. This approach led to significant overpredictions of the embrittlement of the vessel, and consequent overestimates of the PTS risk. These conservatisms are absent from our model.

(2) Treatment of Fracture Toughness Scatter as Aleatory: The aleatory model of fracture toughness uncertainty described in Section 7.7.1.2 differs from the epistemic treatment of toughness uncertainty adopted in all pervious probabilistic studies of PTS. In these studies the result of a particular trial in the calculation was the prediction that the vessel *had* or *had not* failed. While this epistemic treatment is inconsistent with our current understanding of the physics of cleavage fracture, the difference in the mean TWCF estimates produced by these two different approaches is small (all other factors being held constant).

(3) RT_{NDT} Bias Correction: While the restrictions on model development detailed in Section 3.1.1 require that the basis of our model be non-toughness metrics (i.e., RT_{NDT}) our model recognizes that RT_{NDT} is not a direct measure of the fracture toughness transition temperature. Indeed RT_{NDT} is by intention a conservative approximation to the true fracture toughness transition temperature, overestimating this value (an implicit conservatism) by 65°F (18°C) on average, and up to 200°F (93°C) in some cases. Our model removes this conservative bias (on average), but in the process, introduces a non-physical model uncertainty. This model uncertainty, which cannot be removed as long as we rely on RT_{NDT}-based metrics, should be regarded as an implicit conservatism in our results. This bias correction significantly reduces the estimated annual through-wall cracking frequency.

7.7.2.3 Method for Estimating Vessel Crack Initiation Probability from the Probability of Initiation of Individual Cracks in the Vessel

Our treatment of the uncertainty in crack initiation fracture toughness (K_{Ic}) as aleatory necessitates use of a different methodology for estimating the probability of crack initiation in the vessel from the probabilities of initiation of the many individual cracks throughout the vessel from that adopted in the calculations used in [SECY-82-465][§§]. In previous probabilistic studies of PTS, the uncertainty in K_{Ic} was modeled as being epistemic, meaning that for any individual simulation, there existed a single value of K_{Ic}. Consequently, if the probabilistic computer code simulated that the applied fracture driving force ($K_{applied}$) resulting from a PTS transient ever exceeded K_{Ic} for any of the

§§ The discussion in this section also applies to the mathematical combination the probability of individual cracks propagating through-wall to estimate the probability of the vessel developing a through-wall crack.

flaws in the vessel, the vessel failure probability was set to 1 (a certainty) and further calculations for that vessel were not performed because a vessel cannot fail twice. When K_{Ic} uncertainty is correctly modeled as being aleatory (as it is in our model), a different approach is needed because the result of each simulation run is not vessel non-failure (probability 0) or vessel failure (probability 1), but rather vessel non-failure (probability 0) or vessel failure *probability* ($0 < \text{probability} \leq 1$; in practical terms vessel failure probability is usually a very small number that is ***not*** close to 1). In this situation, the appropriate representation of the vessel failure probability is the complement (meaning the difference from 1) of the joint (meaning combined) probability of non-failure of all of the flaws in the vessel [Fang 03], which can be expressed mathematically as follows:

Eq. 7-2 $$P_{FAIL(VESSEL)} = 1 - \prod_{j=1}^{n} \left(1 - P_{FAIL(j)}\right)$$

where n is the total number of flaws simulated to exist in the pressure vessel. This equation can be stated in words as follows: *the probability that the vessel will fail is 1 minus the probability that all of the cracks in the vessel do not fail*, or, even more simply: *in order for the vessel to not fail <u>all</u> of the cracks in it must not fail.*

During the many public meetings that have been held during the course of the PTS reevaluation project, concerns have been expressed that this methodology for estimating the vessel failure probability is both inappropriate and overly conservative. The following alternative probability formula has been proposed:

Eq. 7-3 $$P_{FAIL(VESSEL)} = \underset{j=1}{\overset{n}{MAX}} \left(P_{FAIL(j)}\right)$$

This equation states that the failure probability of the vessel is the maximum of the individual failure probabilities associated with the many individual cracks in the vessel. The appropriateness of Eq. 7-2 rather than Eq. 7-3 when estimating the total probability associated with system failures (vessels) that might result from many individual causes (cracks) can be easily understood by way of analogy. Consider the "system" to be an individual human life and consider the "failure" to be death. Below, we provide two examples to illustrate the differences between Eq. 7-2 and Eq. 7-3, and the appropriateness of Eq. 7-2:

<u>Example 1</u>: Hypothetical individual #1 leads a very controlled life and (so) is subject to only one cause of death (cancer). The individual's annual risk of dying of cancer is 2%. In this situation, this individual's total annual risk of death is estimated to be 2% by either Eq. 7-2 or by Eq. 7-3.

<u>Example 2</u>: Hypothetical individual #2 is less careful than hypothetical individual #1 and (so) is at risk from more than one cause of death. The individual's annual risk of dying from any one of four causes is as follows: cancer=2%, AIDS=1%, skydiving=½%, gunshot=¼%. Clearly individual #2 has a greater annual death risk than individual #1, yet Eq. 7-3 estimates their annual death risks to be identical: MAX(2%, 1%, ½%, ¼%), or 2%. Conversely, Eq. 7-2 estimates individual #2's annual death risk to be {1-(1-0.02)*(1-0.01)*(1-0.005)*(1-0.0025)}, or 3.7%.

It can also be noted that for the particular situation of interest here (PTS-induced failures of nuclear RPVs containing cracks), the numerical differences between the failure probabilities estimated by Eq. 7-2 and Eq. 7-3 is actually very small because, as illustrated in Figure 7.5, for the great majority of the time, only one crack in a vessel has a probability of through-wall cracking that exceeds zero. It was for this reason, that Meyer assessed the differences between Eq. 7-2 and Eq. 7-3 to be practically insignificant [Meyer 03].

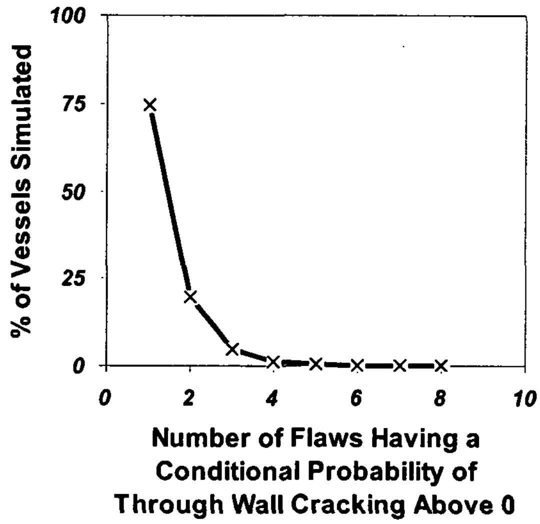

Figure 7.5. Number of flaws simulated that have a conditional probability of through-wall cracking that exceeds zero (Oconee at 60 EFPY).

7.8 Through-Wall Cracking Model

Provided that the results of a particular trial for a particular simulated flaw result in an estimation of $CPI > 0$, FAVOR will check to see how far the simulated crack will propagate into the vessel wall before it arrests permanently (if it arrests at all). The through-wall cracking model is itself composed of the following component models:

- Fracture driving force
  - o LEFM driving force
- Crack growth resistance
  - o cleavage crack arrest
  - o upper shelf ductile tearing model
  - o property gradient model

The probability of through-wall cracking is determined by comparing the fracture driving force ($K_{applied}$) to the resistance to further crack growth, which is expressed as a value of cleavage crack arrest toughness (K_{Ia}). Additionally, once a propagating crack has arrested the potential for re-initiation at some later time in the transient is assessed relative to the material's resistance to crack initiation in either cleavage (K_{Ic}) or by ductile tearing ($K\{J_{Ic}\}$, and the associated *J-R* curve). For each simulation where FAVOR calculates a value of $CPI > 0$, it then conducts 100 deterministic through-wall cracking analyses. The outcome of each of these deterministic simulations is either that the crack propagates all the way through the thickness of the vessel[***], or that the crack arrests before it reaches the outer diameter. The percentage of the trials that result in through-wall cracking is then multiplied by the *CPI* value to estimate the *CPTWC*.

In the following two subsections, we discuss the key features of the through-wall cracking model (Section 7.8.1) and the major differences between our model and that used in previous investigations of PTS risk (Section 7.8.2) [SECY-82-465, ORNL 85a, ORNL 85b, ORNL 86]. These sections address only the crack growth resistance models because the fracture driving force models are the same as used for crack initiation. [*EricksonKirk-PFM*] provides a detailed discussion of the through-wall cracking model.

7.8.1 Key Features

Our model of the resistance of ferritic steels to through-wall cracking includes both a cleavage crack arrest model and a model for re-initiation of a crack by ductile tearing on the upper shelf[†††]. These models include the following characteristics:

- Crack arrest toughness model
  - o a temperature dependency of crack arrest toughness that is universal to all ferritic steels and is not influenced by irradiation
  - o a scatter in crack arrest toughness that is universal to all ferritic steels and is not influenced by irradiation

*** In practice, when the crack extends 90% of the way through the wall thickness the vessel is considered to have failed.

††† The through-wall cracking model also accounts for the possibility of re-initiation in cleavage, but for these purposes the crack initiation model described previously in Section 7.7 is used.

- a finite lower bound to the distribution of (scatter in) crack arrest toughness values (i.e., a value of fracture driving force below which cleavage fracture *cannot* occur)
- a model that positions the crack arrest transition temperature depending on the crack initiation transition temperature, and recognizes that the temperature differential between the crack initiation and crack arrest transition temperatures depends on the amount of prior hardening (i.e., irradiation damage) experienced by the material

- Upper shelf ductile initiation and tearing model
  - a temperature dependency of upper-shelf toughness that is universal to all ferritic steels and is not influenced by irradiation
  - a scatter in upper-shelf toughness that is universal to all ferritic steels and is not influenced by irradiation
  - a linkage between the magnitude of the fracture toughness on the upper shelf and the fracture toughness transition temperature

These characteristics are all motivated by an understanding of the physical processes responsible for both cleavage crack arrest and for ductile crack initiation on the upper shelf. While the numerical coefficients of our models are obtained empirically (i.e., obtained by fitting toughness data), the functional forms of the fits are physically motivated. This physical basis provides an additional benefit in that it helps provide assurance that the models apply to all conditions of interest (i.e., to a variety of RPV steels and welds subject to range of irradiation conditions).

Our physical understanding of both cleavage crack arrest and of ductile crack initiation also provides important guidance regarding how the uncertainty in fracture toughness should be modeled. As was the case for cleavage crack initiation toughness, it is recognized that the physical processes responsible for both cleavage crack arrest and for ductile crack initiation make the uncertainty in these toughness values aleatory in nature [***EricksonKirk-PFM***], and it is so modeled in FAVOR [***Williams***].

7.8.2 Major Changes

Relative to the models used in the studies that established the technical basis to the current PTS Rule [SECY-82-465, ORNL 85a, ORNL 85b, ORNL 86], our model has the following *major* differences (see [***EricksonKirk-PFM***] for a comprehensive discussion of *all* differences):

(1) Allowance of Ductile Tearing and Inclusion of Crack Arrest Resistance at $K_{applied}$ Values Above 200 ksi√in (220 MPa√m): In all former studies of PTS (including our own study reported in [***Kirk 12-02***]) the resistance to crack arrest was truncated at 200 ksi√in (220 MPa√m) because this is the highest value allowed by the ASME code K_{Ia} curve. However, ample evidence from large-scale experiments exists demonstrating that crack arrest above 200 ksi√in (220 MPa√m) does occur, indicating the inappropriateness and over-conservatism of the 200 ksi√in (220 MPa√m) limit. Moreover, no allowance was ever made in former studies of the possibility for an arrested crack to re-initiate by ductile tearing on the upper shelf despite the fact that the resistance to crack initiation on the upper shelf ranges between 100 and 200 ksi√in (110-220 MPa√m) for ferritic RPV steels both before and after irradiation. We have eliminated this apparent oversight in our through-wall cracking model. As shown in Figure 7.6, the combined effect of these two changes is a reduction in the TWCF by a factor of 4–5 (at lower levels of embrittlement) down to a reduction factor of ~1.5 as embrittlement increases. Allowing cracks to arrest at $K_{applied}$ values above 200 ksi√in has resulted in cracks being arrested at shallower depths, which in turn makes re-initiation by either cleavage or ductile fracture more difficult. Thus, removing the conservatism of the 200 ksi√in (220 MPa√m) limit on K_{Ia} more than

compensated for the non-conservatism associated with assuming that re-initiation in a ductile mode cannot occur.

(2) A Separation between the K_{Ic} and K_{Ia} Curves that Depends on the Degree of Irradiation Embrittlement: In all studies of PTS risk predating this reevaluation, the temperature separation between the K_{Ic} and K_{Ia} transition curves was held fixed irrespective of the material condition, as has always been the practice for the ASME K_{Ic} and K_{Ia} curves. However, because ferritic steels harden to an absolute limit [Wagenhofer 01], the separation between the two curves depends upon the degree to which the material is hardened, with more hardened (more irradiated) materials having smaller separations [Kirk 02a]. This is also supported by ample empirical evidence [Wallin 98b]. We have not performed a sensitivity study to assess the effect of this model change. However, comparison of the temperature differential between the K_{Ic} and K_{Ia} curves adopted by our current model (see curve of Figure 7.7) with the constant temperature differential of ~30°C (~86°F) previously assumed (i.e., the temperature separation between the ASME K_{Ic} and K_{Ia} curves) demonstrates our new model reduces the crack arrest capacity of higher toughness materials (i.e., materials having a T_o value of ~60°C (~140°F) or less) because the greater K_{Ic} to K_{Ia} curve separation adopted by our model reduces the of value of K_{Ia} at a fixed K_{Ic}. Conversely, the crack arrest capacity of more embrittled materials (i.e., materials having a T_o value of ~60°C (~140°F) or more) is greater in our model than it is in the ASME model.

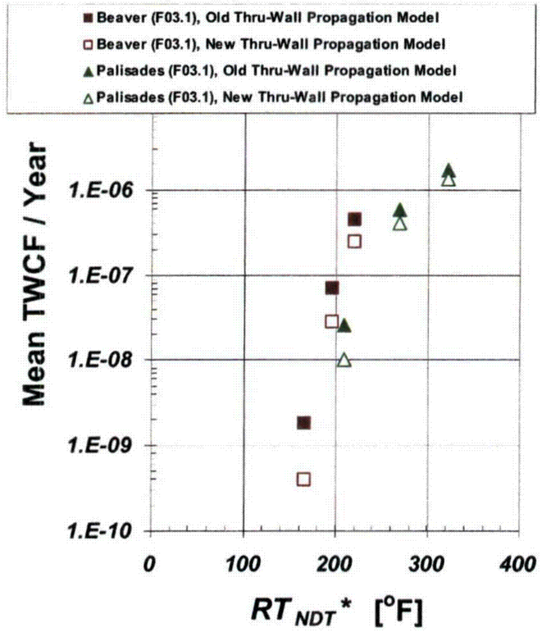

Figure 7.6. Combined effects of allowing K_{Ia} to exceed 200 ksi√in and allowing for ductile crack re-initiation on the upper shelf. Open points show TWCF results when K_{Ia} is allowed to exceed 200 ksi√in and ductile crack re-initiation is permitted. RT_{NDT}* is defined in [*Kirk 12-02*].

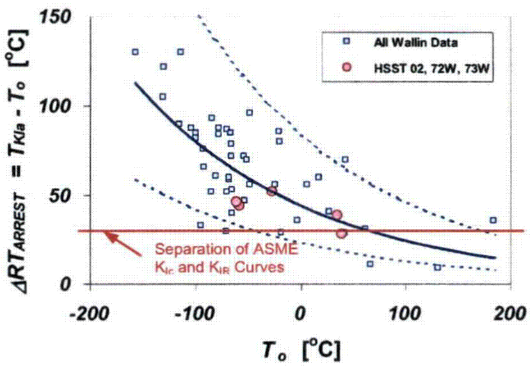

Figure 7.7. Comparison of temperature separation between crack initiation and crack arrest toughness transition curves assumed in our current calculations (blue curve) with the constant separation of ~30°C (~86°F) assumed by previous calculations

7.9 Probabilistic Fracture Mechanics Code FAVOR

7.9.1 Implementation of PFM Model

As shown in Figure 7.8, FAVOR is composed of three computational modules: (1) a deterministic load generator (**FAVLoad**), (2) a Monte Carlo PFM module (**FAVPFM**), and (3) a post-processor (**FAVPost**). Figure 7.8 also indicates the nature of the data streams that flow through these modules.

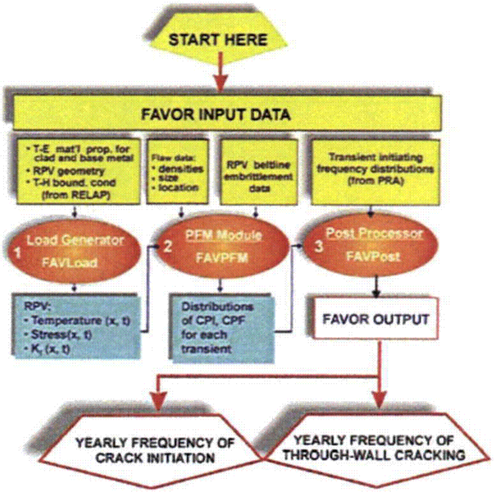

Figure 7.8. FAVOR data streams flow through three modules: (1) FAVLoad, (2) FAVPFM, and (3) FAVPost

FAVLoad takes as input the time histories of pressure, temperature, and heat transfer coefficient defined by the RELAP TH analysis. These inputs are used along with a 1D transient heat conduction equation to estimate the time-dependent variation of temperature through the vessel wall. These time-dependent temperature profiles are used, along with the RELAP pressure history, in a linear elastic stress analysis to estimate the time history of applied-K_I, which is passed to FAVPFM for further analysis.

The FAVPFM module implements the logical specification of the PFM model within a series of nested loops illustrated in Figure 7.9. These loops step through the TH time history and implement the Monte-Carlo trials necessary to estimate the conditional probabilities of crack initiation and of though wall cracking. The probabilities estimated by FAVOR (complete with uncertainties) are *conditional* in the sense that, within the FAVPFM module, the TH transients are assumed to occur.

The FAVPFM module provides the capability to model the variation of radiation damage in the *beltline region* of an RPV with as much detail as the analyst considers necessary. Only that portion of the beltline that is proximate to the active core need be modeled because the fast-neutron flux, and thus the radiation damage, drops to nearly zero within a foot beyond the fuel region. Within this region (active core ±1-ft. (0.3-m), the vessel is represented as a combination of "major regions," with each major region representing a different plate, weld, or forging each having (potentially) a unique combination of mean copper content, mean nickel content, mean phosphorus content, and unirradiated RT_{NDT}. Each major region may be divided into as many "sub-regions" as the analyst feels are necessary to represent accurately both the axial and azimuthal variation of fluence. Sufficient discretization is adopted so that each sub-region is effectively subjected to the same fluence throughout. In this way, the complex variation of embrittlement throughout the vessel wall that is caused by variations in both material and radiological conditions is represented to the model. It should be noted that this material/radiological model is a considerably more accurate representation of reality than the models adopted in the calculations performed to support SECY-82-465 and the IPTS studies. In these earlier calculations, the entire vessel was presumed to be made out of the most irradiation-sensitive material, and all of this material was assumed to be subjected to the peak fluence that occurred anywhere in the vessel.

The last FAVOR module, FAVPost, combines the conditional initiation and through-wall cracking probabilities and combines these, through a matrix multiplication, with the frequency histograms for each TH sequence provided by the PRA analyses. In this way, the complete distribution of TWCF (per operating year) is estimated.

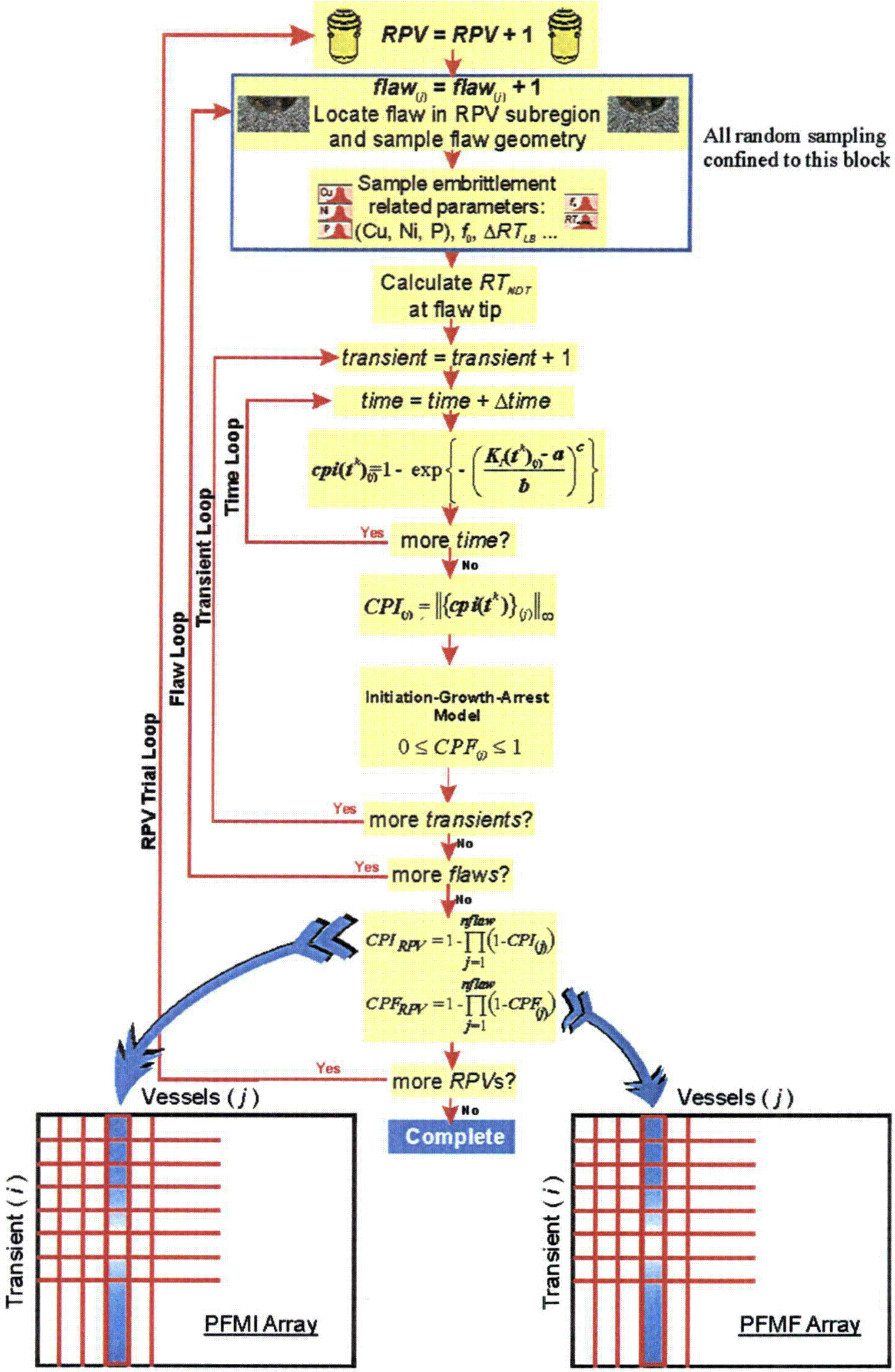

Figure 7.9. **Flow chart for improved PFM model implemented in FAVPFM showing the four primary nested loops – (1) *RPV Trial Loop*, (2) *Flaw Loop*, (3) *Transient Loop*, and (4) *Time Loop***

7.9.2 Discretization of the Reactor Pressure Vessel

FAVOR utilizes discretizes the RPV beltline into one "major regions" for each axial weld, circumferential weld, plate, and forging. The major regions are further subdivided into iso-fluence "subregions." To model accurately the complex variation of fluence with azimuth and axial location (see Figure 7.10) a large number of sub-regions was necessary (15280, 19651, and 67076 subregions for Beaver Valley, Oconee, and Palisades, respectively). The neutron fluence maps were provided for 32 and 40 EFPY were used, and were linearly extrapolated to estimate fluence for longer operational durations.

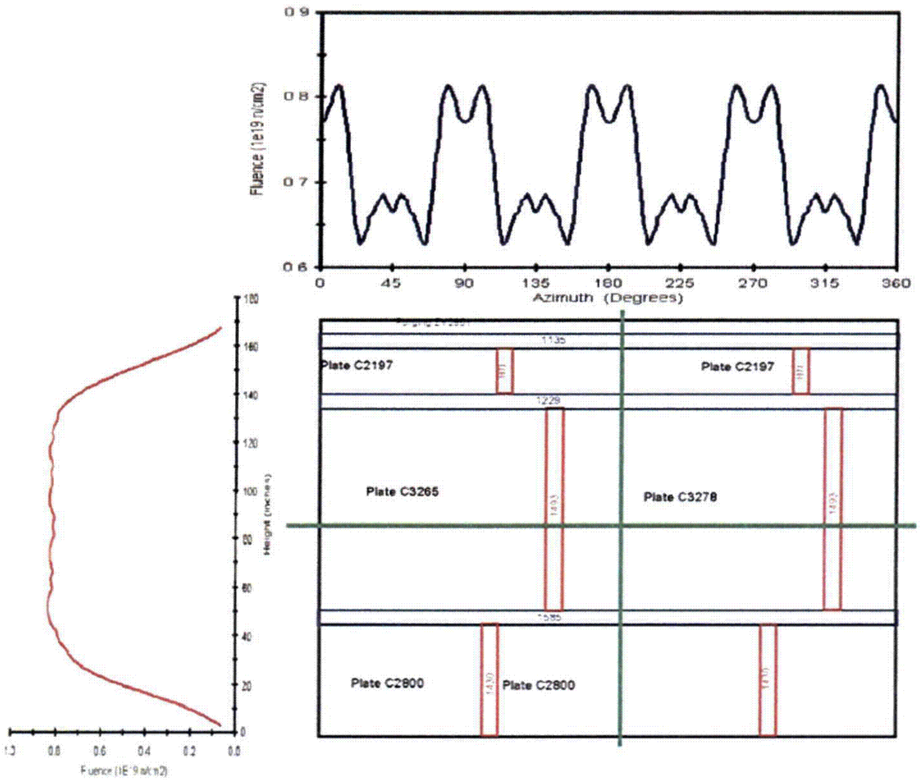

Figure 7.10. Rollout diagram of beltline materials and representative fluence maps for Oconee Unit 1

7.10 Experimental Validation of Linear Elastic Fracture Mechanics

Extensive experimental/analytical investigations performed at ORNL during the 1970s and 1980s examined the accuracy with which LEFM models could be expected to predict the failure of nuclear RPVs subjected to both simple loadings (pressure only) and to much more complex loadings (PTS conditions) [Cheverton 85a, Cheverton 85b]. These investigations all featured tests on thick-section pressure vessels (see Figure 7-11), and aimed to reproduce, as closely as practical in a laboratory setting, the conditions that characterize thermal shock of a nuclear RPV. These conditions include the following:

- fracture initiation from small flaws
- severe thermal, stress, and material toughness gradients
- biaxial loading
- effects of cladding (including residual stresses)
- conditions under which warm pre-stress may be active

- combined stress and toughness gradient conditions that can promote crack initiation, arrest, re-initiation, and re-arrest all during the same transient
- due to these various gradients, the possibility of conversion of fracture mode from cleavage to ductile and back again all during the same TH transient

The three test series were as follows:

- The first series of tests employed ten intermediate test vessels (ITVs), three with cracks located at a cylindrical nozzle and seven with cracks located remote from any geometric discontinuities. These tests were aimed at investigating the ability of LEFM to predict the fracture response of thick section vessels containing relatively deep flaws (20 to 83% of the 6-in. (152.4 mm) vessel wall) at test temperatures ranging from lower shelf to upper shelf. A variety of nuclear grade RPV plates, forgings, and weldments were tested.
- The second series of tests comprised eight thermal-shock experiments (TSEs). The purpose of these experiments was to investigate the behavior of surface cracks under thermal-shock conditions similar to those that would be encountered during a large-break loss of coolant accident (LBLOCA) (i.e., a rapid cooldown in the absence of internal pressure).
- The third series of tests included two experiments that subjected ITV specimens to concurrent pressure and thermal transients. These "pressurized thermal shock experiments," or PTSEs, sought to simulate the effects of a rapid cooldown transient combined with significant internal pressure. Thus, these experiments simulated TH conditions characteristic of smaller break LOCAs.

These investigations support the following conclusions:

- ITV Experiments:
    - LEFM analyses very closely predicted actual fracture pressures for thick-wall pressure vessels.
    - Methods for calculating fracture toughness from small specimens were successfully used in applications of fracture analysis of thick flawed vessels.
- Thermal Shock Experiments (TSEs):
    - Multiple initiation-arrest events with deep penetration into the vessel wall were predicted and observed.
    - Surface flaws that were initially short and shallow were predicted and observed to grow considerably in length before increasing significantly in depth.
    - Warm pre-stress was observed to limit crack extension through the wall under LOCA conditions.
    - Small-specimen fracture mechanics data successfully predicted the fracture behavior of thick pressure vessels.
    - Crack arrest occurred in a rising stress field.
- Pressurized Thermal Shock Experiments (PTSEs):
    - Warm pre-stress is effective at inhibiting crack initiation for conditions under which crack initiation would otherwise be expected (i.e., $K_{applied} > K_{Ic}$).
    - Crack arrest toughness values (K_{Ia}) inferred from conditions prototypic of PTS loading agree well with other experimental measurements, suggesting the transferability of laboratory toughness data to structural loading conditions.

- LEFM predictions of crack initiation, growth, and arrest behavior successfully captured the response of the vessel to the transient; however some details were not exactly predicted (two initiation-run-arrest events were predicted whereas one was observed).

With regard to this final bullet item, it should be noted that exact agreement between deterministic predictions and individual experiments cannot be expected when the physical processes that underlie those experiments produce large aleatory uncertainties (as is the case with K_{Ic} and K_{Ia} data; see Sections 7.7.1.2 and 7.8.1, respectively). Such disagreement does not in itself condemn the methodology, but rather reveals that the precision of any single prediction is limited by the precision in our knowledge of the controlling material properties.

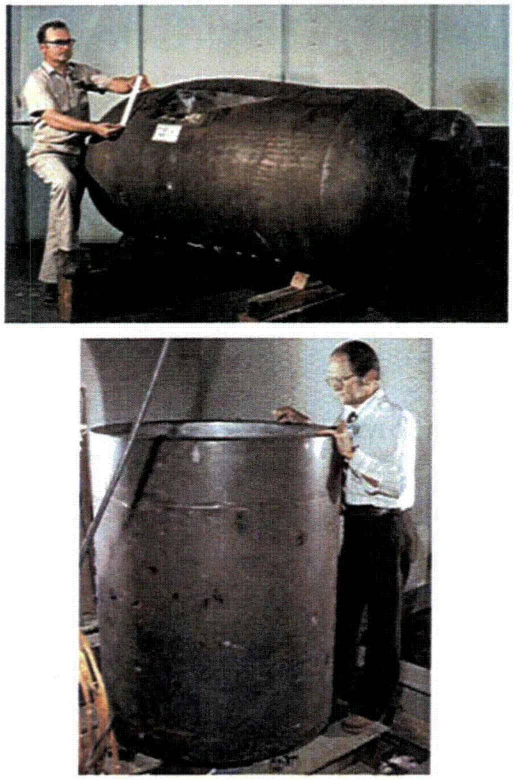

Figure 7-11. Test vessels used in the ITV and PTSE test series (top) and in the TSE test series (bottom)